Bimodal Electric Tissue Ablation (BETA):

An investigation of the ablative potential of combining alternating and direct current in the liver.

By

DARREN KLASS

MBChB, MRCS, FRCR

This thesis is submitted for the Doctor of Medicine degree at the Faculty of Medicine and Health Sciences, University of East Anglia, Norwich.

December 2010

© This copy of the thesis has been supplied on condition that anyone who consults it is understood to recognise that its copyright rests with the author and that no quotation from the thesis, nor any information derived there from, may be published without the author's prior, written consent.

ABSTRACT OF THESIS

Primary and secondary liver cancer account for significant morbidity worldwide. Radiofrequency ablation (RFA) provides patients with a chance of cure or disease control. The technique however has limitations associated with the high rate of tumour recurrence, thought in part to be due to the inability to completely envelop the tumour in a zone of ablated dead tissue. Bimodal Electric Tissue Ablation (BETA) combines direct current with conventional RFA with a resultant increase in the ablation zone size, and an effect on the needle that makes it much harder for tissue to adhere to it.

To explore the effects of BETA, *ex vivo* and *in vivo* studies were conducted.

BETA was found to create larger ablation zones compared to conventional RFA ($p<0.0001$). The hypothesis for this observation is the net movement of water through tissue, a process termed electroosmosis. Analysis of samples treated with BETA and conventional RFA showed a significantly higher hydration percentage following ablation with BETA ($p<0.0001$). Temperature distribution studies demonstrated cytocidal temperatures at 5, 10, 15 and 20mm from the electrode following BETA ($p<0.0001$).

In order to assess the effects of BETA *in vivo*, large animal studies were conducted. Twelve pigs underwent four 'open' conventional RFA cycles and four BETA cycles. These studies showed significantly larger ablation zones following BETA compared to conventional RFA ($p<0.0001$), with no local complications observed.

The inflammatory response to BETA was investigated; pig Major Acute Phase Protein, Serum Amyloid A, Haptoglobin and C Reactive Protein assays were analysed pre and post ablation. The proteins peaked at 48 and 72 hours and all returned to normal levels at termination.

The outcome of this research demonstrates BETA to produce significantly larger ablation zones due to increased hydration of the ablated tissue, with superior temperature distribution and comparable systemic and clinical effects in animal models.

If you can fill the unforgiving minute

With sixty seconds' worth of distance run -

Yours is the Earth and everything that's in it,

And - which is more - you'll be a Man my son!

Rudyard Kipling 1865-1936

CONTENTS

Chapter 1. Literature Review

Chapter 2. Ex Vivo Studies for optimisation of Ablation Parameters

Chapter 3. Hydration Studies

Chapter 4. Temperature Distribution Studies

Chapter 5. *In vivo* Porcine Studies

Chapter 6. Response to BETA - Biochemical Markers and Acute Phase Protein Studies

SUMMARY of FIGURES and TABLES

Chapter 1

Figures

Chapter 2

Figures

Graphs

Schematics

Tables (Appendix 1)

Table 2.1 - shows the control sample size calculations together with the minimum, maximum and means for each radiofrequency energy value measured. The interquartile ranges and standard deviations are also shown.

Table 2.2 - shows the experimental sample size calculations together with the minimum, maximum and means for each radiofrequency energy value measured. The interquartile ranges and standard deviations are also shown.

Table 2.3 - shows the matrix of tested parameters. Each experiment is shown together with the parameters, the size of the ablation zone (cm), the total time of the experiment with RF switched on (s), mean maximum short axis diameter of the ablation zone (cm), the standard deviation (SD) and the 95% Confidence Interval (95% CI).

Tables

Table 2.4 - shows a summary of the ablation zone sizes obtained for the initial ablation matrix including the range and standard deviation (SD).

Table 2.5 - shows the mean sizes of the ablations obtained with 500mA and 600mA respectively. The standard deviation, 95% confidence interval and standard error of the mean (SEM) and ranges are listed in addition.

Table 2.6 - demonstrates the results using 600mA of RF power with no DC (RF), simultaneous DC (9V) and RF (DC/RF) and 300 and 600 seconds of pre RF DC respectively. The Mean, standard deviation, range and standard error of the mean are listed.

Chapter 3

Figures

Graphs

Tables

Table 3.1 - demonstrates each group, with the corresponding values obtained from the hydration analyser. The mean percentage hydration following ablation is tabulated for each parameter with the associated standard deviation (SD), range and the standard error of the mean (SEM).

Tables (Appendix 2)

Tables 3.2 – 3.6 - demonstrate the results of each hydration experiment. The percentage of weight loss registered during drying process - water content (%M), percentage of the sample which remained on the pan after humid evaporation - solid tissue content (%D), the humid/dry mass ratio - part of sample which vaporised during drying process (%R) and residual mass (g) are tabulated in each experiment.

Table 3.7 - explanation of the parameters for each experiment.

Chapter 4

Figures

Figure 4.1 - demonstrates tissue reaction to thermal ablation.

Figure 4.2 - illustrates heat efficacy. In order to decrease the risk of recurrence, an effective heating target volume (the tumor with a margin of normal liver) is necessary. Increasing the amount of electric current (unidirectional arrows) can increase the heat deposition in tissue. Heat conduction decreases with increasing distance from the tip of the electrode (bidirectional arrow), microbubble formation (stars) and charring (dots) adjacent to the electrode. Heat sink due to the adjacent vessel results in insufficient heating and subsequent recurrence.

Figure 4.3- thermadata TD2C temperature logger with LCD display of current temperature, alternating between the two electrodes

Figure 4.4 - graphical display of temperature data following analog-digital conversion by the software.

Figure 4.5 - four temperature probes (silver) placed 5, 10, 15 and 20mm from the electrode (black)

Graphs

Graph 2.1 - illustrates the temperature trend of the control group and the BETA group for each distance (5mm, 10mm, 15mm and 20mm) from the electrode.

Tables (Appendix 3)

Table 4.1 - lists temperatures at each distance from the electrode at each 30 second time interval for the control (600mA RF) and the BETA (9V simultaneous DC and 600mA RF, no pre RF DC) experiments.

Tables

Table 4.2 - lists the mean temperatures at each distance from the electrode at each 30 second time interval for the control (600mA RF) and the BETA (9V simultaneous DC and 600mA RF, no pre RF DC) experiments.

Chapter 5

Figures

Figure 5.13 - shows conventional RFA (left) with a fibrotic ablation (black arrowheads) and BETA (right) with a larger, but similar fibrotic zone of ablation (grey arrowheads). Both are surrounded by normal (arrows) liver parenchyma. No intense inflammatory reaction is seen.

Graphs

Graph 5.1 - demonstrates the size ranges for each of the groups of animals for control and corresponding BETA experiments, with standard error bars.

Graph 5.2 - demonstrates the mean sizes for each of the groups of animals for control and corresponding BETA experiments, with standard error bars.

Graph 5.3 - demonstrates the mean animal weights pre and post surgery and the mean difference between the two weights.

Graph 5.4 - demonstrates the individual animal weights pre and post surgery and the difference between the two weights. The animals have been coded according to the termination dates. 1 & 2 – non-recovery, 3 & 4 – 2 day, 5 & 6 – 14 day, 7 & 8 – 28 day and 9 & 10 – 56 day termination animals.

Tables (Appendix 4)

Table 5.1 - demonstrates the largest short axis diameter ablation zone for each control and corresponding BETA experiment at post mortem examination. The mean, standard deviation (SD) and 95% confidence intervals (95% CI) are tabulated.

Tables

Table 5.2 - demonstrates the summary of the 0d and 2d animal data, the mean, median, standard deviation (SD), standard error of the mean (SEM), 95% confidence interval (95% CI) and ranges are listed.

Table 5.3 - demonstrates the summary of the 14d animal data, the mean, median, standard deviation (SD), standard error of the mean (SEM), 95% confidence interval (95% CI) and ranges are listed.

Table 5.4 - demonstrates the summary of the 28d animal data, the mean, median, standard deviation (SD), standard error of the mean (SEM), 95% confidence interval (95% CI) and ranges are listed.

Table 5.5 - demonstrates the summary of the 56d animal data, the mean, median, standard deviation (SD), standard error of the mean (SEM), 95% confidence interval (95% CI) and ranges are listed.

Chapter 6.

Graphs

Tables

Table 6.1 - tabulates the results for the mean Haptoglobin levels at each time point, including the standard deviation (SD), standard error of the mean (SEM), 95% confidence interval (CI) and range.

Table 6.2 - tabulates the individual Haptoglobin levels for each animal at each time point.

Table 6.3 - tabulates the results for the mean CRP levels at each time point, including the standard deviation (SD), standard error of the mean (SEM), 95% confidence interval (CI) and range.

Table 6.4 - tabulates the results for the CRP levels at each time point for each animal.

Table 6.5 - tabulates the results for the mean SAA levels at each time point, including the standard deviation (SD), standard error of the mean (SEM), 95% confidence interval (CI) and range.

Table 6.6 - tabulates the results for the SAA levels at each time point for each animal.

Table 6.7 - tabulates the results for the mean pMAP levels at each time point, including the standard deviation (SD), standard error of the mean (SEM), 95% confidence interval (CI) and range.

Table 6.8 - tabulates the results for the pMAP levels at each time point for each animal.

Table 6.9 - summarises the mean values for each liver function, LDH, Albumin and Bilirubin at each specified time point tested, with the corresponding 95% confidence interval (Radostits et al, 2005).

Table 6.10 - tabulates the results for the mean ALP levels at each time point, including the standard deviation (SD), standard error of the mean (SEM), 95% confidence interval (CI) and range.

Table 6.11 - tabulates the results for the ALP levels at each time point for each animal.
tabulates the results for the ALP levels at each time point.

Table 6.12 - tabulates the results for the mean ALT levels at each time point, including the standard deviation (SD), standard error of the mean (SEM), 95% confidence interval (CI) and range.

Table 6.13 - tabulates the results for the ALT levels at each time point for each animal.

Table 6.14 - tabulates the results for the mean AST levels at each time point, including the standard deviation (SD), standard error of the mean (SEM), 95% confidence interval (CI) and range.

Table 6.15 - tabulates the results for the AST levels at each time point for each animal.

Table 6.16 - tabulates the results for the mean γ-GT levels at each time point, including the standard deviation (SD), standard error of the mean (SEM), 95% confidence interval (CI) and range.

Table 6.17 - tabulates the results for the γ-GT levels at each time point for each animal.

Table 6.18 - tabulates the results for the mean LDH levels at each time point, including the standard deviation (SD), standard error of the mean (SEM), 95% confidence interval (CI) and range.

Table 6.19 - tabulates the results for the LDH levels at each time point for each animal.

Table 6.20 - tabulates the results for the mean Bilirubin levels at each time point, including the standard deviation (SD), standard error of the mean (SEM), 95% confidence interval (CI) and range.

Table 6.21 - tabulates the results for the Bilirubin levels at each time point for each animal.

Table 6.22 - summarises the mean values for each marker tested (Sodium (Na), Potassium (K), Urea and Creatinine) at each specified time point tested, with the corresponding 95% confidence interval (Radostits et al, 2005).

Table 6.23 - tabulates the results for the mean Na levels at each time point, including the standard deviation (SD), standard error of the mean (SEM), 95% confidence interval (CI) and range.

Table 6.24 - tabulates the results for the Na levels at each time point for each animal.

Table 6.25 - tabulates the results for the mean K levels at each time point, including the standard deviation (SD), standard error of the mean (SEM), 95% confidence interval (CI) and range.

Table 6.26 - tabulates the results for the K levels at each time point for each animal.

Table 6.27 - tabulates the results for the mean Urea levels at each time point, including the standard deviation (SD), standard error of the mean (SEM), 95% confidence interval (CI) and range.

Table 6.28 - tabulates the results for the Urea levels at each time point for each animal.

Table 6.29 - tabulates the results for the mean Creatinine levels at each time point, including the standard deviation (SD), standard error of the mean (SEM), 95% confidence interval (CI) and range.

Table 6.30 - tabulates the results for the Creatinine levels at each time point for each animal.

ACKNOWLEDGEMENTS

Firstly, I am grateful and indebted to Mr SA Wemyss-Holden and Dr JFA Cockburn for their constant support, encouragement, constructive appraisals and patience during the supervision and writing up of this thesis – you provided me with an open template with which to delve into thermal ablation and importantly, the unknown science behind BETA. This was only made possible by your clinical and research experience, your understanding of thermal ablation and the open three-way conversation during our endless discussions.

Secondly, I am indebted to Mr S Thomson and NHS Innovations East for their support and belief in BETA; in particular, Mr Thomson's incredible persistence and drive for clinical progress. This research would not have been possible without your input and support.

Thirdly, my sincere thanks to Dr P Musonda at the University of East Anglia for his support and guidance during the statistical power calculations and study design. Dr C Chrysochou for her assistance and advice with statistical analysis throughout the study and Dr AP Toms for his training support. To Fran, Frances and Glynis at the Norwich Radiology Academy and Sam Andrews for their moral support and assistance.

Last, but certainly not least, I would like to thank my family, especially my wife Tracey and son Joshua whose patience, understanding and love enabled me to complete this work.

This is dedicated to:

Mark Jules Levy (מושי חיס נן אברהס) *19 Nov 1967 – 20 Jul 2008,*
Valhalla, NY, USA
Acute Myeloid Leukaemia

Mary Thelma Miller 23 Dec 1942 – 24 Oct 2006
Johannesburg, South Africa
Bronchogenic Carcinoma (Small Cell)

זכור

Chapter 1:

Bimodal Electric Tissue Ablation:

Radiofrequency Ablation and Competing Therapies.

Introduction.

The liver is, second only to lymph nodes, the most common site for metastatic disease irrespective of the primary tumour (Bruix et al, 2001). Liver metastasis from colorectal carcinoma is the leading cause of cancer-related morbidity and mortality in the West (Bruix et al, 2001). Worldwide, primary hepatocellular carcinoma (HCC) is one of the ten most common cancers (Bruix et al, 2001). Sub-Saharan Africa and Asia are high-risk regions, where HCC constitutes 10%–50% of all malignancies, occurring in 30/100,000 men annually (De Sanctis et al, 1998). The median survival of patients with non-resectable colorectal metastases is 6–12 months and the majority of patients with colorectal liver metastases present with unresectable disease (Pereira, 2007). For those patients presenting with organ-confined disease, surgical resection remains the only curative treatment (Gazelle et al, 2004, Garrean et al, 2008). Surgical resection has until recently been the only established treatment modality with the potential for cure for both primary HCC and metastatic hepatic neoplasms. Survival in patients with surgically resected HCC range from 55% to 80% at 1 year and 25% to 50% at 5 years (De Sanctis et al, 1998). Recent retrospective studies have shown surgical resection to provide superior survival rates compared to radiofrequency ablation (RFA) when treating HCCs between 3 and 5cm in diameter, however for tumours less than 3cm, RFA has comparable recurrence free survival rates to resection (Huang et al, 2010). A meta-analysis has reinforced these findings for HCC (Zhou et al, 2010). Otto et al compared RFA to hepatic resection as a first-line treatment of colorectal liver metastases (CRLM) and demonstrated shorter time to progression and higher local recurrence rates for RFA, but no difference in survival (Otto et al, 2010).

Systemic chemotherapy can provide improvement in median survival time for some patients, however patients who have advanced disease not suitable for resection, rarely survive beyond 5 years (Ahmed et al, 2004). Improved surgical and anaesthetic technique, post operative advancements in intensive care and an overall improvement in patient care, allows 80% of the liver volume to be resected with a mortality of 5% or less (Matsumata et al, 1995). Bilobar or bulky disease and the need to leave sufficient residual functional hepatic parenchyma after resection to support post hepatectomy hepatic function are the cardinal factors decreasing chances of complete resection, or any surgical options for that matter. With these factors in mind, strategies and pathways designed to increase the number of patients who are candidates for complete surgical treatment of liver metastases have emerged and are continuing to be developed.

Neoadjuvant chemotherapy (Adam et al, 2001), preoperative portal vein embolisation (Abdalla et al, 2001) and 2-stage resection procedures (Adam et al, 2000) contribute immensely to increasing the number of patients who are candidates for surgical curative treatment.

The techniques described, although increasing the potential of each patient for cure, still leave the majority of patients with liver-only metastases from colorectal carcinoma unsuitable for complete surgical resection. This decision is largely based on metastatic load and distribution in the liver.

For patients where resection is not an option, other techniques can be used in an attempt to achieve complete or partial tumour destruction depending on tumour load, distribution and histological grade (Cascinu and Wadler, 1996, Kuvshinoff and Ota, 2002, Kim et al, 2006a, Gervais et al, 2009).

For those patients with hepatocellular carcinoma (HCC), liver transplantation is currently considered to be the best treatment for small tumours (Brillet et al, 2006) as it eliminates both the tumours and the underlying cirrhosis – thus preventing new tumours from developing. Surgical resection as in metastatic disease is otherwise the best chance of cure. However, this does not eliminate the causative agent and many of these patients will develop further primary liver tumours following resection (Kim et al, 2003). Tumour progression and co-morbidities associated with HCC often prevents patients from undergoing transplantation or resection, thus necessitating a less invasive, but effective treatment. For these patients, RFA (Choi et al, 2000, Galandi and Antes, 2004, Cabassa et al, 2006, Delis et al, 2006, Kim et al, 2006b, Lencioni et al, 2008) or transarterial chemo-embolisation (TACE) (Yamada et al, 1983, Yamada et al, 1990, Livraghi et al, 2000, Goldberg and Ahmed, 2002, Buijs et al, 2008) and selective intra-arterial radiotherapy (Kennedy et al, 2007) are the only modalities which give the patient a possible chance of disease control or cure.

Recently, RFA has been viewed as a first line treatment for patients with small (<5cm diameter) solitary hepatocellular carcinoma (HCC) and well-preserved liver function. Peng et al (Peng et al, 2010) treated 247 patients with a solitary HCC ≤5 cm and liver status scored as Child-Pugh class A. The overall 5, 7 and 10-year survival rates were 59.8%, 55.2%, 33.9% respectively. Similar studies by Liu et al (Liu et al, 2010a) have demonstrated RFA to provide similar survival outcomes compared to resection for tumours less than 5cm. This however is not mirrored in the literature and hepatic resection still remains the treatment of choice for these patients (Zhou et al, 2010).

General.

Currently, the most widely used tumor ablative technique for treatment of colorectal liver metastasis is radiofrequency ablation (RFA), which has been shown to be safe and feasible in patients with unresectable hepatic tumors (Goldberg et al, 1996a, Goldberg et al, 1996b, D'Ippolito and Goldberg, 2002, Lencioni et al, 2005). Outcomes following RFA are difficult to interpret, as most of the papers in the literature describing recurrence rates following RFA report recurrence per lesion and not per patient. A further difficulty is the reporting of outcomes for a set group or population with mixed tumor types as well as the use of a variety of techniques of ablation with differing equipment (Abdalla et al, 2004, Mulier et al, 2005). One of the most important factors to consider however is the immature follow-up data. Abdalla et al reported a 1-year survival of 78% and a 3-year survival of 46% for percutaneous RFA (Abdalla et al, 2001).

Livraghi et al (Livraghi et al, 1997) and Solbiati et al (Solbiati et al, 1997a, Solbiati et al, 1997b) performed the largest clinical trials in the late 1990s. Livraghi et al. treated 11 patients with 17 hepatic metastases and one primary cholangiocarcinoma using a single probe. On follow-up CT at 6 months, just under 67% of the lesions showed complete response and the remaining 6 lesions a partial response. The recurrence rates again were quoted per lesion rather than per patient, which is a common theme in the literature, making clinical and technical success per patient difficult to interpret.

Solbiati et al. (Solbiati et al, 2001) reported a recurrence rate of up to 40% overall, but 12% of patients were found to have recurrence at a treatment site at 1 year following RFA.

Abdalla et al published data on patients treated with RFA only, RFA and resection and resection only. The recurrence rates were 84%, 64% and 52% respectively for each of the groups (Abdalla et al, 2004). These results may in part reflect the poor prognosis of the disease.

Such recurrence rates have meant RFA has been reserved as an adjunctive tool to resection, when the chance of complete resection is not possible. RFA is used alone or in combination with resection. In many cases, recurrence following resection leaves the clinician with RFA as the only option for disease control (Choi et al, 2004, Yang et al, 2006).

Recent retrospective studies in the literature have sought to confirm resection as the treatment of choice for metastatic disease and primary liver cancer. Gleisner et al (Gleisner et al, 2008) published retrospective data from a major hepatobiliary centre between 1999 and 2006. 258 patients with colorectal liver metastases underwent hepatic resection alone or in conjunction with RFA. The median size of the largest lesion treated was 3.0 cm. One hundred and ninety-two patients (74.4%) underwent resection alone, 55 patients (21.3%) underwent resection and RFA and 11 patients (4.3%) underwent RFA alone. The results showed patients who underwent resection alone had a better disease-free survival than those who underwent resection and RFA or RFA alone. However the tumour load, distribution and number were not calculated in the

data analysis. Given the need for resection coupled with RFA one can infer lesions were present which could not be resected and needed further treatment. These patients will always have worse outcomes than patients with single, resectable lesions.

Recent meta-analyses by Zhou et al (Zhou et al, 2010) questioned the literature and the consensus of resection rather than RFA for small HCC. Zhou conducted a systematic review and meta-analysis of trials comparing RFA with HR for small HCC between 1997 and 2009. A total of 1411 patients: 744 treated with RFA and 667 treated with hepatic resection (HR) were included in the analysis. The overall survival for tumours larger than 3cm was significantly higher in patients treated with resection than in those treated with RFA at 3 and 5 years. The local recurrence rate of RFA was higher than resection, however as expected, the resection group encountered more post-operative morbidity. For tumors ≤3 cm resection was comparable to RFA for survival. These findings are similar to recently published studies comparing resection to RFA (Huang et al, 2010, Hung et al, 2010, Kudo, 2010, Liu et al, 2010b).

Hur et al (Hur et al, 2009) compared outcomes in patients with single colorectal metastases. The retrospective analysis included 67 consecutive patients with solitary colorectal liver metastases treated by resection or RFA. Forty-two patients underwent resection and 25 patients, RFA. The 5-year overall and local recurrence-free survival rates after resection (50.1% and 89.7%) was higher than following RFA (25.5% and 69.7%). The interesting finding in this study was the outcomes in patients with tumours smaller than 3cm (n = 38). In this subset of patients, the 5-year survival rate for resection or RFA was similar: overall survival (56.1% vs 55.4%) and local recurrence-free survival (95.7% vs 85.6%). Neither of the differences was shown to be statistically significant. The tumour size, treatment method and primary node status were shown to be significant prognostic factors. These prognostic factors, coupled with resection margin, local extension of the tumour, response to chemotherapy and preoperative portal vein embolisation have also been described as significant (Nikfarjam et al, 2009). Leblanc et al (Leblanc et al, 2008) published a similar study design to Hur et al in 2008 comparing outcomes in the same 3 groups. No statistical difference in survival between the 3 groups (RFA alone vs RFA and resection vs resection alone) at 2 years was demonstrated.

A large retrospective study published by Gillams and Lees (Gillams and Lees, 2009) describes a five-year survival rate of 24-33% in 309 patients with colorectal metastases, treated with RFA. These results are superior to any published data relating to chemotherapy and approach the five-year survival rates quoted for resection.

The largest retrospective study to date comparing resection to RFA for hepatic colorectal metastases (HCM) was published by Reuter et al (Reuter et al, 2009). This retrospective review of patients treated between 1995 and 2007 describes 192 patients undergoing either resection or RFA alone for metastatic disease. As expected the time to recurrence for RFA patients was

shorter than for resection (12.2 vs. 31.1 months; $p < 0.001$). Recurrences at the site of treatment for each modality were more with ablation (17%) than with resection (2%). Distant hepatic recurrences were found in 33% of ablation patients vs. 14% in the resection group, however this may in part be due to disease load before treatment. The largest lesion in the ablation group was 5.3cm and 3.2cm in the resection group. Nodal involvement, too, was higher in the ablation group (63% vs 50%); both of these have been shown to be significant prognostic factors (Hur et al, 2009, Nikfarjam et al, 2009) and must be borne in mind when interpreting the results. The results did, however confirm resection to be the treatment of choice for colorectal metastases.
Otto et al (Otto et al, 2010) evaluated the use of RFA as first-line treatment in patients presenting with colorectal metastases (CRLM) within the first year after colorectal surgery. Resection was performed in patients who were deemed not amenable to RFA due to number, size, or location of metastatic lesions. Local recurrence at the site of ablation or resection occurred in 32% and 4% ($p<0.001$), new metastases apart from the site of previous treatment in 50% and 34% ($p=0.179$) and systemic recurrence in 32% and 37% ($p=0.820$) of the patients after RFA and surgery, respectively. Time to progression was significantly shorter in patients primarily treated with RFA (203 vs. 416 days; $p=0.017$). Otto demonstrated that despite striking differences in local tumour recurrence and shorter time to progression, survival in patients with early CRLM was independent of treatment modality.

Treatment of hepatocellular carcinoma (HCC) however is not as simple to define as metastatic disease. HCC is associated with significant co-morbidities, which do not often accompany metastatic disease. These include cirrhosis, liver failure and its associated results, poor nutritional status, and abnormal clotting. These often have a major impact on the clinical team's decision to treat and the method chosen for treatment. Consequently these factors are often the reason why patients are excluded from the option of transplantation.
As a result of the confounding influence of co-morbidities, data establishing RFA as an effective treatment for HCC compared to resection or repeat resection is scarce in the literature, with only a single non-randomised trial published to date (Rampone et al, 2009, Zhou et al, 2010).
Several observational studies have suggested that RFA may have survival benefits similar to hepatic resection (HR; excision of diseased lobe of the liver) in cirrhotic patients affected by hepatocellular carcinoma (HCC) who are not candidates for liver transplantation (Shimozawa and Hanazaki, 2004). A paper by Molinari (Molinari and Helton, 2009) used a computer generated Markov model to simulate a randomised controlled trial. This confirmed these findings, although the study did not have sufficient power to detect a significant difference at a 5-year interval. In this paper a Markov model was created to simulate a randomized trial comparing survival in patients undergoing hepatic resection or RFA for HCCs less than 5 cm in

diameter. Hepatic resection was shown to be the best option overall, however RFA was shown to be the preferred method if the perioperative mortality of resection was more than 30%, if the percentage of patients with complete resection was less than 60% and if RFA could be performed at least 60% of the time for recurrent disease after a previous ablation. The results of this model only simulate a randomised trial and the results should be viewed with reservation. This small study, however, did highlight the potential place of RFA in the treatment of HCCs. A study by Liang et al (Liang et al, 2008) of 110 patients with HCC recurrence following resection was published in 2008. Sixty-six patients with 88 tumors were treated by RFA and 44 patients with 55 tumors were treated by repeat hepatectomy. The one year survival rates for each group were 76.6% vs 78.6% respectively and the 5 year survivals 27.6% vs 39.9% respectively. Neither of these was found to be statistically significant. The complication rate was higher in the repeat hepatectomy group compared to the RFA group (75% vs 3%), which was significant, confirming our knowledge that surgery does carry with it inherently higher morbidity risks than percutaneous treatments. The interval of recurrence from the initial hepatectomy, diameter of the recurrent tumor and the serum albumin level were significant prognostic factors for overall survival, in keeping with prognostic factors of metastatic groups of patients (Hur et al, 2009, Nikfarjam et al, 2009). The serum albumin level refers to liver function and overall nutritional status of the patients, which if low indicates poor hepatic function and or severe malnutrition.

RFA has been shown to be a relatively low risk procedure, with few complications (Livraghi et al, 2000, Mulier et al, 2002, Zagoria et al, 2002, Livraghi et al, 2003). Those causing delayed discharge, life-threatening injuries or causing significant disability or morbidity (Kong et al, 2009) are defined as major complications. These include liver failure, and uncontrolled haemorrhage requiring additional procedures including surgery or embolisation, tumour seeding and collateral damage to adjacent structures including bile ducts, visceral organs (bowel or solid organs), and diaphragm, as well as pneumo/haemo or hydrothorax requiring drainage (Akahane et al, 2005, Head et al, 2007, Kong et al, 2009). Minor complications include biloma, portal vein thrombosis and skin burns (Akahane et al, 2005). Major complications are infrequent (2.43%) (Rhim et al, 2003) with an overall complication rate of between 8 and 12 % (Mulier et al, 2002, Cheung et al, 2009).

Modified techniques have been described in an attempt to make this occurrence even less. In certain cases, complications such as tumour seeding may upstage a patient's disease (Llovet et al, 2001, Arienti et al, 2006). Efforts have been made to dissipate heat adjacent to the treatment area in an attempt to decrease collateral damage (Hinshaw et al, 2006, Laeseke et al, 2006, Marchal et al, 2006, Liu et al, 2008). The complications associated with radiofrequency ablation will be expanded on in later chapters.

The spectrum of complications, individual rates of occurrence and most importantly its impact on radiofrequency ablation outcome will be discussed in later chapters in depth.

Ablation:

Definition:

Ablation is defined as the direct application of chemical or thermal or cryotherapy from an energy source in an attempt to achieve eradication or substantial destruction of cells (Goldberg et al, 2005).

General.

Ever since the discovery of the heat and its effects on the body, medical applications have continued to increase in number and complexity. Initially the treatments used extremes of heat and cold in order to observe any visible change in the tissue. With time, and the growth of technology, this became more refined and controlled.
Pavy and Siau published the first paper using ablation in the liver in 1903 (Pavy and Siau, 1903). Since then there have been over 8000 papers published on the use of ablation for therapeutic purposes.

There are 4 main categories of ablation in current practice today.

1. Thermal ablation
2. Cryoablation
3. Chemical ablation
4. Irreversible electroporation

Thermal ablation:

This category of ablation uses energy sources that destroy tissue using thermal energy.

These techniques include the following:

1. Radiofrequency
2. Laser
3. Microwave

Cryoablation:

This category of ablation uses extreme cold generated by liquid nitrogen or gases to destroy tissue.

Chemical Ablation:

This category of ablation uses chemicals to induce ablation of tissue.
The methods of chemical ablation are classified according to the universally accepted nomenclature of the primary agent used.

1. Ethanol
2. Acetic Acid
3. Direct Current

Direct Current (DC), although not a chemical agent induces tissue ablation through the polarisation of tissue. This polarisation of tissue is caused by the anode (positive) and the cathode (negative) in the tissue and liberation of various gases, along with electrode corrosion, causes chemically induced necrosis. This will be discussed in Chapter 2 in detail.

Irreversible Electroporation:

This category of ablation uses short pulses (ms) of high voltage direct current to disrupt the cellular membrane, causing irreparable cell damage.

Radiofrequency Ablation:

Definition:

Radiofrequency ablation (RFA) is the induction of coagulative necrosis by a source of alternating current whose frequency is in the Radiofrequency range: 30KHz – 30MHz (Goldberg et al, 2005).

General.

Radiofrequency Ablation (RFA) uses electromagnetic energy, supplied by a radiofrequency (RF) generator to produce heat in tissue with subsequent tissue destruction. Radiofrequency refers to the alternating electric current that oscillates in the range of high frequency (200–1,200 kHz) rather than the emitted wave.

A closed-loop circuit is created by placing a generator, a large dispersive electrode (grounding pad), a patient, and a needle electrode in series.

Both the dispersive electrode and needle electrode are active, with the patient acting as a resistor. An alternating electric field is created within the tissue of the patient. Tissue has relatively high electrical resistance in comparison with the metal electrodes. This causes marked agitation of the ions and charged molecules ions present in the tumor or liver tissue adjacent to that immediately surrounds the electrode. This ionic agitation creates friction and thus heat, which can be tightly controlled through modulation of the amount of radio-frequency energy deposited (Rhim et al, 2001).

The Bioheat equation:

The parameter governing tissue destruction is temperature.
The generation of tissue heat induces cellular death via thermal coagulation necrosis (Dupuy and Goldberg, 2001, Nahum Goldberg and Dupuy, 2001).

The distribution of thermal energy in tissue is governed by the "Bioheat" equation, described by Pennes in 1948 (Pennes, 1998).
He described heat transfer in a human forearm, suggesting the rate of heat transfer between blood and tissue was proportional to the product of the volumetric perfusion rate and the difference between the arterial blood temperature and the local tissue temperature.
The original equation was broken down into 11 separate equations, which explained the heat transfer in detail and is beyond the scope of this thesis.
The equation derived the formula to explain the loss of heat in tissue influenced by the blood circulation. This can be simplified as outlined below.

The loss of heat through conduction in tissues can be explained as follows:

$$Q_{gain} = q_{storage} + q_{loss} + W$$

q can be explained by heat absorption from the surrounding control volumes stored by the tissue, lost through the boundary of the volume and W - work performed by the tissue and metabolic heating.

The two main mechanisms for heat flow inside tissue is through

1. Conduction - the gradient in temperature within the tissue itself drives the flow.
2. Convection of thermal energy by the perfusing blood.

The Fourier law of heat conduction governs the conducted heat flow. The law states that the amount of thermal energy conducted through a medium is proportional to the cross sectional area, the temperature difference and the length of time. It is inversely proportional to the length across the medium.

The Fourier Law of Heat Conduction

$$q = Q/A = -kdT/dx$$

q is the heat flux, defined as the heat per unit area (w/m^2).
Q is the heat rate
dT/dx is the thermal gradient in the direction of the flow. The negative indicates flow of heat is from hotter to colder. If the temperature decreases with *x, q* will be positive and will flow in the direction of *x.* If the temperature increases with *x, q* will be negative, and will flow opposite to the direction of *x*.
k is the thermal conductivity and is used to show that not all materials heat up or retain heat equally well. k is W/m*K, where W is watts, m is meters, and K is Kelvin.

The heat transfer or conduction rate is a scalar and is

$$Q = -kA\,\Delta T/L$$

L is the length of the slab
ΔT is the temperature difference between two different surfaces.
These two equations show that heat can be considered to be a flow. The flow of heat depends upon the thickness of the material, the area, the conductivity and nature, all of which combine to retard or resist this flow.

The bioheat equation can be viewed in a simplified framework, which is more pertinent to radiofrequency ablation.

"coagulation necrosis = (energy deposited x local tissue interactions) – heat lost."

Each of these parameters must be addressed when considering thermal ablation and tissue necrosis (Lobo et al, 2005).
Cellular homeostasis can continue with elevation of temperature to 40 °C. As temperature increases, cells become more susceptible to damage by agents such as radiotherapy and chemotherapy (Ahmed et al, 2003b, Ahmed et al, 2004, Ahmed et al, 2005a). With a mild temperature increase of 42-45 °C. (hyperthermia) prolonged heating at these temperatures will not induce complete cell death. Continued cell growth and function can be observed after long

exposures to hyperthermia. Increasing the temperature to 50-55 °C shortens the time necessary to induce cytotoxicity to less than 10 minutes. 4-6 minutes has been quoted as the minimum time needed at this temperature to induce cell death (Goldberg et al, 1996a, Goldberg et al, 1996b, Goldberg et al, 2000). At temperatures less than 50 °C Goldberg et al 1996 showed no coagulation in *ex vivo* studies. 60-100 °C causes almost instantaneous protein coagulation, which irreversibly damages key cytosolic and mitochondrial enzymes (Dupuy and Goldberg, 2001, Nahum Goldberg and Dupuy, 2001).

Temperatures greater than 105-115 °C, result in tissue boiling, vaporisation and carbonisation (Kruskal et al, 2001). Carbonisation increases the impedance in tissue and limits the ability to deposit heat, limiting the ablation geometry (Goldberg et al, 1996a, Goldberg et al, 1996b, Goldberg et al, 2000).
The "charring" effect of RFA is the ultimate limiter of ablation zone size. The charring effect of RFA on the tissue in immediate contact with the electrode is caused by excessive temperature deposition at the needle tip in a very short time frame. This results in:

1. Adhesion of the liver to the needle. This prevents the needle from sliding out of the tissue easily and safely. The needle is left with adherent pieces of tissue, and subsequent damage to the organ being treated.

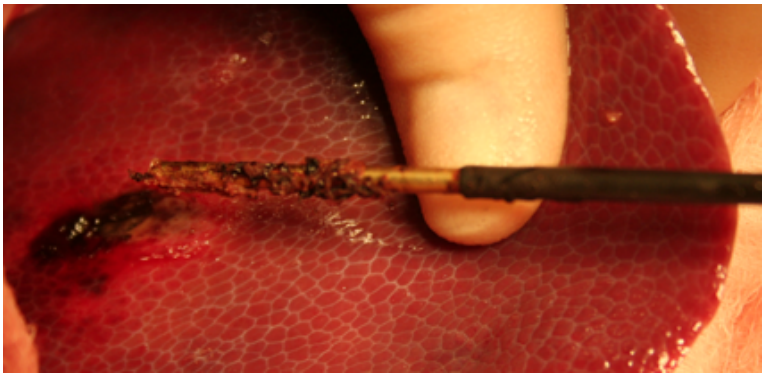

Figure 1.1 Charred tissue adherent to the needle following RFA.

2. Sudden and uncontrollable rise in the impedance of the tissue. The impedance of the tissue is a variable that governs the amount of power deposited in the tissue. As the impedance increases, the RF voltage (V) must increase or the RF current (mA) must decrease in order to balance the equation: V = I X R.

The equation rearranged: R (Ohms) = V (Volts)/I (Amps).

As the impedance increases, the power must increase in order to ensure the same amount of RF current (mA) is delivered to the tissue.
Once tissue reaches an impedance of 900 Ohms, the power required to generate enough heat becomes too great, and it is at this impedance that most commercially available machines stop ablating, switching themselves off as further ablation is so difficult to achieve.
This phenomenon is known as impedance "roll-off" (Lin et al, 2003).
The key aim of ablative technology is to control the heat deposited and the local tissue interactions in order to achieve the desired effects in tissue. Thus the impedance roll-off is delayed for as long as possible in order for the maximum benefit to be gained from the ablation treatment (Lin et al, 2003).

The earliest use of radiofrequency ablation was primarily geared towards neurosurgical and cardiac applications (Taha et al, 1995, Gazelle et al, 2000). Initial studies of percutaneous RF tumour ablation involved the use of monopolar electrodes to induce coagulation necrosis up to 1.6cm (McGahan et al, 1990, Rossi et al, 1990).
Most currently available machines function in the 375-500kHz range (Dupuy and Goldberg, 2001, Goldberg, 2001, Nahum Goldberg and Dupuy, 2001), with the majority of devices being monopolar.

The goal of RF ablation is to intentionally ablate a zone of healthy tissue around the target tumour, analogous to the "surgical margin" described in the literature (Hong and Georgiades, 2010). The margin should be 0.5-1 cm beyond the tumour margin, given the difficulty in accurately identifying the tumour margin macroscopically and to allow for microscopic tumour spread beyond the macroscopic tumour margin. This equates to a 3-4cm ablation created during treatment of a 2cm tumour. The "ablative margin" (Goldberg et al, 2005) decreases the risk of local tumour recurrence, however the limitations of RFA make this margin difficult to obtain with monopolar RFA and a straight ablation electrode. The following describes the modifications used in the delivery of radiofrequency energy to tissue. Each modification described below attempts to increase the ablation zone size and thus decrease the risk of recurrence of tumour.

Bimodal Electric Tissue Ablation (BETA).

Definition.

Applications of Direct Current (DC) to a radiofrequency ablation (RFA) circuit either individually or simultaneously without allowing interference of the DC in the RFA circuit.

Bimodal Electric Tissue Ablation is a novel method of applying DC and RFA to tissue either serially individually or simultaneously in order to increase the ablation zone in the tissue. BETA combines these two energies in an effort to improve the temperature distribution in the tissue. It has been shown that improved temperature distribution in the tissue allows a more uniform distribution of heat and thus increases the ablation zone (Goldberg et al, 1996a).
BETA is thought to increase the hydration of the tissue by a process termed electroosmosis (Reuss, 1809), which will be discussed in detail in later chapters.
These two important factors are hypothesised as critical in the larger ablation zones obtained in the original studies of the earlier BETA study (Cockburn et al, 2007).
In order to understand the context of BETA in ablation technologies, it is important to have an understanding of the modifications and advances made in RFA in an attempt to counteract the limitations placed on RFA by the bioheat equation.
The remainder of this chapter will address this and includes descriptions of modifications in needle design, which attempt to increase the ablation zone size. In addition, adjunctive techniques, which target the ability of the cells to repair following a thermal insult or increasing the sensitivity of the cellular framework to thermal energy, are described.
Finally in this chapter, the history of BETA will be outlined together with a description of competing thermal technologies.

Monopolar RFA:

Definition:

The RF generator supplies RF power to the tissue through an electrode. It is connected to the shaft of the electrode and to a reference electrode. The reference electrode is a large-area conducting pad in contact with the patient's skin in an area of good electrical and thermal conductivity (Goldberg et al, 1996a).

In order for radiofrequency ablation to be deemed successful the entire tumour must be subjected to cytotoxic temperatures. Prior studies have shown that with monopolar radiofrequency ablation, temperature is not uniformly distributed within tissues (Goldberg et al, 1996a). Goldberg et al (Goldberg et al, 1996a) demonstrated that higher electrode tip temperature and longer electrode tip exposures were associated with increased temperature variation. He also demonstrated that the diameter of local coagulation necrosis was a function of the local mean temperature. The ideal would therefore be to heat the tumour uniformly to 50-60 °C, inducing uniform coagulation.
Conventional RF precludes this due to the high temperatures at the electrode tip and the rapid fall off of temperature at increasing distances from the electrode as described by Cosman (Cosman et al, 1984). Together with electrode size, tissue conductivity and blood-flow convection, monopolar RF ablation faces many challenging barriers to enlargement of the ablation volume.

Tissue cooling secondary to vascular flow is a primary determinant of coagulation necrosis size. This effect, known as the "heat sink" effect has been proved by Curley and Hamilton 1997, Goldberg et al 1998 and Patterson et al 1998 (Curley and Hamilton, 1997, Goldberg et al, 1998, Patterson et al, 1998). Coagulation zones obtained in *ex vivo* tissues have been both larger and more reproducible compared to results from *in vivo* studies (Solbiati et al, 1997a, Livraghi et al, 1999).
This is very likely to be a result of the heat sink effect in *in vivo* tissue.

In order to try and decrease the limiting effects of the heat sink, two techniques can be used to alter blood flow through the tissue:

1. Mechanical occlusion
2. Pharmacological modulation of blood flow.

Mechanical occlusion refers to occlusion of the lesser omentum carrying blood to the liver, the porta hepatis. Mechanical occlusion interrupts the flow of blood through the hepatic artery and the portal vein, thus decreasing the blood flow to the liver.
The technique was described by James Hogarth Pringle, published in 1908 (Pringle, 1908). He described a method whereby the portal vein is compressed in the anterior boundary of the foramen of Winslow to arrest hepatic blood flow to allow time to repair liver trauma. The technique was described using ligatures in animal studies and later, mechanical occlusion in patients. The limitation of this technique is the need for adequate surgical access in order to perform the manoeuvre. The technique requires an open or laparoscopic procedure (Iannitti et al, 2002, Hsieh et al, 2004) and thus the advantage of percutaneous techniques are lost. The relatively uncontrolled mechanical occlusion of the entire vascular supply to the liver at the hilum does have the potential for significant morbidity such as portal vein thrombosis (Kim et al, 2004). The theory has been investigated, particularly in recent years with the development of endovascular occlusion techniques. The radiologist has at their disposal both temporary and permanent occlusion techniques. Temporary techniques include inflating an occlusion balloon in the portal vein, occluding supply to the entire liver, or a portal vein branch, thus occluding only the supply to the specific lobe of liver being treated (de Baere et al, 2008).
Using absorbable occlusion material such as gelfoam (Miyamoto et al, 2004) or autologous blood is another alternative, mostly reserved for trauma. Unfortunately mechanical form of external occlusion of the entire porta hepatis has not consistently proved to aid in increasing the ablation zone significantly, and has produced significant morbidity, including portal vein thrombosis (Shen et al, 2003, Hope et al, 2007).
A newer technique being evaluated is the intra-arterial administration of medication to decrease the blood supply to the organ being treated (Hines-Peralta et al, 2006b, Hakime et al, 2007), this technique remains in the pre-clinical trial phase.

Permanent occlusion techniques include embolisation with coils or glue. This technique is used widely in preoperative patients for liver resection. The lobe being resected is embolised 1-2 days prior to surgical intervention to allow the lobe to devascularise. A further technique is also adopted in patients with a small unaffected lobe, where the affected lobe is embolised 6 weeks prior to resection, allowing the unaffected lobe to undergo compensatory hypertrophy. This ensures that following resection; the unaffected lobe is able to carry out normal hepatic function, without compromising the patient's biochemical balance.

Horkan (Horkan et al, 2004) altered blood flow in rabbit models using halothane, adrenaline or arsenic trioxide. Laser Doppler flowmetry was used to monitor peri-procedural hepatic blood flow. Temperature probes were placed in the tissue in the region of the ablation zone and at predetermined distances from the portal vein and electrode to monitor temperature change. Halothane and Arsenic Trioxide reduced hepatic blood flow to 40.3% and 29% of normal, respectively. Adrenaline conversely increased blood flow to 207.8% of normal.

Patterson et al (Patterson et al, 1998) conducted *in vivo* porcine experiments in eight animals to determine the effect of treatment time and hepatic blood flow. Patterson examined the specimens histologically and found vessels less than 1cm from the probe tip strongly predicted the lesion diameter and volume. This negative effect of blood flow on lesion size was confirmed when comparing the two animals that underwent ablations in exactly the same lobe of liver, with and without mechanical vessel occlusion. The ablation zones created with mechanical vessel occlusion were significantly larger than those without mechanical vessel occlusion (3.0cm vs 1.2cm respectively). Lesion volume increased accordingly ($35.0cm^3$ vs $6.5cm^3$). This however has not been a consistent observation in the literature (Hope et al, 2007).

De Baere et al (de Baere et al, 2008) performed targeted hepatic venous occlusion using an endovascular balloon rather than complete portal vein occlusion as described by Pringle in 1908. The results of the portal blood flow occlusion revealed the technique to only be effective for tumours less than 35mm, abutting vessels 4mm or larger.

Further *in vivo* animal studies have been conducted by Horkan et al (Horkan et al, 2004) and Iwamoto et al (Iwamoto et al, 2008) evaluating hepatic blood flow following pharmacological and mechanical occlusion respectively. The findings of mechanical or chemical occlusion on coagulation volume have been investigated in the kidney, a growing target organ for thermal therapy, with similar promising results (Chang et al, 2004).

Radiofrequency Energy Deposition:

Bipolar Ablation:

Definition:

Bipolar radiofrequency ablation uses two active electrodes, placed in closed proximity to each one another to achieve contiguous ablation zones. The electrodes are placed into the tissue and energy is deposited at the active and ground electrodes (Goldberg and Gazelle, 2001, Clasen et al, 2007).

Radiofrequency energy is deposited at both electrodes as opposed to monopolar ablation where the energy at the grounding pad is dissipated over a larger surface area (McGahan et al, 1996). Heat is thus generated at both the active and ground electrodes resulting in larger more confluent ablation zones. The zone of ablation is usually elliptiform, with a longer zone of ablation. Burdio (Burdio et al, 2003a) described a method of bipolar radiofrequency ablation that significantly increased the ablation zone *ex vivo*. The ablation zone could be as large as 4cm depending on the distance between the electrodes.
A paper in the same year by Burdio (Burdio et al, 2003b) described a method whereby a single electrode is used to deliver RF energy in a bipolar manner. Using the bipolar technique, the needle is exposed at two different points along the needle, separated by a non-conductive element. The results using bipolar RF again showed larger zones of ablation and decreased impedance in the tissue during and at the end of the ablation cycle.
A further benefit of bipolar ablation is the reduction of the electric field in the body and a decreased risk of damage to surrounding structures (Buy et al, 2006). Bipolar RFA also allows for use in patients with cardiac pacemakers, as there is no distant circuit created outside the liver as with monopolar RFA.
Bipolar RFA however is not without potential complications, the most obvious being the use of two needles instead of one as opposed to a single needle with a non-conducting element as described above. The use of two needles adds an unnecessary potential for complications during insertion or during ablation. Damage to structures adjacent to the organ during insertion makes this technique less desirable for clinical use. A further limitation is that needles should be placed parallel, between 5 and 30mm form one another and should not touch in order to avoid shorting the electrical circuit (Frericks et al, 2005).

Multipolar RF Ablation:

Definition:

Multipolar RFA is a technique used to apply RF to 3 or more needles placed in a single lesion or multiple adjacent lesions. The RF current flows between 2 electrodes in a random pattern generated by the machine (Callstrom and Charboneau, 2008).

Using the technique of multipolar RFA (Callstrom and Charboneau, 2008, Peng et al, 2011), each electrode is bipolar, with current flowing between electrodes, negating the need for a reference electrode or grounding pad. The system measures the tissue resistance between the 2 electrodes in use at any time, switching between electrodes as the resistance (impedance) increases. A microprocessor divides the RF output between the individual electrode pairs according to changes in tissue resistance. The energy applied, power output, and the ablation time are monitored throughout. As the tissue dehydrates during ablation, the resistance increases. All possible electrode pairs are activated automatically one after the other in a short period of time. The current is therefore able to pass between one electrode of one applicator shaft and an electrode of another applicator shaft independently. The combination of ablations allowed is therefore only limited by the number is electrodes in the tissue (Lee et al, 2007a, Lee et al, 2007b). Once the resistance of an electrode pair increases beyond a specific limit (900 ohms) or when the power output decreases to less than one-third of the preset power output (inadequate power), the electrode pair is excluded from further ablation cycles. Power output is stopped automatically if the resistance of all possible electrode pairs exceeds the limit three times, indicating that maximum energy deposition has extended along all the electrodes and that the coagulation process has ended (Frericks et al, 2005). Lee et al (Lee et al, 2007a, Lee et al, 2007b) demonstrated no significant difference in ablation zone size when compared to monopolar RFA using multi-tine needles; however the complexity of the procedure is increased significantly, depending on the number of electrodes used.
Brace et al (Brace et al, 2009) compared sequential RFA in a cluster electrode setup with the switching technique in order to determine the ablation zone size in *ex vivo* bovine and *in vivo* swine models. Using either sequential or switched application of three cooled electrodes in a 2-cm triangular array in *ex vivo* bovine liver and *in vivo* swine liver models, RF ablation was performed. The protocol for the sequential ablations, involved 12 minutes of RF energy to each electrode with a 5-minute interval between activations. The 5-minute rest period was performed in order to simulate repositioning of the electrodes. Using a multiple-electrode switching system for 12 minutes created the switched ablations. The switched application of RF energy created

larger and more circular zones of ablation than the sequential application of RF energy (25.4cm^2 vs. 18.8 cm^2 cross sectional area for *ex vivo* studies and 17.1cm^2 vs 5.1cm^2 for the *in vivo* studies). The switched application produced higher temperatures and more rapid heating of the tissue; however this method still exposes the patient to unnecessary morbidity in terms of 3 punctures in the liver as opposed to a single puncture.

Multipolar ablation has been shown to increase the ablation zone (Peng et al, 2011), as illustrated above. The use of multiple needles to achieve this however makes this technique unattractive, as the potential morbidity increases due to the number of needles used.

RFA is a minimally invasive technique with a favourable complication profile (Tateishi et al, 2005). The use of multiple needles increases the potential for unnecessary morbidity and thus single needle techniques have been favoured. The single greatest drawback, however, is the difficulty in accurately positioning multiple needles using a percutaneous approach such that a predictable ablation zone can be reliably achieved.

Modification of RF Electrodes:

A key advance in RF technology is RF electrode design. This has improved the size of the ablation zone, without changing the RF generator parameters significantly. Many of the technological developments have become complimentary and part of single electrode design. All the design modifications are aimed at achieving acceptable tissue coagulation and larger ablation zones.

Multi-tine Needles:

Definition:
A single electrode shaft with retractable hooks or tines arranged in a radial manner around the shaft. The hooks are housed in the shaft, and can be advanced forward from the tip of the shaft to release the tines. (LeVeen, 1997).
The number of tines varies depending on design.

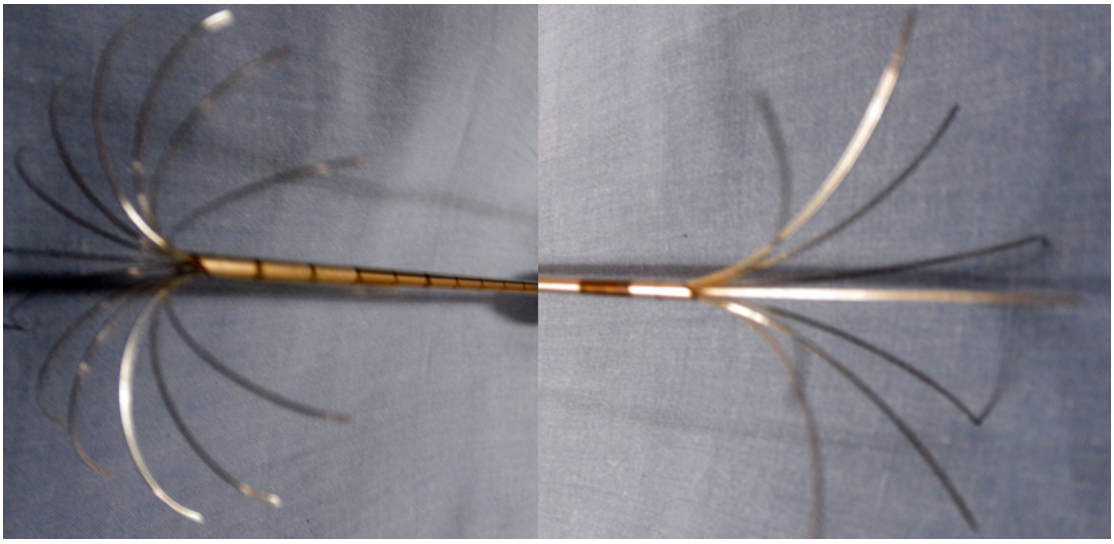

Figure 1.2 LeVeen multi-tine electrode (Boston Scientific, Natick, USA) and the StarBurst (AngioDynamics, Latham, NY, USA).

The volume of necrosis created with RF energy increases with longer tip exposures (Goldberg et al, 1995b). The limitation however is the cylindrical ablation zone created, rather than a spherical ablation zone. A sphere is the most common shape for tumours. A method was

needed to increase the ablation zone size and optimize the geometry.
Rossi et al (Rossi et al, 1996) demonstrated increased ablation zones in tissue by repeatedly inserting RF electrodes into tissue to induce coagulation. This method was cumbersome and not clinically viable given the multiple passes through the organ and the potential for injuring adjacent organs.
Goldberg et al (Goldberg et al, 1995a) studied the use of freestanding electrodes in an array. Experiments using *ex vivo* calf liver were carried out using 3cm arrays for 6 minutes at 70-90 °C. The spacing of the probes, probe configuration and RF application methods were varied. The results of the studies demonstrated that simultaneous RF energy applied to probes placed no more than 1.5cm apart produced larger zones of ablation. At 1.5cm, arrays of 2 probes produced ablation zones of 3cm long axis and 1.5cm short axis. Three probes with similar spacing produced a short axis diameter of 3cm. Four probes placed in a cuboid configuration with similar spacing produced zones of 3.2cm. Probes placed 2cm or more apart produced separate zones of ablation of 1.4cm, with incomplete necrosis between the ablated tissues (Goldberg et al, 1995a). In this configuration residual tumour would be left and recurrence inevitable.
The former probe configurations produced coalescent coagulation volumes of greater than 800% when compared to single probe use. Solbiati et al however highlighted the limitation of this technique, in 1997 (Solbiati et al, 1997b). Accurate placement of 3 or more separate probes into a clinical lesion proved technically challenging, time consuming and therefore not clinically viable. The research however was the precursor to a single probe with multiple hooked arrays or tines.

In 1997 LeVeen described an “umbrella” electrode, which consisted of a single shaft with retractable hooks or tines, arranged in a radial manner around the shaft. The hooks were housed in the shaft, and could be advanced forward from the tip of the shaft to release the tines (LeVeen, 1997). LeVeen applied 50-80W of RF energy for a total of 10-12 minutes to produce spherical lesions measuring up to 3.5cm. LeVeen’s umbrella electrode housed 4 needles, which needed rotating to allow adequate coagulation of all the tissue. This too, proved to be clinically difficult due to the charring of tissue and subsequent adherence to the needle tip.
The charring prevented successful manipulation of the needle without causing a degree of trauma to the tissue. The needle, although not without its shortcomings, is the most popular treatment method for RFA in use today (Cho et al, 2006, Kelekis et al, 2006). Multitine needles are currently manufactured by three commercial companies (Angiodynamics, Queensbury, NY, Boston Scientific, Natick, MA and MIRAS, Invatec, Roncadelle, Italy); the newer modified needle is a 14 to 17G hollow needle with up to 12 tines, thus negating the need for manipulation in tissue. Both needles, although claimed by manufacturers to be superior to one another, produce very similar clinical results (Gulesserian et al, 2006).

A recent advancement in the standard multi-tine technique has been the use of perfusion multi-tine needles. The multi-tine needle marketed by Angiodynamics (StarBurst Xli, Queensbury, NY, USA) utilizes hollow multi-tine needles to infuse small amounts of saline into the tissue from the ends of the needles at a rate of 0.1mL per second. The theory behind the design is to decrease the amount of tissue charring at the needle tips by direct cooling with saline. The direct infusion of saline through the open electrodes was thought to be a novel method of increasing the efficiency of the expandable RFA-needle device by maintaining the tissue impedance at about 80 ohms (Abitabile and Maurer, 2010). This would therefore aid in decreasing the charring at the electrodes, which is encountered with conventional RFA. In this way, higher energy could be delivered to he tissue and thus significantly decrease the treatment time. Each tine is supplied by a separate infusion tube, which supplies each alternate tine on the needle. The tube supplying each tine must be primed before use, a lengthy process that adds time to the procedure. A mechanical pump, attached to the RFA device, controls the infusion. Although there is no randomised control trial comparing this novel technique to any other standard ablation technique, Abitabile and Maurer treated 159 liver tumors (median diameter - 2.0cm) with RFA. 54 tumors were treated according to the manufacturer's standard protocol (Angiodynamics, Queensbury, NY, USA) and 105 tumors according to this novel perfusion technique-using multi-tine perfused open electrodes (Starburst XLi, Angiodynamics, Queensbury, NY) without randomising the patients.

Follow up of the patients was by contrast enhanced computer tomography (CE-CT) at regular intervals post procedure (27 months for standard group vs 23 months for the perfusion group). Data published for the times taken for completion of the procedure (18.9 min in the standard group to 8.0 min in the perfusion group) were significant; however there was no difference in rates of incomplete ablations (Abitabile and Maurer, 2010).

Internally Cooled Electrodes:

Definition:

A conventional RF electrode welded into a dual-lumen 18-gauge insulated cannula.
These chambers communicate at the tip of the electrode, allowing internal cooling of the probe tip with chilled saline (Goldberg et al, 1996b).

Goldberg et al (Goldberg et al, 1996b) described increasing the ablation zone using an internally cooled electrode. The internally cooled electrode is a conventional RF electrode welded into a dual-lumen 18-gauge insulated cannula. These chambers communicate at the tip of the electrode, allowing internal cooling of the probe tip with chilled saline. The saline perfuses the chambers of the insulated needle by means of an external pump, which ensures the saline is continually exchanged, preventing heating of the fluid, which would negate the benefit of tip cooling. This phenomenon causes “heat sink” at the needle tip – whereby some heat is drawn away by the chilled saline within the needle. As a result, heating of the tissues nearest the RF electrode is reduced, allowing greater energy deposition. Greater energy deposition increases tissue heating and coagulation further from the electrode without tissue charring.

Figure 1.3 Cool-Tip ablation electrode (Covidien, Dublin, Ireland) demonstrating tubing (blue and orange) required for perfusion of the needle.

Studies carried out by Goldberg et al (Goldberg et al, 1996b) evaluated the efficacy of needle tip cooling, taking into account the effects of procedure duration (3-60 min), RF output (3-100W; 100-1200mA), electrode tip length (1-4cm) and tip temperatures (15-90 °C). The experiments were performed using *ex vivo* liver and an 18G electrode. The results demonstrated a significant increase in RF energy deposited in tissue. Tip cooling prevented charring with RF energy below 750mA, however with tip temperatures as low was 45-55 °C, charring was still observed above 750mA and RF current was not permitted above 1100mA due to the impedance in the tissue. Decreasing the RF current or treatment duration decreased the ablated tissue volume, as observed with conventional electrode RFA.
Lorentzen (Lorentzen, 1996) applied RF to *ex vivo* calf liver using room temperature perfusate (20 °C). Without using cooling, Lorentzen showed a rapid decrease in temperature from the electrode so that cytotoxic temperatures (>50 °C) were only observed up to 7mm from the needle tip at 420mA. Internal cooling however showed temperatures increasing to 90 °C 5mm from the needle tip using 750mA of RF current and decreased to 50 °C at 16mm. Coagulation diameters were consistently 14mm and 30mm for uncooled and cooled needle experiments respectively. Further experiments by Lorentzen et al demonstrated thermal equilibrium could only be reached in the larger volume of ablated liver after 36 minutes. The findings by Goldberg et al in 1996 were in keeping with the need for longer durations of treatment to achieve the greatest ablation diameters.

Freiser (Frieser et al, 2004) applied current to an electrode continuously perfused with 0.9, 5.85 or 10% NaCl solution. The results showed no correlation between lesion diameter and saline concentration. Perfusion rate rather than content of the solution determined ablation size.
Lee et al demonstrated increased ablation zone size using a perfused internally cooled electrode compared to standard cooled electrodes, with larger ablation zones created using 14.6% NaCl compared to 0.9% NaCl, which highlights the unpredictability of the concentration of saline in determining ablation zone size (Lee et al, 2006).
The lack of predictable correlation between *ex vivo* and *in vivo* ablation zones is well recognised; the addition of perfusion with differing fluid concentrations further compound the lack of predictability and reproducibility. There have been no studies to date demonstrating reproducible and reliable correlation between ablation zones obtained using a perfusate at varying saline concentrations.

Cluster RF.

Definition:

Radiofrequency energy applied to a cluster of three closely placed internally cooled electrodes using a monopolar technique of ablation (de Baere et al, 2001).

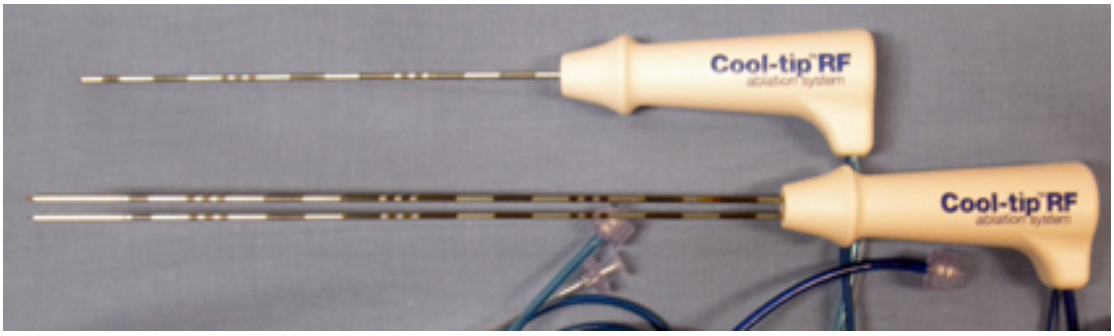

Figure 1.4 Single electrode Cool-Tip needle (top) and a cluster Cool-Tip electrode (bottom)

This technique offers the potential of large volume coagulation necrosis for tumor ablation therapy (de Baere et al, 2001).
Goldberg et al (Goldberg et al, 1998) described using electrodes, placed no more than 1cm apart, in order to create more spherical ablation zones than those seen in ablations using three electrodes placed 2cm or more apart. This may appear contradictory, given the evidence of larger ablation zones with multiple needles; however the theory of having electrodes 1cm apart is that this close proximity creates a single RF field with the 3 electrodes significantly larger than individual probes. Using distances of 2cm or more creates an RF field around each electrode, rather than a confluent RF field (Goldberg and Gazelle, 2001). Goldberg used a pulsed monopolar technique in order to create the confluent ablation zones in this paper, which was responsible, somewhat for the larger individual ablation zones achieved with 2cm spacing. Goldberg (Goldberg et al, 1998) applied this cluster technique to 10 patients with a solitary intra-hepatic metastasis ranging in size from 4.2-7cm. Each was treated for 12-15 min with RF energy ranging from 1600-1950mA. Post ablation imaging revealed coagulation diameters of 5.3cm with a minimum short axis of 4.2cm. The overall shape of the coagulation zone was closer to the shape of the tumor i.e. spherical than to that of a cylinder. The shape of the tumours is an important factor in developing effective ablation protocols for large tumors (Chen et al, 2004). In some cases involving a system of ensuring overlapping ablations using a five-sided prism model (Chen et al, 2004) or computer modeling to enhance the ablation (Liu et al, 2007).

Pulsed RF.

Definition:

High-energy monopolar RF deposition alternated by periods of low energy monopolar RF depending on the impedance of the ablated tissue. If correct parameters and timing are used, periods of low energy RF allow cooling of tissue adjacent to the electrode without decreasing the heat significantly in the deeper tissue (Goldberg et al, 1999).

Current is applied in a continuous fashion at pre-determined parameters until the first time that impedance increases above a predetermined level. The RF is then altered to a pulsed algorithm to allow tissue cooling adjacent to the needle for a period of time, after which a higher current is again applied to a level. The cycle is repeated until the impedance rises above 900 ohms and the RF is switched off. The peak current can be applied in two ways: (1) a constant peak current can be used, where regardless of impedance in tissue, a constant energy is delivered. (2) Variable current strategies, where current is reduced to a minimum for a period after an increase in tissue impedance. Peak current can also be successively reduced if the preceding cycle of high current cannot be maintained for the specified minimum duration (Goldberg et al, 1999).
Goldberg et al (Goldberg et al, 1999) conducted experiments using a high-current, 500-kHz, monopolar RF generator capable of 2,150 mA (150 watts) output. Internally cooled RF electrodes were used, with RF currents ranging from 750-2,150 mA. When the desired current could not be applied without an elevation in impedance, the generator automatically switched to a pulsed-RF technique.
Goldberg then applied this pulsed technique to a cluster of 3 internally cooled electrodes at a peak current of 2000mA, producing ablation zones of 4cm (Goldberg et al, 1999).
Kettenbach et al (Kettenbach et al, 2003) performed saline-enhanced and impedance-controlled radiofrequency ablation cycles on twenty-six patients with fifteen hepatocellular carcinomas and thirty-three hepatic metastases (maximum diameter ≤ 8.6 cm) under general anaesthetic. Results showed increasing ablation volumes with a greater number of radiofrequency applications.

Improving tissue heat conduction:

Saline Infusion.

Definition:

Saline is infused into the tissue via a hollow radiofrequency electrode at a predetermined infusion rate or bolus infusion in order to increase the surface area of the electrode and the conductivity of tissue by creating high ion concentrations at the electrode tip (Goldberg et al, 2001).

Improving tissue heat conduction is an important area of research for improving ablation zones in tissue. As discussed in earlier text, tissue heating, vaporization and charring adjacent to the needle limits conduction of heat through deeper tissues and is the major factor limiting ablation zone diameter.

Improving or maintaining the hydration of tissue is a method of increasing the ablation zone. The conductivity of normal saline is 12 to 15 times higher than that of tissues. In this way the interstitial electrolyte perfusion spreads the applied RF current further into the tissue away from the surface of the electrode, allowing a greater amount of RF energy to be delivered to the tissue without reaching the critical current density and avoiding desiccation and char formation at the electrode–tissue interface (Goldberg et al, 2001, Burdio et al, 2003a, Burdio et al, 2003b). A further possible reason put forward by Goldberg (Goldberg et al, 2001) is that the infusion of fluid during RF application improves the thermal conduction within the tissues by a more efficient rapid and effective method of heat convection over a larger tissue volume. The authors continued to state that the exact mechanisms responsible for the increase in coagulation had not been well characterized.

Livraghi (Livraghi et al, 1997) performed experiments using a 100W, 500kHz monopolar generator during continuous saline infusion. The modified RF electrode was manufactured with three terminal side holes, which were used for saline infusion. The needles were insulated with a 0.1-mm layer of polyvinyl chloride for all but the distal 3 cm. 0.9% sterile saline was infused via a infusion pump at a constant rate of 1 mL/min. Lesion size increased with increasing saline volumes up to a maximum of 10 mL, above which no further increase in lesion size was observed. Maximum lesion diameter measured 1.4 cm in *ex vivo* liver, and 1.2 cm in *in vivo* porcine liver. Without saline pretreatment, lesion diameters were 1.0 cm and 0.8 cm respectively. In his studies, the use of hypertonic saline (5%) did not further increase lesion diameter or length.

Curley and Hamilton (Curley and Hamilton, 1997) infused up to 10 mL/min of normal saline in *ex vivo* liver for 4 minutes during RF application to increase the coagulation diameter from 1.4 to 2.6 cm. Miao et al (Miao et al, 1997) infused 1 mL/min of 5.0% hypertonic NaCl solution in ex vivo liver for 12 minutes during RF application and achieved tissue coagulation of 5.5 cm in diameter.

Ahmed and Lobo (Ahmed et al, 2002, Lobo et al, 2004) have performed saline pretreatment. Before the application of RF energy, 6 mL of NaCl at varying concentrations (18%, 24%, or 36%) was injected into the liver parenchyma surrounding the electrode using a 25-gauge needle. The control tumors (without NaCl injection) measured 3.1 cm, surrounded by viable, well-perfused tumour. 36% NaCl alone produced 2.7cm of patchy necrosis. These findings are in contrast to the observations made by Livraghi et al (Livraghi et al, 1997), where no difference was observed when using 5% as opposed to 0.9% saline. This observation was described by Aube in 2007 (Aube et al, 2007), where continuous infusions of saline concentrations between 0.9% and 25% did not produce any significant differences in ablation zone sizes.

Lobo et al (Lobo et al, 2004) demonstrated NaCl volume and concentration had significant effects on RF-generated heating of agar phantoms. Volumes ranging from 1 - 38mL and nine concentrations ranging from 0 - 35% were used. The effect of altered electrical conductivity was studied by varying the NaCl volume and the NaCl concentration. The mean maximum temperature (91.4 °C), was reached with 3.5 mL of 10% NaCl. This was significantly higher than the mean temperature reached in phantoms containing 0% NaCl (40.3 °C). Heat increases to the maximum temperature correlated strongly with the deposited RF energy, which correlates in theory to a larger ablation zone.

Boehm et al (Boehm et al, 2002) compared ablation zone sizes in an aggressive rat tumour model using internally cooled electrodes. 13 tumors in seven animals were treated with saline enhancement (0.5 mL/min). No statistical difference in efficacy was detected.

Although saline infusion has been shown to increase the ablation zone, the size of the ablation zone is potentially unpredictable at low volume injections and becomes technically challenging in terms of adequate volume injection at higher volumes (Goldberg et al, 2001). Ahmed et al (Ahmed et al, 2002) demonstrated a larger ablation zone using saline infusion; however these tumors were superficial, and artificially induced tumors in subcutaneous tissue. The results of the research conducted by Goldberg et al (Goldberg et al, 2001) demonstrated the unpredictability and sometimes non-viable clinical application of saline infusion.

Lee et al (Lee et al, 2004a) combined acetic acid and hypertonic saline with similar outcome measures to Goldberg's paper in 2001; however the acetic acid-hypertonic saline combination caused significant peritonitis at high concentrations as the solution leaked around the needle and into the peritoneal cavity owing to increased tissue turgor.

Adjuvant techniques for increased Tumour Ablation:

Intratumoral Chemotherapy:

Definition:

The combined application of chemotherapy before or after radiofrequency ablation, in order to increase the tumoricidal effects of both modalities (Goldberg et al, 2001).

Recent advances in delivery of chemotherapeutic agents include the development of liposomal carriers for compounds such as doxorubicin. Liposome particles are completely biocompatible, cause very little toxic or antigenic reaction and are biologically inert. Water-soluble drugs can be trapped in the inner aqueous compartment, whereas lipophilic compounds may be incorporated into the liposomal lipid membrane. Incorporation into liposomes protects the drug from the destructive environment in-vivo. Goldberg et al (Goldberg et al, 2001) postulated that combining thermal ablation with tumoricidal therapies such as chemotherapy might be beneficial in increasing the amount of tumor destruction and in reducing the local rate of tumor recurrence.

Rats were impregnated with tumour and then treated with either
(*a*) conventional monopolar radiofrequency ablation alone:
(*b*) direct intratumoral doxorubicin injection;
(*c*) combined therapy (doxorubicin injection immediately followed by radiofrequency ablation;
(*d*) Radiofrequency ablation and injection of 250 mL of distilled water;
(*e*) no treatment.
No statistical difference in coagulation zone size was found between tumours treated with RF alone and RF with water. Larger ablation zones were produced when RF was combined with doxorubicin. The coagulation zone size was found to be dependant on concentration and timing of doxorubicin administration. The largest coagulation zones observed were with doxorubicin administered within 30 minutes of RF ablation. Goldberg observed histological changes in cells adjacent to the ablated tissue from 0-48 hrs after ablation had occurred. Cell death continued after ablation had ceased, where this phenomenon had not been seen and was not known to occur with radiofrequency ablation alone (Goldberg et al, 2001). In comparison with the pathologic findings with RF ablation alone, conclusive histopathologic coagulative necrosis was observed in a zone adjacent to the coagulated tissue, termed the expanded treatment zone. This difference in morphologic appearance, coupled with the increased time to observe changes compatible with cell death after therapy, suggested the thermal damage from combined RF

ablation and chemotherapy produces cytotoxic effects through mechanisms that are different from the mechanisms of the thermal damage from RF ablation alone.
Kruskal (Kruskal et al, 2001) concurred with this hypothesis, when he, in the same year conducted experiments on live mice livers. Kruskal described five discreet zones following RF ablation extending outwards from the electrode surface:
(1) tissue coagulation,
(2) cellular edema/necrosis
(3) sinusoidal stasis
(4) parenchymal shunting
(5) normal liver tissue.

The zone of sinusoidal stasis occurred at temperatures between 40 and 50 °C, corresponding to the hyperemic zone on histologic analysis described in living ablated tissue (Goldberg et al, 2005a, Goldberg et al, 2005b).
Alterations in permeability and phagocytic activity were first identified at 43°C, where tip temperatures higher than 55 °C always produce local endothelial leakiness to carbon microparticles and inhibit phagocytic activity. It is this hyperaemic zone, which occurs at temperatures between 43 and 50 °C that the potential for adjuvant therapies lies. The sinusoidal stasis and increased endothelial permeability were thought to be potential routes for targeted adjuvant cytotoxic therapy such as chemotherapy to increase cell death and decrease recurrence at the periphery of the ablated tissue.
Monsky (Monsky et al, 2002) supported the hypothesis of the sinusoidal stasis and increased endothelial permeability being a route of entry for chemotherapeutic drugs. Monsky et al conducted experiments using an adenocarcinoma breast model in rats. Intravenous liposomal doxorubicin or intravenous free unencapsulated doxorubicin was administered immediately following RF ablation. The results showed mean intratumoral doxorubicin concentration was 5.6g/g and 1.0 g/g in tumours treated with and without RF ablation respectively. A mean 7.1-fold increase in intratumoral doxorubicin accumulation thus followed RF ablation compared with the amount without RF pretreatment (Monsky et al, 2002).
This accumulation of liposomal doxorubicin was found in a peripheral rim of tumor adjacent to the zone of coagulation, zone 3 as described by Kruskal (Kruskal et al, 2001). Ahmed et al (Ahmed et al, 2003a) proved the same concept of increased intratumoral doxorubicin concentrations with pretreatment RF (Ahmed and Goldberg, 2004).
Goldberg (Goldberg et al, 2002) demonstrated similar findings in clinical trials. Focal hepatic tumors were treated with internally cooled radiofrequency ablation. In addition to undergoing radiofrequency ablation, half of the patients received IV doxorubicin in a long-circulating

stealth liposome carrier 24 hr before ablation. Contrast-enhanced helical CT was performed immediately after radiofrequency ablation and 2–4 weeks after ablation.
For tumors treated with radiofrequency alone, the volume of the lesion had decreased by up to 24% of the initial volume at 2–4 weeks after ablation. By comparison, increased tumor destruction at 2–4 weeks after ablation was seen in the combination group. Goldberg et al attributed the peripheral distribution of increased treatment effect to mechanisms such as the reversible damage to cellular machinery such as the multidrug-resistant membrane efflux pump that is responsible for actively excluding doxorubicin from the cells.

Ahmed and D'Ippolito (Ahmed et al, 2003a, D'Ippolito et al, 2003) conducted further studies on the effects of adjuvant chemotherapy. The results showed significantly improved survival for the animals with combined liposomal doxorubicin and RF ablation.
This evidence suggests that there are several mechanisms by which combination therapy could potentially increase tumor destruction. Latterly there has been much debate as to how to best administer the combination of RF ablation and transarterial chemoembolisation (TACE) (Salman et al, 2002, Maluccio et al, 2006, Ruutiainen et al, 2007). TACE involves the selective catheterization of arteries supplying the tumour followed by the intra-arterial administration of cytotoxics. One school of thought advocates the administration of chemoembolisation first to minimize blood flow before RF ablation and to create higher drug concentrations present at the time of heating. A further alternative hypothesis is the ablation of as much tumour as possible, followed by concentrated deposition of chemoembolic material in the peri-ablational zone.
A third school questions the relative benefit of chemotherapy at all. Mallucio suggests that bland embolisation alone is sufficient to increase ablation efficacy (Maluccio et al, 2006).
The importance and synergy of the chemotherapeutic regimen is well known, however the reason for chemoembolisation followed by RF ablation being more effective is not. The reduction of tumor blood flow following chemoembolisation, combined with the effect of hyperthermia and local chemotherapy was thought to be the reason (Mostafa et al, 2008), however sensitizing the tumor cells with chemotherapy prior to ablation was another hypothesis put forward.

Takaki et al (Takaki et al, 2007) published results of combined chemoembolisation and radiofrequency ablation for treatment of HCC. The results suggested RF ablation combined with chemoembolisation increased the initial therapeutic response and reduced local tumor progression in HCC lesions as large as 5 cm in maximum diameter compared with RF ablation alone. The initial therapeutic response to RF ablation alone decreased as tumor size increased. A recent randomized control trial by Cheng et al (Cheng et al, 2008) treating HCCs larger than 3cm showed TACE and RFA in combination to be superior to TACE alone or RFA alone with reference to the response rates at 6 months and the overall survival.

The size of the particles for chemotherapeutic delivery has also been evaluated in determining the effect of TACE and RFA (Ahmed et al, 2005b). The results from this study demonstrated that not only the nanoparticle size but also the circulation time of the chemotherapeutic agent and chemotherapeutic agent itself could influence the intratumoral drug accumulation and consequently the size of tissue coagulation.

The unpredictability of direct injection of any cytotoxic agent leaves the patient at high risk of potential catastrophic complications (Seki et al, 1998) as demonstrated recently (Chiu et al, 2009). Although extremely rare, massive hepatic infarction described by Chiu et al illustrates a significant morbidity risk for an otherwise relatively safe, minimally invasive procedure.

Bimodal Electric Tissue Ablation.

History.

Bimodal Electric Tissue Ablation (BETA) was first performed by Dr John Cockburn, a consultant radiologist at the Norfolk and Norwich University Hospital in a home laboratory in Norfolk, United Kingdom in 2005. The idea to add cathodic direct current (DC) to alternating current (AC) ablation occurred to him following a discussion with his father regarding DC electrolysis. On studying papers on DC ablation by Norderstrom (Nordenstrom, 1983) and Berendson (Berendson and Simonsson, 1994, Berendson and Olsson, 1998), in which the authors describe pale swelling of the cathodic tissue, Dr Cockburn theorised that the increased volume of tissue was a consequence of increased hydration. This theory was furthermore strengthened by authors describing desiccation of tissue at the anode during DC ablation (Samuelsson and Jonsson, 1980). Dr Cockburn believed opposite hydration effects were occurring at the cathode. Accordingly, as standard radiofrequency ablation (RFA) causes desiccation of tissue it would be reasonable to test the hypothesis that adding cathodic DC to the ablation needle circuit would cause a larger ablation zone to be formed.

In home experiments conducted in January 2005, a commercially available AC-DC transformer (240V AC – variable voltages from 1.5V-12V, Maplin's Electronics, United Kingdom) was used to construct a circuit whereby a commercially available RFA device (RF3000, Boston Scientific, Natick, MA, USA) was connected in parallel to a DC circuit. A grounding pad from a diathermy machine was used to line a plastic dish and a tissue sample of lamb liver was ablated.

The needle electrode was a truncated multitine needle (Angiodynamics, Queensbury, NY, USA) with the tines removed. Electrical connections were made using crocodile clips. The RF3000 was set to deliver 20W and each ablation was allowed to proceed until roll-off. In an attempt to prevent alternating current from destroying the DC circuit, a 1mH inductor was inserted.

Multiple further experiments were performed over a period of months in the laboratory in Coltishall, Norfolk, UK. During these experiments it was found that larger ablation zones were created when 9V of cathodic DC was delivered to the tissue. Furthermore, pre-treating the tissue with cathodic DC for a period of minutes prior to starting the RF current appeared to create even larger ablation zones.

The early findings by Dr Cockburn were discussed with Mr. Simon Wemyss-Holden, a consultant hepatobiliary surgeon, who had experience of DC ablation and animal experiments (Wemyss-Holden et al, 2000a, Wemyss-Holden et al, 2000b, Wemyss-Holden et al, 2002, Wemyss-Holden et al, 2003).

It was decided that BETA should be subjected to scientific rigour in a series of animal experiments. Professor Guy Maddern was approached and an agreement was reached regarding the use the University of Adelaide animal research facility at the Queen Elizabeth Hospital in South Australia. Part funding for this work was gained from an Education Award awarded to Dr Cockburn and Mr. Wemyss-Holden by the Royal College of Radiologists in the United Kingdom. Dr Cockburn funded the remainder of the research personally (Cockburn et al, 2007).
There was still a need for a machine independent of feedback algorithms and Dr Cockburn approached the Department of Engineering at Cambridge University for assistance. Mr. Davor Dukic constructed an ablation machine according to Dr Cockburn's specifications – broadly based on the RF3000 ablation device.
The output of the device, termed Mark I, was insufficient to ablate tissue and Dr Cockburn and Mr. Wemyss-Holden travelled to Australia with an RF3000 and the parallel DC circuitry to perform the *in vivo* experiments in October 2006.
Over a 2-week period, 144 ablations were performed in 12 Large White X Duroc pigs in compliance with the Animal Research and Ethics Committee at the University of Adelaide. The data was analysed by an independent statistics company affiliated to the University of Adelaide. Using an ANOVA test, they demonstrated that BETA produced larger ablation zones compared to standard RFA ($p<0.0001$) (Cockburn et al, 2007). Further experiments were conducted at the animal research facility in Adelaide using the RF3000 machine under the indirect supervision of Dr Cockburn and Mr. Wemyss-Holden, who formulated the design and co-authored, reviewed and revised the peer reviewed publications (Dobbins et al, 2008, Dobbins et al, 2008a, Dobbins et al, 2008b). In 2006/7 Health Enterprise East (now NHS Innovations East) were approached in a bid to fund further experiments. BETA won the Health Enterprise East Innovation award in 2007 and went on to claim first prize in the medical devices category of the National NHS Innovation Awards in 2007.
In September 2007, Dr Cockburn accepted a personal invitation from Professor S Nahum Goldberg to evaluate BETA in his ablation research facility at Harvard University (Boston, MA, USA). These experiments (unpublished data) showed BETA did not augment the effect of internally cooled electrodes. The effect of cooling an electrode has been discussed earlier in this chapter. The experiments did highlight the need for a fixed mA machine with which to test BETA as opposed to adding DC to a commercially available RFA device with built-in impedance feedback algorithms as had been the case with all BETA research until then.
In 2008 a fixed mA BETA machine, labeled Mark II was manufactured by EG Technology in Cambridge, United Kingdom. This machine is the mainstay of all the experiments described throughout this thesis and will be described in detail in Chapter 2 of this thesis.

Figure 1.5 Clockwise from top left, laboratory set-up, BETA Mark II machine, DC supply, and digital/analog convertor.

BETA proved that larger ablation zones could be achieved using a simple method of increasing the ablation zone.

BETA does not require the complex circuitry described in bipolar and multi-polar ablation devices earlier in this chapter. The lack of any adjunct measure in an attempt to increase the ablation zone such as saline or alcohol injection, or chemotherapy provided BETA with a unique technological advantage in the field of thermal ablation. BETA utilises a Monopolar RFA circuit with the addition of a parallel DC circuit. The initial results obtained in the early *ex vivo* experiments and the animal research demonstrated the technique to be robust.

Not altering the RFA circuit, but merely adding a simple parallel circuit avoided the limitations of each of the techniques described previously in the chapter.

Importantly, as highlighted, a machine without impedance feedback and a fixed mA delivery was needed in order to test the variability and robustness of BETA and to prove the early theories of Dr Cockburn regarding the increased hydration.

This required a well constructed *ex vivo* experimental design and a complimentary *in vivo* animal study.
This thesis describes in detail the methods and results of the experimental design.
In each chapter, the background is discussed in detail, together with the results of each experiment conducted. Each chapter is outlined by a specific aim, which demonstrates the attributes of this new technology. In the later chapters, the biochemical effects and safety of BETA are demonstrated and discussed in detail.

Before this research is described, it is important to understand and be familiar with competing technologies and their risk/benefit profile, in order to appreciate each study design and the rationale behind the study design.
The following are competing technologies in the field of ablation. These encompass thermal ablation (heat and cold), chemical ablation and irreversible electroporation.

Microwave Ablation:

Definition:

The application of microwave radiation in the region of the electromagnetic spectrum using electromagnetic frequencies from 900 to 2450 MHz in order to produce thermal coagulation in tissue (Hamazoe et al, 1995).

The microwave tissue coagulator was developed in 1979 by Tabuse to aid in the transection of hepatic parenchyma during liver resection. It proved to be an excellent device for aiding in hemostasis. Microwave ablation, a recent development in the field of tumour ablation was described in 1995 by Hamazoe (Hamazoe et al, 1995) for the treatment of inoperable Hepatocellular Carcinoma (HCC).
Microwave radiation refers to the region of the electromagnetic spectrum with frequencies from 900 to 2450 MHz (Carrafiello et al, 2008, Hope et al, 2009, Sun et al, 2009, Lubner et al, 2010). This type of radiation lies between infrared radiation and radio waves. Water molecules (H_20) are polar and asymmetric. Electromagnetic radiation has electric charge, which flips between positive and negative. Microwave radiation oscillating at 9.2×10^8 Hz (920MHz), causes the charge to change signs nearly 2 billion times a second. With higher frequency microwave devices (2.5GHz), this is increased to almost 6 billion times a second, thus in theory more energy is deposited in the surrounding tissue. Microwave ablation (MWA) offers many of the benefits of RF ablation and has several other potential advantages that may increase its effectiveness in the treatment of tumours (Brace et al, 2005, Brace et al, 2007a, Brace et al, 2007b). The potential benefits of microwave technology include consistently higher intratumoral temperatures and faster ablation times. Compared with conventional monopolar radiofrequency ablation using a single needle, microwave ablation is thought to produce larger ablation zones (Hines-Peralta et al, 2006, Yu et al, 2010). *In vivo* animal and clinical studies however have not substantiated this. Xu and Wright both showed no significant difference in ablation zone size when comparing microwave and RF ablation therapies (Xu et al, 2004, Wright et al, 2005). Microwave therapy is thought to have the added flexibility of using multiple applicators and is able to heat cystic masses optimally. Microwave ablation does not use current for energy deposition as does RF energy and therefore does not require the placement of grounding pads. Recent studies have shown MWA to have a similar safety profile to RFA (Liang et al, 2009). Recently published data by Liang et al described a 3.6% complication rate in 1136 patients. Complications ranged from liver abscess and empyema, to pleural effusions requiring chest drain insertion.

The inflammatory profile of microwave has been demonstrated to be superior to RFA (Ahmad et al, 2010), however the study did not highlight a number of significant variables, including length of anaesthetic.

A further potential benefit of MW ablation was thought to be less influence by the "heat-sink" effect of adjacent blood vessels due to the mechanism of energy delivery. Although a theoretical benefit, this does not seem to have translated into larger ablation zones in practice (Wright et al, 2005). Historically, the majority of microwave devices available were not designed for percutaneous use. The microwave antennae are too large to be placed safely into the tumour, necessitating an open approach. Until recently, this has been a major limiting factor in microwave ablation. Seki et al (Seki et al, 1999) described results using microwave ablation with a custom designed antenna in 15 patients. Although the follow up was short (<37 months) and the tumour size small (< 3cm) the study did show microwave ablation to be a viable option for percutaneous treatment, however the results were no better than using RF energy. Brace et al described lesion diameters of 3.8cm using a 17G antenna (Brace et al, 2005), however due to the extremely high temperatures produced in the microwave cord delivery system, the needle requires continuous cooling via a pump in order to reduce the temperatures to an acceptable level (Brace et al, 2009). This extreme and potentially hazardous heating of the microwave antennae cord poses significant risks of additional morbidity to the patient or theatre staff due to inadvertent skin burns resulting from touching the cord, or the cord resting against the patient during the procedure (Liang et al, 2009).

Shibata et al (Shibata et al, 2000) described survival rates of patients after open microwave ablation, which were not significantly better than RF survival rates, but the patients were subjected to significantly more invasive procedures (all required laparotomy for surgical access to the liver). Xu et al (Xu et al, 2004) conducted a retrospective data analysis of 97 patients with HCC treated over 4 years with percutaneous RF or microwave ablation, with no significant difference in results. Similar findings were published by Wright et al (Wright et al, 2005) a year later showing no significant difference in ablation zone size when compared with RF ablation in hepatic porcine models. Hines-Peralta et al (Hines-Peralta et al, 2006) conducted *ex vivo* and *in vivo* experiments using a 2.4GHz microwave machine and a surgical applicator, producing large ablation zones. For *ex vivo* liver, maximum short-axis coagulation diameter achieved was 7.6 cm (150W, 20 minutes). The *in vivo* studies produced short axis coagulation diameters of 5.7cm (100W, 8 minutes). The unusual finding in this study was the significantly larger ablation zone *in vivo* than the corresponding result for *ex vivo* liver following microwave ablation (150W of power for 8 mins). This has not been described before in the literature and the reason for the findings are unclear. Hines-Peralta et al (Hines-Peralta et al, 2006) attributed these findings in part to the lack of influence of the heat sink effect of perfused tissue to ablation zone size. Electrochemical composition of the tissue was thought to be another contributing factor.

Although promising, the study used a microwave antenna produced by the manufacturer (Microsulis, Denmeade Hampshire, England) which is not for percutaneous use and thus limits the potential use and impact of the results. The lack of the heat sink effect seen in microwave ablation was postulated as the reason for complete histological destruction of tumour cells seen with microwave ablation, compared to RF and cryoablation (Bhardwaj et al, 2009); this has never been proved conclusively.

Sun et al (Sun et al, 2009) compared ablation zones of two cooled shaft microwave antennae (KY2000-915 and KY2000-2,450, Kangyou Medical, Beijing, China). The machines operated at 915 MHz and 2,45 GHz respectively. Studies were carried out in *in vivo* porcine livers. The results of the study showed larger ablation zones at all power levels (40W, 60W and 80W) for short axis diameter measurements. The results are the first showing a 915 MHz cooled-shaft microwave antenna increasing the ablation zone when compared to the 2,4 GHz antennae. These promising results may be due to the following reasons according to the authors. (1) The wavelength of 915 MHz microwaves is longer than that of 2,450 MHz microwaves. This leads to deeper penetration into the tumour and tissues. (2) The energy attenuation of 915 MHz microwaves is less than that of 2,450 MHz microwaves; this means that more electromagnetic energy can be converted to heat energy. This translates into larger and deeper heat deposition and larger ablation zones (Gao et al, 2010). Shaft cooling allows a higher power output (100 W) to be used for tumor ablation without shaft overheating. More microwave energy can thus be delivered into tumor tissue. Despite the promising results by the authors, the largest ablation zone created with 80W of energy was 3.8cm. Kuang et al (Kuang et al, 2007) showed larger ablation zones using a cooled shaft antenna with a 2,4 GHz microwave machine, again no larger than 3.8cm.

Five studies (Marlow et al, 2006) and one randomised control trial (Shibata et al, 2002) have compared microwave ablation and RFA.

RFA tumours had a more complete ablation at follow-up (96%) compared to the tumours treated with microwave ablation (89%). These results can in part be attributed to a larger area of ablation achieved with RFA than with MCT. The lower rate of complete ablation in microwave tumours has led to a higher rate of recurrence in comparison to those treated by RFA.

The first clinical trial using microwave ablation in the North America was conducted by Iannitti et al (Iannitti et al, 2007). In this particular study single and clustered antennae ablation volumes were measured in terms of size. The clustered ablation volumes were significantly larger than the volumes of the single antennae, a finding that has been noted in RFA studies. Recently, a study (Hompes et al, 2010) comparing microwave and RF ablation with matched hepatic tumours concluded microwave ablation to produce highly variable and suboptimal ablation zones, again raising doubt as to the effectiveness of this thermal ablation technology.

Laser Ablation

Definition:

The induction of tissue damage by heat photocoagulation. An infrared light wavelength of between 800 and 1100 nm is applied to tissue by means of an optical fibre (Amin et al, 1993).

Since laser photocoagulation for tumor destruction was introduced in 1983, a Neodyium Yttrium-Aluminum-Garnet (Nd-YAG) laser has been successfully employed to treat a wide range of liver malignancies by using two procedures: (1) laser-induced thermotherapy, which uses a single cannulation needle and (2) laser ablation (LA), where laser light is delivered to the tumour with multiple bare-tip 300-nm fibers inserted into thin needles.
Nd-YAG (wavelength of 1,064 nm) and diode (wavelength of 800–980 nm) lasers are most commonly used. Laser light delivered into tissue is absorbed by tissue-specific chromophores and photon energy is transferred into heat to produce thermal injury (Amin et al, 1993, van Hillegersberg, 1997). Tumours are thus destroyed by direct heating, using low-power laser light energy, with the tip of the laser fibres placed directly into the tumour, termed contact mode laser therapy (Izzo, 2003). Laser ablation has been shown to be effective in treating HCCs smaller than 4cm (Vogel et al, 1998, Pacella et al, 2008, Pompili et al, 2010). The technique, like all the thermal ablation therapies has a relatively low complication rate (Amin et al, 1993, Vogl et al, 1995, Vogl et al, 2004, Vogl et al, 2008). Amin et al (Amin et al, 1993a) compared laser ablation to ethanol ablation. Laser-induced necrosis greater than 50% of the tumour volume was achieved in 87% of tumours and complete necrosis was found in 52% of tumours. None of the tumours, however showed complete ablation and almost 50% showed no change following laser ablation.
A further study of laser ablation for liver metastases by Amin in the same year (Amin et al, 1993b) demonstrated similar findings. Tumour necrosis of greater than 50% was seen in 82% of the tumours. 100% necrosis was achieved in 38%. Metastases smaller than 4cm in diameter were treated more effectively and required fewer treatments than tumours larger than 4 cm.
Lees and Gillams 1999 compared RFA using a single or triple cluster electrode to laser ablation. 125 nodules were treated with RFA and 49 with laser ablation. The RFA treatment times were shorter (60 mins) than the laser ablation times (90 mins). RFA achieved 92% complete ablation using the single electrode. Catalano (Catalano et al, 2001) demonstrated an increase in diameter of 68% in nodules treated with laser ablation, compared to 58% for RFA (Marlow et al, 2006).
A major limitation of laser ablation has been the incomplete ablation rate of tumours. Dick et al (Dick et al, 2003) quoted an ablation rate of 50% of tumour volume.

Arienti (Arienti et al, 2008) published a multi-centre analysis on the rate and type of complication associated with laser ablation. Major complications were associated with using higher energies and the application of the technique in high-risk locations. The study recommended using laser ablation for small HCCs rather than larger tumours.
Rosenberg (Rosenberg et al, 2009) treated sixty-four patients with metastasis to the lung. The average tumor size was 2.0 cm and fewer than less than half of the patients (31 of 64) were treated completely.
Pompili et al (Pompili et al, 2010) performed laser ablation on 9 patients awaiting liver transplantation for HCC. A 25% recurrence rate occurred during the waiting time to liver transplantation. Complete necrosis was only found in 66% of the lesions, with partial necrosis (50-99%) in 25% and partial necrosis (1-49%) in a single nodule.
Puls et al (Puls et al, 2009) treated 180 liver metastases with laser ablation and achieved an effectiveness rate 85.6% demonstrated on MRI 24–48 hours after treatment. The local tumour progression rate was 10% after 6 months. The vast majority of patients had tumour volumes of less than $5cm^3$, which again reinforced laser ablation for small hepatic lesions.
The possible limitation of ablation zone size demonstrated using laser ablation has encouraged researchers to experiment with combination therapies (TACE) as has been done in the development of RFA. Maataoui combined Mitomycin embolisation with laser ablation in rat model and demonstrated reduced tumour growth using this combined therapy opposed to laser ablation or TACE alone (Maataoui et al, 2005). This has not translated into larger animal trials or clinical trials, which may be due to the inherent limited clinical application of laser ablation for treating liver tumours.

Cryoablation:

Definition:

The freezing of tissue to temperatures of -160 to -180 °C to achieve cell necrosis by means of a cryoprobe (Ravikumar et al, 1987) .

Cryoablation or cryosurgery uses the same principles as thermal ablation to cause cell destruction and necrosis by means of freezing.
Temperatures of -160 to -180 °C are achieved by means of liquid nitrogen or argon gas circulating through a cryoprobe at temperatures of -200 °C or lower (Ravikumar et al, 1987, Korpan, 2008). The freezing process lasts for about 8 minutes. A pioneering paper (Ravikumar et al, 1987) in 1987 described the use of cryoablation with or without resection. 50% of the patients treated had residual disease, however the use of cryoablation increased following this early clinical paper.
In 1991 Ravikumar et al published a retrospective 5-year study of cryosurgery in liver tumour treatment. 32 patients were treated predominantly for colorectal metastases. A median follow-up of 24 months revealed a 28% cure, with 34% of patients having recurrence of the disease. The study did however highlight only a 9% recurrence rate at the treatment site. The remaining patients with recurrence had either active recurrence in another site in the liver or distant metastases.
Onik et al (Onik et al, 1991) described a 22% technical failure rate, and a 78% overall recurrence rate (including the technical failures), however a mean survival of 21 months for those with recurrence.
Adam et al (Adam et al, 1997) reported no recurrences for hepatocellular carcinoma at a mean follow-up of 16 months and a 44% local recurrence rate for metastatic disease; survivals were 63% and 52% respectively.
In the group of patients with metastases, survival was related to the tumour size and absence of residual disease.
In 1997 Korpan published a retrospective study of 137 patients over a ten year period undergoing a variety of cryosurgical procedures for liver metastases (Korpan, 1997) with no documented significant morbidity; a promising paper for the use of cryosurgery for liver tumours, however a significant potential complication was described by Weaver et al in 1995.
Seifert and Morris (Seifert and Morris, 1999b) published a world survey on the complications of cryoablation, which described an infrequent, but potentially fatal complication of cryoablation, termed the “Cryoshock Phenomenon”. The cryoshock phenomenon is a syndrome of multiorgan

failure, severe coagulopathy and disseminated intravascular coagulation (DIC), similar to septic shock but without systemic sepsis. This potentially fatal complication was described by Weaver et al in 1995 (Weaver et al, 1995) and referred to as the cryoshock phenomenon by Morris et al in 1996 (Morris et al, 1996). The cryoshock phenomenon was responsible for two patient deaths that had large central lesions treated with cryoablation (Weaver et al 1995). Cryoshock causes severe DIC necessitating repeated infusions of fresh-frozen plasma, cryoprecipitate, platelets, and tranexamic acid in order to restore the normal clotting cascade. The survey on complications of cryosurgery evaluated both prostate and hepatic treatments. The survey demonstrated that cryoshock is responsible for almost 20 percent of mortalities reported with cryotherapy. The incidence of the cryoshock phenomenon however is extremely low (1%). In the survey, 6 of 21 liver patients with reported cryoshock died. It is thought the occurrence of cryoshock is related to the volume of freezing and to the number of freeze–thaw cycles (Seifert and Morris, 1999, Seifert et al, 1999). It was recommended cryotherapy be used in smaller tumours to avoid this uncommon but potentially fatal complication. This recommendation was supported by the relatively low complication rate of prostatic cryotherapy. The difference in the incidence of cryoshock between hepatic and prostate cryotherapy was thought to be related to the volume of tissue frozen and possibly the differences in tissue response to cryoablation. The liver is prone to release cytokines after insult, with the release of TNF-α and IL-6 within the liver parenchyma stimulating the clotting cascade and a severe inflammatory response. The low volume of ablated tissue is a significant factor in decreasing the complications associated with cryoablation; however cryoablation is still responsible for the largest inflammatory reaction compared to RFA and microwave ablation (Ahmad et al, 2010). In a recent study comparing the inflammatory reaction caused by cryoablation to RFA and laser ablation, cryoablation caused significantly higher liver transaminase levels, white blood cell count and cytokine levels compared to RFA or laser ablation, with comparable volumes of destruction of liver parenchyma.

Seifert published a case series of 49 patients treated with cryotherapy for metastatic disease (Seifert et al, 2000). A 57% recurrence rate was quoted. This was preceded by a study by the same author in 1999 (Seifert and Morris, 1999a), where a 33% local recurrence rate at the cryosite was quoted. Seifert attributed the high recurrence rate in cryotherapy to a discrepancy between the ice ball size and the actual tissue volume treated. This high recurrence rate caused great concern in a patient group with a technically successful ablation. The findings contradict descriptions of the ice ball created being easier to see during and after treatment than with RFA (Jansen et al, 2005), the well formed ice ball seen may only represent that area of tissue at tumoricidal temperatures and not the entire treatment zone. Tumoricidal temperatures have been reported to be between –20°C and –50°C and incomplete treatment is followed by rapid local

tumour recurrence. The region of ablated tissue produced by a 3 mm cryoprobe after 20 min of freezing is only about 2.8 cm in diameter, although the ice ball diameter measures 4 cm which may be a reason for incomplete ablation and the high recurrence rate. A recent study evaluating the accuracy of MRI in determining the zone of cryoablation showed contrast enhanced MRI to be an accurate predictor of ablation zone size, compared to the majority of studies to date using ultrasound (van den Bosch et al, 2009).

A further complication is cracking of the ice ball (Seifert and Morris, 1999, Schmit et al, 2010); this may be associated with technique and the number of freeze-thaw cycles. Techniques used in cryotherapy are a major contributory factor to recurrence and complication rates (Martin, 2006). Cracking of the ice ball often occurs when the cryoprobe is removed from the cryosite. The fracture of the ice ball can result in major hemorrhage, rebleeding from the site, bile leaks and recurrence (Seifert and Morris, 1999, Joosten et al, 2005, Martin, 2006).

Overall, significant complications occur in 0–30% of patients undergoing cryotherapy. Besides the potentially fatal cryoshock phenomenon and the ice ball cracking, haemorrhage, subcapsular haematoma, abscess formation and biliary fistula have been reported (Teague et al, 2002, Joosten et al, 2005).

High tumour recurrence rates after hepatic cryotherapy have been described: Yan et al (Yan et al, 2006) reported local recurrence rates of 85%, which, coupled with the possibility of the cryoshock phenomenon and significant complications, makes cryotherapy an unattractive treatment in the liver.

To date, there are no comparative studies evaluating the efficacy of cryoablation and radiofrequency ablation (Marlow et al, 2006). A study by Niu et al (Niu et al, 2007) compared resection to resection and cryotherapy for liver metastases. Only small lesions were treated by cryoablation due to the cryoshock risk associated with large volume tumours. This decision highlighted by the authors demonstrates the limitations of cryotherapy in treating larger tumours and may in part illustrate the fate of cryotherapy in treating small volume tumours in smaller organs.

A study by Permpongkosol et al (Permpongkosol et al, 2007) evaluating ablation zone size and relative temperature of the tissues during cryoablation revealed the kidney to be the tissue with the most sensitivity to freezing when compared to liver and lung.

The study identified a potential use for cryotherapy – small renal tumours. Small renal tumours (<3cm) have an incidence of 10-40% (Dominguez-Escrig et al, 2008). The natural history and biological behaviour of these tumours are not yet well understood, and thus the management remains controversial (Dominguez-Escrig et al, 2008). Surgery remains the choice for young healthy patients; for increasing non-surgical candidates, cryotherapy may have a role (Dominguez-Escrig et al, 2008, Kunkle and Uzzo, 2008); long-term survival studies are awaited.

Chemical Ablation:

Ethanol Ablation:

Definition:

Application of 90-100% Ethanol into tissue, causing chemical necrosis/ablation of tissue (Solbiati et al, 1985).

In the early 1980s, alcohol was described for a number of ablative techniques.
The techniques included treatment of renal cysts, celiac plexus blocks and parathyroid ablative techniques (Solbiati et al, 1985, Livraghi et al, 1986, Livraghi and Vettori, 1990, Lencioni et al, 2010). Based on the findings of these early studies, clinical application of alcohol ablation developed. Ethanol Ablation is used for a number of applications. It can be injected into the renal, bronchial and hepatic arteries to ablate the target tissue, injected into oesophageal varices to cause an intense inflammatory reaction, sclerosing the vessel and injected into large renal and hepatic cysts, ablating the cyst wall (Livraghi et al, 1986). Alcohol has many advantages: it is readily available, simple to use, low in cost, non-viscous and immediately toxic. The toxicity of alcohol is due to dehydration and intracellular coagulation which causes immediate necrosis of the tissue and then a secondary fibrotic reaction, thrombosis, and vascular occlusion.
The indications for use in malignancy are similar to those for any percutaneous ablative procedure described previously. They include: inadequate response to systemic chemotherapy, refusal or unfit patient for surgery and tumours, which can easily be identified on ultrasound or CT (Livraghi et al, 1986). Livraghi et al (Livraghi et al, 1986) conducted an early study using ethanol ablation to treat tumours less than 4cm. The number of treatments needed was directly proportional to tumour size. 3 of the 12 tumours showed no response to treatment, but the remaining 9 lesions responded to treatment, with 50% showing a 100% volume reduction. Livraghi et al (Livraghi and Vettori, 1990) conducted a larger study in 1990, treating 35 patients with HCC. 30 of the 35 patients had complete remission. The remaining 5 patients (14%) all showed residual disease on CT follow-up, and all had lesions larger than 3.5cm. Long-term follow up showed a recurrence rate of 29%.
A limitation however emerged for ethanol ablation early on in its use; multiple treatments are needed for each tumour to attain complete ablation. Although ethanol is cheap and readily available, multiple treatments incur multiple admissions and multiple follow-up appointments, including imaging. In Livraghi's study of 50 HCCs (Livraghi and Vettori, 1990), an average of 10 treatments was needed for the tumours.

More recently, ethanol ablation has been combined with RFA to increase the ablation zone (Goldberg et al, 2000, Sakr et al, 2005). The uneven distribution of all injected therapies throughout the target tissue, both adjunct and chemical, has dramatically limited therapeutic efficacy for larger tumors and metastatic liver cancer (Goldberg et al, 2000).

Brunello et al (Brunello et al, 2008) published a randomized control trial in 2008 comparing ethanol ablation to RFA. The majority of patients underwent a single session of treatment. A complete response at 1yr was seen in 25 ethanol ablation patients (36%) and 46 (65%) RFA patients. The limitations of this study however was the one-shot technique used for ethanol ablation rather than the multiple applications normally needed for treatment. This would have influenced the complete response rate at 1yr and the cost effectiveness of the ethanol ablation given the need for additional admissions for treatments.

The ASERNIP review in 2006 (Marlow et al, 2006) reported on 12 studies, 7 randomised control trials, (Lencioni 1999; Lencioni 2003; Lin 2004; Lin 2005; Olschewski 2001; Shiina 2000; Shiina 2005), 1 quasi-randomised control trial (Livraghi, 1999) and 4 retrospective comparisons (Catalano 2000, Catalano 2001, Luo 2005), and (Nakamura 2004) comparing ethanol ablation with RFA.

Lencioni and Lin reported on tumour response rates for RFA vs ethanol ablation (87% vs 82% respectively). RFA also achieved a lower recurrence rate and fewer new lesions. During the first year of follow-up RFA had a 10% recurrence rate and ethanol ablation 16%, which increased to 14% and 34% respectively at 2 years. At one and two years, the event-free survival was 86% and 64% respectively for each author in the RFA treatment group compared to the ethanol ablation treatment group (77% and 43% respectively for each author).

A more recent meta-analysis of randomised or quasi-randomised control trials comparing RFA to ethanol ablation by Bouza et al (Bouza et al, 2009) showed RFA to be superior to ethanol ablation in terms of survival and local disease control. Six studies were included in the meta-analysis, however the overall complication rates for RFA were higher when compared to ethanol ablation (19% vs. 10%), with major complication rates of 4.1% and 2.7% respectively.

Cho et al (Cho et al, 2009) conducted a systematic review of randomised control trials comparing RFA and ethanol ablation, which too showed RFA to be superior to ethanol ablation for treatment of HCCs, with improved survival of patients at 3 yrs. The most conclusive evidence however was published by the Cochrane Collaboration (Galandi and Antes, 2004) in 2009 where both the overall survival and the event free survival favoured RFA over ethanol ablation.

High-Intensity Focused Ultrasound (HIFU):

Definition:

The application of wideband focused ultrasound to tissue over a short period of time (0.5-1s), producing an acoustic wave, which is absorbed by the tissue and converted to heat (Hynynen and McDannold, 2004).

High-Intensity Focused Ultrasound (HIFU) may in future provide a non-invasive therapeutic option and therefore it would be prudent to discuss this briefly.
HIFU utilises a focused ultrasound transducer array with approximately 200 elements, which generates the ultrasound beam at a frequency between 0.9–1.3MHz, which can be manually adjusted by the operator (Hynynen and McDannold, 2004). The diameter of the transducer can range from 40mm (Luo et al, 2009) to 160mm (Hynynen and McDannold, 2004), depending on the clinical application and the depth from the skin surface to the tumour.
The use of ultrasound in clinical practice has historically been for diagnostic purposes and simple needle guidance for percutaneous biopsies and therapy.
Ultrasound technology now allows the use of focused ultrasound energy for therapeutic purposes such as tissue ablation and hemostasis (Skinner et al, 1998). HIFU is being promoted as a noninvasive method to treat certain primary solid tumors and metastatic disease, to ablate foci of ectopic electrical activity in the heart, and to achieve hemostasis in acute traumatic injuries to the extremities and visceral organs (Dubinsky et al, 2008). HIFU differs to conventional diagnostic ultrasound, not in the frequency of the ultrasound waves, but in the focused wideband ultrasound waves produced. At high intensities, ultrasound can result in tissue heating and necrosis, cell apoptosis, and cell lysis (Haar and Coussios, 2007, Dubinsky et al, 2008).
The focused beam means this effect can be achieved in deep tissues. At high enough acoustic intensities, cavitation results. Microbubbles form which interact with the ultrasound field and grow, eventually imploding, causing a shockwave through the tissue and mechanical damage to immediately adjacent structures.
Unlike radiofrequency ablation, ultrasound is completely noninvasive and can be used to reach tumours that are deep within the body, provided there is an acoustic window to allow the transmission of ultrasound energy. Without this acoustic window, successful HIFU requires rib resection (Jin et al, 2010), converting a non-invasive treatment into one with surgical morbidity risk. Ultrasound has been used to try and increase temperature in tissues since the 1950s; the majority of the work must be credited to Fry et al (Fry 1954) and Lynn et al in the 1940s.

Most of the early attempts failed, however in the 1980s, ultrasound was used to treat renal calculi, a process known as extracorporeal shockwave lithotripsy (ESWL). A rediscovery of HIFU for the treatment of tumors occurred in the 1990s with the refinement of modern technology, in particular, advanced imaging methods such as MR thermometry (Dubinsky et al, 2008). HIFU can produce almost instantaneous cell death by coagulation necrosis to selected regions of tissue has made it a candidate for tumour treatment. HIFU suffers all the limitations of ultrasound; any tissue deep to bones suffers from acoustic shadowing which limits view and thus treatment. Gas in bowel cannot be penetrated by HIFU, just as it cannot be with diagnostic sonography. The sound waves are reflected back to the transducer and are interpreted as acoustic impedance or acoustic noise. With diagnostic sonography, these reflected sound waves are of such low energy that there is no adverse effect from them. The reflected waves in HIFU are of very high energy and can produce burns in the tissues that lie between the transducer and the target. This may in part be overcome by interstitial ultrasound delivery devices (Lafon et al, 2007), which may decrease the risk of such adverse effects of HIFU and also increase some of the therapeutic applications. This technology is in development (Lafon et al, 2007). The use however of HIFU continues to grow and to date both animal and human studies for the treatment of hepatocellular carcinoma (HCC) (Li et al, 2007, Zhang et al, 2009, Jin et al, 2010), renal cell carcinoma, pancreatic cancer, sarcomas, urinary bladder tumours, and prostate carcinoma have been published (Dubinsky et al, 2008). Effective treatment of hepatocellular carcinoma has been demonstrated when trans-arterial chemoembolisation is performed prior to HIFU (Leslie and Kennedy, 2007, Maruyama et al, 2008, Jin et al, 2010). This appears not only to reduce the vascularity of the tumour and in doing so decrease heat loss through perfusion, as in RFA. It also increases the acoustic absorption coefficient, allowing lower acoustic powers to be used (Leslie and Kennedy, 2007). Given its low cost and intrinsic therapeutic and operational safety, HIFU has the potential to become a popular method for both oncological and non-oncological applications. Advances in treatment targeting, real-time treatment monitoring (Kopelman et al, 2006a, Kopelman et al, 2006b) and speed of ablation are needed before this can happen.

Irreversible Electroporation (IRE)

Definition:

The application of short (microsecond to millisecond) high voltage direct current pulses via contact electrodes to cells or tissues, creating aqueous pores in the cellular membrane (permeabilising), leading to cell death (Rubinsky, 2007).

In 1754 Nollet studied the release of a static electrical generator on the skin (Rubinsky, 2007). Fuller published the first article on irreversible electroporation in 1898 (Rubinsky, 2007), in which he reported the bactericidal effects caused by multiple high voltage discharges on a water sample.

IRE is included in non-thermal ablation techniques including electrochemotherapy and supraporation. The true clinical application of IRE was derived from the utilization of reversible electroporation for electrochemotherapy (Dev and Hofmann, 1994); a method in which genes, monoclonal antibodies or drug uptake into eukaryotic cells is significantly increased when electrical pulses (typically a sequence of eight 100 ms pulses of approximately 1000 V/cm) are used to temporarily increase cellular membrane porosity for insertion into cells (Al-Sakere et al, 2007).

Supraporation, another non-thermal method to kill tissue, is achieved by means of nanosecond electrical pulses in the tens of nanoseconds range and 40–80 kV/cm of field strength (Al-Sakere et al, 2007).

Initially, the cell death created by irreversible electroporation during reversible electroporation was considered highly undesirable. However, further investigations on the use of irreversible electroporation as a method of permanent cellular destruction for oncology have led to its clinical application in tumor ablation. The study of Davalos et al (Davalos et al, 2005) showed that IRE could ablate substantial volumes of tissue without inducing a thermal effect. This study provided the initial platform for the use of IRE in surgery.

Edd et al (Edd et al, 2006) demonstrated the application of IRE in liver. In this study, single 20-ms-long square pulse of 1000 V/cm, were applied to rat livers. Following application of IRE, the treated areas in exhibited microvascular occlusion, endothelial cell necrosis, and diapedeses, resulting in ischemic damage to parenchyma and pooling of erythrocytes in the hepatic sinusoids. An important observation made, was the preservation of the large blood vessel architecture immediately adjacent to the area of treatment.

This observation is critical to the application of IRE in liver, given the limitations of RFA immediately adjacent to large vessels due to the heat sink effect. The importance of this

observation is the potential of IRE to treat tissue immediately adjacent to vessels without damaging the vessel and without the risk of an incomplete treatment zone, due to insufficient heating of tissue as found with thermal ablation.

In 2007 Al-Sakere et al reported the use of IRE for tumour treatment *in vivo* using mouse models. The study demonstrated IRE to be effective for tumour treatment. The authors noted results to be affected mainly by electric field strength. Trains of a large number of short pulses resulted in the best antitumor effects (up to 92% of tumor ablation). Histological specimens demonstrated vascular congestion induced by IRE pulses, which should contribute to tissue hypoxia and may thus further contribute to tumor cell death. Twenty-four hours after the application of the pulses, all treated tissue was necrotic. An original observation reported is the detection of diffused Terminal deoxynucleotidyl transferase (TdT)-mediated dUTP Nick End-Labeling (TUNEL) staining first in the cytoplasm around the cell nucleus, and later, around the cells. TUNEL staining detects breaks in DNA strands, associated with cell apoptosis. The evidence of TUNEL staining initially around the nucleus and subsequently in the intercellular space indicates the lack of resealing of the plasma membrane. The damaged DNA spreads out of the nucleus and out of the cell due to the lack of the natural membrane barrier. This observation is the hallmark of irreversible electroporation.

Guo et al (Guo et al, 2010) demonstrated the efficacy of IRE in HCC in a rodent model. Hepatomas were grown in 30 rats divided into treatment and control groups. IRE (8 x 100μs 2,500V) pulses were applied to the treatment group and magnetic resonance imaging scans were performed at baseline and 15-days to determine tumour reaction. Additional groups of treated animals were sacrificed at 1, 3, and 7 days post treatment and the livers assessed histologically. Magnetic resonance images showed significant reductions in tumor size within 15 days following therapy. Pathology correlation studies demonstrated progression from viable HCC tissues before treatment to extensive tumor necrosis and full regression in 9 of 10 treated rats 7 to 15 days after treatment.

Lee et al (Lee et al, 2010) conducted studies on normal porcine liver; utilising ultrasound (US), magnetic resonance (MR) imaging and computed tomography (CT) for follow up with histology for comparison.

The mean diameter of the ablation zones was 33.5mm ± 3.0, achieved in a mean procedural time of 6.9 minutes per ablation.

The current literature describing the effects of IRE on tissue is limited to animal models, however the promising results and lack of complications (Lee et al, 2010), together with the independence of the technique from the bioheat equation and thus the heat sink effects encountered with thermal ablation techniques provides IRE with a significant platform to challenge thermal ablation techniques.

Conclusions:

Radiofrequency ablation is a safe technique with good results when compared to resection as outlined in this chapter.

It does however suffer a number of limitations, which inevitably limit its ability to create large ablation zones and thus its clinical effectiveness. The heat created at the tip of the needle rapidly rises in excess of 80 °C Celsius, leading to vaporisation and charring of tissue, which is a significant factor limiting its efficacy, as well as causing tissue to adhere to the needle. As outlined and described in this chapter, various methods have been adopted in an attempt to increase the ablation zone; the majority have proved unsuccessful.

The multi-tine needle (LeVeen, 1997) and the cool-tip needle are currently commercially available needles, which have been successful in increasing the ablation zone. The multitine needle however has limitations in that rather than creating a large spherical ablation zone with a single needle, each tine creates an ablation zone, which coalesce to form a larger ablation zone, however this is not ideal. The cool-tip needle requires continuous perfusion, which is an added potential complication in the ablation process.

Multiple needles require accurate positioning for an effective ablation and also increase the complexity of the procedure and potential for increased morbidity due to multiple liver punctures.

Saline, water or acetic acid infusion, although in theory should provide larger ablation zones due to the maintenance of hydration in the tissue during the ablation cycle, suffers form an erratic distribution in the tissue and although available commercially, have fallen out of favour.

Adjunct chemotherapy improves the zone of ablation, however has not been adopted as a routine procedure in loco regional tumour therapy.

Objectives for this research:

The main objective for this research at its inception was to prove BETA produced larger ablation zones than conventional RFA. We however elected to do this using a custom made ablation machine in order to ensure the results were not influenced by complex algorithms incorporated in the commercially available ablation generators.
The purpose of this research was not to just prove the concept of BETA, but to prove the hypothesis of electroosmosis (movement of water from the cathode to the anode) and examine the distribution of heat in tissue.
Following the *ex vivo* studies, *in vivo* studies were conducted to prove BETA produced larger ablation zones *in vivo.* In addition, our objectives were to determine if BETA caused a significant inflammatory response or significant hepatic or renal biochemical derangements.

In summary this researched aimed to meet the following objectives:

1. Prove BETA produced larger ablation zones than conventional RFA.
2. Determine the parameters that produced the largest ablation zones.
3. Examine the hydration in ablated *ex vivo* tissue following BETA and conventional RFA in order to prove the hypothesis of electroosmosis occurring during electrolysis.
4. Examine the temperature distribution in *ex vivo* tissue at fixed distances from the electrode.
5. Replicate the results of BETA in animal models in order to establish BETA as being safe *in vivo.*
6. Examine the biochemical and physiological response of the animal models to BETA and RFA.
7. Examine the hepatic and renal biochemical response to BETA and conventional RFA.

Chapter 2:

Bimodal Electric Tissue Ablation:

Ex Vivo Studies for optimisation of Ablation Parameters.

Introduction:

Electrolysis.

Hopsley first described electrolysis of human tissue in 1908. The effects of direct current on the human body were studied and indeed became the life work of BE Nordenstrom (Nordenstrom, 1985, Nordenstrom, 1992, Nordenstrom, 1994a, Nordenstrom, 1994b). He described the body as being made up of a circulatory system, comprising the vascular system, and a separate, but critically important electrical circuit. Described as Biologically Closed Electrical Circuits (BCEC), the Vascular Closed Circuit (VCC) represents the first BCEC identified. The walls of blood vessels are electrical resistors. Arteries and veins can therefore function as relatively closed conducting cables for ions in the blood. An external moving magnetic field can induce flow of these ions in the loops or vessels. The Vascular-Interstitial Closed Circuit (VICC) is an important additional circulation between the blood circulation (Harvey 1628) and lymphatic circulation (Rudbeckius 1653, Nordenstrom, 1992). In his early work, Nordenstrom applied voltage between two electrodes in tissue and found that 10V of direct current applied to a tumour which is polarised anodic, leads to a series of electrochemical changes, which leads to either partial or complete resorption of the tumour. Azavedo et al (Azavedo et al, 1991) published a single case of complete radiological resolution of a breast tumour after applying 10V of direct current (DC) for 2 hours. The tumour showed signs of regression at 2 days and mammography bi-annually and at 2 years demonstrated no radiological evidence of the tumour. The mechanism behind this phenomenon was thought to be polarisation of the tissue. The charge at the electrode will attract ions of the opposite charge, and attraction of some of the anions or cations will lead to an overshoot excess of ions of equal polarity at the electrode. The resultant charging of the body results in blocking of the Sodium and Potassium pumps, and consequent cellular function is impaired.

Charging the peritoneal fluid in rats tested this principle. The purpose – to create an uphill electrostatic force that was too large for the Sodium pump to work against, thus impairing its function and creating an electric field in the peritoneal fluid (Nordenstrom, 1994a). The charge created in the peritoneal fluid by a platinum electrode eventually equalled the electrode charge. An electrode placed in the subcutaneous tissue, too, reached the same charge as the electrode. These experiments were conducted between 1984 and 1986, after which 3 voluntary patients with inoperable cancer volunteered for clinical experiments.

Theoretically it was assumed that blocking the ions pumps would interfere with cellular function. Cancer cells being more susceptible to changes would be affected more than normal cells, and thus the spread of cancer would be arrested. The patients had electrodes placed in a

subcutaneous location close to the tumour. The treatment involved using direct current increased in a stepped method. The current ranged from -83 to -200 volts and then was increased stepwise to 230 volts in patient 1, to 400V in patient 3. The results differed, but the patients exposed to higher voltages underwent larger volumes of tumour regression, with minor clinical symptoms related to the high voltages.

Electrolysis in tissue causes decomposition of water and oxidation or reduction of substances dissolved in the water (Berendson and Simonsson, 1994, Berendson and Olsson, 1998).
At the anode, hydrochloric acid, oxygen and chlorine gas form according to the following equation:

$$2H_2O = O_2 + 4H^+ + 4e^- \quad (1)$$

$$2Cl^- = Cl_2 + 2e^- \quad (2)$$

Chlorine spreads to surrounding tissue by diffusion, causing bleaching of the tissue. Liberated hydrogen ions spread by migration and diffusion. Hydrogen chloride and Chlorine are known to be toxic to tissue.
At the cathode, Sodium Hydroxide (NaOH) and Hydrogen gas (H_2) are formed (Wemyss-Holden et al, 2000a).
More recently electrolysis has been used in the treatment of tumours in rat (Wemyss-Holden et al, 2000, Wemyss-Holden et al, 2000a) and porcine models (Wemyss-Holden et al, 2000, Wemyss-Holden et al, 2000b). Electrolysis uses a small direct current (80-100mA) passed between two electrodes, the anode (positive) and cathode (negative) thus polarising the tissue and causing the formation of the toxic gases described by Berendson. The electrolytic process itself causes small changes in tissue temperature, but not enough to cause cell death secondary to the thermal effects (David et al, 1985, Baxter et al, 1998). The electrolytic process is long; treatment times are up to 3hrs depending on the tumour size.
Shorter treatment times would require larger currents (Teague et al, 2002).
With the results published by Nordenstrom and Azavedo (Azavedo et al, 1991, Nordenstrom, 1994a) work was carried out on the feasibility of electrolysis and its effects on rat livers by Wemyss-Holden et al (Wemyss-Holden et al, 2000a). Within thirty seconds of starting electrolysis, gas production was observed in the form of bubbles emanating from both the anode and cathode. This is the toxic gas formation described by Berendson. A discrete zone of discolouration was evident in the liver surrounding the anode, which is due to the chemical necrosis caused by the chlorine gas production (Berendson and Simonsson, 1994). The areas of discolouration increased in size as treatment progressed.

The results of the study showed no severe effects on liver function, and no severe systemic complications during the electrolytic procedures. The electrolytic areas were seen as discrete foci of fibrosis at 6 months. The time for treatment however was in excess of 40 minutes, a significant limitation.

The findings of this study lead to a larger study on the effects in pigs (Wemyss-Holden et al, 2002b). The electrolytic lesions increased with dose and separation of electrodes, with predictable healing at 6 months, and no systemic complications reported. The findings again were similar to a smaller study conducted by Wemyss-Holden et al (Wemyss-Holden et al, 2000).

Wemyss-Holden et al (Wemyss-Holden et al, 2002a) conducted a pilot study on 5 patients undergoing liver resection for colorectal metastases. The purpose of the study was to demonstrate the clinical safety and effectiveness of electrolysis in patients. A single metastasis was treated with electrolysis before being resected. The treated metastasis was examined following liver resection to determine the degree of necrosis. The study showed electrolysis to be well tolerated and safe. Additionally, it demonstrated total destruction of the malignant tissue at the site of electrolysis.

A study examining the effects of electrolysis in inoperable pancreatic lesions (Wemyss-Holden et al, 2003) showed electrolysis to be safe and well tolerated.

BETA combines the effects of direct current (DC) and radiofrequency energy in order to increase the ablation zone (Cockburn et al, 2007). The effects of both direct current and radiofrequency energy as separate treatment modalities have been described in detail in the literature and have been highlighted in Chapter 1 of this thesis. The effects of BETA have been described using a commercially available RF device coupled to a DC transformer (Cockburn et al, 2007). The effects of BETA however have not been evaluated using a range of DC values, using DC pre treatment prior to RFA and at a variety of DC voltages. In order to determine the effectiveness of BETA a machine needed to be designed which allowed both DC and RFA to be administered simultaneously as well as separately. The commercially available machine used by Cockburn et al included an impedance feedback algorithm, which modulated the RF power delivered to the tissue. This power modulation allows for fluctuations in the RF delivery to ensure the RF power delivered to the tissue did not cause excessive heating early in the treatment cycle. This impedance feedback algorithm had to be removed in order for more precise monitoring of ablation zone size at specific RF power levels.

The design of the machine will be discussed in more detail in the materials and methods section.

Objectives of the Study:

To determine the parameters which produce the largest ablation zones in *ex vivo* liver.

The DC time before RFA, the DC voltage and the RF power was examined.

Materials and Methods:

***Ex vivo* Liver**

Ex vivo livers for the laboratory experiments were obtained from a local butcher (JC Fines & Sons, Coltishall, Norfolk UK).

The fresh bovine livers were delivered to the local butcher from a local abattoir.

Immediately following slaughter of the animal, the livers were excised en-bloc and placed in a sealed vacuum packed bag ready for delivery.

The livers were stored in the abattoir at 0 to 4 °C, the industry standard for refrigeration of meats (Foods Standards Agency, UK) and delivered to the butcher the following day, ready for collection.

Before beginning experiments, each liver was washed and prepared in the same way.

- Each liver was cleaned by removing the falciform ligament and adherent omentum to the visceral side of the liver.

- The redundant free edge of the portal vein in the porta hepatis was dissected free and discarded.

- The liver was then placed on a large PVC cutting board for preparation.

Discussions regarding the use of the whole bovine liver for experiments were discussed amongst the chief investigator and both supervisors.

All *ex vivo* experiments published in peer reviewed journals conduct *ex vivo* ablations in a large plastic container with a shallow saline solution in order to allow the electrical circuit to be completed (Goldberg et al, 1998b). Placing the liver directly onto the reference-grounding pad creates a bipolar circuit, which in itself is a modification on the essential monopolar technique used in this research. This important factor necessitates that in order for the electrical circuit to be completed, the saline must act as a conductor of electricity to the reference-grounding pad, placed at least 20cm from the liver.

This point was discussed with Dr SN Goldberg of the University of Harvard, Boston, Massachusetts, USA. Dr Goldberg has published a number of papers on radiofrequency ablation and designed the Cool-tip needle. Dr Goldberg is regarded as the world authority on Radiofrequency Ablation. He stressed the need for the grounding pad to be placed a distance from the liver and for the solution to be normal (0.9%) saline.

The liver itself however can either be ablated as a whole liver (Goldberg et al, 1998b), or as individual blocks of liver dissected into cubes (Lee et al, 2006). Both of these methods are accepted by peer-reviewed journals.
The purpose of our research includes proving the theory that electroosmosis, which will be discussed in later chapters, has a synergistic effect on radiofrequency ablation.
The investigator and supervisors felt it would be prudent to cut the liver into blocks measuring 10 x 10 x 10cm in order to ensure that:

1. There was no risk of causing overlapping ablations in the liver. This may be problematic if the electrode is placed into the liver at an angle, and a subsequent ablation, although 10cm away is influenced by this previous ablation.

2. There was no risk of affecting the relative hydration in the liver post ablation. If two ablations were close to one another, this may influence the relative hydration in the liver, as RFA causes desiccation. Surrounding factors would therefore have influenced the subsequent hydration measurements discussed in later chapters.

The liver was initially scored with a sharp knife, in order to mark out equal blocks of tissue. (Figure 2.1)

Figure 2.1 whole bovine liver scored in preparation to be cut into 1000cm^3 blocks.

The liver was then dissected into equal blocks measuring 10 x 10 x 10 cm (Lee et al, 2004a, Lee et al, 2004b, Lee et al, 2004b). The left lobe of the bovine liver, as in a human one is much thinner than the right lobe and proved to be unsuitable in many instances for production of suitable blocks of liver. These were discarded.
The pieces of liver were then immersed in a warm saline bath of 30 °C (Lee et al, 2005). The bath was changed regularly throughout the day once the temperature decreased to below 27 °C . This was in order to ensure the livers were kept at between 26 and 30 °C (Lee et al, 2004b, Haemmerich et al, 2005).
The saline bath prevented the liver blocks from drying out and also ensured each block of liver used was at the same temperature for each experiment.
Large veins traversing the liver were avoided to ensure the blocks used were of homogenous density.
In *ex vivo* liver, the relative low impedance of large cavernous venous channels creates an artificially larger ablation zone, and therefore to ensure reproducible results, these were avoided.

Saline Solution:

In order to complete the circuit *ex vivo*, the block of liver used for each experiment was placed into a large shallow PVC container with a shallow volume of 0.9% Sodium Chloride solution (Saline).
The concentration of the saline, although not important in terms of conduction of electricity, is essential in maintaining the intracellular concentration of Sodium in the bovine livers.
Each litre of 0.9% saline contains 154mmol of Sodium, an essential ion in both humans and animals. As in human blood, the normal Sodium concentration range in bovine blood is 130-155mEq/L. This has a 10% error value to allow for laboratory fluctuations.
Ensuring the saline used at all times was 0.9%, ensured the liver would not be subjected to fluctuations of intracellular sodium concentrations which may influence how the liver reacted to ablation.
For BETA to occur there must be a closed electrical circuit, and with the grounding pad not in contact with the liver the saline provides a medium of electrical transport. The grounding pad used in the experiments was placed at least 20cm from the liver in order to prevent a bipolar effect from occurring.
The saline solution was produced using normal table salt, measured out to 9g of salt dissolved into 1L of tap water. The salt was measured to 9g on a commercially available digital scale and dissolved into 1L of water at 26 °C.

The temperature of the water was monitored using a commercially available digital thermometer, produced for the food industry.
The thermometer is waterproof and can be left in a solution for continual temperature measurement.

Perspex Container for cut Liver Blocks:

The cut liver blocks proved to be extremely difficult to work with initially.
Without support from the surrounding liver, fresh liver is extremely mobile and difficult to immobilise in order for an electrode to be inserted, and for the electrode to be placed perpendicularly into the tissue.
A Perspex box was thus commissioned for manufacture by the engineering department at the University of East Anglia (Figure 2.2).

Specifications:

- Internal dimensions of the box 10 x 10 x 10cm.

- Floor of the box was to have multiple holes drilled into the Perspex measuring 1cm in diameter each, at equidistant intervals. The holes allowed the saline to flow into the box and complete the electrical circuit.

- The sides of the box were solid, and glued to one another.

- Removable lid with a hole drilled into the centre to allow the electrode to be inserted through it (Figure 2.2).

- A "floating platform, a mirror of the removable lid which had a hole drilled into the centre to allow for the electrode to be placed through it. The Medical Engineering department and the Norfolk and Norwich University Hospital manufactured the platform.
  The floating platform had Perspex spacers glued to the underside of the platform to allow the platform to be placed onto the liver, but not be flush with the liver surface. The electrode could then be placed through the two holes and into the liver, thus ensuring that the needle was perpendicular to the liver surface for each ablation. (Figure 2.4)

- 4 Perspex spacers were glued to the underside of the Perspex box in order for the underside to "float" 0.5cm above the PVC container holding the saline.
  The reason for this addition to the Perspex box was to ensure a gap between the box under surface and the container. Having these two surfaces in close contact may have prevented saline from entering the holes in the floor of the Perspex box. (Figure 2.2)

The Perspex box was then used for each experiment in the *ex vivo* study and ensured each experiment was reproducible and accurate.

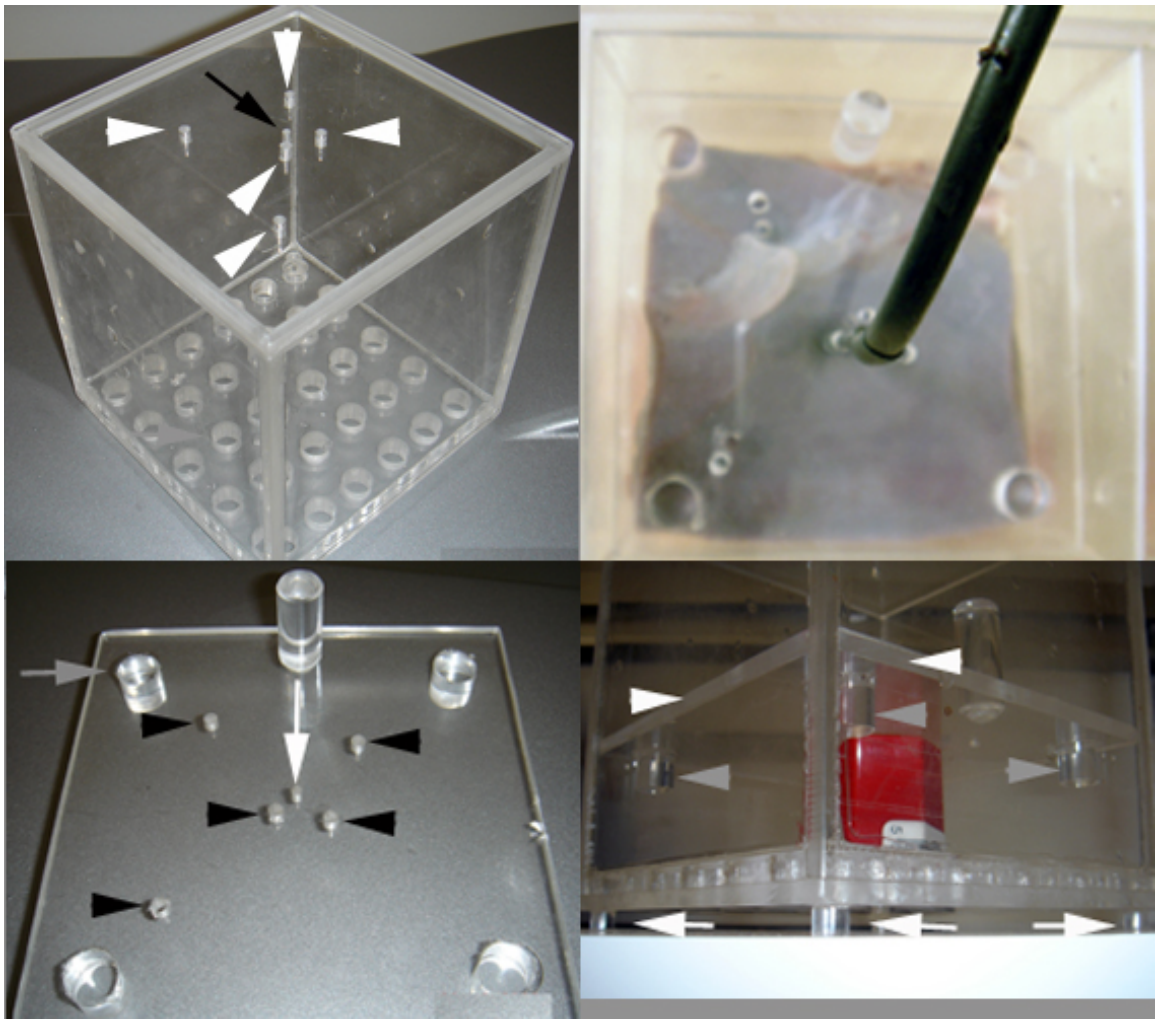

Figure 2.2 clockwise from top left, Perspex box with holes drilled into the lid to accommodate temperature probes (white arrowheads) and the electrode (black arrow) and multiple holes drilled into the floor (grey arrowheads) to allow for saline contact during ablation, electrode insitu with a piece of liver in the box. Perspex box showing legs (white arrows), which raise it to allow for saline to contact the liver and thus electrical conduction. A floating platform (white arrowheads) with legs, which is placed on the liver in order to keep the temperature probes and electrode perpendicular. Floating platform showing legs (grey arrows), multiple holes for temperature probes (black arrowheads) and a hole for the electrode (white arrow)

The BETA Machine:

The BETA device was manufactured for purpose by EG Technology, Cambridge, UK.
The prototype BETA system (Mark II) allows controlled amounts of radiofrequency (RF) and DC electrical current to flow through tissue, resulting in tissue ablation. The machine creates a circuit by inserting a probe into tissue, directing electrical current on the effected area, which travels to a grounding pad attached to the patient, providing the return path.
The DC signal at the probe is negative when referenced to the grounding pad.
The RF generator box produces an RF signal at 470 kilohertz (kHz), produced by the RF generator box.
The RF current and voltage are monitored by outputs from the box providing DC signals in proportion to the RF signals.

Circuit description:

The 470 (kHz) RF source feeds four 50 watt (W) amplifiers arranged in parallel (U3, U4, U5, U6). The outputs are combined in two stages (in L1 and L5 initially and then in L3) and the 200W output is then transferred to the probe via an impedance matching transformer (L4).
There is no impedance feedback algorithm built into the circuit.
The DC is inserted into the circuit across the RF decoupling capacitor (C3). This capacitor protects the DC power supply from the RF signal by effectively shorting out the DC terminals at the RF operating frequency. The remainder of the RF circuit is employed purely to measure the RF current through, and the voltage across the ablation probe.
L2 is a current transformer whose output is rectified (D3) and filtered before being buffered and temperature compensated by U2.
The RF voltage level is rectified (D1) and filtered before being buffered and temperature compensated by U7.
Not shown on the schematic (Schematic 2.1) is the input to the power amplifiers to allow control of the output power. The ‘input’ is a current source, which has to be pulled down in order to decrease the output voltage. The connection to the box is made using a 25 way D connector (Schematic 2.1).

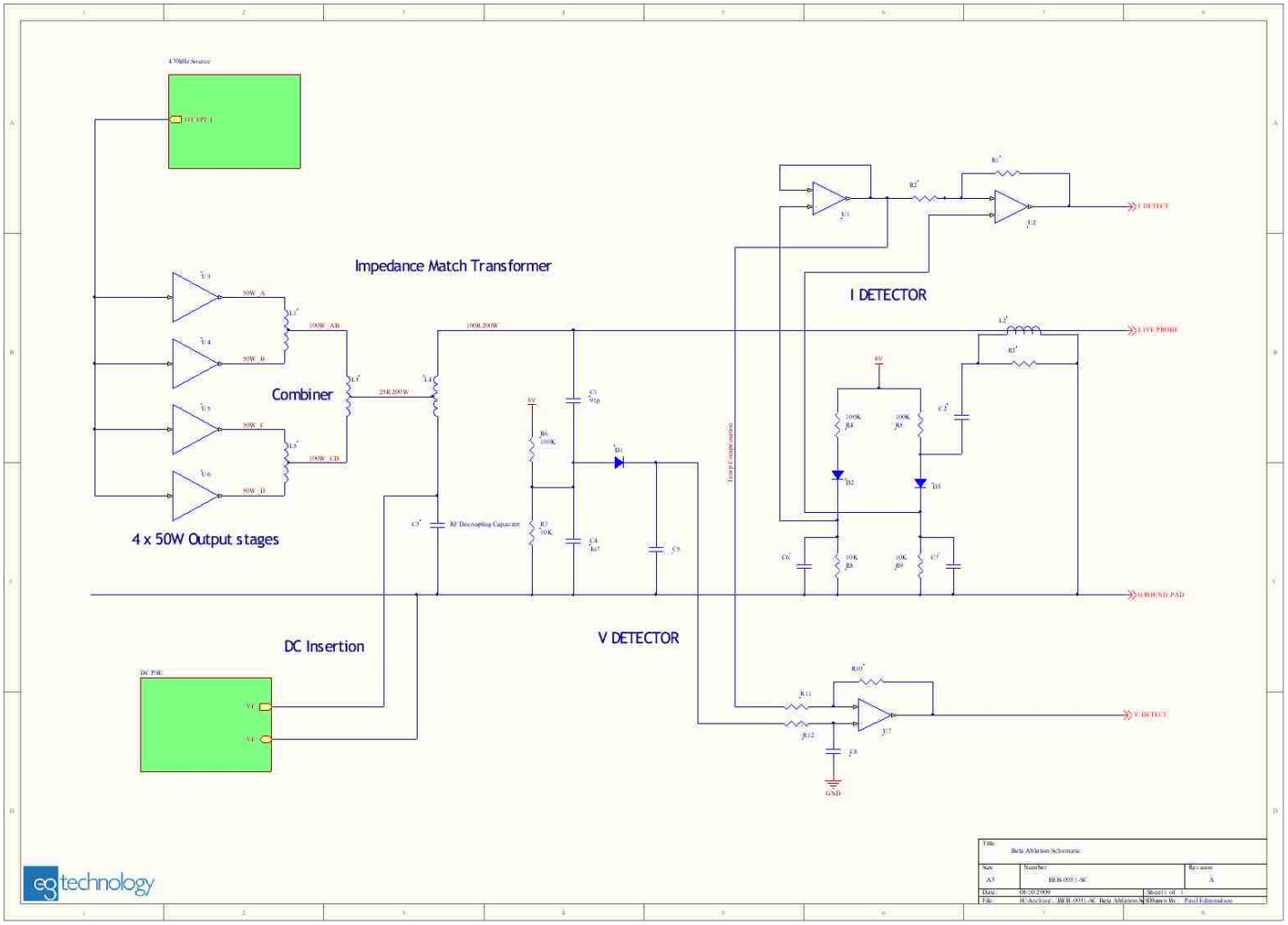

Schematic 2.1 Circuit diagram of the BETA Mark II machine

Control Method:

The prototype machine (Mark II) (Figure 1.5) is controlled from a PC/laptop running specially developed software (EG Technology, Cambridge, UK). An analogue to digital converter captures the current and voltage signals. An algorithm then calculates the required setting and provides a signal to the power control (pin 7) input on the RF amplifier based on the desired RF power setting (mA).

The user is able to adjust the RF power (0-2000mA), the DC voltage (0-50V) and the DC and RF times (0-2000 seconds).

The software program (Figure 2.3) allows the user to program up to 15 steps for each ablation cycle.

Each step requires the user to input 3 variables – time (seconds), RF power (mA) and DC (volts).

Figure 2.3 software interface controlling the Mark II machine

For DC to be delivered alone the RF power must be 0mA, and for RF power to be delivered alone the DC voltage must be 0V.
Similarly DC and RF may be delivered simultaneously by adding a DC value and RF value. The cycle will not begin if a time for the RF cycle is not inputted.
The user must also choose a maximum impedance value, which will end the ablation cycle, effectively simulating 'roll-off'.
The impedance value is measured in ohms with a range of 0-2000 ohms.
For each ablation cycle, 900 ohms was chosen as above 900 ohms was the value accepted in the literature for roll-off. Above 900 ohms the impedance is too high for any amount of RF energy to be deposited in tissue and indicates ablated tissue (Lin et al, 2003).
The user can also control the cycle and the RFA can then be shut off - based on elapsed time rather than roll-off. This is particularly important when pre treating tissue with DC prior to the ablation cycle.

The Ablation Cycle:
The hypothesis for this research required comparison of BETA to standard radiofrequency ablation (RFA) using the same RF power for the control (RF alone) and for the BETA experiment.
Early studies evaluating BETA have done so using a commercially available RFA generator, the Radionics RF3000 (Boston Scientific, Natick, MA). This RFA generator had a DC transformer connected in parallel (Cockburn et al, 2007).
The current BETA generator as described has not been evaluated previously and a large research matrix was designed in order to determine the parameters needed to produce the largest ablation zone.

A matrix was designed using the following parameters:

1. Time of DC current application before standard RF ablation is commenced. This is referred to as the pre-RF DC. DC is applied to the liver using the electrode as the cathode and the reference-grounding pad as the anode (Nordenstrom, 1983, Probstein, 1994). The measurements for this phase of the experiments were 0, 300, 600, 900 and 1800 seconds of pre-RF DC.

2. Strength of DC current (Volts)
   3, 9, 18 and 36 volts were chosen as the variables for DC magnitude. The values chosen are based on work done by Nordenstrom (Nordenstrom, 1985), which was presented at the Fleischner Lecture in 1985. (Table).

3. Strength of AC current (mAmps)
   A variety of current strengths were chosen for the study based on the literature and described in chapter 1. The radiofrequency currents chosen initially, 500, 750, 1000, 1500 and 2000mA can be attributed to work by Solazzo et al (Solazzo et al, 2007) in *ex vivo* bovine studies, however this pertains to the higher currents, namely 1000, 1500 and 2000mA (Table 2.3, Appendix 1).

Given the variables, a matrix was designed using each of the variables in each group to produce a matrix (Table 2.3, Appendix 1).

The parameters used where no DC voltage was applied represent the control group of experiments.

105 combinations were used initially to determine the largest ablation zone.

A meeting was held early on in the research, during the study design stages with Dr P Musonda, Medical Statistician, University of East Anglia in order to discuss power calculations for the above research matrix.
Dr Musonda recommended dividing the *ex vivo* study into two separate phases in order to determine power calculations for the entire research matrix and once satisfactory results were produced, to begin a second phase of the *ex vivo* study.

Phase I:
Conduct each experiment in the research matrix (n=4) in order for power calculations to be determined.
The following measurements would be recorded for each experiment.

- DC Pre-time
- DC Voltage
- RF Power
- Time of roll-off
- Largest diameter of the ablation zone.

Phase II:

Identify the set of parameters, which produce the largest ablation diameter and produce a large number of experiments for each parameter (n > 15).

In addition the volume of the ablation would be calculated.

The standard in the literature for volume calculation for RFA is the volume of an ellipse or of a sphere (Mulier et al, 2003, Ahmad, 2004, Stippel et al, 2004).

A spherical volumetric calculation was used for these experiments as the geometry of the lesions produced, had 2 similar measurements for the axis perpendicular to the long axis of the ablation probe r_1 and r_2. The measurement for the ablation zone along the long axis of the electrode r_3 was often considerably larger than r_1 and r_2 and thus proved to be unsuitable for these calculations.

Volume of a sphere:

$$V = 4/3\pi r^3$$

Volume of an ellipse:

$$V = (4/3)\ \pi.r_1.r_2.r_3$$

In phase II of the experiments, in addition to the generator parameters and the roll-off time, each of the 3 radii were measured and documented for volume measurements. Each radius was measured 3 times and the average of the 3 measurements was used as the final measurement. This was to ensure the final measurements recorded for each ablation zone represented a reliable measurement.

The technique for each experiment conducted was exactly the same, in order to produce reliable and reproducible data.

Each block of tissue was placed into the Perspex box, which was positioned in the large PVC container with a shallow volume of 0.9% sodium chloride solution (Figure 2.4). The level of the sodium chloride solution was measured out to a depth of 1cm from the floor of the Perspex box. This ensured that 1cm of the block of the liver was submerged in the saline solution, allowing for electrical conduction.

The foil grounding pad was placed at the opposite end of the container, immersed in the saline. The foil grounding pad measured $100cm^3$.

The electrode was then inserted into the centre of the block of liver with at least 1cm of insulated electrode placed into the liver in addition to the 3cm exposed active electrode tip.

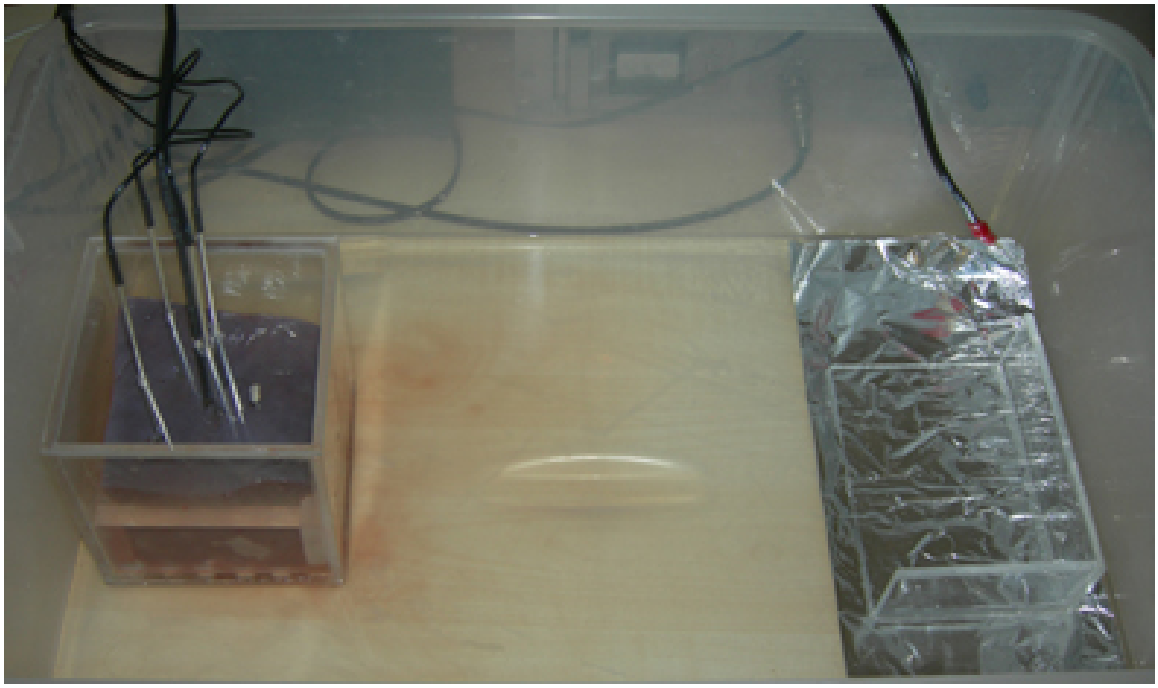

Figure 2.4 Perspex box containing piece of liver with electrode (black rod), temperature probes (silver rods) in situ. Foil grounding pad placed 20cm from the liver.

The parameters for each experiment were then entered into the software program.
Each experiment conducted was assigned a file name according to the parameters used and the date of the experiment.
A control experiment had no DC and there for was labelled according to the time assigned to the experiment in seconds, the RF power (mA) and the DC voltage. As each experiment continued until there was roll off of the RF power, a random time was selected in order to ensure the experiment never continued to this time; 3600 seconds was chosen.

For each control experiment referred to in this thesis, the control refers to RFA with no DC, using the same RF power (mA) as the corresponding BETA experiments.

The format of assigning labels to each BETA experiment was as follows.

DC pre(s). RF pre(mA) . DC power pre(V) . RF time(s). RF power(mA). DC(V)

Using this format, a BETA experiment with 300s of pre-DC at 9V with 600mA of RF would be written as follows:

300 . 0 . 9 . 3600 . 600 . 9

A control RF ablation that did not have a DC component was shortened to exclude the DC parameters and was written in the following format.

RF time(s) . RF power(mA) . DC(V)

A control RF ablation using 600mA would therefore be assigned a label a label as follows.

3600 . 600 . 0

If the BETA experiment involved no pre-DC time, but DC was used in conjunction with RF immediately at the onset of the experiment, the format above was used.
For an experiment with no pre-DC, but RF and DC running simultaneously with parameters of 600mA RF power and 9V of DC, the experiment was labelled as follows.

3600 . 600 . 9

Each experiment was automatically saved by the software program with a date and time stamp, however in order for the information stored to be easily accessed and referenced, each ablation was assigned a further number at the end of the label in order to record the number of ablations conducted on a particular day using the same parameters.
The first ablation using specific parameters was not assigned a number, in other words regarded as the first.
Each subsequent experiment was assigned a number after a hyphen, indicating the number of times the experiment was conducted in a single day.
This was recorded by the software was follows.

300 . 0. 9 . 3600 . 600 . 9
300 . 0. 9 . 3600 . 600 . 9 - 1
300 . 0. 9 . 3600 . 600 . 9 - 2

This format indicated that 3 experiments using the same parameters were conducted in a single day.

The BETA experiment was then commenced. The software program monitored the impedance of the liver continually during the entire cycle of RFA.
With only DC being applied to the liver, the impedance was not measured.
Current was delivered to the liver at 70mA and a set voltage.

Once RFA is commenced, the software program measures the impedance in the tissue and adjusts the RF power (Watts) and RF Voltage according to the impedance, to ensure the programmed mA remains constant.
Once the impedance increases to above 900 ohms, the program terminates and generates an excel file containing the parameters described and a graph incorporating each of the parameters (Graph 2.1).

The 900 is the value at which roll-off occurs (Lin et al, 2003) during RFA in the liver as described in chapter 1.
This is where the impedance in the liver is too large to enable any transfer of heat into the liver and further ablation.
The impedance value where the machine automatically ends the ablation can be adjusted before commencing the ablation. The value ranges from 1 to 2000 ohms.
Experience in the literature dictates that above 900 ohms, no ablation takes place and commercially available ablation machines have 900 ohms preset as the roll-off value.

Immediately after ablation, the block of liver was removed from the Perspex box in preparation for dissection and measurement of the ablation diameters.
A rigid brass rod was inserted into the block of liver before it was removed from the Perspex box, along the electrode tract in order for the block to be cut exactly parallel to the direction of the electrode. This ensured that the measurements are taken in the middle of the ablated tissue and that each measurement was identical and reproducible.

3 separate measurements were taken of each diameter and the average of the 3 was recorded in a research notebook and on the excel spreadsheet generated by the software program.
The data was recorded in the following manner in the research notebook under the date for that day.

Assigned label ablation dimensions (d1.d2.d3 cm) impedance time to roll-off

A typical entry into the research notebook would be as follows.

300 . 0 . 9 . 3600 . 600 . 9	**2.6 x 2.4 x 5.2 cm**	**85 ohms**	**1268 s**
300 . 0 . 9 . 3600 . 600 . 9 - 1	**2.4 x 2.2 x 4.8 cm**	**90 ohms**	**1198 s**
300 . 0 . 9 . 3600 . 600 . 9 - 2	**2.9 x 2.9 x 5.8 cm**	**75 ohms**	**1318 s**

This data was the recorded on a large spreadsheet with each parameter in order from control to experiments.

The parameters were recorded and a mean of the largest ablation diameter was calculated for each experiment.
Volumes were calculated for those experimental parameters, which produced the largest ablation zones.

Once each experiment had been performed four times (n = 4), it was decided to include 600mA to the RF power group for selected parameters. 600mA produced a large ablation zone in a reasonable period of time, compared to 500mA
The reasons for this will be expanded upon in the results section of this chapter.
The parameters chosen were based on the largest ablation zone sizes overall using a set mA. To expand on this further, regardless of the mA, the parameters for a given MA, i.e. Pre DC and DC voltage were analysed and those parameters producing the largest ablation size were then chosen for the 600mA set of experiments (Table 2.3, Appendix 1).
Each of these parameters were performed four times (n = 4) and included in the results submitted for statistical analysis to Dr P Musonda for power calculation.
600mA was not included in the initial matrix of parameters however experiments were conducted at 300mA, 400mA, 450mA, 600mA and 650mA in addition to the parameters set out in the original matrix.
The addition of the 5 combinations above increased the total combination number to 110.

Results:

In total 1017 experiments were conducted in order to determine the set of parameters, which produced the largest ablation zone.
Initially, each parameter was tested (n=4) in order to perform power calculations.
This data was examined in conjunction with Dr P Musonda and power calculations performed.
Following power calculations, each parameter was examined (n=6) in order to determine the parameter, which produced the largest ablation zone.
The results are expressed as means ± standard deviation (SD) for normally distributed variables or the median and the interquartile range for non-normal variables. Differences in maximum short axis diameter between tissue receiving standard RFA or BETA were tested with ANOVA. A *P* value <0.05 was considered statistically significant. SPSS 17 was used for all statistical data analysis. The sizes quoted refer to the maximum short axis measurement unless specified.

Phase I:
Initial experiments were carried out (n=4) and power calculations performed. Following power calculations, each experiment was conducted to a total (n=6) according to the power calculations.

Appendix 1:
Table 2.1 shows the control sample size calculations together with the minimum, maximum and means for each radiofrequency energy value measured. The interquartile ranges and standard deviations are also shown.

Table 2.2 shows the experimental sample size calculations together with the minimum, maximum and means for each radiofrequency energy value measured. The interquartile ranges and standard deviations are also shown.

Overall Estimates:

Sample Size 1.33 and 2.09

p (0.8)

SD1 (0.23)

SD2 (0.48)

Estimated sample size for two-sample comparison of means

Test Ho: m1 = m2, where m1 is the mean in population 1
and m2 is the mean in population 2

Assumptions:

alpha =	0.0500 (two-sided)
power =	0.9000
m1 =	1.33
m2 =	2.09
sd1 =	.23
sd2 =	.48
n2/n1 =	1.00

Estimated required sample sizes:

n1 =	6
n2 =	6

A total of 12 experiments are needed at 80% power (JM, 1993, B, 2005).

Phase 2:

Following the results of the power calculations, each parameter was tested a minimum of 6 times (Table 2.3, Appendix 1).

Table 2.3 shows the matrix of tested parameters. Each experiment is shown together with the parameters, the size of the ablation zone (cm), the total time of the experiment with RF switched on (s), mean maximum short axis diameter of the ablation zone (cm), the standard deviation (SD) and the 95% Confidence Interval (95% CI).

Figure 2.1 shows graphical representation of all the experiments conducted at each parameter.

The RF power at 1500 and 2000mA was too excessive and caused almost immediate roll-off, with no definable ablation zone. These experiments will be expressed as N/A in the tabulated results (Appendix 1-Table 2.3).

Similarly DC voltages of 18 and 36V with pretreatment times of 1800 seconds did not allow any ablation to take place. This will be discussed later in the chapter – these are also expressed as N/A in the results table (Appendix 1-Table 2.3).

500mA initially produced larger ablation zones sizes (Table 2.4), when compared to 600mA, however the mean ablation times for simultaneous RF and DC was significantly longer than those experiments using 600mA (1809 seconds vs 891 seconds; $p < 0.0001$).

mA Ranges	Mean (cm)	N	SD	Min (cm)	Max (cm)	Range	Variance
400mA	**1.2**	**6**	**0.06**	**1.1**	**1.3**	**0.2**	**0.004**
450mA	**1.27**	**6**	**0.08**	**1.2**	**1.4**	**0.2**	**0.007**
500mA	**1.64**	**6**	**0.17**	**1.4**	**1.9**	**0.5**	**0.03**
600mA	**1.58**	**6**	**0.12**	**1.5**	**1.8**	**0.3**	**0.014**
650mA	**1.42**	**6**	**0.12**	**1.3**	**1.6**	**0.3**	**0.014**
750mA	**1.29**	**6**	**0.08**	**1.2**	**1.4**	**0.2**	**0.006**
1000mA	**1.05**	**6**	**0.1**	**0.9**	**1.2**	**0.3**	**0.011**
Total	**1.35**	**42**	**0.22**	**0.9**	**1.8**	**0.9**	**0.05**

Table 2.4 shows a summary of the ablation zone sizes obtained for the initial ablation matrix including the range and standard deviation (SD).

Figure 2.5 demonstrates ablation zones obtained with conventional RFA (top) and BETA (bottom)

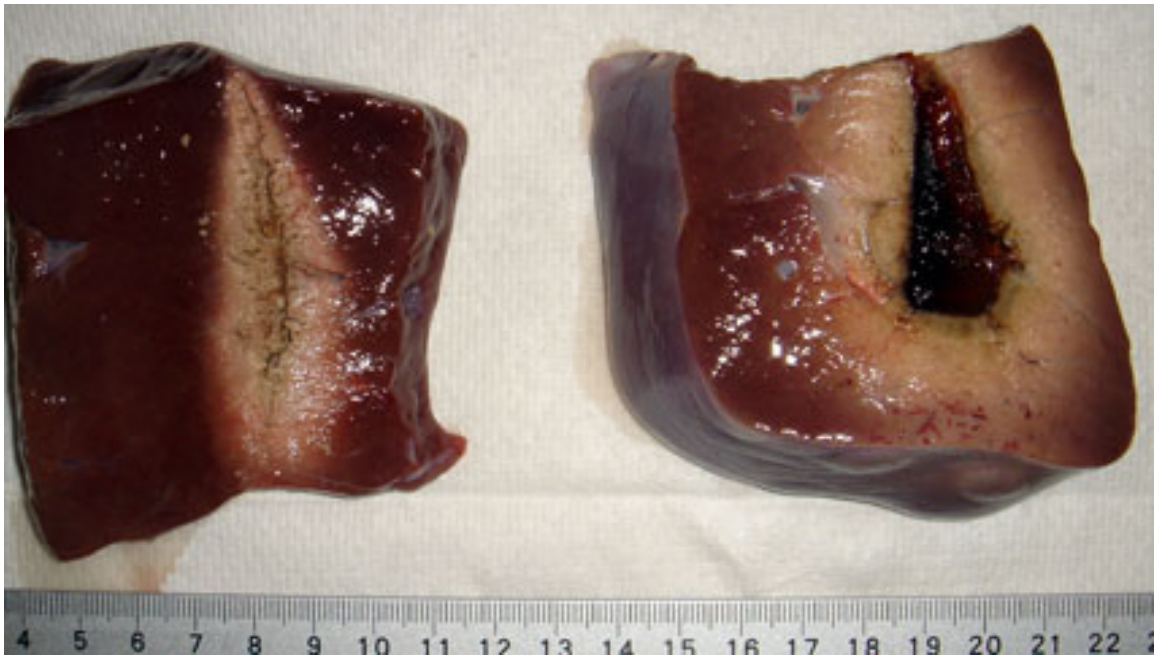

Figure 2.6 demonstrating conventional RFA (left) and BETA (right)

The use of 500mA equates to a mean ablation time of over 30 minutes compared to just over 14 minutes for 600mA using sequential DC/RF with no pretreatment.
600mA was therefore chosen as the RF power, which produced the largest ablation zone ($p < 0.0001$).
This decision was confirmed later with larger comparative groups of 500mA and 600mA using simultaneous 9V of DC with no pre-RF DC (Table 2.3, Appendix 1)

	N	Mean (cm)	SD	SEM	95% CI for Mean (cm)		Min (cm)	Max (cm)
					Lower	Upper		
500mA BETA	**15**	**2.68**	**0.26**	**0.07**	**2.53**	**2.83**	**2.5**	**3.6**
600mA BETA	**82**	**2.84**	**0.42**	**0.05**	**2.74**	**2.93**	**2**	**4.4**
Total	**97**	**2.81**	**0.4**	**0.04**	**2.73**	**2.89**	**2**	**4.4**

Table 2.5 shows the mean sizes of the ablations obtained with 500mA and 600mA respectively. The standard deviation, 95% confidence interval and standard error of the mean (SEM) and ranges are listed in addition.

The difference between the ablation zone sizes using 500mA compared to 600mA was not statistically significant (p=0.168). An interesting observation was the larger mean ablation zone obtained with 600mA compared to 500mA when a larger group was sampled, however this was not significant (p=0.168) and is therefore probably due to chance.

Table 2.5 shows the mean sizes of the ablations obtained with 500mA and 600mA respectively. The standard deviation, 95% confidence interval and standard error of the mean (SEM) and ranges are listed in addition.

The results of the experiments showed 9V of DC to produce the largest ablation zones, with a decrease in ablation diameter with increasing DC voltage. This conflicts with the data obtained by Cockburn et al (Cockburn et al, 2007). This will be discussed later in the chapter (Table 2.3).

No statistical difference was detected between the size of the ablation zone with no DC pre treatment, compared to 300s (p= 0.591) and 600s (p=0.624) of DC pre treatment (Graph 2.2 and 2.3).

	Mean (cm)	N	SD	Min (cm)	Max (cm)	SEM
RF	**1.586**	**85**	**0.17**	**1.2**	**2.1**	**0.02**
DC/RF	**2.837**	**82**	**0.42**	**2**	**4.4**	**0.05**
300s DC	**2.794**	**31**	**0.23**	**2.1**	**3.3**	**0.04**
600s DC	**2.797**	**30**	**0.23**	**2.4**	**3.4**	**0.04**

Table 2.6 demonstrates the results using 600mA of RF power with no DC (RF), simultaneous DC (9V) and RF (DC/RF) and 300 and 600 seconds of pre RF DC respectively. The Mean, standard deviation, range and standard error of the mean are listed.

Graph 2.1 illustrates the graph produced by the BETA software program following an ablation cycle.
Graph 2.2 illustrates the ranges and confidence intervals for BETA with 600mA and simultaneous DC with no pre-RF DC, 300 seconds of pre-RF DC and 600 seconds of pre-RF DC
Graph 2.3 illustrates the means and confidence intervals for BETA with 600mA and simultaneous DC with no pre-RF DC, 300 seconds of pre-RF DC and 600 seconds of pre-RF DC

The ablation zones decreased slightly in size when DC was applied for 900 seconds and 1800 seconds respectively, which will be discussed later in the chapter.
BETA produces significantly larger ablation zones using 9V of DC compared to standard RFA (600mA) ($p < 0.0001$).
BETA produces an ablation zone 1.8 times the diameter of that produced by of standard RFA ($p < 0.0001$).
BETA produces an ablation zone 1.8 times the diameter of that produced by standard RFA ($p < 0.0001$) when 9V of DC is applied to RF with no DC pretreatment (Graphs 2.2 and 2.3).

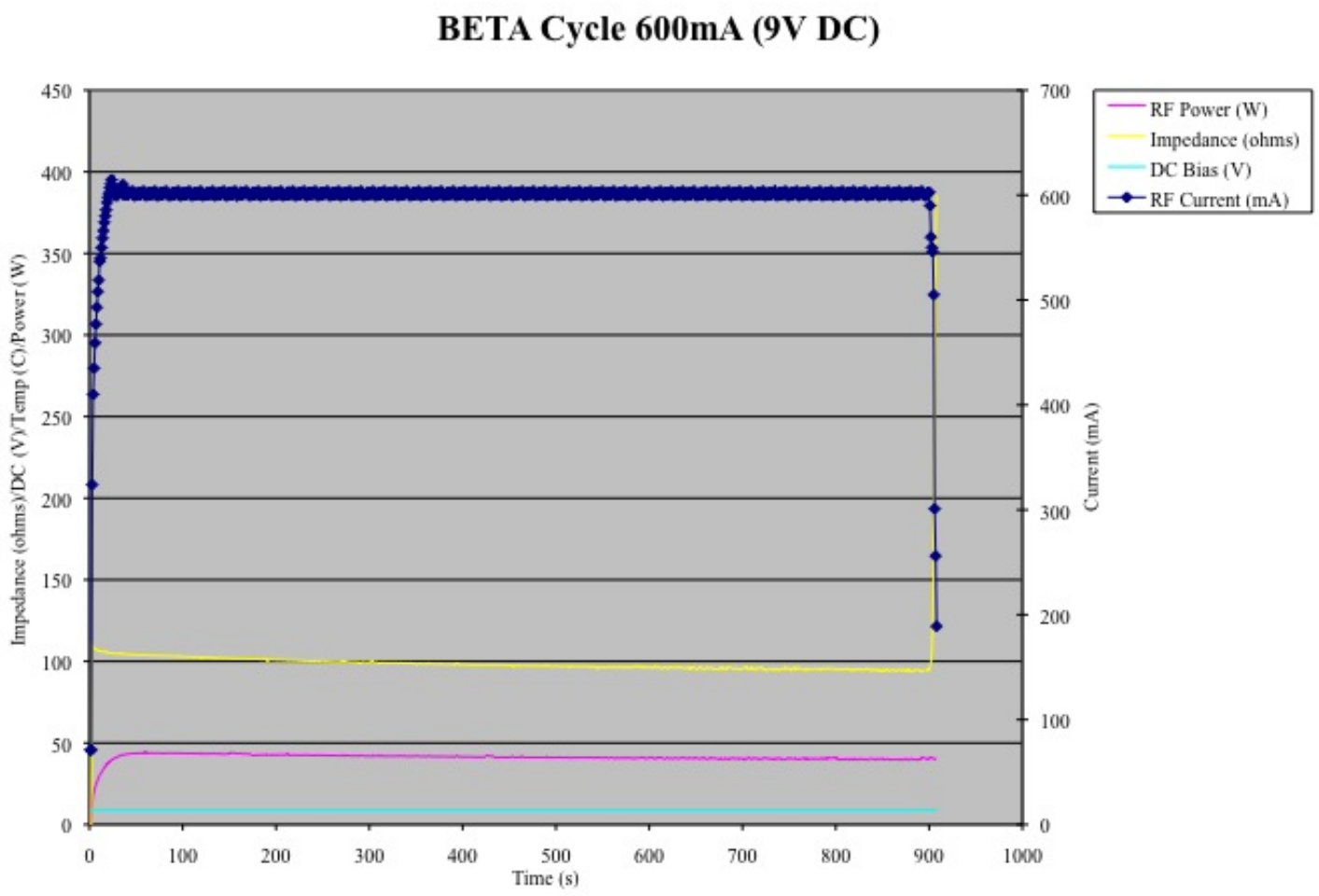

Graph 2.1 illustrates the graph produced by the BETA software program following an ablation cycle.

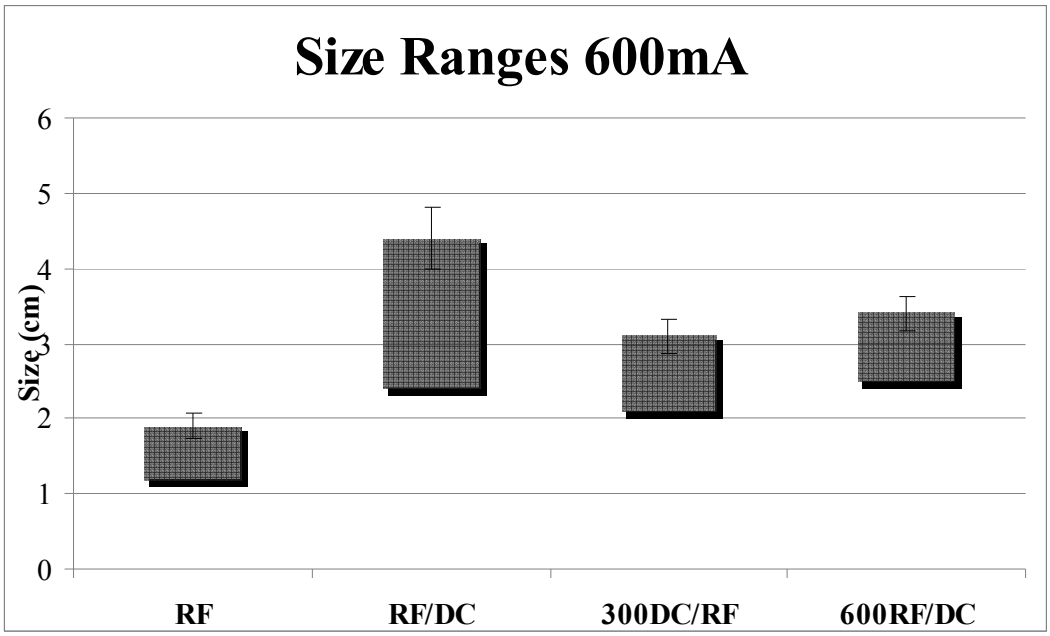

Graph 2.2 illustrates the ranges and confidence intervals for BETA with 600mA and simultaneous DC with no pre-RF DC, 300 seconds of pre-RF DC and 600 seconds of pre-RF DC compared to controls (RF) using 600mA with no DC.

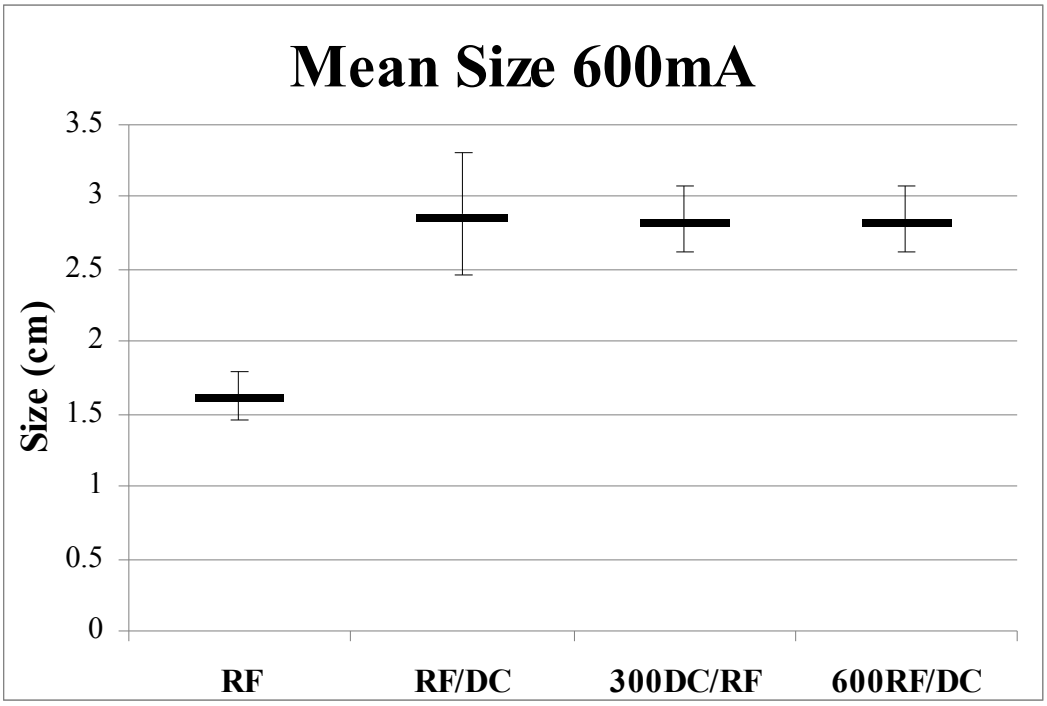

Graph 2.3 illustrates the means and confidence intervals for BETA with 600mA and simultaneous DC with no pre-RF DC, 300 seconds of pre-RF DC and 600 seconds of pre-RF DC compared to controls (RF) using 600mA alone.

Discussion:

General:

In chapter 1 Radiofrequency Ablation was defined and discussed in detail.
The inherent disadvantages of the technique were highlighted with reference to the literature. Modifications on the technique of radiofrequency ablation were discussed and reference made to improvements in technique. Emerging procedures using radiofrequency ablation and adjunct techniques such as chemoembolisation in order to increase the ablation zone demonstrated the need for a technique, which produced reliable, and reproducible ablation zones, which were larger than the standard ablation zones achieved with radiofrequency alone.
Radiofrequency ablation and its uses are well known, as are the uses of direct current. Combining direct current and radiofrequency ablation in order for the simultaneous use in a single circuit had not been described in the literature prior to 2007.
Cockburn and Wemyss-Holden, the inventors of BETA trialled BETA using a commercially available RF device (Cockburn et al, 2007) and a DC transformer. This research represents the first attempt to evaluate BETA using a purpose built device. Many have described modifications of RF, few have succeeded in producing reliable ablation zones larger than standard RF, and no paper has been found which describes detailed data on the effects of BETA using a machine designed for this use.
It is proposed this research gives a unique insight into the effects and workings of BETA in producing large ablation zones.
This discussion will address DC in relation to RFA, including DC power, time for DC, RF power and simultaneous RF and DC application.

Parameters of BETA:

General

BETA can be divided into two separate phases.
Phase 1 is that phase of the ablation where direct current is applied to the tissue, with the electrode acting as the cathode and the grounding pad as the anode. As described this causes the release of gases at the cathodic electrode and reference anodic grounding pad (Samuelsson and Jonsson, 1980, Samuelsson and Jonsson, 1981, Samuelsson, 1981), establishing an electrical osmotic gradient referred to as an electro-osmotic gradient by Nordenstrom (Nordenstrom, 1983, Nordenstrom, 1998). No radiofrequency energy is applied at this point. The operator determines the amount of direct current and the time for DC delivery.
Phase 2 is the combination of radiofrequency energy and direct current applied to the electrode simultaneously the duration of this phase is dependent on the roll-off of the radiofrequency ablation.

Effect of direct current: The pre – RF phase
The effects of direct current applied to tissue have been described (Samuelsson and Jonsson, 1980, Samuelsson and Jonsson, 1981, Samuelsson, 1981) in detail in the literature. The electrochemical gradient created by DC in the tissue causes electro-osmosis (Reuss, 1809, Nordenstrom, 1983) and chemical necrosis through the creation of gases and sodium hydroxide at the cathode.
The amount of direct current and the time of application of direct current in the pre – RF phase have an impact on the size of the ablation zone, as demonstrated by the results of the ex-vivo study (Appendix 1-Table 2.3). This relationship is not a linear one and the size of the ablation zone is impacted by the time of DC application to a certain extent, however more importantly is influenced by the DC power applied (volts).
Cockburn et al (Cockburn et al, 2007) demonstrated a linear relationship of ablation zone size and time of pre – RF DC up to 600 seconds, thereafter there was no significant difference in ablation zone size when DC was applied for longer than 600 seconds.
9 volts of DC was applied in the study.
The purpose of this study was to determine the parameters, which would create the largest ablation zone, varying both the DC pre time and the DC voltage. The size of the ablation zone increased with increasing DC voltage to 9 volts, however the ablation zone decreased in size when 18 and 36 volts were applied to the tissue, irrespective of the time of pre DC (Appendix1-Table 2.3).

The size of the ablation zone increased with increasing pre – RF DC time to 10 minutes, but there was no increase in the ablation zone sizes with 15 and 30 minutes respectively (Appendix 1-Table 2.3). An interesting observation was the destruction of the tissue immediately adjacent to the electrode. The destruction of the tissue was not due to excessive charring or burning of the tissue, but rather it appeared the destruction was due to chemical necrosis of the tissue (Figure 2.7).

Figure 2.7 demonstrates a central linear area of chemical necrosis representing tissue immediately adjacent to the electrode. No RF energy could be delivered to the tissue due to the extensive liquefactive necrosis along the electrode.

This only appeared to occur with high DC voltages (18 and 36 volts) and long DC times (15 and 30 minutes). This correlates with the chemical necrosis described (Wemyss-Holden et al, 2000b) in the literature, however this phenomenon associated with DC application and subsequent RF ablation has not been described previously. The most likely cause of this phenomenon is the chemical necrosis caused by the DC followed by heating of the tissue (Samuelsson and Jonsson, 1980, Samuelsson and Jonsson, 1981), causing the tissue immediately adjacent to the electrode to liquefy. A theory for the decreasing ablation zone sizes at these high DC voltages with long pre – RF DC times may be a result of excessive toxic gas release at the cathode causing rapid necrosis of the tissue adjacent to the electrode.

The most extreme of these observations was at 36 volts with 30 minutes of pre – RF DC. At this extreme, no radiofrequency energy was deposited in the tissue, and roll – off occurred within seconds of radiofrequency energy being applied. Dissection of the block of liver revealed a large 'cavernous' tube along the length of the electrode (Figure 2.7) with no ablated liver tissue. The liver adjacent to the electrode appeared discoloured with thick liquid replacing the normal liver adjacent to the electrode. This had the appearance of necrotic liquefied liver parenchyma. The results of the *ex vivo* study demonstrate the ablation zones to be the largest with no pre – RF DC at 9 volts which is in contradiction to the results published by Cockburn et al (Cockburn et al, 2007) where the ablation zone was larger following 600 seconds of pre - RF DC. In this study the mean ablation diameters for 300 seconds and 600 seconds of pre – RF DC were not significantly different,. This finding does not decrease the significance of Cockburn et al's early work with BETA; it must be borne in mind, the number of experiments performed using the parameters in the current study were larger than those published in the 2007 paper.

The most significant observation in the study was the effect of applying no pre – RF DC to the tissue, and applying DC and RF simultaneously.
This observation proved to be statistically significant when compared to the controls for the same RF power (Table 2.10), but no statistical significance was observed between the ablation zones where no pre – RF DC was delivered and where 300 and 600 seconds of pre – RF DC was delivered (Tables 2.11 and 2.12).

This observation means the treatment time could be decreased by at least 5 minutes without decreasing the size of the ablation zone significantly.
This important observation may prove to be extremely important in the application of BETA in the clinical scenario. Electrolysis is a slow process, which is one of the cardinal reasons for it not being adopted as a method of tumour ablation.

Effect of RF Power

RF power refers to the amount of milli-ampheres (mA) delivered to the tissue. The mA delivered is dependant on Ohm's Law, which described mathematically:

$$\mathbf{V = I \times R}$$

The RF power or current (I) is dependant on the relationship between the voltage of RF delivered and the resistance in the liver tissue. The computer software adjusts the RF wattage

and the RF voltage according to the impedance in the liver in order to maintain the current delivered.

The impedance of the liver fluctuated depending on the temperature of the liver and the age of the liver. A high impedance in the liver resulted in a high RF wattage and RF voltage for a given RF current. With a very high RF wattage, the liver ablated too quickly and the resultant ablation zone was smaller than expected. Cool liver temperatures (<20 °C) resulted in high liver impedances (>100 ohms) and livers, which were older than 3 days, resulted in high impedances (>100 ohms). The reasons for this are unknown. However, given the findings early in the study, only livers a maximum of 48 hrs old were used. This was relayed to the butcher supplying livers and this was then conveyed to the abattoir. Later in the study, the livers were vacuum packed as soon as they were removed from the animal, ensuring maximum preservation of the tissue. The temperature findings, however relate to the literature in terms of temperatures of the *ex vivo* liver. Lee et al (Lee et al, 2005, Lee et al, 2006, Lee et al, 2006) utilised the same methodology for his *ex vivo* experiments as was used throughout the *ex vivo* work of this research. Room temperature saline baths were utilised throughout the study and the livers, once cut into the blocks to be used for the experiments warmed up to room temperature extremely quickly. Some authors used frozen livers, which were thawed overnight and used for experiment at temperatures of 18-22 °C (Mertyna et al, 2007). I did not need to freeze livers as I had a dependable source of fresh, chilled livers.

The RF parameters set out in the matrix were modified early on in the study, as the largest mA achieved given liver impedances of between 70 and 80 ohms was 1000mA. 1500 and 200mA were not achievable due to the design of the BETA machine and a lack of sufficient RF voltage in the machine needed to achieve these high powers.
Radiofrequency settings of 500, 750 and 1000mA were tested (Table 2.4). As radiofrequency power increased, above 600mA, the size of the ablation zone decreased. This finding is not in keeping with the findings of Solazzo (Solazzo et al, 2007) or Goldberg (Goldberg et al, 1998a), however Solazzo et al achieved large ablation diameters using a pulsed algorithm. Rhim et al (Rhim et al, 2001) described a new generation of ablation machines which had RF power capabilities of more than 150 W, in order to deposit more energy in the tissue, however the findings in this study demonstrate a decreasing ablation zone size with RF power of 750 and 1000mA. This may be due to the lack of impedance feedback algorithms present in all of the commercially available ablation devices. Impedance feedback allows the machine to adjust its settings in order to continue to deliver a set amount of RF power (watts) to the tissue. In this way, the RF current and RF voltage will be reduced in order for the machine to deliver adequate RF power. Our machine allowed only the RF current to be set and once the ablation cycle had

commenced, the software program adjusted the RF power and voltage in accordance with the changing impedance of the liver.

500mA produced the largest ablation zones, however the roll off using 500mA was often extremely lengthy (>45 minutes). This in a clinical context would not be clinically effective, given an ablation zone using 600mA would be of similar size, but taking half the time to achieve (Appendix 1-Table 2.3). Following completion of each parameter of the original matrix (n = 6), achieving an 80% power statistically, parameters were repeated using 600mA as the RF power.

This proved to produce a large ablation zone (Table 2.10) compared with controls, with no statistical difference between the mean ablation diameter produced at 500mA and 600mA (Table 2.7).

Parameters at 600mA were then repeated in order to determine whether any statistical difference could be determined between simultaneous RF and DC only, and pre – RF DC deliver for 300 and 600 seconds.
The results of this revealed no statistical difference (Table 2.11-2.13).

The Effect of simultaneous RF and DC delivery

Simultaneous RF and DC delivery alone, without any pre – RF DC delivery produced similar ablation zone sizes to those ablations where DC was delivered in the pre – RF phase and then simultaneously with RF. The difference in ablation zone sizes was not significant (Table 2.11-2.13).
Simultaneous RF and DC delivery appeared to produce the same effects in the liver regarding electroosmosis with simultaneous RF delivery as long as the ablation continued for a sufficient period of time. The period of time needed for the effects of the DC to become apparent was 600 seconds. Ablation that rolled off before 600 seconds were smaller and there was resistance to the electrode being removed from the tissue. In these instances, adherent liver was found on the electrode, similar to the observations in the control group, where RF was applied in isolation without any DC. In these groups, the charred liver adhered to the electrode and only through force and damage to the liver could the electrode be removed, however significant liver tissue adhered to the electrode in these controls (Figure 2.8).

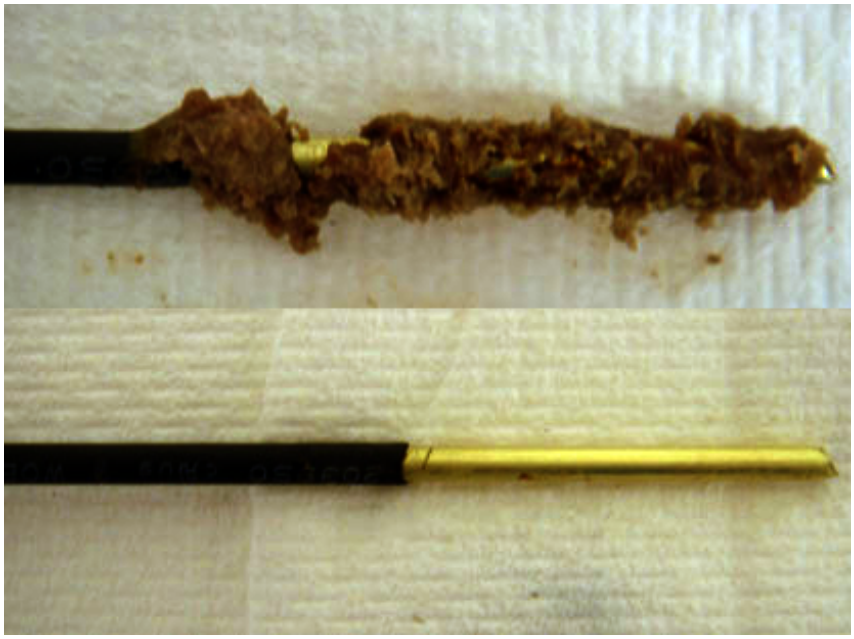

Figure 2.8 charred adherent tissue following conventional RFA (top) and the appearance of the needle following BETA (bottom)

This finding is common with conventional RFA and was highlighted by Cockburn et al (Cockburn et al, 2007). This often leads to trauma to the liver tissue and although not described in the paper, Wemyss-Holden described the site of needle entry into the liver bleeding post ablation, whereas this did not occur following BETA.

Figure 2.9 Conventional RFA (left) demonstrating a smaller ablation zone with the needle track (arrowheads) removed completely due to adherence to the electrode. BETA (right) demonstrating a larger ablation zone and the blackened tissue, (white arrows) which remains insitu with electrode removal.

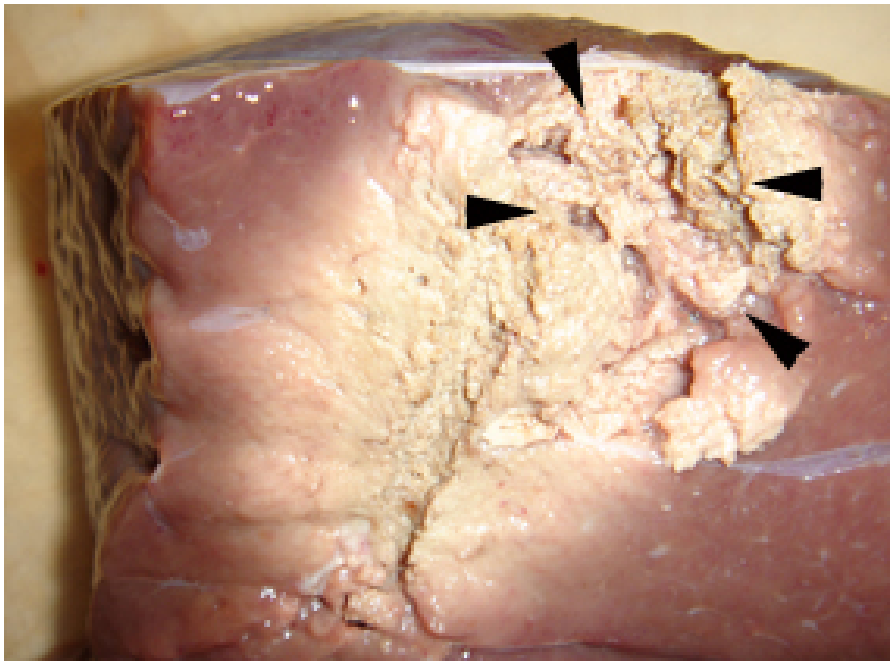

Figure 2.10 damaged liver (arrowheads) resulting from needle removal following conventional RFA.

The haemorrhage was not significant and was easily controlled. However, in percutaneous treatments, direct visualisation of the surface of the liver does not occur and therefore any haemorrhage will not be clinically apparent until it causes signs such as hypotension and tachycardia.

Given the effects of DC, ablations with a run off of less than 600 seconds, encountered with RF parameters of 750 and 1000mA had similar results with liver adherent to the needle, however this was significantly less than the effects seen with RF ablation alone. This was not seen using RF parameters of 500 and 600mA as the run off for these parameters was in excess of 600 seconds. The chemical reaction occurring at the cathode as described by Samuelsson and Jonsson (Samuelsson and Jonsson, 1980, Samuelsson, 1981) with hydrogen formation occurred in all experiments. This reaction could be observed visually with gas bubble formation at the cathode (Figure 2.11).

Figure 2.11 gas bubble formation at the cathode during BETA

Ablation zone sizes were not statistically significant when 18 or 36 volts of DC was applied simultaneously with RF ablation. The damage observed with long periods of 36 volts as described earlier was not seen (Figure 2.7). Given the potential for tissue damage with high voltages and the results of the ablations using 9, 18 and 36 volts (Appendix 1-Table 2.3), no benefit to using more than 9 volts is seen. This is in keeping with finding by Nordenstrom (Nordenstrom, 1983). A further phenomenon described by Cockburn et al (Cockburn et al, 2007) is the swelling of the liver adjacent to the electrode (Figure 2.12). This is again only seen with BETA and not conventional RFA.

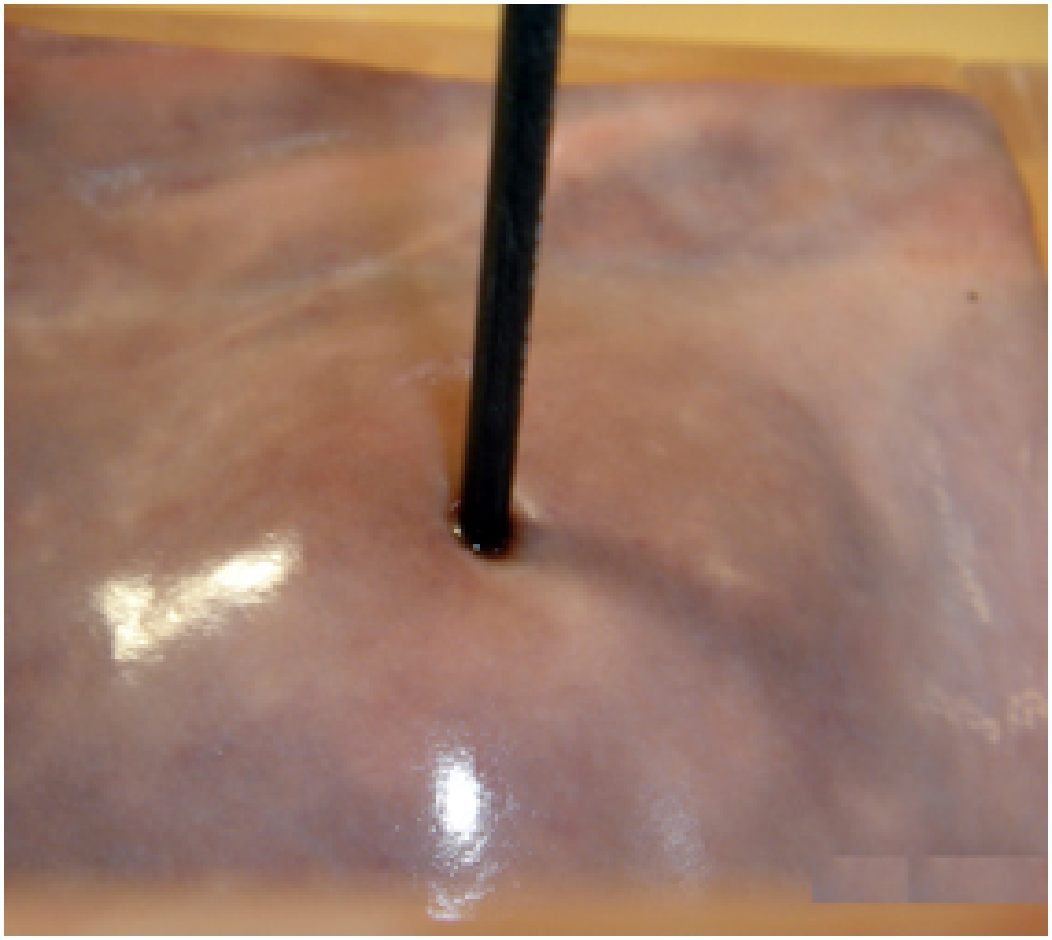

Figure 2.12 Swelling on the surface of the liver observed with BETA

A hypothesis for this is the increase in hydration of the liver due to electroosmosis. This is discussed in Chapter 3 in more detail.

Limitations of Research:

Limitations to this research model were identified, however I did not feel the results were influenced significantly by these limitations.

1. The tissue used for the *ex vivo* studies was bovine liver. The tissue used for the *in vivo* work was porcine. Although the tissue type differed, the reason for using the bovine livers as opposed to porcine livers was primarily the larger size of the bovine livers and therefore the ability to utilize more tissue for ablation per liver.

2. The porcine liver, as discussed in chapter 5 has 3 lobes, which limits the amount of tissue available to create large ablation zones. The bovine liver has a large right lobe, similar to the human liver, which allows for larger ablation zones.

3. The fluid medium used for transmission of current in the bath during all experiments was tap water with NaCl added, in order to obtain 0.9% saline. This fluid medium is not physiological and therefore could, in theory affect the results, due to conventional osmosis into the liver. The livers were placed in the saline bath, only to allow for electrical conduction and each experiment was conducted in the same way, each control ablation and BETA was performed using the same experimental design and therefore each liver was exposed to the same amount of fluid medium. The reason I decided to use normal saline was due to the fact that the water needed changing regularly throughout the day in order to maintain the temperature and replacing it with physiological saline was not thought to be practical.
   The saline bath was maintained between 26 and 30 °C. This is not core body temperature, however the temperature dropped in the saline bath relatively quickly and it was not felt to be practical to maintain the water at 37 °C due to the added complexity of a water heater and the lack of water circulation in the batch, which would lead to vast temperature differences in different parts of the saline bath.

During the study design I decided on the 26-30 range for practicality, however a number of studies in the literature use cool water (Mertyna et al, 2007), which undoubtedly affect the ablation zone size as discussed earlier in this chapter.
The convention in the literature is to utilise liver in the temperature range 25-30 °C (Lee et al, 2005, Lee et al, 2006, Lee et al, 2006), and I thought this to be the most practical, although the ideal would have been body temperature livers.

Conclusions:

1) BETA produces larger ablation zones in *ex vivo* liver compared to controls using the same RF power.

2) There is no statistically significant difference between the ablation zone sizes produced with simultaneous RF and DC alone compared to those produced with 300 or 600 seconds of pre – RF DC.

3) 9 Volts of DC current produces the largest ablation zones. 18 and 36 volts cause chemical necrosis of the tissue immediately adjacent to the electrode, with this becoming significant with long periods of pre – RF DC (30 mins).

4) No statistical difference is seen comparing the ablation zone sizes produced with 18 and 36 volts with no pre – RF DC, compared to 9 volts.

5) 600mA produced similar BETA zone sizes to 500mA BETA zones, but the ablation is completed in almost half the time with 600mA compared to 500mA.

6) The ideal parameter for producing a large ablation zone in reasonable time is 9 volts of direct current combined with 600mA of RF power simultaneously, with no pre – RF direct current delivery.

Chapter 3:

Bimodal Electric Tissue Ablation:

Hydration Studies.

Introduction:

General.

BETA combines direct current and radiofrequency ablation increasing the resultant ablation volume when compared to controls.

The hypothesis of this study is based on the evidence described by Nordenstrom (Nordenstrom, 1983). Direct current applied to the radiofrequency circuit polarises the electrode and the grounding pad, creating an anode and a cathode. The electrical current passing between the anode and cathode creates an electrochemical gradient known as an electroosmotic gradient (Nordenstrom, 1983). This electroosmotic gradient was first described by FF Reuss (Reuss, 1809) in 1809.

Electroosmosis:

Frederick Reuss first described the process of movement of water molecules from the cathode to the anode - termed Electroosmosis (Reuss, 1809) in 1809 in the Proceedings of the Imperial Society of Naturalists of Moscow. Reuss demonstrated that when influenced by an externally applied electric field, water migrated through porous clay diaphragms to the cathode. This finding was understood then to be the result of clay, sand and other mineral particles carrying negative surface charges when in contact with water. A charged surface will attract positive ions present in water and repel negative ions. The positive ions predominate next to the charged surface, hence application of an electric field results in a net migration towards the cathode. Electroosmosis has been used extensively in mining and construction, as a method of dewatering soil (Probstein, 1994).

It is its qualities of attracting of water to the cathode that provides the basis of BETA. Nordenstrom described in detail the theory of electroosmosis in necrotic tissue (Nordenstrom, 1983). Necrotic tissue increases in weight early on in the autolytic process due to accumulation of calcium in the tissue. Measurements of ionic concentration in necrotic tissue show that the weight and the swelling seen are due to an influx of water, sodium and chloride ions. Necrosis leads to the release of proteolytic enzymes, which increase the osmotic properties of the tissue, this causes water to enter the tissue due to the osmotic gradient created. A space between cells (the intercellular space) allows water and solutes to accumulate and is essential to cellular function. As water and solutes move into cells from the intercellular space, the space is filled by further water and solutes. Attractive forces between cells decrease as cells begin to undergo autolysis, which further increases the intercellular spaces. The structural features of water depend greatly on its ability to form bonds between the electrons of its hydrogen and oxygen atoms. In ice, the lowest energy level of water, the hydrogen bonded clusters form tetrahedrons.

As ice melts the tetrahedron bonds decrease with the increasing energy content of liquid water. Triple, double and unbonded water molecules increase in number as the tetrahedron bonds break, as water approaches vapour these decrease even more in number to the highest energy state of water vapour. There is a significant difference in energy between a tetra bonded water molecule and an unbonded one; the estimate is in the region of 2.7kcal/mole (Nordenstrom, 1983). Water possesses a permanent dipole moment and orientates itself in an electric field. This dipole moment also develops when the molecule is exposed to an electric field.
Water transport by means of fixed electrical charges was demonstrated by an experiment using cotton wool in a glass U-tube. The cotton wool was packed in the bend of the tube to form small "capillaries". The spaces between the cotton fibres served as channels, similar to intercellular spaces. Water is poured into the tube and platinum electrodes immersed in the water. As an electrical potential is applied between the two electrodes, water moves from the positive to the negative side of the system until equilibrium is reached between the hydrostatic and electroosmotic pressures. The flow of water against the hydrostatic pressure is a form of "active" transport (transport against an energy gradient). This transport of water (referred to as Type I electroosmotic water transport by Nordenstrom) is able to take place without the concomitant electrolysis of the water molecules.

Type I Electroosmosis.

If an electric field is strong enough to break up water molecules clustered together, the molecules undergo "structuring" or field orientation. The dimensions of the matrix of "capillaries" are important, as they must be small enough to prevent hydrostatic return of the water molecules. If these conditions are met, water will move with the electrical field in a predictable way. The direction of water flow in electroosmosis is determined by the surplus of fixed charges of the capilliaries in the electric field. The rate of transport of the water however depends on several factors: the magnitude of the electric field, the porosity of the membrane (the number and size of the pores) and the magnitude, density and geometry of the fixed charges. If the electric field is placed close to the membrane or matrix, the electric field is strengthened. Capillary channels also play an important role in water transport and equilibrium. If capillary channels are too large, the hydrostatic pressure will cause water return. This effect will lengthen the time to achieve equilibrium or may prevent it completely.

Type II Electroosmosis.

Type II electroosmosis is more complex than type I, diffusion and electrophoretic migration of ions in an electric field determine where the recombined water molecules will be found. The transport mechanism of migration depends on the mobility of ions. In an experiment using litmus paper, Nordenstrom proved protons were produced at the anode and hydroxyl ions at the cathode using 10V of direct current applied to platinum electrodes soaked in water. The ions migrate in the electric field and recombine to form water. The differing mobility of the ions result in a net transport of water to the cathode. Water transport in type II electroosmosis increases as the voltage increases and occurs immediately as an electrical field is created. The dielectric induction and structure of water molecules adjacent to the anode and cathode serve as the initial prerequisites for the oxidation and reduction reactions taking place. Water molecules become orientated in an optimal way to consume electrons from the cathode and donate electrons to the anode.

The products then diffuse into the electric field, a mechanism compatible with the slow transport of OH^- and H^+ from the respective electrodes to the area of recombination, which is a barrier resistant to the passage of protons and hydroxyl ions. In the case of tissue, this area of recombination represents the cellular membrane and the intercellular space.

Type III Electroosmosis.

Type III electroosmosis depends on the behavioural differences of anions and cations. Cations may become hydrated, but anions do not (Nordenstrom, 1983). Cations carry water molecules absorbed on their surfaces when ions migrate in the electropositive part of an electric field. This is not mirrored by the anions in the opposite direction. There is thus a net electrophoretic water transport, which may be viewed as a basic form of “mediated” transport. Mediated transport refers to transport across a membrane by a membrane transport protein. In this case the cation serves as the “mediator” or carrier of the water molecule. Once the cation and water molecule enters a region of high pH (the region surrounding the cathode), the water molecule is released from the cation carrier.

Type IV Electroosmosis.

Type IV electroosmosis refers to a partial function of electroosmosis. This type of electroosmosis occurs in molecules close to a charged electrode within a matrix, which does not need to be lined with fixed charges. These inductions cause a net attraction of water to any charged electrode, regardless of its polarity.

Pressure changes and Electroosmosis.

An important question is whether electroosmosis can occur at low voltages, voltages low enough not to create electrolysis of water. Helmholtz observed electrolysis at 1.64V in 1879 and Bartoli at 1.23V in 1978 (Nordenstrom, 1983). H_3O^+ and its polymers form with type III electroosmosis that are connected with the transport of water during electrolysis, transport pressures play an important role during electrolysis and Nordenstrom conducted experiments in order to understand this behaviour further. His experiments using cotton wool in a U tube revealed a linear relationship between the rising voltage and hydrostatic pressure.

Nordenstrom applied 20V of current for 2 minutes each to electrodes in the U-tube. The results showed two pressure phases, the first, a slow pressure phase that occurred due to gas formation at the electrodes as discussed previously. The slow pressure phase is only observed at higher voltages. The second phase, the rapid pressure phase is observed at both high and low voltages (0.4V up to 20V) (Nordenstrom, 1983).

Given these findings related to pressure change, Nordenstrom described the four types of electroosmosis in terms of pressure.

Type I is characterised by its dependence on a surplus of fixed negative or positive charges, otherwise referred to as “fixed charge electroosmosis”. The rapid change of pressure correlates directly with the magnitude of the voltage applied across a matrix.

Type II electroosmosis can also be described as “electroosmosis by ionic recombination” and does not require fixed charges in the matrix. Type II involves electrolysis of water, diffusion and migration of H^+ and OH^- and the recombination into water. The elevation of pressure in type II is slow and not related to the magnitude of the voltage applied.

Type III electroosmosis is closely related to type II; its mechanism is based on ionic hydration of cations only. Cations carry water and water polymers from the electropositive to the electronegative part of the field. Type III electroosmosis can be described as “cationic electroosmosis”.

Type IV electroosmosis occurs close to charged electrodes which produce an attractive force on close water molecules by induction. In this type of electroosmosis the water molecules move to the closest electrode regardless of the polarity. Type IV electroosmosis can be described as “field-induced osmosis” and can be regarded as a special case of type I electroosmosis, where in type IV electroosmosis, the charged electrodes include the functions of the applied field and fixed charges.

Nordenstrom went on to prove this in human and animal tissue, using lung tissue to replace the cotton wool in his initial experiments. These electroosmotic experiments revealed the human and animal lung behaved in exactly the same way as cotton wool.

BETA produces a significantly larger ablation zone than standard RFA (Chapter 2). The hypothesis of this is the production of a cathodic electrode and the net movement of water to the cathode during the ablation cycle. This net movement of water keeps the tissue hydrated and thus allows for larger ablation zones.

The theory of electroosmosis has been proven by Nordenstrom et al, but demonstration of ablated tissue of higher hydration post ablation compared to standard RF was essential in proving our hypothesis of electroosmosis as a cause for the larger ablation zone observed with BETA. The effects of DC on tissue have been described in chapter 2. These observations are well described in the literature (Samuelsson and Jonsson, 1980, Nordenstrom, 1983). The hydration of tissue post ablation, has only recently been described in the literature (Brace et al, 2010).

Objective:

The objective of this study is to prove electroosmosis to be responsible for the increased size of the ablation zone obtained with BETA, by proving an increase in mean tissue hydration of ablated tissue following the application of BETA.

Materials and Methods:

Liver.

The liver used in this study was prepared for the ablation process as outlined in Chapter 2.
Following the ablation process as outlined in Chapter 2, a brass rod was placed along the ablation path in the liver created by the ablation electrode. The 10 x 10 x 10 cm block of liver was removed from the Perspex box with the brass rod in situ and placed onto a plastic cutting board.
A sharp knife was used to cut along the brass rod, parallel to the direction of the ablation electrode in order to determine the longest ablation diameter.
Following measurement for volume calculation, a sharp scalpel (no. 11) was used to remove four equal sizes of ablated tissue for hydration analysis 0.5 cm from the centre of the trough created by the ablation electrode at 12, 3, 6 and 9 o'clock.
The measurement was taken perpendicular to the long axis of the ablation volume, at the level of the longest short axis measurement.
Four equal sizes of ablated liver were removed from the ablated liver volume, each piece from a distance of 0.5cm from the centre of the trough created by the ablation needle. This was to ensure enough tissue could be taken for hydration analysis and that the areas of sample could be reproduced in either control or experimental liver samples.
Each of the four samples measured 0.5 x 0.5 x 2cm and had a combined minimum weight of 5 grams.
The samples were placed immediately into the sample pan of the hydration analyser for hydration measurement. The remainder of the liver was then discarded.

Moisture Analyser.

The device used for moisture analysis is a commercially available moisture analyser (MAC 50/1, Radwag, Radom, Poland) (Figure 5.1).
The MAC series of moisture analysers are designed to provide the user with a variety of maximum weights of samples for analysis, with a differing degree of accuracy at each extreme for each of the MAC analysers.
Following discussion with the technical department in Poland a MAC 50/1 moisture analyser was purchased for moisture analysis of the ablated liver samples.
The MAC 50/1 (Figure 5.1) has a maximum drying capacity of 50g, which also represents the calibration weight of the machine. The reading unit measures to 0.1mg (0.0001g) with an accuracy of 0.001% for measurements greater than 1.5g. The drying chamber measures 120 x 120 x 20mm with a disposable aluminum drying pan measuring 90mm in diameter. The

maximum drying temperature is 160 °C, with the option of increasing the drying temperature to 250 °C, however the manufacturer did not recommend this. The moisture analyser is sold with both a conformity declaration for safety and electromagnetic stability. The MAC analyser has a large LCD which provides the user with information regarding ambient temperature within the drying chamber, elapsed time of the drying process, the program number and information regarding the sample itself including weight changes and hydration status expressed in percentages (Figure 5.2), this will be discussed in more detail.

Figure 5.1 the Radwag MAC 50/1. Heating element (white arrow), disposable tray (white arrowhead) and LCD display (grey arrowhead)

Figure 5.2 Hydration analyser during the drying process. The heating element raises the temperature in the drying chamber (white arrowhead); the temperature within the drying chamber is displayed on the LCD screen (grey arrow) together with the elapsed time (white arrow), mass reading (black arrow) and the cycle setting (white arrowhead).

Machine Calibration.

Prior to first use, the manufacturer recommends calibration of the machine regarding temperature measurement and weight measurement. Following initial calibration of the machine, the analyser is to be placed on a level surface. Individually raising or lowering the back footrests of the machine can adjust the exact position of the analyser. The machine contains a small circular spirit level, which indicates the exact orientation of the machine on the surface. The machine footrests must be adjusted until the spirit level is in the centre of the circle, indicating an exact level position. The machine has an optimum function with an ambient room temperature of 15 – 40 °C and humidity not in excess of 80% at 31 °C and 50% at 40 °C. The temperature and humidity of the laboratory are centrally controlled and do not exceed these recommendations.

Temperature.

The manufacturer, on initial use and weekly recommends temperature calibration. Thereafter or following prolonged inactivity of the machine (more than 3 weeks) or following transport of the machine. On initial setup, the analyser undergoes a temperature stabilisation period or self-heating period, which may last up to 4 hours. This is an automated feature.

Temperature calibration requires a separate thermometer, which can withstand temperatures in excess of 160 °C. A thermometer is placed into the drying chamber through a small aperture in the drying chamber window. The temperature calibration process is initiated on the machine and the user is required to increase or decrease the temperature display on the machine according to the external thermometer reading in order to calibrate the internal thermometer. This process lasts 15 minutes.

Following temperature calibration, the data must be saved and the analyser recalibrated weekly.

Weight.

The scale of the analyser was calibrated daily due to the importance of weight measurement in the hydration analysis. A machined 50g weight was used for this purpose. The weight calibration process was initiated on the machine and the 50g weight placed in the centre of the drying pan. The machine self calibrated according to the known weight of the machined 50g weight. The accuracy of the scale could be easily checked thereafter throughout the day by means of a calibration test. This was conducted after each hydration analysis. The 50g weight is placed in the centre of the drying pan and the machine calculates a difference between the known weight and the measured weight and displays this difference to an accuracy of 0.0001g. If the accuracy is less than 0.00001g, the machine scale must be recalibrated.

Hydration Analysis.

Three separate drying programs are available to the user on the MAC series: manual, automatic and time defined. The automatic setting ends the moisture analysis once the sample does not undergo a weight change for intervals of 20, 50, 120, 180 or 240 seconds, depending on the degree of accuracy required. An interval of 120 seconds is recommended for solid foods, achieving an accuracy of 0.001%. The automatic analysis must be further defined by means of the maximum chamber drying temperature and the drying profile. The maximum drying temperature was not adjusted and was left at 160 °C. The drying profiles consist of the following:

1. Standard profile – rapid heating to 160 °C.
2. Quick profile – rapid intense heating in a short period of time. The drying temperature is increased to 30 °C above the maximum set (160 °C) for 180 seconds, after which the temperature decreases to the set temperature chosen.
3. Mild Profile – Temperature increases to maximum in t_1, where the user predefines t_1.
4. Step Profile – Temperature increases in steps tmp_1, tmp_2, tmp_{max}, at intervals t_1, t_2, t_3. The user determines each of these variables.

A standard drying profile was chosen for the hydration analysis.

Hydration Analysis Display.

An LCD (Figure 5.2) displayed the elapsed time of the drying process, the drying profile, the maximum temperature and the weight interval setting chosen.

A large set of LCD numbers in the centre of the display changed continually throughout the drying process indicating the following changes to the sample:

- $\%^M$ - Percentage weight loss of the sample
- $\%^D$ – Part of dry mass received in drying process in percent. This is part of the sample, which remained on the pan following humid evaporation.
- $\%^R$ – Humid/dry mass ratio in percent. This is the part of the sample, which vaporised during drying and correlates with the $\%^M$.
- g – mass change. The mass of change registered during the drying process.

The most important of these parameters is the $\%^M$. This indicates the percentage of weight loss of the sample, through the drying process, which correlates with the water content of the sample. The larger the $\%^M$, the greater the moisture content of the sample.

Drying Process.

Following removal of the four pieces of ablated liver from the block of liver, the hydration analyser was zeroed and the four pieces placed in the centre of the drying pan. As soon as the lid of the drying chamber was closed, the drying process was initialised automatically. A circular halogen lamp heated the sample continually (Figure 5.1). The machine measures changes in weight of the sample continually with an accuracy of 0.0001g. For this study an automatic cut-off setting of 3 was chosen. This setting dictates the machine measures the sample continually, until there is no weight change in the sample for 120 seconds. The lack of weight change indicates complete desiccation of the sample (Figure 5.3). The program terminates and the results of the drying process, namely $\%^{M}$, $\%^{R}$, $\%^{D}$ and g are displayed on the LCD. These results were recorded in the research folder and on an excel spreadsheet.

Figure 5.3 Fresh unablated liver (left) and liver following complete dehydration process

The following ablation parameters were tested for percentage hydration.

- Normal unablated liver as reference.
- 600mA of RFA – Control
- No pre – RF DC, 600mA of RFA with 9V of simultaneous DC.
- 300 seconds of pre – RF DC and 600mA of RFA with 9V of simultaneous DC.
- 600 seconds of pre – RF DC and 600mA of RFA with 9V of simultaneous DC.

Results.

The results are expressed as means ± standard deviation (SD) for normally distributed variables or the median and the interquartile range for non-normal variables. Differences in hydration percentage between tissue receiving standard RFA or BETA were tested with ANOVA. A *P* value <0.05 was considered statistically significant. SPSS 17 was used for all statistical data analysis. The hydration is quoted in percentage and sizes quoted refer to the maximum short axis measurement of the ablation zone unless specified.

A total of 75 experiments were conducted (n=15).
Normal liver hydration was tested in addition to each ablation group (n=15).
Prior to each hydration analysis, the ablation zone was measured for maximum short axis diameter and scrutinised using the ANOVA test.

Hydration Studies

Groups	N	Mean (%)	SD	SEM	95% Confidence Interval for Mean		Min (%)	Max (%)
					Lower Bound	Upper Bound		
Normal Liver	**15**	**72.19**	**2.65**	**0.68**	**70.73**	**73.66**	**68.16**	**77.99**
Standard RFA Control	**15**	**46.91**	**2.91**	**0.75**	**45.29**	**48.52**	**42.38**	**53.31**
9V-600mA BETA	**15**	**51.54**	**3.98**	**1.03**	**49.33**	**53.74**	**40.44**	**56.57**
300s 9V-600mA BETA	**15**	**51.61**	**3.16**	**0.82**	**49.86**	**53.36**	**46.53**	**57.01**
600s 9V-600mA BETA	**15**	**52.25**	**2.62**	**0.68**	**50.8**	**53.7**	**47.72**	**56.39**
Total	**75**	**54.9**	**9.41**	**1.09**	**52.73**	**57.06**	**40.44**	**77.99**

Table 3.1 demonstrates each group, with the corresponding values obtained from the hydration analyser. The mean percentage hydration following ablation is tabulated for each parameter with the associated standard deviation (SD), range and the standard error of the mean (SEM).

The intergroup analysis demonstrated a significant difference between the control group and the group with no DC pre-treatment ($p < 0.001$) (Table 3.3).
The intergroup analysis did not demonstrate a significant difference between the groups treated with 300 seconds or 600 seconds of pre RF DC ($p = 0.55$) or between the 600 seconds pre-treatment group and the group with no pre RF DC ($p = 0.56$) and between the 300 seconds pre-treatment group and the group with no pre-treatment ($p = 0.953$).

Graph 3.1 demonstrates the range of hydration percentages for the control group, the experimental groups and for normal unablated liver for reference, with corresponding error bars.
Graph 3.2 demonstrates the mean hydration percentages for the control group, the experimental groups and for normal unablated liver for reference, with corresponding error bars.

Appendix 2:
Tables 3.2 – 3.6 demonstrate the results of each hydration experiment.
The percentage of weight loss registered during drying process – water content (%M), percentage of the sample which remained on the pan after humid evaporation - solid tissue content (%D), the humid/dry mass ratio - part of sample which vaporised during drying process (%R) and residual mass (g) are tabulated in each experiment.

Table 3.7 - explanation of the parameters for each experiment.

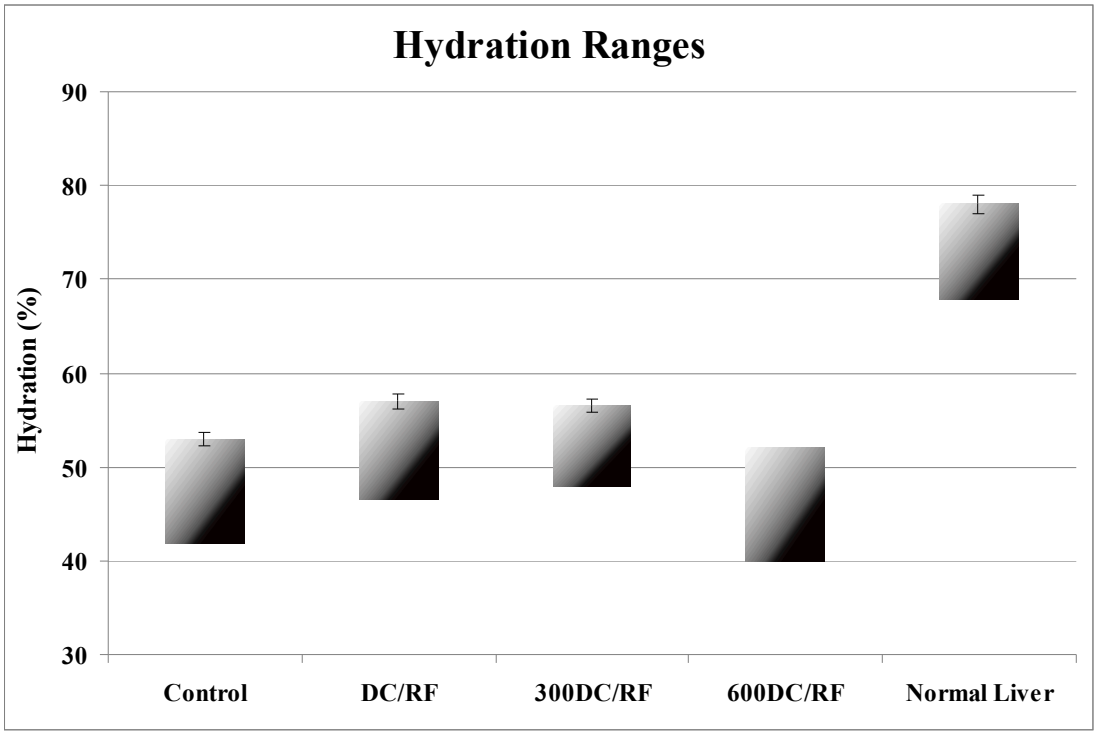

Graph 3.1 The range of hydration percentages for the control group, the experimental groups and for normal unablated liver for reference, with corresponding error bars.

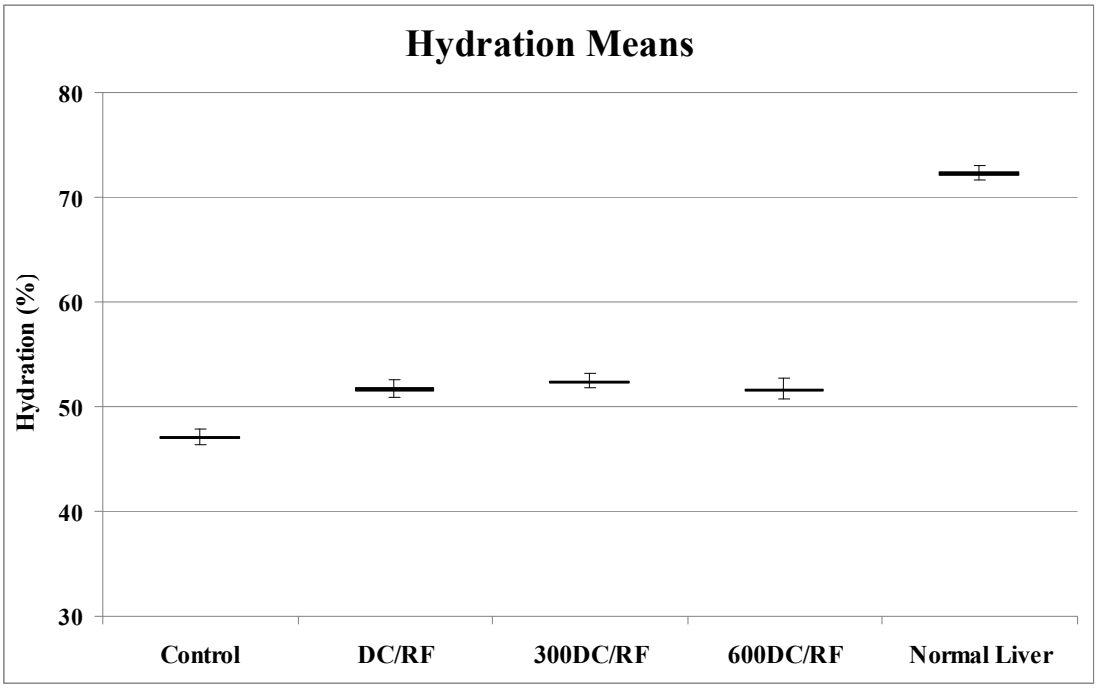

Graph 3.2 The mean hydration percentages for the control group, the experimental groups and for normal unablated liver for reference, with corresponding error bars.

Discussion.

Introduction.

In Chapter 2, the results of *ex vivo* BETA compared to control RFA were described.

The ability of BETA to produce large ablation zones is due to the polarisation of the ablation electrode and its effects on the surrounding tissue (Samuelsson and Jonsson, 1980, Samuelsson and Jonsson, 1981, Nordenstrom, 1983). The chemical necrosis caused in the tissue is due to the formation of gases at both the anode and cathode (Samuelsson and Jonsson, 1980, Samuelsson and Jonsson, 1981) and has been discussed. The effects of electrolysis in inducing chemical necrosis have been described (Wemyss-Holden et al, 2000a, Wemyss-Holden et al, 2000b, Wemyss-Holden et al, 2002) in detail in the literature. The role of electroosmosis in maintaining the hydration of liver during ablation with radiofrequency energy however has not been described in the literature.

General.

Electrolysis in tissue polarises the tissue at the anode and cathode causing liberation of gases at each electrode (Samuelsson and Jonsson, 1980). The paper in 1980 described the volumes and relationship of gas formation to the current delivered. The minimum voltage for chlorine gas formation at the anode was 1.5V (Samuelsson and Jonsson, 1980).
Electroosmosis was well described by Nordenstrom (Nordenstrom, 1983) using a series of experiments in a U-tube and later in tissue.

The key limitation of radiofrequency ablation is the charring of tissue immediately adjacent to the needle (Goldberg et al, 1996a, Goldberg et al, 1996b). The initial observation of BETA by Cockburn and Wemyss-Holden was the lack of charring of the needle and the ease of removal of the needle from the tissue. This finding was highlighted in their paper in 2007 (Cockburn et al, 2007). The theory behind this lack of charring was that of electroosmosis.
During the development of the Mark II machine, it was thought the hydration could be measured during the ablation cycle.
The ablation machine manufactured by EG Technology (Cambridge, United Kingdom) originally had specifications which included four hydration analysers. These analysers consisted of four stainless steel rods, arranged in parallel, which acted as resistors in the tissue. The software program could be manipulated to measure the resistance in the tissue at specified intervals from every second, to 200-second intervals. During the resistance measurements, the

radiofrequency and the direct current were switched off; this interval lasted 100 milliseconds (ms) and allowed the tissue resistance to be determined between each of the rods. The measurements were expressed as numbers, but no units were attached to these measurements, as there was no calibration performed for the analysers. This proved to be a major stumbling block for hydration analysis initially. The lack of calibration meant that before any measurement could be taken, a constant reading would have to be quantified and regarded as the standard for which each measurement after this could be measured. Water was first used in order to obtain a reading, which was thought to be constant. The hydration/resistance analysers were placed in shallow tap water during a series of radiofrequency experiments in order to determine the resistance in water. The readings were extremely variable between each experiment and varied between each resistance electrode. The lack of a calibration device in the machine itself meant that even with reliable measurements in water, the significance of a difference in the readings received from the hydration analysers could not be interpreted.
A further limitation encountered during the hydration measurements was the temporary suspension of the ablation cycle in order to obtain a resistance measurement. The effect of this extremely short but possibly significant break in the ablation cycle was unknown, however did not appear to be compatible with a clinical scenario. The lack of calibration or consistent data readings in a constant test medium such as water lead to discussion regarding the scientific reliability of the hydration measurements obtained from the machine itself.
For this reason a request was made to the manufacturer to disconnect the hydration analysers from the machine and alternatives were looked into.

The MAC analyser proved to be the most reliable and most suited device for the hydration analysis. The machine can be easily calibrated and checked to ensure correct measurement and the data is easy to interpret.
The results of the hydration analysis show a significant difference in the hydration of the ablated tissue between control and BETA experiments. This proved the theory of electroosmosis occurring with electrolysis and the simultaneous application of radiofrequency used in BETA. We believe, given the results of Nordenstrom's work (Nordenstrom, 1983), type II electroosmosis is responsible for the hydration changes in the tissue. As the time of DC voltage application is increased, the hydration in the ablated tissue increases significantly when compared to the control ablations, however the observed increase in hydration is not significant within the groups of experiments treated with BETA, regardless of the amount of time pre-RF DC is applied to the tissue. The observations are consistent with the observations in chapter 2 with regards to the size of the ablation zone when either simultaneous DC and RF are applied or if 300 seconds or 600 seconds of pre-RF DC are applied to the tissue prior to the application of simultaneous DC and RFA. These findings, too, are in keeping with the findings of

Nordenstrom (Nordenstrom, 1983) and thus support the theory of electroosmosis in BETA.

An important observation with BETA however is the relatively consistent hydration measurements and corresponding size measurements.

The results however show no significant difference in the degree of hydration of the ablated tissue between simultaneous DC and RF only, 300 seconds of pre-RF DC and 600 seconds of pre-RF DC. This is entirely consistent with the results of the size and volume analysis of the three groups. Although there is a gradual increase in size as DC is applied for longer to the tissue, this is not statistically significant, and no scientific inference can be made from the results. The difference is purely an observational one.

Attempts to maintain the hydration in tissue during ablation have been described in the literature. These range from pretreatment with varying concentrations of saline (Livraghi et al, 1997, Ahmed et al, 2002) to the instillation of saline through an infusion electrode (Boehm et al, 2002, Burdio et al, 2003).

These techniques have been described with varying degrees of success. Ahmed et al (Ahmed et al, 2002) described pre ablation saline instillation as a bolus, however the benefits of the technique seem to only become evident with highly concentrated volumes of saline. This technique demonstrates the impact of increasing the hydration of the ablated tissue, however a significant increase in the size of the ablation zone was only evident in tumours treated with 36% saline.

This observation was not demonstrated by Freiser or Aube et al (Frieser et al, 2004, Aube et al, 2007), in contrast, both Freiser and Aube demonstrated no effect when the concentration was increased, however Freiser did demonstrate an increase in the ablation zone when the perfusion rate of saline was increased.

Boehm et al (Boehm et al, 2002) compared saline infusion to internally cooled electrodes and showed no significant difference in outcomes in animals treated with either technique.

The literature demonstrates the lack of consensus regarding whether the saline infusion rate or the concentration of saline are responsible for the increase in the size of the ablation zone. Increasing the hydration of the tissue however, does increase the size of the resultant ablation zone.

BETA, in contrast to saline infusion does not require complex infusion pumps, accurate placement of irrigation catheters or the risk of morbidity associated with multiple punctures of tissue. The debate regarding the exact mechanism of action of the saline infusion however leaves a significant question regarding its clinical application. A manufacturer (Angiodynamics, Latham, NY, USA) has adopted this saline infusion technique into their clinical application of RFA, however, to date, there is no conclusive data to support saline infusion and improved survival.

Although the exact composition of the change in electrolytes in the tissue following BETA was not examined, this does not seem to be an important factor.
The consistency of the hydration data and the correlation with the ablation zone size proves BETA to be reliable and reproducible.

Limitations of this Research:

Limitations to this research model were identified; however I did not feel the results were influenced significantly by these limitations.

The same limitations as outlined in chapter 2, with regard to the temperature of the livers and the use of normal saline as opposed to physiological saline were encountered.
The use of normal saline, particularly in this aspect of the research study may have had a more influential effect on the outcomes of the hydration studies due to the potential for osmosis and thus increased hydration in the liver. Both the control ablations using 600mA alone and the BETA experiments were conducted using the same experimental design and thus were subject to the same potential osmotic gradients. I did not feel this limitation affected the results significantly, particularly as the purpose was to determine the relationship of hydration between the experiments and the controls, rather than the absolute hydration values.

Conclusions.

1. BETA causes an increase in the hydration of ablated tissue due to type II electroosmosis.

2. The degree of hydration increases as the duration of the direct current application increases when compared to the control radiofrequency ablation hydration percentage. This is in keeping with the findings of Nordenstrom 1983.

3. There is no significant difference in the degree of hydration in liver treated with simultaneous DC and RFA, 300 seconds of pre DC or 600 seconds of pre DC.

4. The increase in hydration due to electroosmosis results in larger ablation zones.

5. The increase in hydration due to electroosmosis decreases the charring of tissue at the cathode and hence adherence of tissue to the electrode.

Chapter 4:

Bimodal Electric Tissue Ablation:

Temperature Distribution Studies.

Introduction:

General:

The distribution of heat through tissues during radiofrequency ablation (RFA) varies between tissue types (Mertyna et al, 2007). The same parameters used to ablate liver and muscle will produce differing coagulation zones. This is due to the inherent properties of the tissues and their response to heat (Figure 4.1). The margin of ablated tissue is a common site for recurrence as this region of tissue is often exposed to temperatures below 50 °C, which is the minimum amount of heat necessary to cause coagulation necrosis (Goldberg et al, 1996a, Goldberg et al, 1996b, Goldberg et al, 2000). However, this does not occur immediately in ablated tissue. Increasing the temperature to 50-55 °C shortens the time necessary to induce cytotoxicity to less than 10 minutes.

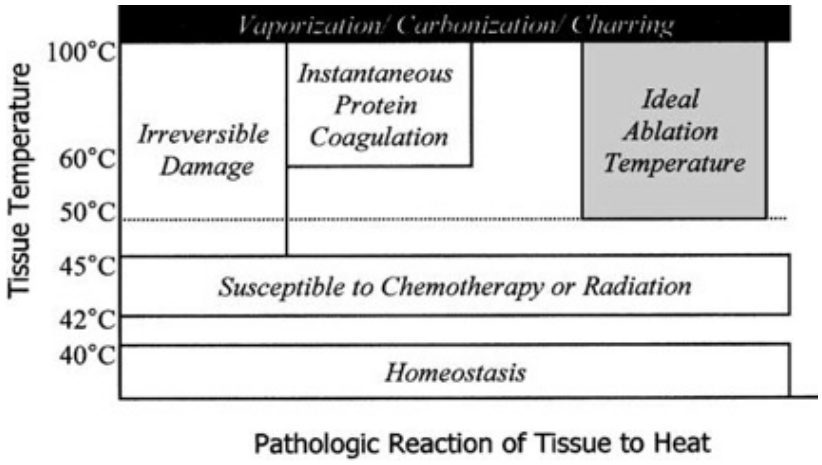

Figure 4.1 demonstrates tissue reaction to thermal ablation (Rhim et al, 2001).

Effects of heat distribution on coagulation zones:

Mertyna et al (Mertyna et al, 2007) describes varying degrees of heat distribution in tissues treated with RFA. The higher the temperature at the margin, the larger the ablation zone. The ablation margin is the most common site for tumour recurrence due to the lowering of temperatures at the periphery of the ablation zone (Figure 4.2).

The tissue at the periphery of the ablation zone reaches temperature of about 46 °C (Goldberg et al, 1998). At these temperatures, cellular homeostasis can continue, however cells become more susceptible to damage by agents such as radiotherapy and chemotherapy (Ahmed et al, 2003b, Ahmed et al, 2004, Ahmed et al, 2005)(Figure 4.1). With a mild temperature increase of 42-45 °C (hyperthermia) prolonged heating at these temperatures will not induce complete cell death. Continued cell growth and function can be observed after long exposures to hyperthermia (Goldberg et al, 1998). The tissue may appear discoloured, however the hyperthermic status does not result in cell death.

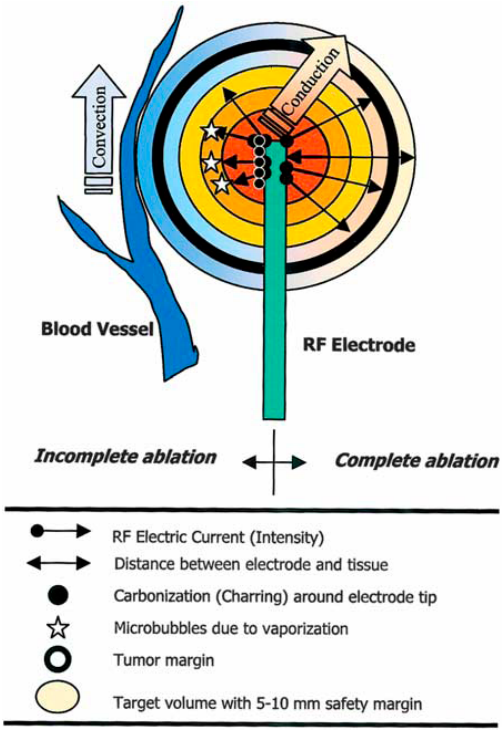

Figure 4.2 illustrates heat efficacy. In order to decrease the risk of recurrence, an effective heating target volume (the tumor with a margin of normal liver) is necessary. Increasing the amount of electric current (unidirectional arrows) can increase the heat deposition in tissue. Heat conduction decreases with increasing distance from the tip of the electrode (bidirectional arrow), microbubble formation (stars) and charring (dots) adjacent to the electrode. Heat sink due to the adjacent vessel results in insufficient heating and subsequent recurrence (Rhim et al, 2001).

A number of techniques have been employed in an attempt to increase the temperature at the periphery of the tumour. The most commonly adopted technique has been modulation of blood flow through the liver (Goldberg et al, 1998). The modulation of blood flow has been shown to increase the ablation zone (Goldberg et al, 1998, Shen et al, 2003, Horkan et al, 2004, Miyamoto et al, 2004, Hakime et al, 2007, de Baere et al, 2008, Iwamoto et al, 2008) in tissue by mechanical techniques, such as the Pringle manoeuvre (Pringle, 1908, Shen et al, 2003), pharmacological modulation of blood flow (Goldberg et al, 1998, Horkan et al, 2004) or endovascular occlusion of the hepatic artery (Goldberg et al, 1998, Horkan et al, 2004). These techniques all increase the ablation zones, when compared to RFA alone, however altering the portal blood flow by means of pharmacological means poses a risk of morbidity to the patient, which could be avoided.

BETA increases the ablation zone significantly when compared to controls as described in chapter 2. The ablation zone measurements however included only that tissue completely ablated by the RF energy (white zone), and not the surrounding tissue exposed to hyperthermic temperatures (red zone) (Goldberg et al, 2005a). The degree of hyperthermia experienced by these tissues may lead to delayed cellular necrosis, however this could not be determined in the *ex vivo* setting.

Measurement of the tissue temperatures in the ablated liver was necessary in order to determine the extent and degree of tissue heating caused by BETA and to evaluate the temperature distribution of BETA in tissues compared to conventional RFA.

Objective:

The objective of this study is to determine the temperature distribution within *ex vivo* liver during BETA compared to conventional RFA.

Materials and Methods:

Liver.

The liver used in this study was prepared for the ablation process as outlined in Chapter 2. Following the ablation process (Chapter 2), a brass rod was placed along the ablation path in the liver created by the ablation electrode. The 10 x 10 x 10 cm block of liver was removed from the Perspex box with the brass rod in situ and placed onto a plastic cutting board.
A sharp knife was used to cut along the brass rod, parallel to the direction of the ablation electrode in order to determine the longest ablation diameter.

Perspex Box.

The Perspex box was utilised as described in Chapter 2.
Holes were drilled into the lid and platform to ensure the temperature probes could be positioned exactly the same distance form the electrode each ablation cycle and to ensure that the probes were placed into the liver parallel to the ablation electrode (Figure 2.3). A slight angle toward or away from the electrode would result in falsely increased or decreased temperature readings for each ablation cycle. The temperature probes were placed 1.5cm into the liver in order for the tip to be at the centre of the active electrode tip in the liver and at 5, 10, 15 and 20 mm from the active electrode (Figures 2.2 and Figure 2.4).

Temperature Probes.

The temperature probes used for the study are commercially available temperature probes, attached to a digital data logger.
The Thermadata Temperature Data Logger TD2C MKII (ETI Ltd) is a portable data logger housed in a waterproof case (Figure 4.3). The data logger has a range of -40 to +125 °C Celsius with a resolution of 0.1 degree Celsius and an accuracy of ±0.5 °C. The data logger has a memory capacity of 2000 readings per temperature probe. The temperature can be sampled from 10 seconds to every 255 minutes. A 10mm Liquid Crystal Display (LCD) alternates between the temperature probe readings every 10 seconds and allows the user to monitor live temperature readings. The data logger is designed to meet EN 12830, S & T, C & D specifications.
Following a single experiment, the temperature probes were removed from the liver and the data logger attached to a PVC cradle, which connected to a software program on the laptop used for the ablation settings.

Courtesy of http://thermometer.co.uk

Figure 4.3 Thermadata TD2C temperature logger with LCD display of current temperature, alternating between the two electrodes

The data obtained through the ablation cycle is then displayed as a Graph (Figure 4.4), with each temperature probe assigned a separate colour. The analog data is then displayed in a table format which can be saved as a text or an excel document for analysis.

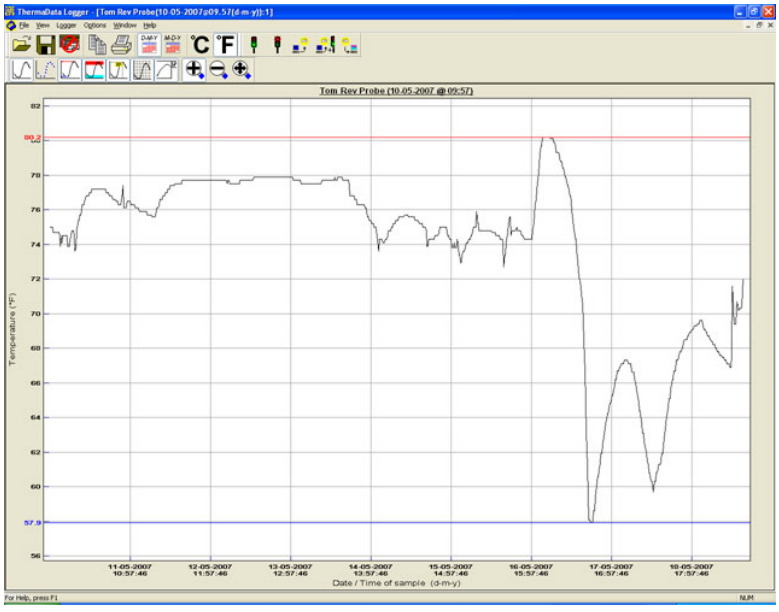

Courtesy of http://thermometer.co.uk

Figure 4.4 Graphical display of temperature data following analog-digital conversion by the software.

The software program of the data logger automatically synchronises with the time and date of the computer to allow for accurate time determination according to the times generated by the BETA software program.
Following the download of the temperatures for a particular ablation cycle, the data logger was reset in preparation for the next ablation cycle.
Each data logger has 2 temperature probes (Figure 4.3) and thus 2 data loggers were used in order to obtain data at four set distances from the electrode (5, 10, 15 and 20mm, Figure 4.5). Each temperature probe was inserted 15mm into the liver in order for the tip of the probe to be level with the centre of the long axis of the active electrode, in order to obtain reproducible, reliable readings throughout the data collection.

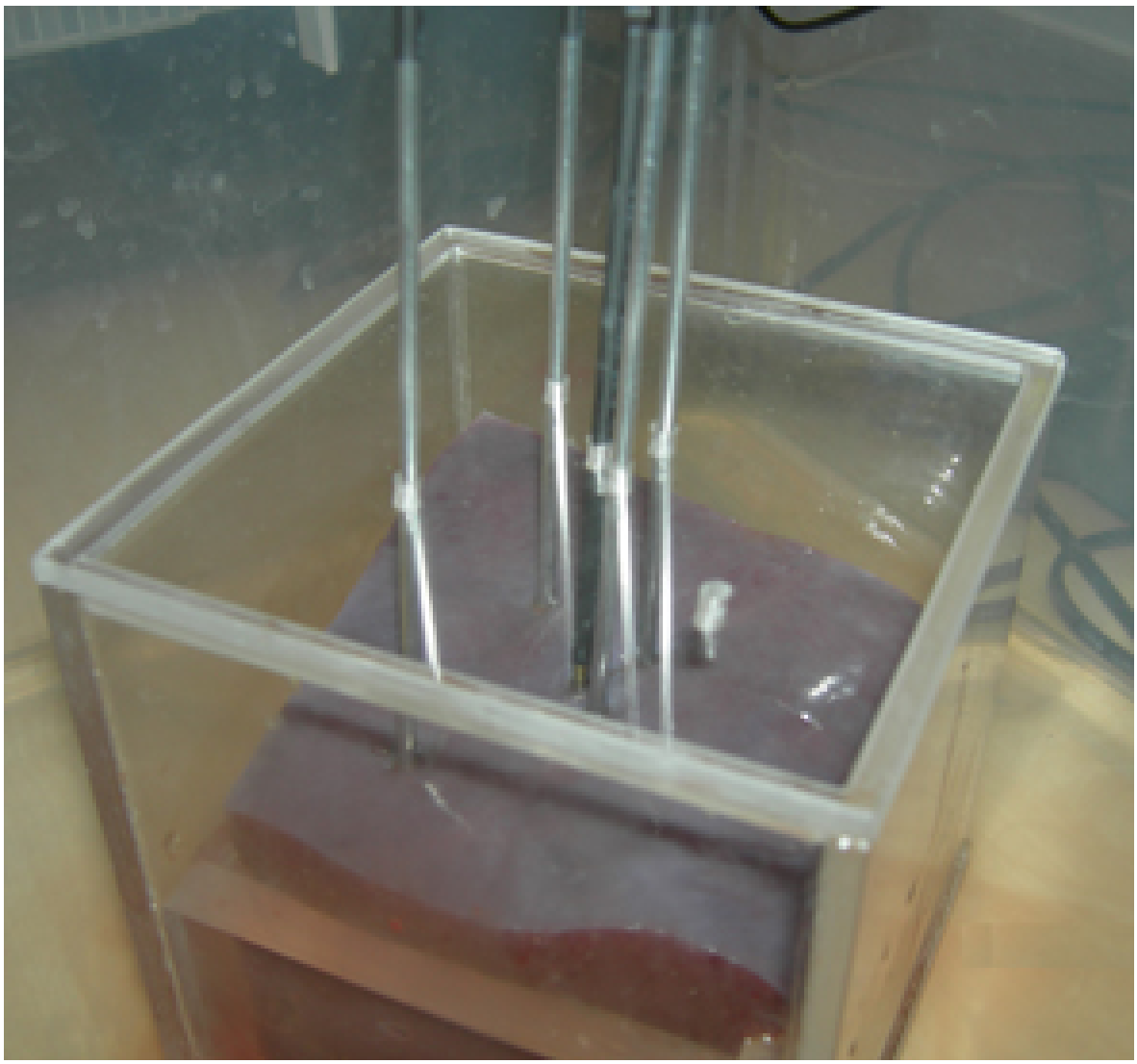

Figure 4.5 four temperature probes (silver) placed 5, 10, 15 and 20mm from the electrode (black)

Results.

The results are expressed as means ± standard deviation (SD) for normally distributed variables or the median and the interquartile range for non-normal variables. Differences in temperature at each distance from the electrode (5mm, 10mm, 15mm and 20mm) at each time interval (30 seconds) between tissue receiving standard RFA or BETA were tested with a linear regression model.

A *P* value <0.05 was considered statistically significant. SPSS 17 was used for all statistical data analysis. The temperature data is quoted in °C unless stated and distances from the electrode are quoted in millimetres (mm).

The experiments were conducted comparing RF alone (600mA control) to BETA using simultaneous DC and RF (9V DC and 600mA) with no pre RF DC (n=20).

Temperature readings were recorded at 30 second intervals at 5mm, 10mm, 15mm and 20mm from the probe (Appendix 3).

In addition, each ablation zone was measured for comparative analysis.

The temperature data was analysed using SPSS 17 software.

Each data point was compared to the corresponding data point at each distance from the probe. Each data point demonstrated a significant difference at each distance from the probe ($p < 0.0001$).

Initially the BETA data was subjected to statistical scrutiny to determine the significance of temperature variance at the four points. The temperature difference at each distance from the electrode was statistically significant when each of the distances were compared ($p<0.0001$).

Appendix 3:

Table 4.1 lists temperatures s at each distance from the electrode at each 30 second time interval for the control (600mA RF) and the BETA (9V DC and 600mA) experiments at 5, 10, 15 and 20mm from the electrode.

Table 4.2 lists the mean temperatures at each distance from the electrode at each 30 second time interval for the control (600mA RF) and the BETA (9V simultaneous DC and 600mA RF, no pre RF DC) experiments.

Graph 2.1 illustrates the temperature trend of the control group and the BETA group for each distance (5mm, 10mm, 15mm and 20mm) from the electrode.

Each temperature experiment yielded an ablation zone (n=20). The ablation zone was examined and the maximum short axis diameter was recorded and the ablation volume calculated. The mean maximum short axis diameter for the control group was 1.56cm and 3.01cm for the BETA group ($p<0.0001$).
The mean ablation volume for the control group was $5.03cm^3$ and $26.79cm^3$ for the BETA group ($P<0.0001$).

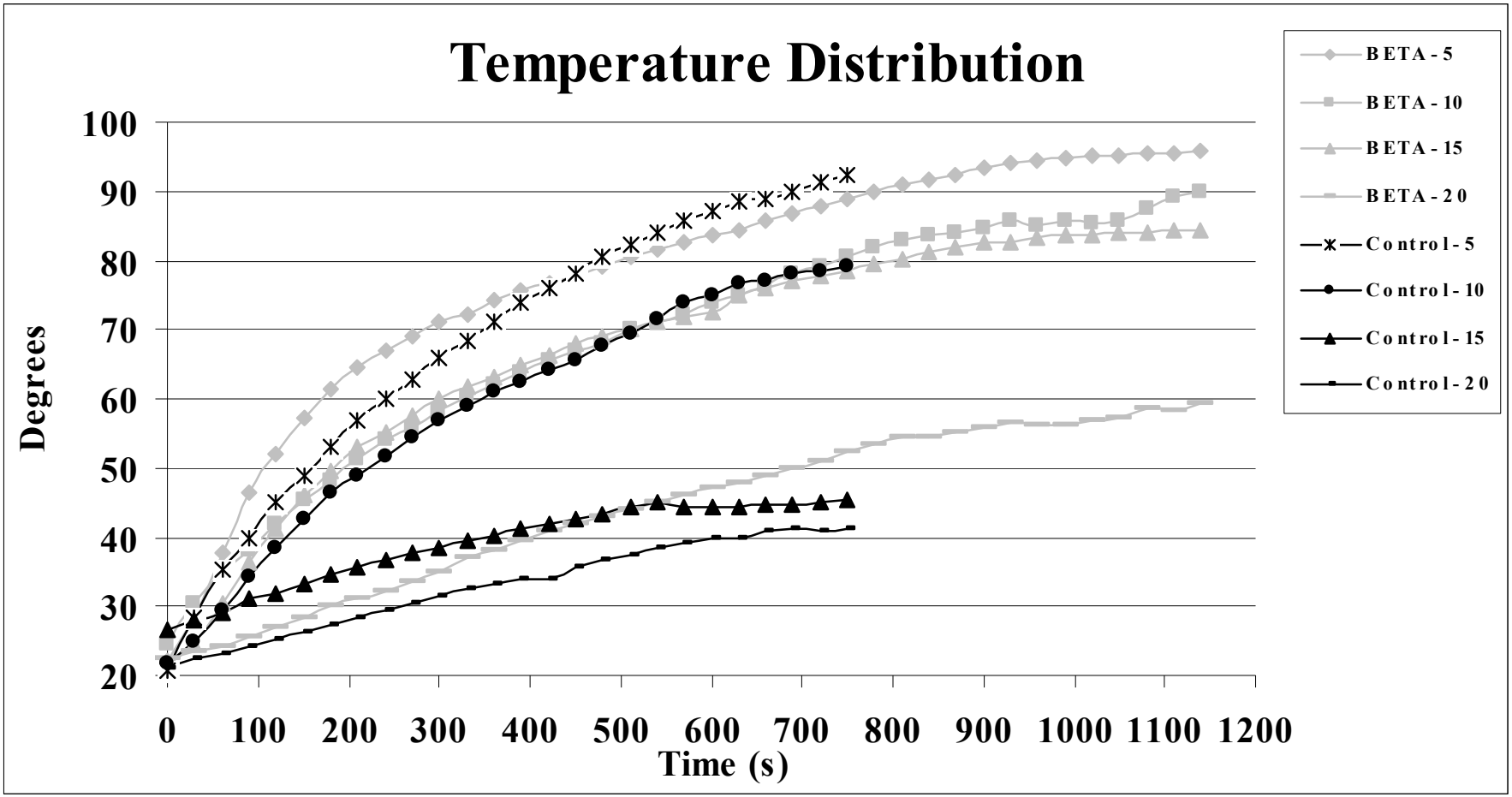

Graph 2.1 illustrates the temperature trend of the control group and the BETA group for each distance (5mm, 10mm, 15mm and 20mm) from the electrode.

Discussion:

The results of the *ex vivo* study (Chapter 2) showed BETA produced statistically larger ablation zones than control experiments.

The poor temperature distribution of RFA due to the limitations of the bioheat equation is thought to be a cause of recurrence at the periphery of tumours (Ke et al, 2010). Ke et al created residual areas of tumour in rabbits implanted with VX2 by ablating the tumours with RFA at 55, 70 and 85 °C. The study demonstrated an increase in local tumour volume and metastatic disease in subjects treated with 55 °C of RFA compared to the 70 and 85 °C animals. Although this study highlights a limitation of RFA, the ablation times used for the study were 5 mins in each group. At temperatures of 50-55 °C, a minimum of 6 minutes is required to induce cell death (Goldberg et al, 1996a, Goldberg et al, 1996b, Goldberg et al, 2000), this may in part be the reason for the rapid recurrence at such low temperatures.

Temperature distribution in the tissue provides an objective determination of the ablative technique to heat the tissue sufficiently to cause coagulative necrosis. Mertyna et al (Mertyna et al, 2007) compared the temperature distribution in 3 different types of normal tissue, including liver. The tissue temperature was monitored at 5mm, 10mm, 15mm and 20mm from the active electrode. Following ten minutes of RF application, the maximum temperature at the margin of the ablative zone was 51.6 °C. At this temperature a minimum of 6 minutes would be needed in order to cause cell death (Goldberg et al, 1996a, Goldberg et al, 1996b, Goldberg et al, 2000). The temperature at the ablative margin is an important factor in determining the probability of recurrence. If the temperature is below 50 °C, the risk of recurrence is high, as the cellular enzymes are much less likely to be denatured. Above 50 °C, for 6 minutes or more is the minimum needed to cause cellular necrosis, and thus decrease the risk of recurrence.

Liu et al (Liu et al, 2010) treated 107 hepatic tumours with RFA (HCC group - 69 lesions and colorectal liver metastases group 38 lesions). The post-ablation margins were calculated using CT and MRI at 1-month post treatment then 3 monthly for a year and biannually thereafter. The results showed a minimum post-ablative margin of 0.4cm (P=0.020) and tumour size smaller than 2.5 cm (P=0.001) significantly correlated with local control for the HCC group. This was not seen in the colorectal liver metastases group, where a 0.4cm margin showed recurrence rates higher than HCC. This finding suggests a “safety margin” larger than 0.5cm, which correlates with the accepted 1cm safety margin following surgical resection.

Goldberg et al (Goldberg et al, 1998) compared the temperatures in tissues following pharmacological modulation of blood flow into the liver in an attempt to determine whether decreasing the blood flow to the liver would result in higher temperatures in the ablation zone. Goldberg compared the ablation zone size and temperatures in tissue at 5mm, 10mm, 15mm and

20mm from the electrode using Halothane to decrease the blood flow, Vasopressin to increase the blood flow, normal blood flow and *ex vivo* livers. These were compared to normal flow through the liver during RFA. The temperature in the tissues was measured after 10 minutes of RF ablation. Increased temperatures were observed 10 and 15 mm from the electrode following Halothane administration, and decreased temperatures were observed at these distances with the administration of Vasopressin. At 5mm from the electrode the temperatures were higher in the Halothane experiments than normal blood flow, but this was not significant. The reason for this is probably due to the degree of ablation at 5mm from the electrode being similar. A significant decrease in temperature was observed 5 mm from the electrode after vasopressin administration compared to normal blood flow (62.5 °C vs 87 °C). Temperatures at all distances in *ex vivo* tissue were slightly higher than those observed in the *in vivo* studies, however the differences were not statistically significant when compared to the Halothane results. This important observation demonstrates a correlation between the *ex vivo* temperature measurements and *in vivo* modulated experiments.

The temperature measurements in the *ex vivo* liver at 5mm, 10mm and 15mm from the electrode measured 95 °C, 76 °C and 60 °C respectively using a cool-tip electrode. These temperature measurements correlated with a mean coagulation diameter of 3.4cm.

The results of the BETA study show a statistically significant difference at 15mm and 20mm from the electrode compared to the control experiments.

The temperature at 20mm from the electrode tip reached a maximum temperature of 59.4 °C at 1140 seconds and a maximum of 84.4 °C at 1140 seconds 15mm from the electrode. This distance translates to an ablation diameter of 3cm, which given the average ablation zone diameter would correlate with the ablative margin.

At 15mm the temperature reached 50 °C after 210 seconds and 60 °C after 300 seconds. At 20mm, the temperature reached 50 °C after 690 seconds and remained above 50 °C until roll-off at 1140 seconds.

An interesting observation during this study was the apparent higher temperatures obtained with the control RFA at specific time points compared to BETA.

At 5mm – The temperature increased faster using BETA than the control (Graph 4.1, Table 4.1) to 400 seconds, thereafter the control ablation temperature was higher until roll-off, however the roll-off temperature for BETA was higher than the roll-off temperatures for the control group.

At 10mm - The temperature increased faster using BETA than the control (Graph 4.1, Table 4.1) to 500 seconds, thereafter the control ablation temperature was higher until roll-off, however the roll-off temperature for BETA was higher than the roll-off temperature for the control group.

The reason for this observation is uncertain. It may be due to rapid heating initially with BETA, however the difference was not significant at these time points and the sudden increase in the

temperature observed with the control group demonstrates the rapid rise in temperature caused by RFA causing charring and vaporization of tissue, thus limiting the effects of RFA and poor heat conduction. The effects of this are observed in these experiments where the tissue temperature at 15 and 20mm failed to reach cytocidal temperatures.
At 15mm and 20mm – This was not observed and BETA remained significantly higher at all time points during the ablation cycle. An important observation is the lack of cytocidal temperatures at 15 and 20mm in the control group, demonstrating the poor tissue conductivity using conventional RFA. The temperatures at 15 and 20mm remained abovea cytocidal temperature of 50 °C for a mean time of 8 minutes (Graph 4.1, Table 4.1).

The mean ablation zone diameter measured 3.01cm, however this is the "white" ablation zone (Goldberg et al, 2005a, Goldberg et al, 2005b) and does not take into account the "red" zone of hyperemia surrounding the "white" coagulation zone. The area of tissue between 15mm and 20mm is likely to correspond to the "red" ablation zone described as the hyperaemic zone surrounding the ablation zone. With temperatures of above 50 °C at the 20mm margin (corresponding to a 4cm diameter ablation zone), BETA may provide a potentially larger area of treatment when using adjunctive therapies such as IV doxorubicin (Goldberg et al, 2001, Goldberg et al, 2002, Ahmed et al, 2003a, Ahmed and Goldberg, 2004, Ahmed et al, 2005). A heat sensitive encapsulated endovascular chemotherapeutic agent (Celsion Corporation, 2010) is currently undergoing clinical trials regarding efficacy and patient tolerance. The drug - encapsulated doxorubicin covered with a heat sensitive liposome (Thermodox, Celsion, NY, USA). Thermodox is designed to deliver high concentrations of anti-cancer drugs directly to those cancer cells that survive RFA (Celsion Corporation, 2010). In conjunction with ablating the centre of the tumour, RFA simultaneously activates Thermodox to release its encapsulated doxorubicin, killing the remaining viable cancer cells throughout the heated region, including the tumour margins. An important advancement in the development of ThermoDox is the heat sensitive delivery of the drug to those cells exposed to temperatures of 40 °C and above. ThermoDox increases the delivery of the drug at the desired tumour site has the potential to reduce drug exposure distant to the tumour site and thus decrease associated side effects of endovascular chemotherapy.
The advantage that BETA has is the high temperatures at 20mm from the electrode tip. Although the ablation zone is limited to 3cm, the adjacent tissue is exposed to hyperthermic temperatures in excess of the 40 °C needed to activate the heat sensitive liposome.
A number of studies have been conducted measuring ablation zone size and temperature in tissue using either a monopolar or bipolar technique using cooled electrodes with or without saline perfusion (Lee et al, 2004a, Haemmerich et al, 2005, Lee et al, 2005, Lee et al, 2006, Aube et al, 2007, Mertyna et al, 2007). Lee et al (Lee et al, 2005) conducted a study to

determine ablation zone size and temperature using a combination of monopolar, simultaneous mono-polar and bipolar modes. The temperature readings were taken at 15mm from the electrode in the monopolar modes and at equidistant points (15mm) between the multipolar and bipolar modes. The mean final-temperature values were 89°C and 91°C for the conventional monopolar modes respectively. The mean final temperature for sequential monopolar mode was 67°C and in the bipolar group 105°C. Importantly using the multipolar and bipolar technique requires precise placement of electrodes and increases the morbidity risk associated with the procedure. The mean final temperature at 15mm for BETA was 84.4°C compared with the monopolar modes, and significantly higher than the sequential monopolar modes. The bipolar mode reached 60°C in the fastest time, whereas monopolar RFA with 0.9% NaCl reached 60°C after 9 minutes, with 6% NaCl after 6 minutes and with sequential monopolar RFA after 16 minutes.

The BETA experiments reached 60°C after 5 minutes with a single electrode and no saline infusion. Although the saline infusion does increase the ablation zone and improve tissue heating, saline infusion can be unpredictable (Goldberg et al, 2001, Ahmed et al, 2002). BETA is reproducible and does not require additional techniques to maintain hydration or improve tissue heating as the DC circuit fulfills this by electroosmosis (Reuss, 1809, Nordenstrom, 1983, Probstein, 1994).

The importance of tissue temperature during thermal ablation has been reinforced by a number of studies in the literature, both laboratory based and clinical, using computer modeling not only to determine tissue heating with regard to safety of adjacent structures (Liu et al, 2008), but also the importance of tissue temperature during MR guided procedures (Chung et al, 1999, Keserci et al, 2006, Lepetit-Coiffe et al, 2010). The temperature of the ablated tissue and the transmission of heat through the tissue are essential in determining the effectiveness of thermal treatments and predicting possible recurrences (Ke et al, 2010).

BETA transmits heat through tissue more efficiently than standard RFA as demonstrated by this study. The mean temperatures 20mm from the active electrode in this study demonstrate hyperthermia in the tissue, which has not reached complete ablation, making this a prospect for thermal sensitive adjuvant therapies. The omission of saline infusions to increase tissue conductivity makes BETA more predictable and decreases the morbidity risks associated with multi-polar techniques.

Limitations of this research:

Limitations to this research model were identified; however I did not feel the results were influenced significantly by these limitations.

The same limitations as outlined in chapter 2 and 3, with regard to the temperature of the livers and the use of normal saline as opposed to physiological saline were encountered.
The liver temperatures remained similar throughout the experiments evaluating the temperature distribution in both controls and the BETA models. The aim of this study was to study the temperature distribution in the liver during ablation and therefore the temperature of the liver at the commencement of the ablations was not influenced particularly by the decision to keep the saline bath at 26-30 °C and I did not think the experiments were compromised by the saline bath temperature.

Conclusions:

1. BETA reaches cyitocidal temperatures in ablated tissue faster than control RFA.

2. The mean temperatures at 5mm, 10mm, 15mm and 20mm are significantly higher following BETA compared to standard RFA.

3. Tissue remains above cytocidal temperatures up to 20mm from the active electrode for longer than standard RFA due to the longer time needed to produce a BETA lesion.

4. BETA provides a larger potential cyitocidal zone for thermosensitive chemotherapeutic agents, increasing the ablation zone.

5. BETA produces a similar mean end-temperature profile to multipolar and bipolar techniques, but with decreased potential morbidity given the single electrode needed.

6. BETA reaches temperatures in excess of 60°C up to 15mm from the active electrode faster than multipolar and bipolar modalities described in the literature.

Chapter 5:

Bimodal Electric Tissue Ablation:

In Vivo Porcine studies.

Introduction.

General.

The *in vivo* animal experimental research on BETA is discussed in this chapter. The results of the ablation zone sizes in terms of maximum diameter and volume and the histological appearance are discussed in detail.

The animals' reaction to the surgery is presented in terms of biochemical blood analysis and inflammatory marker measurement in chapter 6. The immediate, short and intermediate term morbidity of the animals post procedure are discussed in detail with special reference made to complications arising at surgery due to BETA. These include local and systemic complications.

In vivo data on BETA has been published (Cockburn et al, 2007, Dobbins et al, 2008, Dobbins et al, 2008a, Dobbins et al, 2008b), however this is work using a commercially available radiofrequency ablation device and an externally attached DC transformer as described in chapter 1. The data presented below is the first published using a custom made BETA machine, designed specifically for the purpose of providing RF ablation without internal feedback circuitry, combined with an optional direct current circuit. Data regarding the animals' inflammatory response to BETA has not been previously described in the literature however. It is against this background that my research began on 1 January 2009.

The Heat Sink Effect.

In Chapter 1, the effects of the heat sink effect were discussed in detail. The heat sink effect described by Curley (Curley and Hamilton, 1997) and Goldberg (Goldberg et al, 1998a, Goldberg et al, 1998b) has an important effect on the size of the ablation zone (Figure 4.2). The results from *ex vivo* and *in vivo* studies show a consistent decrease in the size and volume of the ablation zone when comparing the same modality in *ex vivo* and *in vivo* experiments (Cha et al, 2009). The effects of heat sink are important to this research. There has been no direct comparison of BETA *ex vivo* and *in vivo*. Cockburn et al (Cockburn et al, 2007) described findings in *in vivo* porcine models, however the *ex vivo* findings have not been published in a peer reviewed journal. The results of the *in vivo* BETA research will provide invaluable data regarding the influences of the surrounding vessels in the liver on BETA and the resultant ablation zones.

Morbidity Studies.

Short and intermediate term morbidity studies will be conducted in order to assess the effects of the surgical intervention, complications related to tissue heating and the response of the liver to the ablation (Dobbins et al, 2008a). The studies will be conducted post mortem following termination of 2 animals at specific intervals following ablation. The intervals will be immediately (terminal anaesthesia), 2 days, 2 weeks, 4 weeks and 8 weeks.

An essential aspect of the *in vivo* research is the possible complications of BETA in a live animal. These complications may be systemic or local. Radiofrequency ablation is known to be a safe technique with few systemic or local complications.

a. Systemic Complications:

Systemic complications are few and consist of potential cardiac complications from direct current and the inflammatory reaction caused by BETA. There have been no significant cardiac complications observed with electrolysis. However, Nordenstrom did describe cardiac symptoms including chest discomfort and breathlessness in a patient treated with electrolysis (Nordenstrom, 1994). This occurred at high (>50 volts) voltages and as soon as the voltage was decreased, the symptoms ceased. The inflammatory response in animals to electrolysis has been described, with no adverse effects noted in the literature (Teague et al, 2004a, Teague et al, 2004b). Teague et al used C-reactive protein (CRP) a well known and common acute phase protein as a marker for an acute inflammatory reaction. This marker is well known and widely accepted for this use. Tumour Necrosis Factor alpha (TNF - α) and Interleukin - 1 Beta (IL - 1β) are further markers of acute inflammation which have been used for assessment of inflammatory response in the porcine species (Kruse et al, 2008). Inflammatory marker analysis requires careful preparation of the blood sample and are analysed by means of enzyme linked immunosorbent assays (ELISA) (Hiss et al, 2003). The ELISA is an expensive assay and requires specialist laboratory services as well as trained veterinary pathologists. The markers provide an objective measurable and reliable determinant of the animals' response to the intervention.

b. Local Complications.

The local complications encountered in radiofrequency ablation relate largely to electrode placement or the thermal therapy itself (Rhim et al, 2004).

The placement of the electrode and complications related to it are mainly encountered in percutaneous image guided interventions (Rhim et al, 2004). The *in vivo* animal experiments are largely performed on superficial tissue specifically implanted for purpose (Ahmed et al, 2002) or are performed on the liver using an open surgical approach (Cockburn et al, 2007).

Bleeding following electrode placement occurs in less than 2% of cases, and is more common with multiple electrode insertions and bleeding disorders (Rhim et al, 2004). Infection is a further complication infrequently seen, and less so with percutaneous procedures.

Non-target organ damage is a local complication associated with larger ablation zones and ablation procedures close to vital structures. Immediate structures at risk of thermal damage include the gallbladder, bile ducts and bowel.

Careful pre-ablation planning is essential to ensure that the risk of thermal damage to adjacent structures is minimalised (Rhim et al, 2004).

Damage to the diaphragm is a further complication, which may cause severe pain, hinder the cough mechanism and cause a post ablation pneumonia, or pleural effusion (Wong et al, 2009).

Grounding pad burns are a potential significant complication (Rhim et al, 2004). In the case of BETA, burns may result from the high energy delivered by the radiofrequency device or the direct current. The risk of burns from the radiofrequency energy is thought to be small, as the proposed energies to be used (600mA) are significantly lower than high energy RFA (Solazzo et al, 2007) used by Solazzo et al. A risk does exist regarding the grounding pad and the effects of the anodic polarity of the pad. As described in chapter 2, the electrode is assigned a negative (cathodic) polarity and the reference grounding pad a positive (anodic) polarity. The toxic gas formation at the anode, namely chlorine (Samuelsson and Jonsson, 1980), combined with the desiccation cause by type II electroosmosis (Nordenstrom, 1983) may cause significant burns at the grounding pad site.

Objectives:

The objectives of this study were to determine the ablation zone size and volume of BETA experiments compared to standard RF ablation; the associated local and systemic complications caused by the intervention and the intermediate morbidity of the study subjects.

Materials and Methods.

In vivo Porcine Experiments Ethical Approval.

The *in vivo* experimental procedures undertaken during the course of this study are subject to the United Kingdom Animals (Scientific Procedures) Act 1986 (the Act). The Act, administered by the UK Home Office, regulates all scientific procedures in living animals which may cause pain, suffering, distress or lasting harm and provides for the designation of establishments where procedures may be undertaken, the licensing of trained individuals who perform the practical techniques and the issue of project licenses for specified programs of work.
This study complied with all applicable sections of the Act and the associated Codes of Practice for the Housing and Care of Animals used in Scientific Procedures and the Humane Killing of Animals under Schedule 1 to the Act, issued under section 21 of the Act.
The number of animals used were the minimum that is consistent with both scientific integrity and regulatory acceptability, consideration having been given to the welfare of individual animals in terms of the number and extent of procedures to be carried out on each animal. On the basis of physiological similarities to man and its general suitability as a surgical model and on comparative *in vivo* and *ex vivo* investigations, the domestic pig was chosen (Cockburn et al, 2007, Dobbins et al, 2008a).

Site of *in vivo* porcine studies.

The *in vivo* porcine studies took place at Huntingdon Life Sciences, Huntingdon, United Kingdom in the Department of Large Animal and Avian Studies led by study director Mrs V Ross. Huntingdon Life Sciences provides a comprehensive range of integrated development services to the pharmaceutical, biopharmaceutical, chemical, crop protection, and veterinary and food industries. Originally the company concentrated upon nutrition, veterinary and biochemical research, however expanding services led to the incorporation of pharmaceuticals, crop protection products, food additives and industrial and consumer chemicals.
The Huntingdon Life Sciences site houses animal maintenance buildings, surgical suites large enough to accommodate large livestock with fully equipped surgical suites with the ability to conduct procedures under general anaesthetic. The surgical team consists of eight Veterinary surgeons and anaesthetists and a full theatre staff team.
The site houses facilities for post mortem examination, including pathologists examining both gross pathological and histological specimens. The chemical pathology services on site provide blood analysis of biochemistry and hematology.

Animal Subjects:

Ten domestic large White hybrid female pigs were used for the *in vivo* experiments, obtained from Huntingdon Life Sciences Stock. The pigs were aged between four and five months with mean weight of 66.7 kg (Range 60-80.5kg). The pigs were selected from a pool of animals on the basis of bodyweight, with the aim of using pigs close to the target bodyweight of an average human subject (60-70 kg). All animals received the same experimental treatment apart from the two terminal anesthesia animals, which arrived on the day of surgery with no acclimatisation. The subsequent animals arrived at the testing site 14 days prior to surgery to allow for aclimatisation.

The animals were identified by means of numbered ear tags, initially by a temporary number and subsequently by the allocated permanent individual animal number for this study. The study number in conjunction with the (temporary or permanent) animal number constituted a unique identification.

The pigs followed exactly the same experimental treatment (discussed later in the chapter), however the times of termination differed as follows:

Each group consisted of 2 pigs:

Group 1 were terminated immediately post procedure and will be referred to as non-recovery animals

Group 2 were terminated at 2 days.

Group 3 were terminated at 2 weeks (14d).

Group 4 were terminated at 4 weeks (28d).

Group 5 were terminated at 8 weeks (56d)

Animal Management.

The two non-recovery animals used initially were delivered directly to the operating theatre without any formal pre-surgery acclimatisation. All other animals were allowed an acclimatisation period of at least 14 days prior to surgery. Only healthy animals were allocated to the study.

The animals were group-housed in floor pens, which are of concrete construction, in a building, which provides a satisfactory range of environmental conditions for the species. At the time of surgery, pigs were selected from the pool of animals available on the basis of bodyweight, with the aim of using pigs close to the target bodyweight of 60-70 kg.

Each pen contained concentrate feed containers and an automatic valve drinker for the supply of drinking water. In the period from immediately before surgery (at the time of premedication) until the surgical wounds were considered to have sufficiently healed by attending veterinary surgeons, the animals were housed individually. All the large animal housing buildings have

natural lighting, which may be supplemented with fluorescent strip lighting as necessary. Ventilation fans control ambient humidity and can be adjusted as necessary.
During the post-operative recovery period, the animals were provided with supplementary heat by means of overhead infrared lamps if they showed signs of hypothermia or had a prolonged post-operative recovery.

Diet and Water Supply.
Pigs were fed twice daily, on an individual basis from Day 7, with a pelleted concentrate ration which nominally contains no antibiotics, growth promoters or other non-nutritional additives. Those pigs undergoing surgery were fasted on the morning of surgery. The amount of feed offered was adjusted as necessary on a group or individual basis in accordance with standard husbandry practice and with the Study Director's authorisation. The concentrate feed did not contain any chemical contaminants or microorganisms of types, or at concentrations, which could interfere with the integrity of the study, and therefore no general contaminant analyses were conducted o the feeds. A 200g sample of each batch of feed used in the study was retained at -20°C for possible subsequent analysis in the event of equivocal findings. This sample was never needed for analysis.
Fresh drinking water (Anglian Water mains supply) was supplied *ad libitum* throughout the study. The water is supplied by Anglian Water; its guidelines on water quality from the EEC directive relating to water for human consumption (80/778/EEC), and conforms to the United Kingdom Water Act 1989 and subsequent amendments. Results of routine physical and chemical examination of drinking water at consumers' taps as conducted by the supplier, are made available to Huntingdon Life Sciences as regular summaries.

Veterinary Care.
From the time of allocation until termination of the study the animals were inspected by a veterinary surgeon if there was a health related query relating to the general health of the animal or resulting from the surgical procedure. In addition a review of relevant clinical health records, bodyweight, food consumption data, etc. was undertaken by the Study Director and documented prior to surgery. Details of all routine prophylactic or therapeutic treatments given, and any peri- and post-operative treatments given (including antibiotics and analgesics in the form of opioids and/or NSAIDs such as meloxicam), were entered in the study records. All treatments needed for the animals post operatively were considered as approporiate to the integrity of the animal study. This however did not pertain to the two non-recovery animals delivered directly to the operating theatre. Each of the animals however was inspected by a veterinary surgeon on delivery to assess their general health and condition.

Inclusion/Exclusion criteria and removal of animals from the study.

Only clinically healthy animals were selected for surgery as determined by a veterinary surgeon prior to delivery to the operating theatre. This again did not include the two non-recovery animals; these animals were examined on delivery to the operating theatre by a veterinary surgeon. Any subsequent perioperative complications such as compromised wound integrity (wound dehiscence); anaesthetic death or stroke excluded the animal from the study. If this was the case, the animal was immediately replaced, however this did not occur in this study. Inclusion in the study was confirmed by a successful surgical procedure and application of both BETA and standard radiofrequency ablation, in addition to a successful, uneventful recovery from anaesthesia (except in the case of the two non-recovery animals)**.**

If an animal that satisfied the inclusion criteria initially developed illness, injury, complication (including wound infection, haematoma or wound dehiscence), or another adverse event, which prevented the animal from completing the study; this animal could be removed from the study on the basis of consultation between the Study Director, the attending veterinary surgeon and/or myself.

If this decision were taken without my presence, notification would be made as soon as possible. It was agreed that this would, if practical be done before the test animal was removed. In such a case the Study Director following consultation with the attending veterinary surgeon and myself would replace the animal upon approval.

Experimental Procedures.

Anaesthetic Administration.

Surgical procedures were conducted on two pigs in any one-day, one pig in the morning and one in the afternoon. At the time of surgery, each pig was premedicated with the following: Midazolam 0.1mg/kg, Medetomidine 0.03mg/kg, Ketamine 20mg/kg via intra-muscular injection in the housing building. Once sedated, the animal was transferred to the operating theatre. Peripheral venous access was obtained via a vein in the ear. The venous access was used for induction and maintenance of anaesthesia, analgesia, bolus anaesthesia and intravenous fluid administration. In the case of the non-recovery animals, the peripheral cannula was used to administer terminal Phenobarbitone. The animal was intubated with a 6.5 – 7.5mm (mean 7.0mm) cuffed endotracheal tube in the supine position following induction of anaesthesia. In all animals except for the non-recovery animals, 20mg/kg of Co-Amoxiclav was administered intravenously for anti-biotic prophylaxis and all animals received 0.4mg/kg of Meloxicam, a non-steroidal anti-inflammatory as pre-emptive analgesia via intra-muscular injection. When deemed stable, transferred to the operating theatre. General anaesthesia was induced and maintained via the intravenous route. The following anaesthetic agents were used: Propofol (10mg/mL) infused at a rate of between 15.8mL/hr and 63.0mL/hr, Remifentanil (4mcg/mL)

infused at a rate of between 37.8 and 378mL/hr and Midazolam (1mg/mL) infused at a rate of 72.45ml/hr to 170.1mL/hr. The rates of infusion were titrated by the anaesthetist according to the non-invasive blood pressure, exhaled carbon dioxide, pulse and oxygen saturation measurements and the animals' response to pain.

Midazolam is an ultra short-acting Benzodiazepine with anxiolytic, hypnotic, amnestic, anti-convulsant, skeletal muscle relaxant and sedative properties. It is fat soluable and has a half-life of approximately 2 hrs, making it a commonly used sedative and pre-anaesthetic agent.

Metomidine is a synthetic drug used as both a surgical anaesthetic and analgesic. It is a crystalline white alpha-two adrenergic antagonist that can be administered as an intravenous drug solution with sterile water. It is often used in combinations with opioids as premedication used in combination with Butorphanol and Ketamine via intramuscular route to produce general anaesthesia for short periods.

Ketamine is classified as an NMDA receptor antagonist. At high, fully anesthetic level doses, Ketamine has also been found to bind to opioid μ and σ receptors. It induces a state referred to as dissociative anaesthesia as well analgesia, hallucinations, elevated blood pressure and bronchodilation. Ketamine is primarily used for the induction and maintenance of general anaesthesia, usually in combination with some sedative drug such as Midazolam.

Propofol is a short acting intravenously administered hypnotic agent. It is commonly used in veterinary practice for the induction and maintenance of general anaesthesia and sedation for mechanically ventilated animals and procedural sedation. Chemically, Propofol is unrelated to barbiturates, and has largely replaced Sodium Thiopentone for induction of anaesthesia, as recovery from Propofol is more rapid and "clear" as compared to thiopental. Propofol is not considered an analgesic, so opioids such as Fentanyl may be combined with Propofol to alleviate pain.

Remifentanil is a potent ultra short-acting synthetic opioid analgesic drug. It is administered during surgery to relieve pain and as an adjunct to an anaesthetic, often in combination with Propofol as in the case with all of the animals in this study. The use of Remifentanil has made possible the use of high dose opioid and low dose hypnotic anesthesia, due to synergism between Remifentanil and various hypnotic drugs and volatile anesthetics.

Co-Amoxiclav is a combination anti-biotic containing amoxicillin, a β-lactam anti-biotic with potassium clavulanate, a β-lactamase inhibitor. With increased use of the penicillins, bacteria developed an enzyme on their cell walls called β-lactamase, rendering them resistant to all penicillinase antibiotics. The addition of a β-lactamase has however increased spectrum of action and restored efficacy against amoxicillin-resistant bacteria that produce β-lactamase. The increased spectrum of Co-Amoxiclav includes some anaerobic bacteria in addition to the gram-positive bacteria in the spectrum. This makes Co-Amoxiclav an ideal anti-biotic for surgical

prophylaxis in clean abdominal wounds (no perforation of the bowel) as it is effective against skin commensial organisms, commonly gram positive and some bowel organisms, commonly gram negative or anaerobic.

The pigs were supported on a warming pad in the supine position (dorsal recumbency) (Figure 5.1). Body temperature was continually maintained within a physiological range using heating blankets if necessary. However, in all cases heating of the animal was noted rather than cooling. Just before beginning the surgical procedure, pre-dose blood samples were drawn for Acute Phase Proteins (APPs) and biochemical markers.

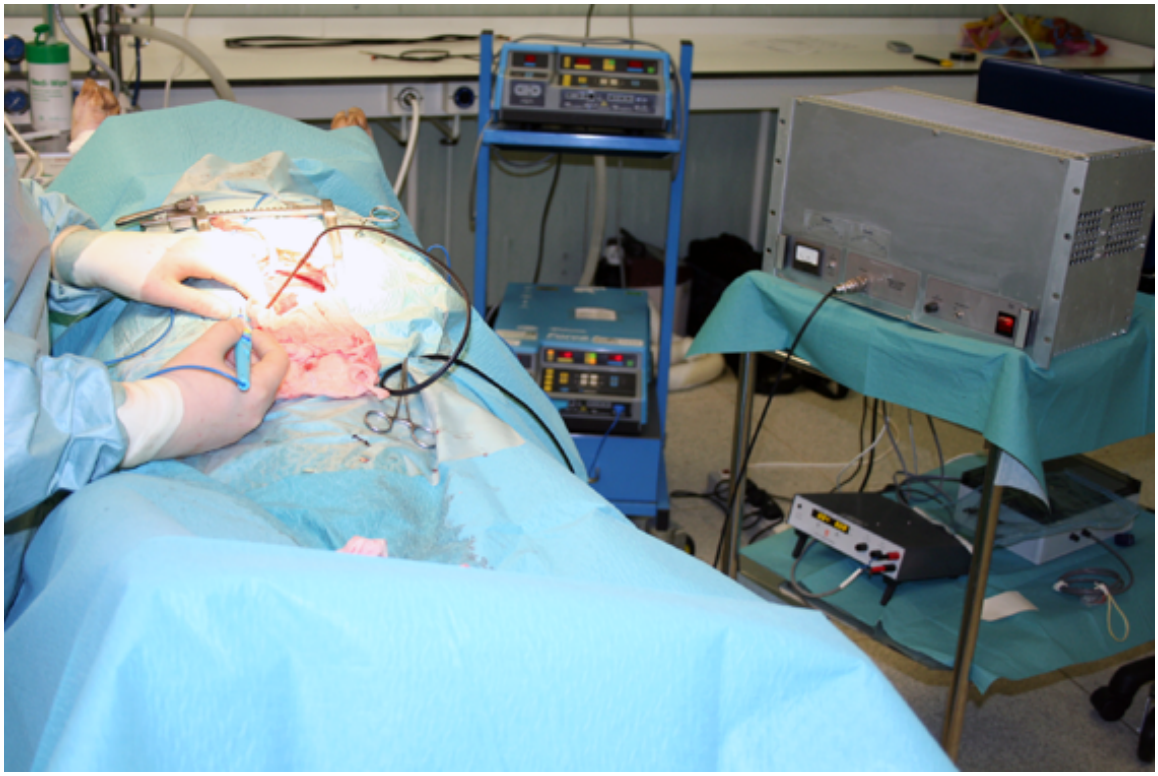

Figure 5.1 demonstrating the operating theatre setup. Supine animal with midline laparotomy to expose the liver and electrode insitu.

Blood Analysis.

An important aspect of the *in vivo* porcine studies is the animals' reaction to the insult of BETA. The anaesthetist monitored the animals' physiological reaction to the general anaesthetic, laparotomy and series of ablative procedures intra-operatively continually. Temperature, blood pressure and heart rate were documented. The physiological monitoring continued in the recovery period until the animal was deemed safe to return to the animal housing. Following return to the animal housing the animals were monitored daily until termination. General health

status, food consumption and wound care were assessed daily. The blood analysis provided an objective measurable assessment of the animals' reaction to the surgery and the ablative procedures.

A biochemical profile and a series of inflammatory markers specific to the porcine species (Alava et al, 1997, Eckersall et al, 1999, Hiss et al, 2003, Grau-Roma et al, 2009, Pineiro et al, 2009) were obtained for analysis. The nature of the biochemical profile and Acute Phase Proteins (APPs) will be discussed in detail in Chapter 6.

Surgical Approach.

Under full general anaesthesia, in the dorsal supine position, the abdominal skin was cleaned with anti-septic and a site immediately overlying the position of the liver, over the upper aspect of the right abdomen was shaved for application of the grounding pad needed for the BETA (90cm^2). A further small grounding pad was placed on the medial aspect of the hind leg for surgical cautery.

An upper abdominal midline laparotomy was performed from the xiphfisternum caudally for 15-20 cm to expose the liver (Figure 5.2). The size of the midlne laparotomy incision was based on adequate exposure of the liver in order to complete 8 ablations and also to decrease the incidence of incisional hernias post surgery. Mr Wemyss-Holden encountered this problem during his work in Adelaide (unpublished data). Careful consideration was made regarding the surgical incision for the animals. A too large an incision would increase the risk of surgical morbidity such as infection, delayed recovery, increased analgesic requirements post surgery, increased risk of incisional hernia formation, wound dehiscence and abscess formation. A small incision would limit the surgical access to the liver and prolong the surgery, increasing the risk of anaesthetic complications. Poor access to the liver increases the risk of damage to adjacent structures and possible ablation of non-visualised vital strictures such as the porta hepatis, bowel, diaphragm and gallbladder. Given the times to termination, careful planning of the incision was considered in order to decrease the associated surgical and anaesthetic risk without compromising the access to the liver for the ablations.

The rectus sheath was incised alone the linea alba and the peritoneum exposed. The liver was mobilised, however no ligaments were incised.

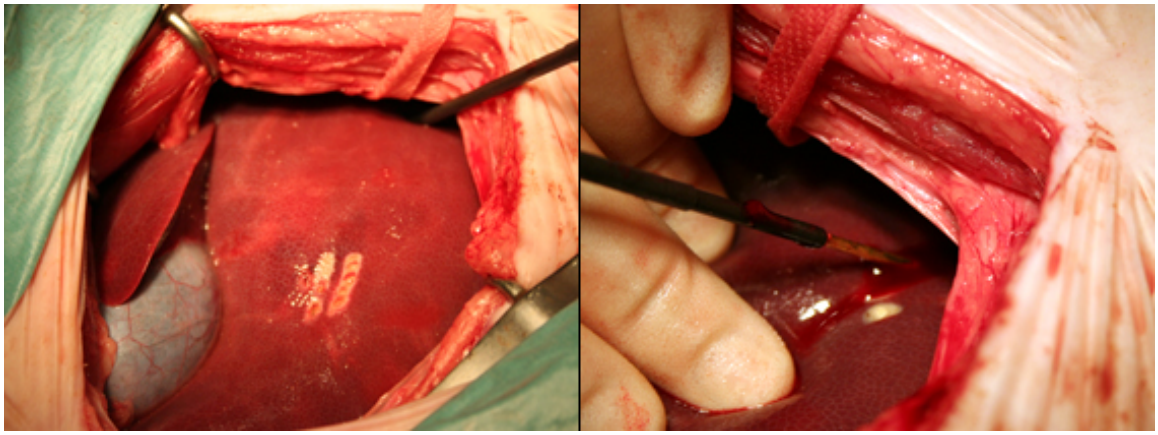

Figure 5.2 demonstrating mildine laparotomy to expose the liver. The liver was mobilised in order to access the posterior aspects of the 3 lobes (right)

The pig liver is conventionally described as having three main lobes: the right lateral, the median and the left lateral lobes. Deep interlobular fissures divide the lobes. The median lobe is further subdivided by a deep umbilical fissure, which extends almost up to the hilum, giving the appearance of two separate median lobes, which can be assigned the terms left and right median lobes (Court et al, 2003, Court et al, 2004)(Figure 5.3).

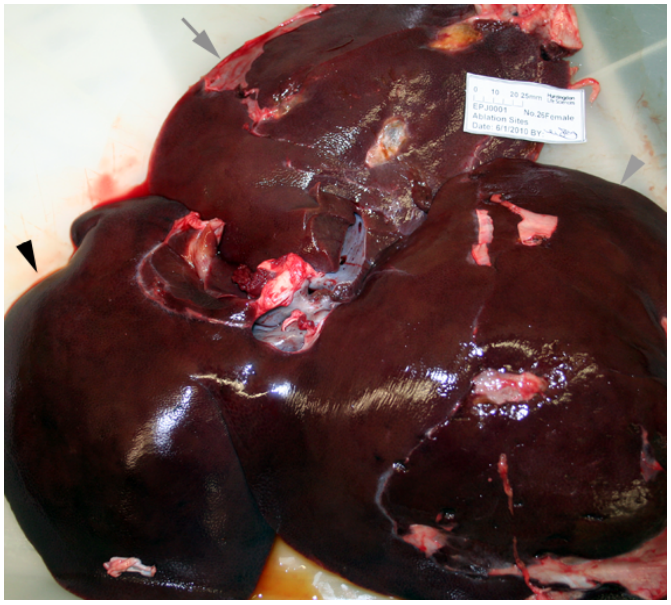

Figure 5.3 demonstrating porcine liver anatomy. Left lobe (grey arrow), median lobe (grey arrowhead) and the right lobe (black arrowhead)

The median lobes were treated as separate lobes for the purpose of this study and allowed a control and a BETA cycle to be performed in each. Unlike the human liver, the left lateral lobe is consistently the largest of all the lobes – if the median lobe is to be considered as two separate halves.

The caudate lobe adjoins the right lateral lobe on the visceral surface and is usually identified by the presence of a small fissure, which partially separates it from the right lateral lobe. The inferior vena cava (IVC) is intra-parenchymal and runs through the caudate lobe. The gallbladder lies partly within the substance of the right median lobe, and poses potential problems with regard to thermal injury when ablations are performed in this lobe. This potential hazardous area was avoided during the ablations. Saline soaked swabs were placed lateral to the right lateral lobe to improve access to the liver by pushing the lobe anteriorly and medially. The swab was placed between the liver and the abdominal wall and ribcage.

Specific sites were chosen in the liver in order to avoid overlapping ablation zones, to improve examination post mortem and importantly to avoid vital structures such as bowel, kidney, portal vein, gallbladder and diaphragm.
The abdominal incision was held open by self-retaining retractors.
During the surgical procedure, the abdominal viscera were kept moist by frequent saline irrigation. If danger of possible thermal damage to adjacent viscera was encountered, a moist saline swab was placed between the liver to be ablated and the visceral structure for protection.
Two suitable sites were identified in each lobe in order to perform a control and a cycle of BETA. The anterior segment of the lobe that is thinner than the posterior segment of the lobe was chosen for the control and the posterior, larger segment of the lobe was chosen for the BETA cycles (Court et al, 2003). The sites of ablation were documented on a diagram of a porcine liver to ensure the sites of each ablation could be easily identified at post mortem examination. Each ablation was individually annotated according to a predetermined symbol indicating a control RFA or a BETA site.

The control RFA sites were marked as follows (Figure 5.4):
Control 1: Single line
Control 2: Two parallel lines
Control 3: Three parallel lines
Control 4: Four parallel lines

The BETA sites were marked as follows:
Test 1: Single dot
Test 2: Two dots
Test 3: Three dots
Test 4: Four dots

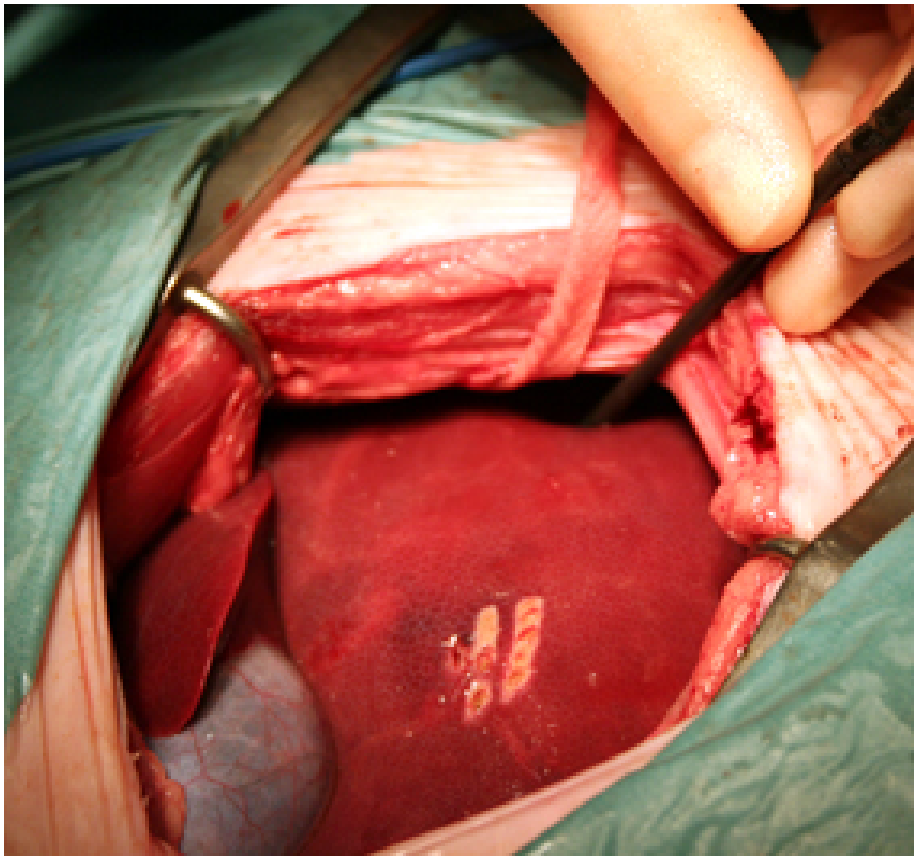

Figure 5.4 shows the liver marked after the second control ablation

Ablation Procedures.

The results of the *ex vivo* ablations described in chapter 2 were the basis for the parameters used in the initial ablation planning for the *in vivo* studies.

No pre-RF DC was to be used and a DC voltage of 9V combined with RF current of 600mA produced the largest ablation zones in a reasonable timeframe.

The mark II ablation machine used for the *ex vivo* studies was used for the *in vivo* animal studies. The mark II machine has no impedance feedback algorithm and is an impedance based ablation machine. The impedance in the *ex vivo* livers ranged from about 80 ohms to 120 ohms depending on the age of the liver and temperature of the liver. For this impedance, RF current of 600mA produced RF power of between 25 and 30 Watts, this was deemed to be the ideal power range for BETA in *ex vivo* liver.

Day 1:

The first day of the scheduled *in vivo* animal studies consisted of two animals, one in the morning and one in the afternoon undergoing terminal anaesthesia.

Following preparation of the animals as described above, the electrode was prepared for use in the first animal. As in the *ex vivo* studies, a brass electrode was used for all the ablations. The brass electrode was insulated with 3cm of exposed electrode for the ablations. A 2.5mm solid brass rod was used for all the *ex vivo* studies, however this was deemed too large for use in the animals and after consultation with the supervisors, a 2mm brass rod was used to decrease the potential injury to the liver.

The brass rod was placed in cold sterilisation solution for 15 minutes prior to use.

Two sites were identified in each lobe of the liver prior to commencement of the series of ablations.

A small incision was made in the liver capsule and the electrode placed into the liver, perpendicular to the liver surface, in order to aid in dissection of the ablation zones post mortem. The electrode was inserted into the liver with careful observation to ensure the entire exposed length of needle entered the liver. A commercially available grounding pad was placed on the animal's skin, immediately overlying the liver on the right side of the abdomen as described previously.

The parameters were then entered into the machine and the ablation cycle started by a member of the veterinary team in accordance with Home Office guidance.

The veterinary surgeon performed all the procedures to ensure continuity of technique and to decrease the potential for surgical error or incorrect use of the electrode. In accordance with Home Office guidance, the researcher is allowed to assistant the licensed veterinary surgeon but may not partake in any practice which may harm the animal in any way. For this reason it was decided I assist in surgery for the first animal to ensure adequate mobilisation of the liver and to identify the sites for ablation. This was only performed in the first animal and all the subsequent surgeries were performed by the veterinary surgeon with no assistant.

The first control ablation revealed the impedance in the liver to be considerably lower than the *ex vivo* liver. An impedance of between 50 to 60 ohms was recorded during the ablation cycle. The machine did not adjust for the low impedance as is found in commercially available ablation machines and thus the ablation cycle continued with an RF current of 600mA and a resultant power of between 15 and 18 Watts. Two cycles of a control ablation and BETA were performed and only a single control ablation reached roll-off. Both the BETA cycles and a control ablation did not reach roll-off and were terminated at 40 minutes (2400 seconds) by the machine. The decision to terminate the ablation cycle at 40 minutes was due to time constraints and the clinical inappropriateness of an ablation cycle taking almost an hour to roll off.

Both supervisors and I agreed to this and the remaining ablations were carried out with a maximum of 40 minutes per cycle if roll-off was not achieved.
The long ablations resulted in the first surgery taking over 6 hours to complete and thus the second animal was postponed for the following week.

Day 2:
The postponed animal surgery took place with only a single animal scheduled for surgery on this particular day; the reason for this was to ensure all the subsequent ablations would continue as per the study protocol.
The animal was prepared in the same way as described for the first animal.
In order to overcome the impedance and subsequent low RF power encountered with the first animal, 3 separate parameters we tested as 3 separate controls in animal two. The anterior aspects of the lobes were used for this purpose in order to preserve the larger posterior lobes for the BETA cycles. RF currents of 750mA, 675mA and 700mA were tested initially. 750mA resulted in over 30 watts of RF power being delivered to the liver; this caused a very fast roll-off of 126 seconds.
675mA resulted in RF power of 23 watts, which produced run-off at 782 seconds. 700mA produced roll-off at 435 seconds, similar times to the *ex vivo* control experiments and this parameter was attempted again with a similar roll-off time (510 seconds). The results of the parameters were discussed by telephone with the supervisors and it was agreed for 700mA to remain the RF current for the remainder of the BETA cycles. The liver was to be examined post mortem and if the ablation zones appeared suitable and comparable to the *ex vivo* studies, 700mA would remain as the RF current parameter for the in-life animal studies. A further control ablation at 700mA was performed and subsequently four BETA cycles using 9V of DC and 700mA of RF power.

Day 3:
Two surgeries consisting of 8 ablations per animal were scheduled for day 3. The animals ablated would be terminated at 2 days post ablation and the liver examined for ablation zone measurement and assessed for visceral thermal injury. The animals were prepared as per protocol and 8 ablations were carried out in each experimental animal. Following the results of the first 2 animals, the technique used for ablations was discussed in detail by the researcher and supervisors. The impedance was discussed at length to ensure reliable reproducible results. The Mark II machine used in the in-life animal studies has no impedance feedback algorithm, resulting in a constant RF current being applied to the tissue and the RF power (watts) and RF voltage changing to compensate for impedance changes. High impedance was observed in the animal liver immediately following application of both BETA and standard RF. The reason for

this is unknown and there is no documented evidence in the literature on this phenomenon. This problem may well have been encountered in research, however the impedance feedback algorithm in commercially available RFA machines would compensate for this and thus not be an observed phenomenon, however this was noted during the *ex vivo* research, but had no observable consequence on the ablation cycle or size of the resultant ablation zone. The high impedance was only observed for the first 20-30 seconds of the ablation cycle and the impedance then rapidly decreased to settle at 50-60 ohms as described. Given this observed impedance phenomenon, the RF current was "stepped" rapidly from 600mA to 700mA in order to prevent premature burning of the tissue during the first 30 seconds of standard RFA and BETA. 600mA of RF current was delivered for 30 seconds and then automatically increased to 700mA by the software. Pulsed RFA has been described (Goldberg et al, 1999) in an attempt to increase the ablation zone.

This method of "stepping" follows similar principles, but the intention is to protect the liver during the short high impedance stage encountered immediately following application of BETA and standard RFA. The low RF current delivered will have very little effect on the overall ablation zone size, but allows for the impedance to settle before maximum RF current is delivered to the tissue. This method was then employed for the remainder of the animal studies. The ablations were completed as planned in both animals and both were returned to their pens post surgery for recovery and subsequent termination at 48 hours.

Day 4:

Two surgeries consisting of 8 ablations per animal were carried out according to the protocol. The animals were to be terminated at 2 weeks post liver ablation. During the ablation cycles of the second animal, erratic cycles were observed with BETA, however the standard RF cycles were stable throughout. All connections to the DC transformer were checked and the grounding pad was inspected for adequate contact and to ensure no thermal burns had occurred (Goldberg et al, 2000b). A commercially available voltmeter was used to check the output from the DC transformer to ensure the output was consistent from the machine. The DC voltage at the grounding pad was checked to ensure the electrode was cathodic and the grounding pad anodic. The results were satisfactory and the ablations were continued.

Both animals returned to the pen for recovery following surgery.

The erratic ablation cycles encountered with BETA during the second animal were discussed with both supervisors following completion of the surgery.

Day 5:

Two surgeries consisting of 8 ablations per animal were carried out according to the protocol. The animals were to be terminated at 4 weeks post liver ablation. The ablation cycles were stable throughout the control RFA and the BETA cycles.
The animals were returned to the pen post surgery for recovery.

Day 6:

Two surgeries consisting of 8 ablations per animal were carried out according to the protocol. The animals were to be terminated at 8 weeks post liver ablation. The ablation cycles were stable throughout the control RFA and the BETA cycles.
The animals were returned to the pen post surgery for recovery.

Day 7:

Two surgeries consisting of 8 ablations per animal were carried out according to the protocol. This additional; surgery day was included in order to perform the experiments on the two replacement animals due to the animal death which occurred in animal 19 (2 week termination) and animal 22 (4 week termination) (This is discussed in detail in this chapter). Each animal was to be terminated according to the original termination schedule. The ablation cycles were stable throughout the control RFA and the BETA cycles.
The animals were returned to the pen post surgery for recovery.

Termination Procedures.

1. **Scheduled termination.**

All animals surviving to the scheduled termination times (2 animals immediately post-ablation, and 2 animals each at 2 days, 2 weeks, 4 weeks and 8 weeks post-ablation) were killed by intravenous injection of sodium pentobarbitone and exsanguination by transection of the carotid/jugular vessels according to Home Office guidance. The animals were fasted overnight prior to post mortem examination.

2. **Non-scheduled termination**

If during the study any animal was to die, or had to be killed for humane reasons in the event of severe ill health or clinical intolerance, the animal would be subjected to a detailed macroscopic post mortem examination and full histopathological examination. This agreement was only if the animal did not fulfill criteria for study exclusion, if this was the case, no post mortem examination was performed. If an agreement by the study director and myself was reached and it was decided to include the animal in the study, this animal was then subjected to full post

mortem examination as described.

Macroscopic examination focused on the liver only, however any gross abnormalities observed incidentally in any other tissues immediately adjacent to the liver, or at the grounding pad site were recorded. Samples of such abnormalities would be preserved at the discretion of the pathologist and/or the Study Director. The necropsy team under the guidance and observance of myself excised the liver. Following incision into the peritoneal cavity, the abdomen was examined immediately for blood and free fluid. The free fluid may be a consequence of an ongoing inflammatory reaction, or may be ascites secondary to portal vein thrombosis – an uncommon but described consequence of RFA. The organs immediately adjacent to the liver were examined for injury and the liver was then removed for examination. In all cases the liver was inspected and handled by myself as well as the ablation zone excisions and measurements. The diaphragm was examined for burns and defects, but none were observed and the adherent diaphragm was then discarded (Figure 5.5).

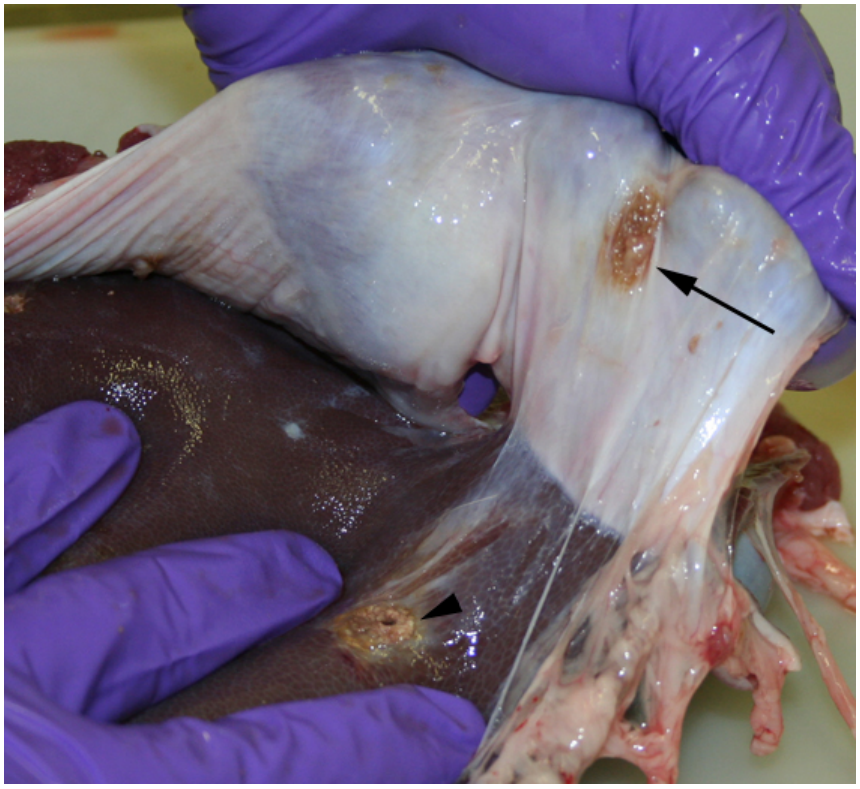

Figure 5.5 shows an ablation site (arrowhead) and a reaction secondary to the ablation on the peritoneal surface of the diaphragm (arrow).

Prior to incision of the liver, the surface of the liver was observed for any abnormality. The annotated sites of ablation were easily identifiable in the non-recovery, 2 day and 2 week terminations, however the markings on the liver in the 4 week and 8 week animals were less

conspicuous and the annotated diagram was used as an adjunct in order to ensure the correct ablation was examined.

Each individual area of ablation was examined and excised. Samples were collected in such a way as to allow subsequent preparation of sections including the centre of the lesion through to normal hepatic tissue beyond the border of the lesion, to allow for accurate measurement of the dimensions of the necrotic, ablated tissue to the border with normal liver parenchyma. The samples were placed on a PVC tray with separate annotations for control and test samples. Once the samples had been examined and measured, the samples were then photographed for macroscopic comparison. The samples were preserved in 10% neutral buffered formalin. Samples were routinely processed (embedded in paraffin wax, sectioned at approximately 4 μm and stained with haematoxylin and eosin) and examined microscopically. Additional stains could be required at the discretion of the study pathologist. Should the standard staining not be sufficient for sample analysis. Photomicrographs of each area of ablation were taken for analysis and subsequent publication.

Results:

Gross Pathological Examination:

The surgical wounds healed well, with no dehiscence or evidence of infection. None of the animals developed abdominal ascites of haemorrhage into the abdominal cavity. The grounding pad sites were unremarkable post surgery in all animals and no thermal burns, either partial or full thickness were observed. No thermal injury was observed in the adjacent organs in any of the experimental animals.

The livers were all intact at removal with no macroscopic evidence of lobar infarction.

Non-Recovery:

The surface of the liver at each of the ablation sites was unremarkable. Each of the ablation sites were excised and examined macroscopically and described according to accepted terminology (Goldberg et al, 2005a, Goldberg et al, 2005b) (Figure 5.6). A clear distinction between the ablated "white zone" and hyperaemic 'red zone" was observed. Careful consideration was taken when measuring the ablation zones in order to ensure the "red zone" was not incorporated into the measurement (Goldberg et al, 2005a, Goldberg et al, 2005b). Three measurements were recorded for data analysis. The measurements consisted of the following:

D1: Diameter of the longest measurement perpendicular to the axis of the electrode.

D2: Diameter of the shortest measurement at the level of the D1 measurement, perpendicular to the axis of the electrode.

D3: Length of the long axis of the ablation, parallel to the axis of the electrode at the site of electrode insertion.

These measurements were used throughout the study, in all experimental animals.

The measurements were validated by two laboratory technicians at Huntingdon Life Sciences present throughout the post mortem examination of the livers as outlines in the study design.

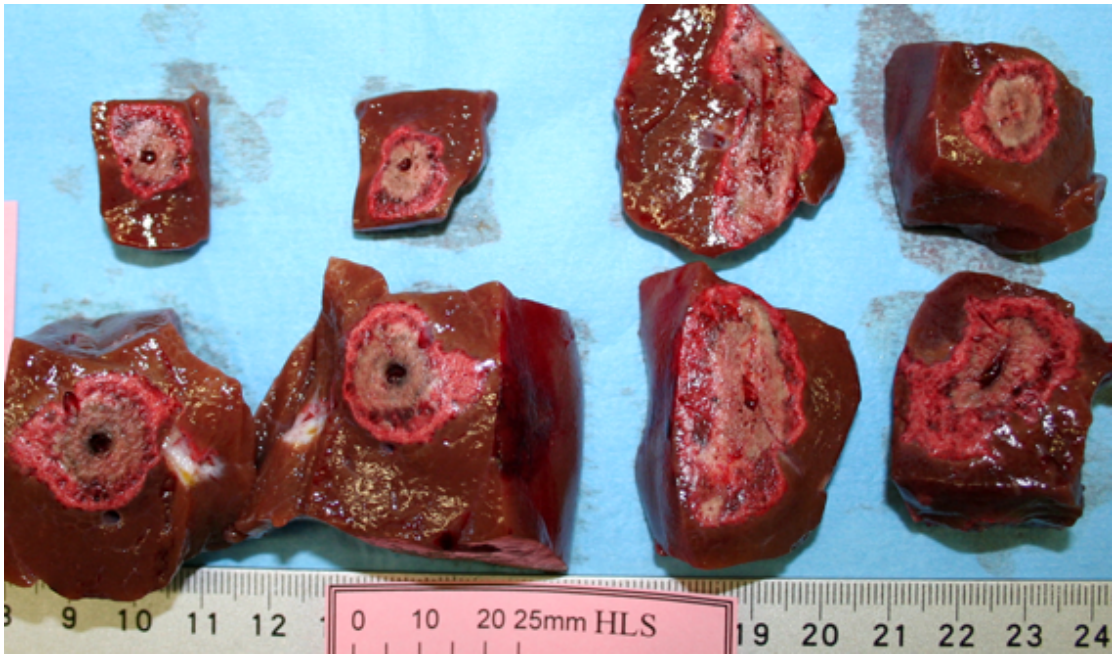

Figure 5.6 ablation specimens. Control (top) and BETA (bottom)

2-day terminations:

The surface of the liver was unremarkable. The sites of ablation were easily identifiable, with only a small incision in the capsule visible. No clot was present at the site of the ablations, but a small amount of fibrinous adhesions between the liver and diaphragm were observed. No hepatic abscesses, biliary thermal injury, or portal vein thrombosis was observed. The stomach, pancreas, right kidney, colon and spleen were normal. Each ablation site was identified and excised for macroscopic examination. The ablation zones were measured according to the terminology described. The ablation zones were well demarcated and easily distinguishable from the surrounding normal liver.

2-week terminations:

Two hours following ablation, the first of the two 2 week termination animals died during recovery in its pen. A post mortem examination was held immediately which was attended by the researcher. The surgical operative notes and anaesthetic notes were examined, however the anaesthetic and surgical notes revealed no significant events peri-operatively. The macroscopic examination of the abdominal cavity was unremarkable, a small amount of blood stained fluid was present however this was due to irrigation during surgery. There was no large peritoneal haematoma and the liver appeared unremarkable.

The liver was excised and examined for evidence of portal vein thrombosis. Biopsies were taken from the lungs, heart, liver and kidneys for histological analysis. The liver was then inspected

for ablation zone measurement and ablation zones recorded.
Following consultation with the study director and according to the approved study protocol, the animal was replaced.
The second and subsequent replacement procedures for 2-week termination animals were uneventful and both animals recovered from surgery and were terminated at 2 weeks according to the study protocol.
In the case of termination at 2 weeks, the diaphragm was adherent to the liver surface and was excised en-bloc to ensure this could be examined more closely following removal. This was probably due to the inflammatory reaction caused by the RFA and BETA. The diaphragm was easily separated from the liver surface by blunt finger dissection (Figure 5.7). The diaphragm did not display any evidence of thermal injury and no perforations were noted. No hepatic abscesses, biliary thermal injury or portal vein thrombosis was observed. The stomach, pancreas, right kidney, colon and spleen were normal. The ablation sites were easily identifiable, as the liver immediately adjacent to the ablated liver appeared to have retracted slightly and revealed the ablate tissue. The ablated tissue was extremely firm, with no evidence of the “red zone” present. Each of the ablation zones was measured as previously described and documented. The size of both the control ablations and BETA appeared to have decreased in size (Table 5.1). The likeliest cause for this is the animals’ response to the ablation. Following an insult the process of healing involves absorption of oedema and of necrotic tissue, in this case the ablated liver. This may have been a factor, but this is purely a hypothesis.

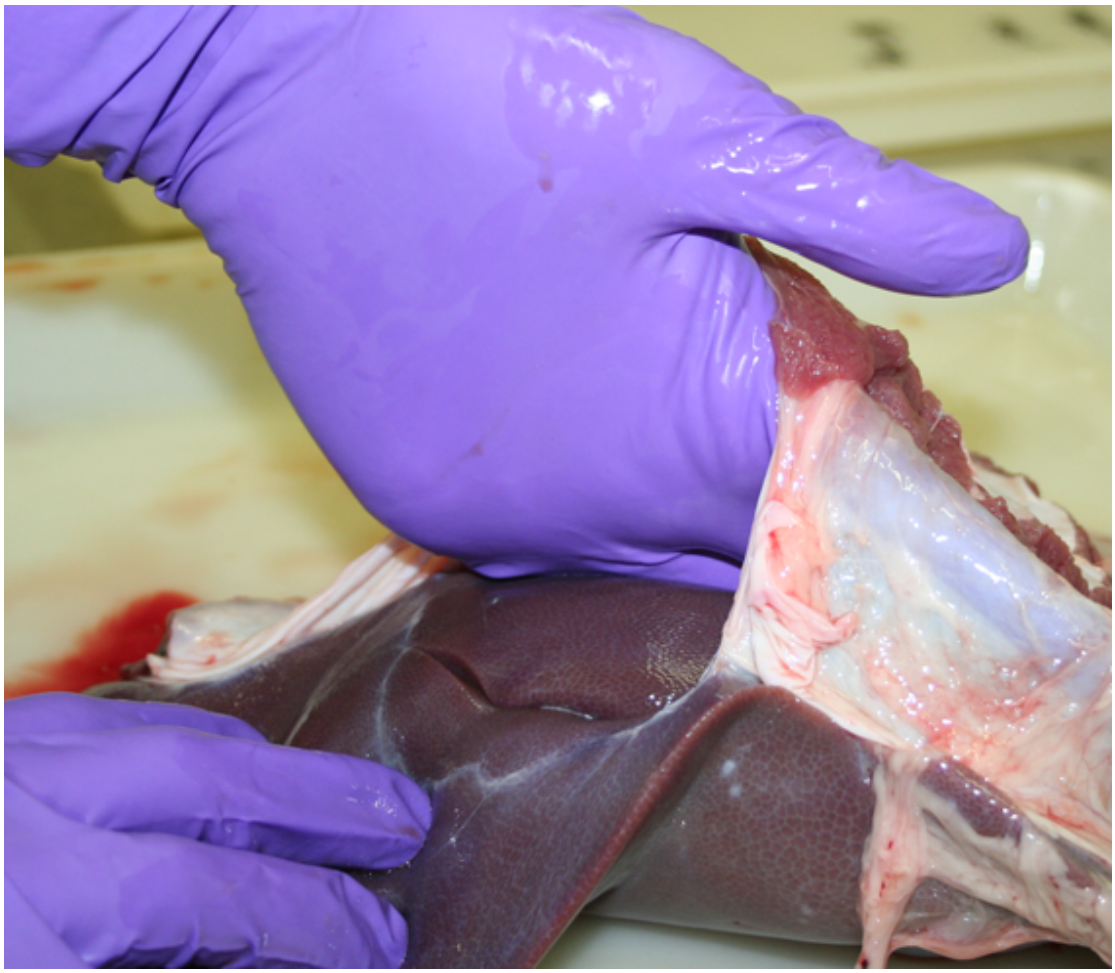

Figure 5.7 the diaphragm was adherent to the liver, however easily separated from the surface.

4-week terminations:

Animal 22 was found dead in its pen on day 4 post surgery. The animal tolerated both the general anaesthetic and the surgery without any clinical concern and with an unremarkable immediate post-operative recovery. On day 1 the animal became unwell, with pyrexia and rigors and was unable to stand. The animal was attended by a veterinary surgeon and the clinical state was deemed stable and probably related to the surgery and anaesthetic. The animal recovered on day 2 and began eating. On day 3 the animal developed anorexia, abnormal gait and began vomiting. The animal was again attended by a veterinary surgeon and analgesia was administered. The animal was deemed stable, but unwell, however the clinical state was not deemed critical, to warrant hospitalisation.

On the morning of day 4, the animal was found dead. A necropsy was conducted the same morning and a large perforated gastric ulcer (4cm) with associated peritonitis was found (Figure 5.8).

The peritoneal cavity was contaminated with partially digested food, with a significant amount of inflammatory ascites. The perforated gastric ulcer and associated peritonitis was considered to be the likely cause of death, and this animal was rejected from the study and replaced. The ulcer was examined histologically and both Neutrophils and Lymphocytes were noted at the ulcer edge. The Neutrophils are acute inflammatory cells, however the Lymphocytes are chronic inflammatory cells, suggesting a chronic ulcer rather than an acute stress ulcer related to the recent surgery. The ulcer primarily involved the mucosa and submucosa, with perforation of the muscularis mucosa. Gastric ulcers occur spontaneously in the pig and can be induced or exacerbated by stress. This observation was made, too by Mr S Wemyss-Holden during his research into electrolysis in pigs (unpublished data). This lesion was thus considered unrelated to the experimental procedure.

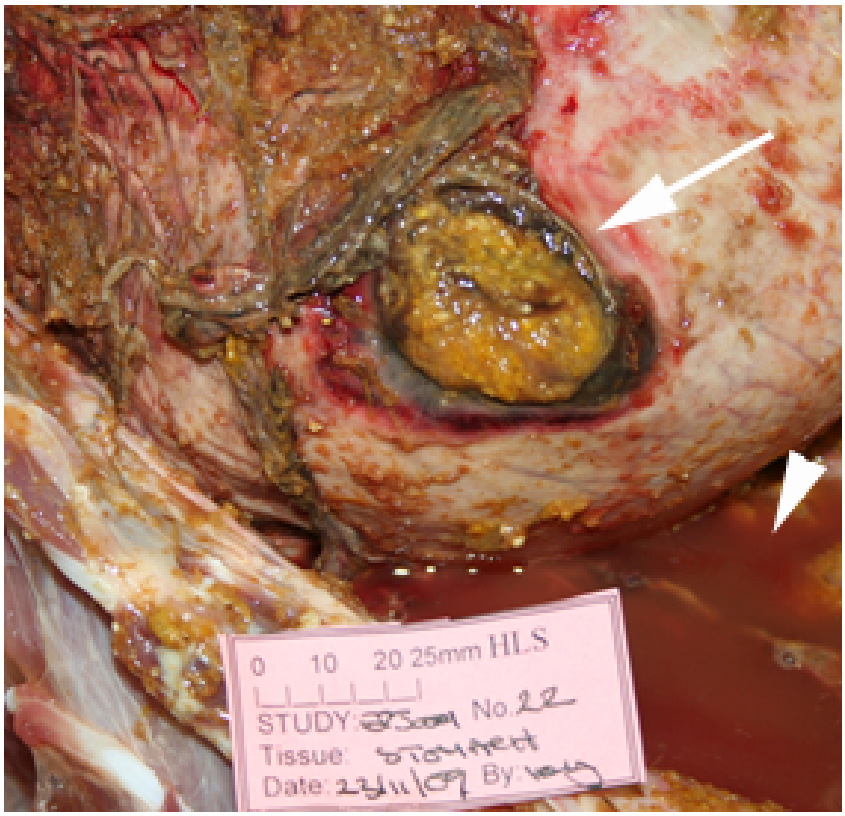

Figure 5.8 shows a perforated gastric ulcer (arrow) and bloodstained peritoneal fluid (arrowhead)

The remaining 4 week termination animal and the subsequent replacement animal underwent successful surgical procedures and recovery and gained weight throughout the 1 month post surgical period. No adverse reactions were encountered. The wounds both healed well with no short or intermediate term complications. At no stage did the animals become unwell and no concerns were raised at any stage by the veterinary staff regarding the animal's recovery and clinical stage throughout the 1month postoperative period.

At post mortem similar observations were documented for both the animals: the diaphragm was adherent to the liver surface and was excised en-bloc to ensure this could be examined more closely following removal. The diaphragm appeared adherent at each site of ablation, but could be separated from the liver with blunt finger dissection. The diaphragm did not display any evidence of thermal injury and no perforations were noted (Figure 5.5). No hepatic abscesses, biliary thermal injury or portal vein thrombosis was observed. The stomach, pancreas, right kidney, colon and spleen were normal. The ablation sites were easily identifiable, as the liver immediately adjacent to the ablated liver appeared to have retracted significantly around the ablation scar, with a small residual scar noted. The ablated tissue was extremely firm, with no evidence of the "red zone" present (Figure 5.9). Each of the ablation zones was measured as previously described and documented. The size of both the control ablations and BETA appeared to have decreased in size compared to the 1 month ablation zones (Table 5.1). The likeliest cause for this is the animals' response to the ablation. Following an insult the process of healing involves absorption of oedema and of necrotic tissue, in this case the ablated liver. This may have been a factor, but this is purely a hypothesis. No evidence of infection, hepatic abscess formation or abnormal inflammatory response was documented.

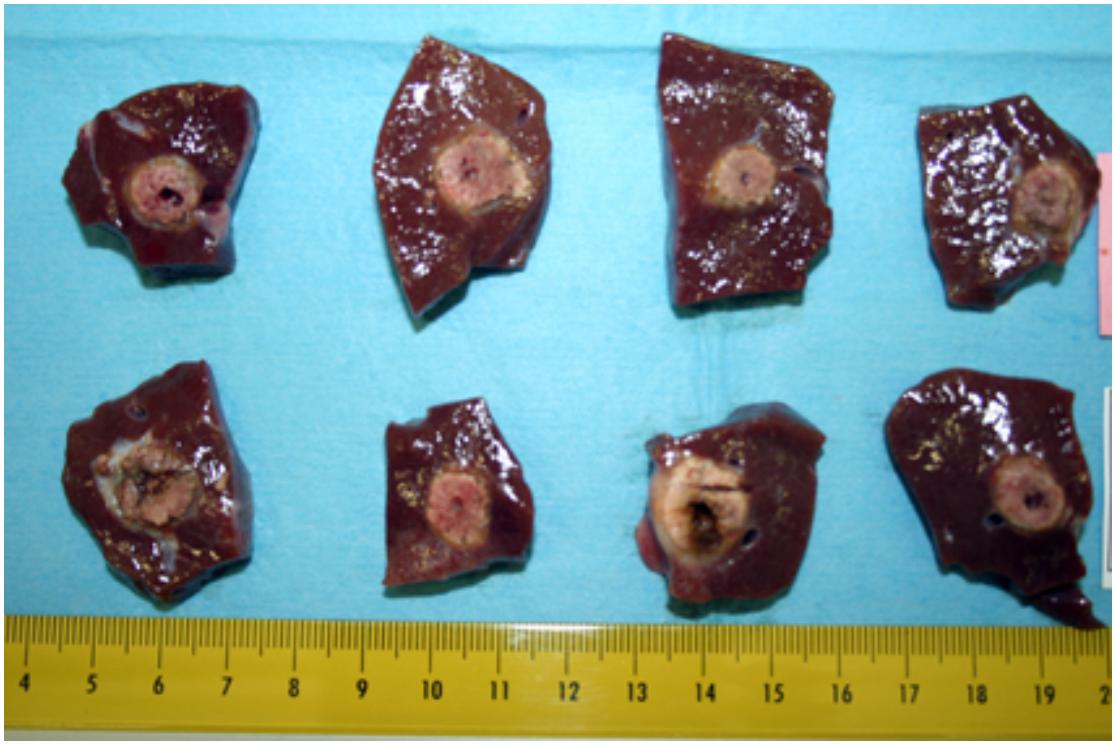

Figure 5.9 showing 28 day termination specimens, control (top) and BETA (bottom)

8-week terminations:

The 8 week termination animals underwent successful surgical procedure and recovery and gained weight throughout the 2 month post surgical period. No adverse reactions were encountered. The wounds both healed well with no short or intermediate term complications. At no stage did the animals become unwell and no concerns were raised at any stage by the veterinary staff regarding the animal's recovery and clinical stage throughout the 2 month postoperative period.

At post mortem similar observations were documented for both the animals: the diaphragm was adherent to the liver surface and was excised en-bloc to ensure this could be examined more closely following removal. The diaphragm appeared adherent at each site of ablation, but could be separated from the liver with blunt finger dissection, however the diaphragm was damaged during this procedure. The reason for this adherent tissue is the intense inflammatory reaction stimulated by the ablations, the difficulty in separating the diaphragmatic surface from the liver was due to established fibrosis following the initial insult (Figure 5.5).

The diaphragm did not display any evidence of thermal injury and no perforations were noted. No hepatic abscesses, biliary thermal injury or portal vein thrombosis was observed. The stomach, pancreas, right kidney, colon and spleen were normal.

The ablation sites were easily identifiable, as the liver immediately adjacent to the ablated liver appeared to have retracted significantly around the ablation scar, with a small residual scar noted (Figure 5.10). The ablated tissue was extremely firm, with no evidence of the "red zone"

present. Each of the ablation zones was measured as previously described and documented. The size of both the control ablations and BETA appeared to have decreased in size compared to the 1 month ablation zones (Table 5.1). The likeliest cause for this is the animals' response to the ablation. Following an insult the process of healing involves absorption of oedema and of necrotic tissue, in this case the ablated liver. No evidence of infection, hepatic abscess formation or abnormal inflammatory response was documented. The decrease in size of the ablation zones however is in contradiction to the results obtained by Dobbins et al (Dobbins et al, 2008a).

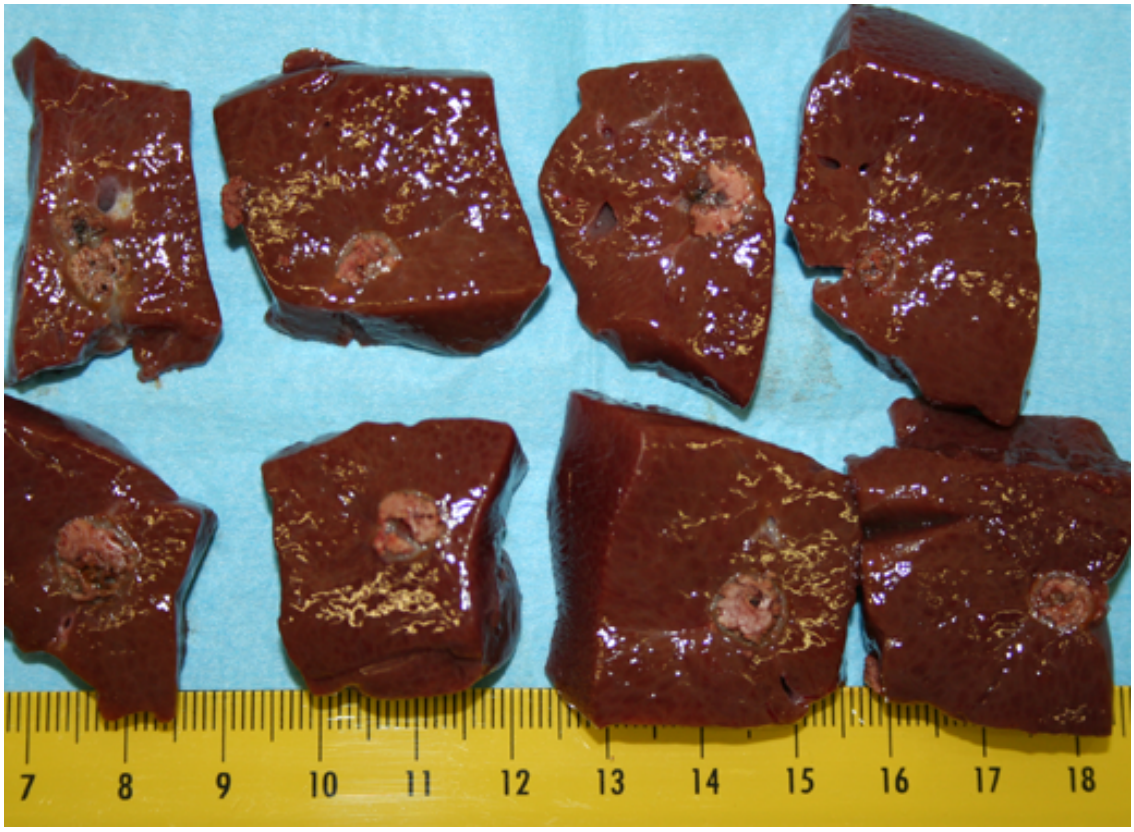

Figure 5.10 shows fibrotic, shrunken ablation sites, control (top) and BETA (bottom)

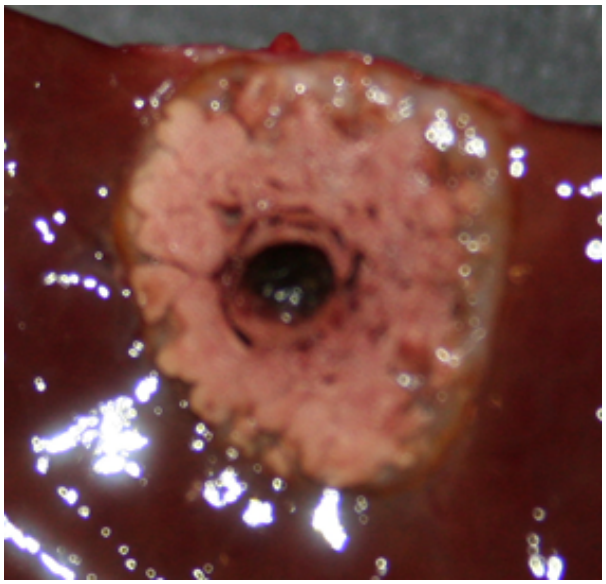

Figure 5.11 Close up of an ablation zone at 56 days. No 'red zone' is seen. The tissue has undergone fibrosis and decreased in size, with a well-demarcated transition between treated tissue and normal liver.

All the histological analysis performed with H and E staining demonstrated cellular necrosis, with no difference in appearance between BETA and conventional RFA. No significant giant cell reaction was noted in the specimens

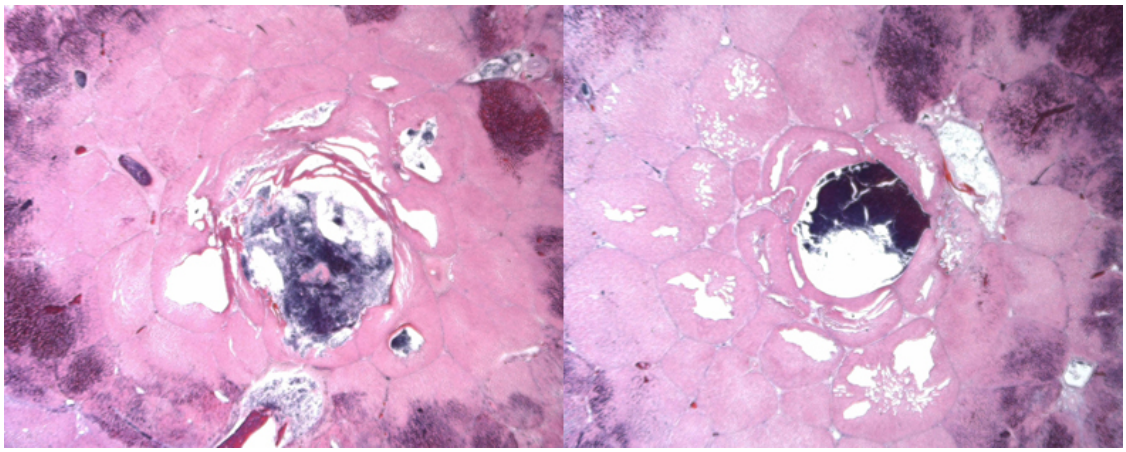

Figure 5.12 H&E staining of control (left) and BETA (right) specimens, with no histological difference observed. No significant inflammatory cell infiltrate is seen.

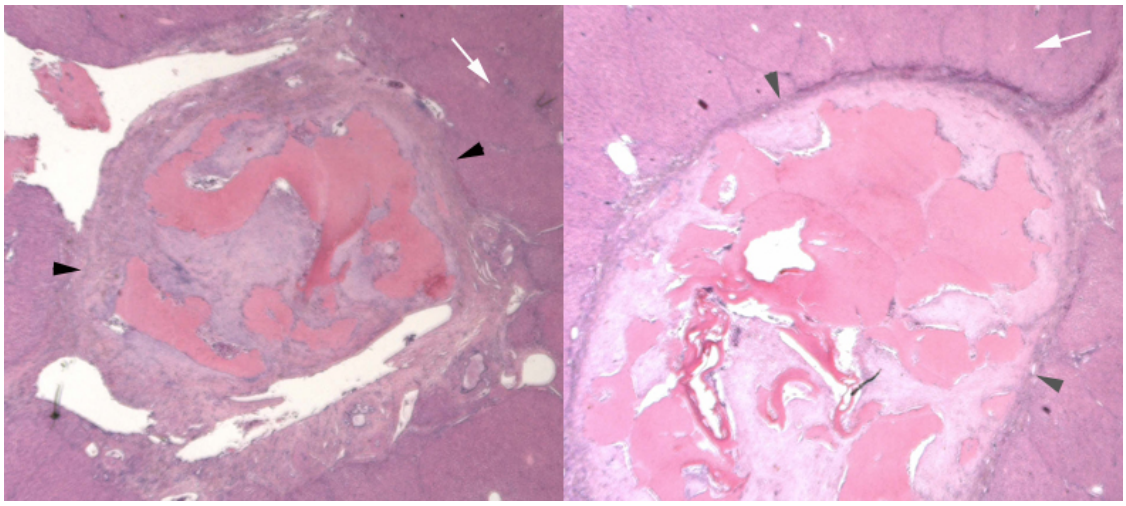

Figure 5.13 shows conventional RFA (left) with a fibrotic ablation (black arrowheads) and BETA (right) with a larger, but similar fibrotic zone of ablation (grey arrowheads). Both are surrounded by normal (arrows) liver parenchyma. No inflammatory cell infiltrate is seen.

The results of the size of each ablation zone in the *in vivo* tissue are expressed as means ± standard deviation (SD) for normally distributed variables or the median and the interquartile range for non-normal variables. Differences in ablation zone size between tissue receiving standard RFA or BETA were tested with ANOVA. A *P* value <0.05 was considered statistically significant. SPSS 17 was used for all statistical data analysis. The size is quoted in millimetres and sizes quoted refer to the maximum short axis measurement of the ablation zone unless specified.
The initial base data will tabulate two sizes for each ablation zone; these refer to the two maximum short axis diameter measurements. The largest of these measurements has been used for all data analysis.

A total of 94 experiments were conducted; Control (n=48) and BETA (n=46).
The each group of animals were scrutinised independently of each other regarding ablation diameter, this is due to the shrinkage of the ablation zone sequentially over time. For this reason, the terminal anaesthesia and 2 day termination animals were assessed as one group, and each subsequent group was assessed independently of each other.

Appendix 4:
Table 5.1 demonstrates the largest short axis diameter ablation zone for each control and corresponding BETA experiment at post mortem examination. The mean, standard deviation (SD) and 95% confidence intervals (95% CI) are tabulated.

For each group of animals (0d and 2d, 14d, 28d and 56d), the BETA zone sizes were significantly larger than the corresponding control RFA zones ($p<0.0001$).

Table 5.2 demonstrates the summary of the 0d and 2d animal data, the mean, median, standard deviation (SD), standard error of the mean (SEM), 95% confidence interval (95% CI) and ranges are listed.

0d and 2d Animals								
					95% CI for Mean			
Animals	N	Mean (mm)	SD	SEM	Lower Bound	Upper Bound	Min (mm)	Max (mm)
0d & 2d Control	24	13.33	2.48	0.51	12.29	14.38	9	18
0d & 2d BETA	22	22.55	4.01	0.85	20.77	24.32	11	29
Total	46	17.74	5.68	0.84	16.05	19.43	9	29

Table 5.2 Summary of the 0d and 2d animal data, the mean, median, standard deviation (SD), standard error of the mean (SEM), 95% confidence interval (95% CI) and ranges are listed.

Table 5.3 demonstrates the summary of the 14d animal data, the mean, median, standard deviation (SD), standard error of the mean (SEM), 95% confidence interval (95% CI) and ranges are listed.

14d Animals								
					95% Confidence Interval for Mean			
Groups	N	Mean (mm)	SD	SEM	Lower Bound	Upper Bound	Min (mm)	Max (mm)
14d Control	8	11.38	1.2	0.42	10.38	12.37	10	13
14d BETA	8	14.88	1.81	0.7	13.37	16.39	12	17
Total	16	13.13	2.33	0.58	11.88	14.37	10	17

Table 5.3 Summary of the 14d animal data, the mean, median, standard deviation (SD), standard error of the mean (SEM), 95% confidence interval (95% CI) and ranges are listed.

Table 5.4 demonstrates the summary of the 28d animal data, the mean, median, standard deviation (SD), standard error of the mean (SEM), 95% confidence interval (95% CI) and ranges are listed.

28d Animals								
					95% Confidence Interval for Mean			
Group	N	Mean (mm)	SD	SEM	Lower Bound	Upper Bound	Min (mm)	Max (mm)
28d Control	8	7.75	2.05	0.73	6.03	9.47	4	9
28d BETA	8	11.5	1.69	0.6	10.09	12.91	9	14
Total	16	9.63	2.66	0.66	8.21	11.04	4	14

Table 5.4 Summary of the 28d animal data, the mean, median, standard deviation (SD), standard error of the mean (SEM), 95% confidence interval (95% CI) and ranges are listed.

Table 5.5 demonstrates the summary of the 56d animal data, the mean, median, standard deviation (SD), standard error of the mean (SEM), 95% confidence interval (95% CI) and ranges are listed.

56d Animals								
					95% Confidence Interval for Mean			
Groups	N	Mean (mm)	SD	SEM	Lower Bound	Upper Bound	Min (mm)	Max (mm)
56d Control	8	5.13	2.03	0.718	3.43	6.82	2	8
56d BETA	8	10.38	1.6	0.56	9.04	11.71	7	12
Total	16	7.75	3.24	0.81	6.03	9.47	2	12

Table 5.5 Summary of the 56d animal data, the mean, median, standard deviation (SD), standard error of the mean (SEM), 95% confidence interval (95% CI) and ranges are listed.

Each of the groups of animals demonstrated a statistically significant difference between the control and the BETA zones.
The 0d and 2d termination animals followed a normal distribution of data, with a statistically significant difference between the control and the BETA groups ($p<0.0001$).
The 14d, 28d and 56d data did not follow a normal distribution and thus logarithmic transformation was performed and ANOVA analysis to determine the significance of the findings.
In each group – 14d, 28d and 56d the results were significant, 14d - $p<0.0001$, 28d - $p<0.005$, 56d - $p<0.001$ when analysed with ANOVA.

Graph 5.1 demonstrates the size ranges for each of the groups of animals for control and corresponding BETA experiments, with standard error bars.

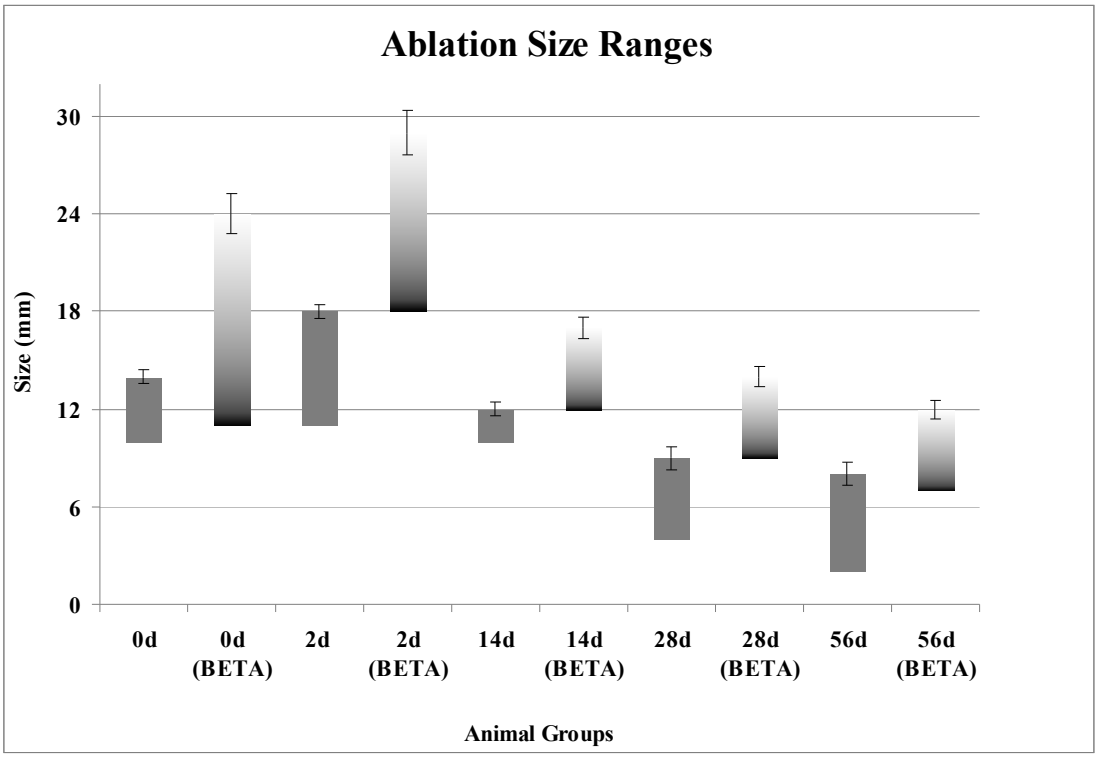

Graph 5.1 The size ranges for each of the groups of animals for control and corresponding BETA experiments, with standard error bars are illustrated.
The control groups are listed as days without the BETA annotation.

Graph 5.2 demonstrates the mean sizes for each of the groups of animals for control and corresponding BETA experiments, with standard error bars.

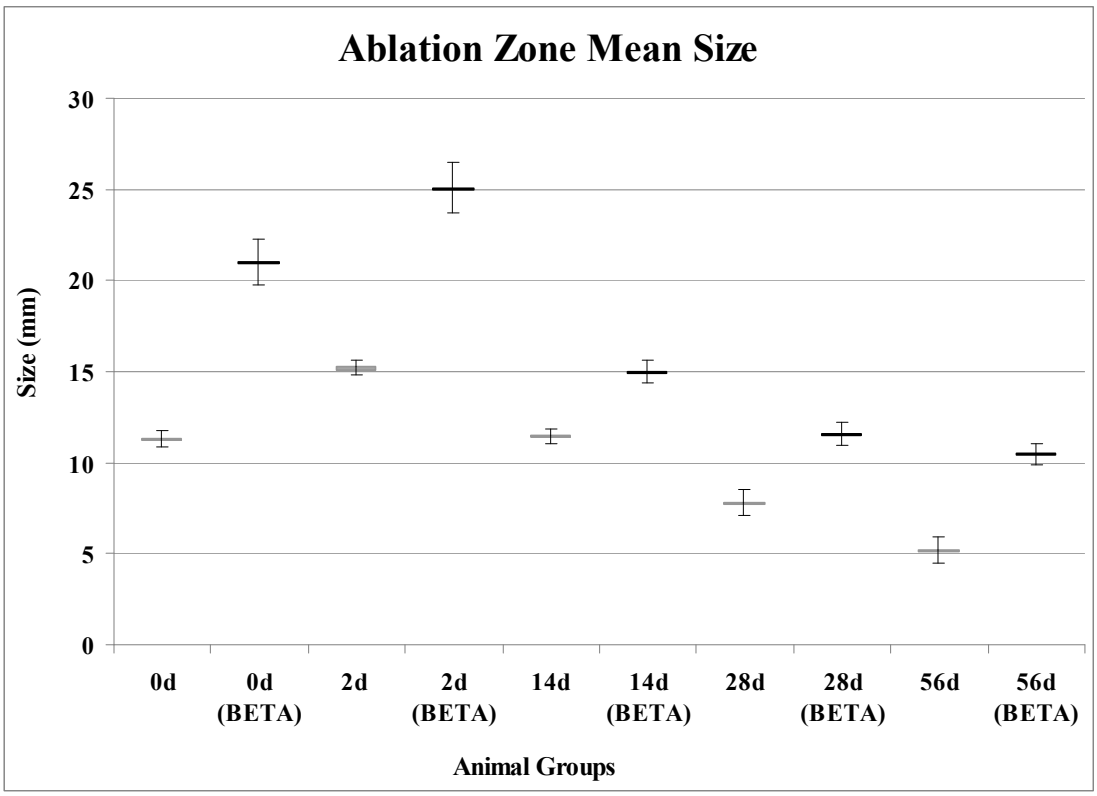

Graph 5.2 The mean sizes for each of the groups of animals for control and corresponding BETA experiments, with standard error bars are illustrated.
(The control groups are listed as days without the BETA annotation).

The animals gained weight following the surgery, mean 19.25 kg (Range 0-30 kg).
The non-recovery animals and 2 day animals were excluded from the weight gain calculations, as the time from intervention to termination was not sufficient to elicit any meaningful change.

Graph 5.3 demonstrates the mean animal weights pre and post surgery and the mean difference between the two weights.
Graph 5.4 demonstrates the individual animal weights pre and post surgery and the difference between the two weights. The animals have been coded according to the termination dates. 1 & 2 – non-recovery, 3 & 4 – 2 day, 5 & 6 – 14 day, 7 & 8 – 28 day and 9 & 10 – 56 day termination animals.

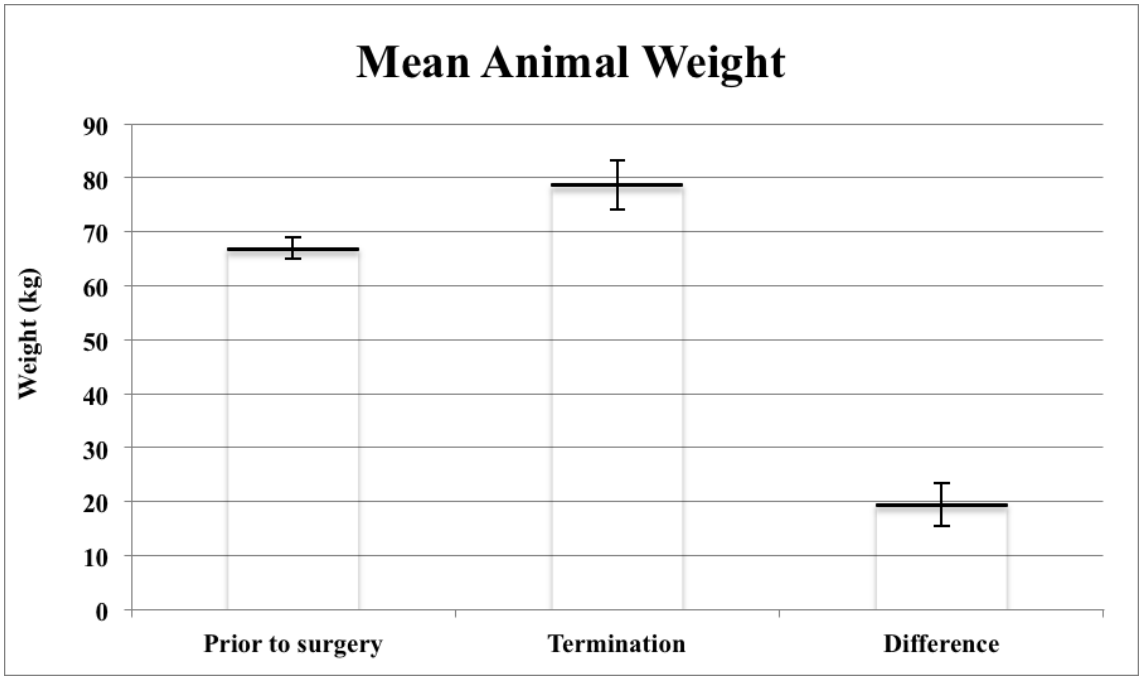

Graph 5. The mean animal weights pre and post surgery and the mean difference between the two weights.

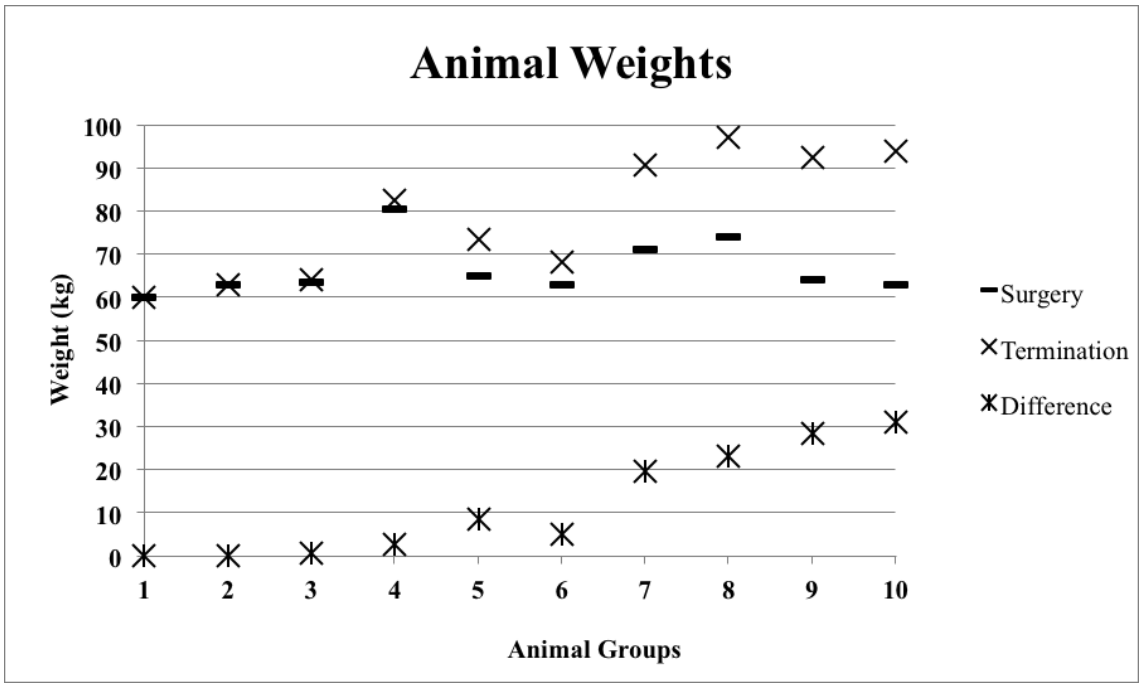

Graph 5.4 demonstrates the individual animal weights pre and post surgery and the difference between the two weights. The animals have been coded according to the termination dates. 1 & 2 – non-recovery, 3 & 4 – 2 day, 5 & 6 – 14 day, 7 & 8 – 28 day and 9 & 10 – 56 day termination animals.

Discussion:

General:

In vivo animal experiments are an essential component to the development of any new medical device or treatment. In the case of medical devices, *ex vivo* experiments provide a safe environment for the researcher to perform a series of experiments in order to determine the efficacy and safety of a device. In the case of BETA, the *ex vivo* experimental work allowed the mark II machine to be tested using a large variety of ablation parameters in order to determine the parameters producing the largest ablation zone. The effects of perfusion of the liver are well documented in the literature (Goldberg et al, 1998b, Nikfarjam et al, 2006, de Baere et al, 2008, Iwamoto et al, 2008), it is accepted the perfusion of tissue and issues relating to the "heat-sink" effect play an cardinal role in ablation zone discrepancy. The safety of devices cannot be tested completely in the laboratory setting and *in vivo* animal studies are essential in order to determine any adverse effects of treatment or unforeseen morbidity associated with a new device or treatment. The effects on perfusion in the liver and the influence of the 'heat-sink' effect on BETA have not been tested using a machine specifically designed for BETA.
During the planning of this research, discussions were held between me and the supervisors regarding methods of access for the ablations. A percutaneous or open approach was considered for the *in vivo* studies. Although percutaneous ablation would replicate clinical practice, we did not feel we would be able to utilise the full liver for ablations, due to the inherent limitations of percutaneous ablation in accessing the subcostal region of the liver and the inherent degradation of the acoustic window when using ultrasound following ablation. During the ablation cycle, gas is formed within the tissue, which limits the transmission of sound through the tissue and degrades the ultrasound image. This limitation would be compounded significantly as 8 ablations were performed in each liver. I felt the possibility of performing inadvertent overlapping ablations due to the limitations of the ultrasound image would potentially compromise the study significantly and therefore, although more invasive, open approach was chosen as the preferred method.

Effects of BETA:

The effects of BETA have been described in the literature (Cockburn et al, 2007, Dobbins et al, 2008, Dobbins et al, 2008a, Dobbins et al, 2008b) since its invention in 2005. A major obstacle in the initial research was the need to place a grounding pad in the subcutaneous tissue rather than on the surface of the skin in order to complete the DC circuit.

Initial animal experiments were unsuccessful when the grounding pad was placed a significant distance from the electrode as with conventional RFA. This was overcome by placing a scalpel blade into the subcutaneous tissue, which was then attached to the anodic DC. The limitations of this meant that this obstacle would have to be overcome in order for this to be accepted as a viable clinical treatment. Placing the grounding pad immediately adjacent to the liver on the skin surface appears to have circumvented this problem. On the first day of *in vivo* ablations, the grounding pad was placed immediately adjacent to the liver on the skin surface and BETA applied to the liver. The DC circuit was completed; however there appeared to be a loss of voltage (1 volt) of DC between the DC transformer and the grounding pad.

This relationship was tested using varying DC voltage to determine whether this loss of DC voltage was a linear, exponential or plateau relationship. Varying voltages from 3 volts to the machine maximum of 50 volts were tested using a commercially available voltmeter to determine the voltage at the grounding pad site.

The relationship appeared to be a stable plateau as the loss of voltage appeared to be 1 volt regardless of the strength of DC voltage applied.

An important observation throughout this research was the lack of any adverse effects caused by polarising the grounding pad (anodic). The adverse effects of anodic polarisation were well described by Dobbins et al (Dobbins et al, 2008a).

The effects of BETA compliment the results obtained in the *ex vivo* experiments and in the published BETA literature to date (Cockburn et al, 2007, Dobbins et al, 2008, Dobbins et al, 2008a).

Following application of standard RFA, the needle chars the tissue and is difficult to remove. As the needle is removed from the tissue, adherent liver from the needle track is removed with the needle (Figure 5.14). This often leads to bleeding from the ablation site, which was easily controlled with manual pressure. This problem however increases the risk of morbidity when the percutaneous method of treatment is used, as the operator is unable to manually control haemorrhage.

This problem was encountered throughout the *in vivo* experiments, with post ablation haemorrhage requiring some manual compression. Following application of BETA, the needle was easily removed from the liver, with little or no adherent tissue (Figure 5.14). The only bleeding encountered from the access site was if a vascular structure was inadvertently injured during the insertion of the electrode. This was easily controlled with manual compression of the bleeding site.

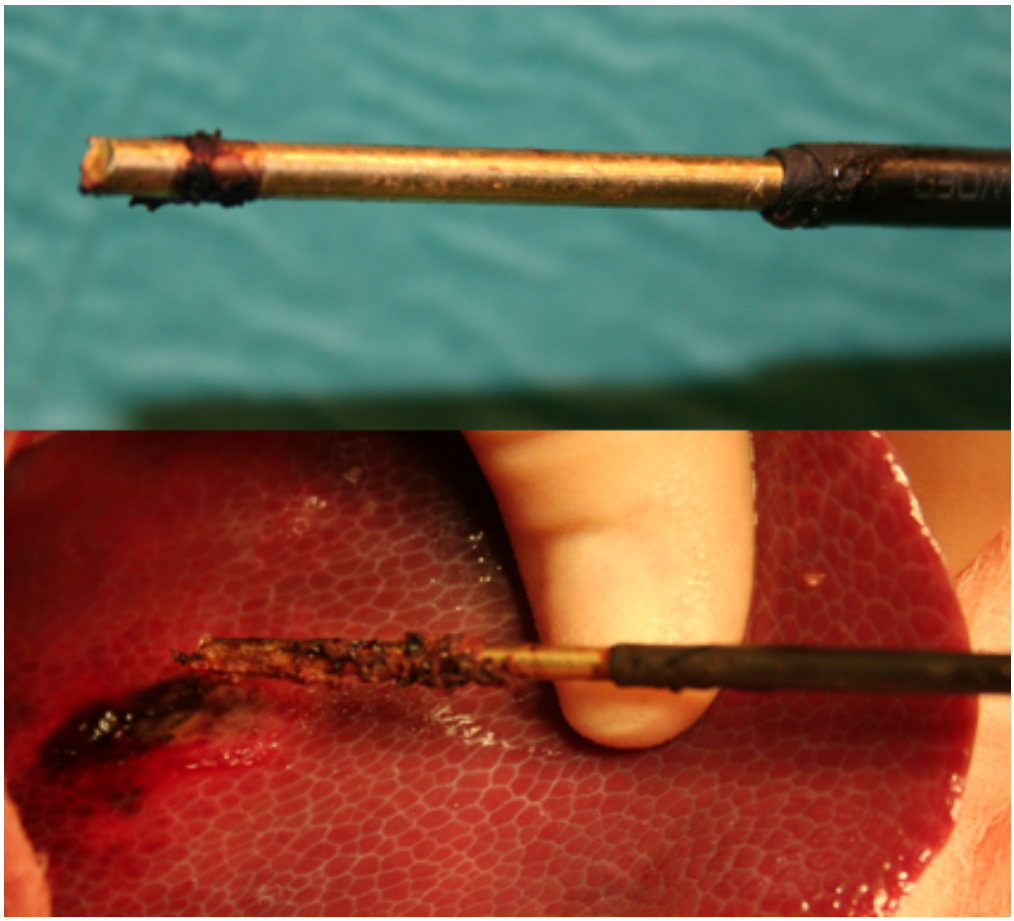

Figure 5.14 the needle following BETA (top), with little adherent tissue compared to conventional RFA (bottom) with a significant amount of adherent tissue

The effects of cathodic DC (Samuelsson, 1981, Berendson and Simonsson, 1994) were evident in the *in vivo* studies as in the *ex vivo* studies. Bubbles were seen at the electrode due to the gaseous liberation described in earlier chapters (Figure 2.11). This confirmed the successful application of cathodic DC to the liver during the BETA experiments.
BETA produced larger zones of ablation when compared to standard RFA; methods have been adopted and tested in order to create larger more confluent zones of ablation with varying results.

Laeseke et al (Laeseke et al, 2005, Laeseke et al, 2006) used multiple electrodes to initially create simultaneous single zones of ablation and then single larger more confluent zones of ablation. This method requires the insertion of multiple needles, which increases the morbidity. Insertion of multiple needles increases the risk of damage to vital structures and removal of multiple needles following conventional RFA increases the risk of haemorrhage following ablation. Laeseke (Laeseke et al, 2007) conducted further studies evaluating multi-tine and multiple needle ablations.

The multiple needle ablations produced larger zones of ablation, but again the risk of increased morbidity with multiple needle insertions.

BETA is able to produce larger ablation zones using a single electrode rather than the needle for multiple needles. Adjunct treatments using ethanol (Goldberg et al, 2000a, Sakr et al, 2005) as an adjunct to RFA have showed promising results, however the effects are often unpredictable and ethanol instillation is not without risk (Chiu et al, 2009). Saline infusion has been widely described in the literature (Livraghi et al, 1997, Burdio et al, 2003) but the efficacy and reproducibility has not been proved conclusively.

Long Term Morbidity:

The long-term morbidity studies are an essential outcome measure when evaluating a new technology. If severe complications develop following the application of a new technology, its safety is brought into question and regardless of the immediate benefits; new medical technology must be proved to be safe with no long-term risks. Before BETA can be considered safe for human trials, the destructive effects as demonstrated in both the *ex vivo* and *in vivo* data must be accompanied by appropriate healing of the treated tissue (Dobbins et al, 2008a). A delayed response to healing or an excessive production of fibrotic tissue may have adverse side effects. The purpose of the study extending the post ablation survival of the animal subjects to 2 weeks, 4 weeks and 8 weeks, provided essential data with regard to the physiological response of the animals to BETA. Radiofrequency ablation has a long established safety profile with very little long term morbidity directly related to RFA, indeed the complications of RFA reported in the literature relate directly to the immediate morbidity associated with the procedure, rather than the long term sequelae thereof (Rhim et al, 2003, Arienti and Pretolani, 2006, Kong et al, 2009). Electrolysis similarly carries an extremely low complication profile (Kinn et al, 1991, Wemyss-Holden et al, 2000, Wemyss-Holden et al, 2002, Finch et al, 2004). The researchers of BETA believed that the combination of these two relatively safe treatments would not alter that safety profile in any way and BETA was expected to behave in a similar way to each of the ablative techniques incorporated into BETA. The purpose of the 2 week, 1 month and 2 month ablations was to demonstrate the safety of BETA and to ensure comparable healing between the control RFA and BETA zones. Data published on the long-term morbidity and hepatic

pathological change demonstrated a favourable safety profile of BETA (Dobbins et al, 2008a). The only complication observed was secondary to the scalpel blade in the subcutaneous tissue. The effect of the scalpel blade was a full thickness burn in the subcutaneous tissue, which progressed to abscess formation. The abscess did not cause any systemic complications, however the abscesses required incision and drainage. The cause of the effects in the subcutaneous tissue were not known and may have been due to "leakage" of RF power from the RF circuit into the DC circuit, resulting in heating of the tissue. Another hypothesis was the effects of the anodic electrode in the subcutaneous tissue (Robertson et al, 1998). The anodic electrode produces hydrochloric acid, chlorine gas and oxygen (Fosh et al, 2002), the cytotoxic effects of the hydrochloric acid and chlorine gas may well be the cause of the necrosis observed at the cathodic electrode site (Dobbins et al, 2008a). No adverse effects were seen at the "anodic" grounding pad site in any of the animal studies conducted during this research. The grounding pad sites did not demonstrate any erythema or burns related to heat production at the sites. No reported sloughing of skin or skin loss was reported in any of the animals.

The healing of the BETA lesions appeared comparable to the standard RFA lesions (Figures 5.9-5.13), the shrinkage of the lesions over time and fibrosis observed from 2 weeks, continuing to the 8 week terminations are entirely consistent with literature of RFA healing (McGahan et al, 1990, Ni et al, 2005, Nikfarjam et al, 2005) and healing following electrolysis (Wemyss-Holden et al, 2000).

The observed healing of BETA lesions observed by Dobbins et al (Dobbins et al, 2008a) was not entirely consistent with the findings in this research. Dobbins et al did not note a significant difference in size of the ablation zones at 2 months compared to the 2 day lesions, however a consistent decrease in the size of the all the lesions was demonstrated consistently throughout this study. The reason for this is uncertain, however a decrease in size is expected following ablation, due to a combination of healing and fibrosis. Dobbins did, however comment on a thick fibrous capsule around the ablation zones at 2 months (Dobbins et al, 2008a). No comment was made regarding the measurement technique.

Animal Deaths:

Two animals died during the study.

Animal 19 (2 week termination) died within 2 hours of the surgery. The animal did not recover from the anaesthesia and post mortem examination did not reveal any cause for the death. The liver itself appeared normal and each of the ablation sites were examined for signs of adjacent visceral or vascular damage, none were found.

Tissue samples were obtained from the heart, lungs, liver and kidneys for routine independent histological analysis. The liver tissue specifically did not demonstrate any signs of hepatic infarction. The cause of death was attributed to the anaesthetic.

Animal 22 (1 month termination) died 4 days after the surgery. Post mortem examination revealed a large (4cm) perforated gastric ulcer (Figure 5.8). The peritoneum was contaminated with partially digested food and a significant amount of inflammatory ascites. On initial inspection, the size of the ulcer suggested it was chronic, however had perforated acutely following the stress of the surgery. The development of gastric ulcers was observed by Mr Wemyss-Holden during his research into electrolysis (unpublished data) and is well recognised. The ulcer occurred on the anterior wall of the stomach a significant distance from the liver and was not secondary to thermal injury form a misplaced ablation electrode.

Samples of the gastric wall and ulcer were obtained for histological analysis.

The histological analysis revealed the prescence of Neutrophils and Lymphocytes.

Neutrophils are acute inflammatory cells, however Lymphocytes are chronic inflammatory cells, indicating chronicity of the ulcer. The size of the ulcer, too suggested chronicity – large perforated ulcers are unusual acutely.

The results of this animal study demonstrate BETA to be a safe technique of thermal ablation. The adverse effects of the positive electrode have been overcome by adjusting the site of the grounding pad and the lack of an invasive mechanism needed for circuit completion as has been demonstrated (Cockburn et al, 2007, Dobbins et al, 2008, Dobbins et al, 2008a, Dobbins et al, 2008b) shows significant advances in the development of BETA for human use. The lack of any significant complications observed during the study demonstrates BETA to be a robust thermal ablation technique with significant advantages over multi-tine RFA techniques. The two deaths encountered during this trial, although notable, was not attributed to the ablations directly. The post mortem results revealed no significant intra-abdominal pathology related to thermal injury and although passed fit for surgery by the veterinary team, the causes of death were related to, but no directly caused by thermal ablation. A single death was reported by Dobbins et al (Dobbins et al, 2008a) and was similarly attributed the anaesthetic rather than directly related to BETA.

Limitations of this Research:

I accept there are a number of limitations with research.

1. Normal liver was utilised and not a tumour model does raise the question of the efficacy of BETA to ablate tumours rather than normal liver.
   This point was discussed and considered extremely carefully prior to making the decision to proceed with the study design.

2. In order to demonstrate BETA's efficacy *in vivo*, an animal model had to be chosen that would simulate a clinical patient. For this reason the White hybrid porcine model was chosen. In order to perform the experiments on a tumour model, VX2 colony would serve as the most appropriate tumour model. This model is costly to initiate and is subject to the United Kingdom Animals (Scientific Procedures) Act 1986 (the Act). The Act, administered by the UK Home Office, regulates all scientific procedures in living animals which may cause pain, suffering, distress or lasting harm and provides for the designation of establishments where procedures may be undertaken, the licensing of trained individuals who perform the practical techniques and the issue of project licenses for specified programs of work. The time and financial constraints on this research made this impossible. A further reason for choosing this particular model was to prove BETA to be safe *in vivo* and to replicate the *in vivo* results as outlined in chapter 2. Although this technology requires validation in tumour models, we felt this was not the primary objective of the animal research. As outlined in Chapter 7, the aim is to validate the technology in a tumour model in the clinical setting, with the ablation parameters used and validated during this research.

3. The use of open ablation as opposed to percutaneous ablation exposed the animals to a laparotomy; however we felt this to be the safest technique in order to ablate the liver according to the study design. Although minimally invasive, percutaneous ablation would have limited the number of potential ablations in each liver and had the potential for overlapping ablations as outlined in the discussion.

Conclusions:

1. BETA produces significantly larger ablation zones compared to standard RFA *in vivo*.

2. BETA can be successfully applied to an animal model using a single grounding pad placed adjacent to the liver on the skin.

3. No significant morbidity is associated with BETA when compared to the literature.

4. BETA demonstrates a favourable long-term morbidity, with no evidence of a delayed adverse event at 2 months.

5. BETA lesions heal in a predictable fashion and are comparable to standard RFA, with no abscess or fistula formation.

6. There is a small loss of DC voltage between the transformer and the grounding pad, however this is constant and does not fluctuate with fluctuating DC voltages.

7. No adverse effects are observed at the ”anodic” grounding pad site due to the formation of hydrochloric acid, chlorine gas or oxygen.

Chapter 6:

Bimodal Electric Tissue Ablation:

Response to BETA –

Biochemical Markers and Acute Phase Proteins

Introduction:

Surgical resection has been shown to be one of the best treatment options for patients with hepatocellular carcinoma (HCC) and colorectal liver metastases as discussed in chapter 1. Only a small number of patients are, however suitable for curative surgical resection at time of diagnosis (Cheung et al, 2009). The commonest cause of the low resectability in this subset of patients are the number of metastases present in the liver, distant metastases (commonly in the lungs), the proximity to vital structures in the liver, such as portal vein and IVC, preventing adequate, safe resection and the inability to preserve amount enough liver to afford normal hepatic function post resection. In a small group of patients, associated comorbidities place the patient at risk of significant postoperative morbidity. Patients with HCC have a further surgical alternative, should liver reserve prove an obstacle for liver resection – liver transplantation. A significant small number of patients however are lucky enough to be successful recipients of donor livers. Ablative techniques provide an alternative in those patients deemed unresectable. The complications of alternative ablation methods to radiofrequency ablation have been discussed in chapter 1. Cryotherapy carries the complication of the cryoshock phenomenon (Seifert and Morris, 1999), which, although low is associated with the volume of tumour treated and can stimulate catastrophic inflammatory cascades, with fatal results (Seifert and Morris, 1999). Seifert et al (Seifert et al, 1999) showed a significant association between serum Aspartate Transaminase (AST) levels and raised plasma TNF-α (Tumour Necrosis Factor – alpha) and IL-6 (Interleukin – 6) levels post procedure in patients undergoing cryotherapy or resection with cryotherapy. The volume of the ice ball and duration of freezing were significantly associated with the AST, TNF-α and IL-6 levels at various times postoperatively. Seifert demonstrated hepatic cryotherapy to be related to cytokine release and hence elevated plasma TNF-α and IL-6 levels which were directly associated with the degree of hepatic cryotrauma. He postulated the mediators were one of the causes of the inflammatory cascade causing cryoshock following large-volume hepatic freezing. Ethanol Injection, although regarded as a safe procedure has recently been associated with complete hepatic infarction (Chiu et al, 2009). Again the volume of tumour treated has a significant influence on the complication rate, however a recent meta-analysis (Bouza et al, 2009) demonstrated RFA to be more effective than percutaneous ethanol injection (PEI) for treatment of HCC.
With the potential complications of other ablative techniques and the reported superior effectiveness of RFA compared with many of the ablative techniques (Marlow et al, 2006), RFA is currently the most common method of ablation for HCC and colorectal metastases (Malczyk and Sutherland, 2009).

RFA is being used on an increasing number of patients, especially those with more advanced underlying liver disease with more tumours and in challenging locations in the liver, which previously were thought to be beyond the safety of successful RFA (Head et al, 2007, Brennan et al, 2008).

This, inevitably, leads to increased complications, some of which have been major (Mulier et al, 2002). A large-scale review of complications of RFA administered to different liver tumors has concluded that the morbidity and mortality associated with RFA is, in fact, higher than previously reported. Marlow et al. (Marlow et al, 2006) demonstrated an overall complication rate associated with RFA to be less than 5% in the referenced literature, however this conflicts with an overall complication rate of 8.9% among 3670 patients described by Mulier et al (Mulier et al, 2002) in literature review to December 2001. The ASERNIP Report No. 56, however contained strict inclusion and exclusion criteria for literature and therefore did not include all papers published regarding radiofrequency ablation to 2006, however 5% or less has been the quoted in the literature. The review evaluated percutaneous, laparoscopic, simple open and combined open approach with an increasing complication rate as the intervention increased in complexity. The review was not limited to HCC and colorectal metastases treatment and included all radiofrequency ablation procedures.

The most common complication quoted in the literature was intraperitoneal bleeding, which encompassed subcapsular haematomas and free intraperitoneal blood. This bleeding is generally not significant, however it highlights the trauma caused when the needle is removed from the liver. Charred liver, which occurs at the needle tip, is adherent and when the needle is removed; it brings amounts of liver tissue with it through the track. This may well contribute to bleeding.

In addition documented cardiac complications, range from vasovagal syncopal episodes to ventricular fibrillation. The vasovagal syncopal episodes may have been related to pain rather than RFA, the 2 ventricular fibrillation episodes were encountered with ablation of carcinoid metastases – a well-known sequelae of treatment of carcinoid tumours by ablation or surgery. The single cardiac death occurred 20 days post RFA and cannot be attributed to RFA directly.

This review of complications is the largest to date (Mulier et al, 2002) and although the overall complication rate is higher than many in the quoted literature, most complications were minor and had little or no influence on the outcome of the treatment. Indeed with more careful scrutiny of the complications, the results are extremely encouraging for RFA and demonstrate the overall safety of this ablative method.

BETA increases the hydration of the ablated tissue by electroosmosis. This decreases the charring at the needle tip and subsequently decreases the amount of adherent tissue at the needle tip following ablation.

The *ex vivo* studies consistently demonstrated little or no adherent tissue at the needle tip upon removal of the electrode from the tissue. These finding were mirrored in the *in vivo* studies. The lack of trauma associated with removal of the electrode from ablated tissue decreases the risk of haemorrhage from tissue following removal of the electrode.

An important question in this research regarding in life animal studies is the inflammatory response to BETA. When researching a new medical device, the physiological response to trauma is important, an inflammatory response may be initiated with little or no observed complications during the procedure, manifesting late with possible fatal consequences. This may be due to a number of factors, namely the insult of the ablation on the tissue being treated and the physiological response of the body to the insult. Cryoshock (Seifert and Morris, 1999, Seifert et al, 1999) may develop with no observed complications during the procedure, however this potentially catastrophic event may be detected only following analysis of biochemical and inflammatory markers (Seifert et al, 1999). Abnormal or normal biochemical and inflammatory markers do not in any way substitute for diligent postoperative care. The pulse, blood pressure, respiratory rate and temperature are all key in determining a developing inflammatory response and in essence, elevated blood markers can only aid in diagnosis are not in any way diagnostic of a severe inflammatory response.

BETA has been shown to be safe in animal studies (Cockburn et al, 2007), however no biochemical analysis was performed to confirm the response to BETA.

Objective:

The objective of this research is to determine the *in vivo* response to BETA. Biochemical markers related to both liver and kidney function and inflammatory factors including specific porcine inflammatory markers will be analysed and discussed.

Materials and Methods.

In vivo Porcine Experiments.

Animal Subjects:

Ten domestic pigs, large White hybrid females were used for the *in vivo* experiments. The animals described in chapter 5 are the same subjects referred to in this chapter, with the same termination schedule. The pigs were aged between four and five months with a mean weight of 66.7 kg (Range 60 – 80.5kg). The pigs followed exactly the same experimental treatment, however the times of termination differed as follows.

Each group consisted of 2 pigs:

Group 1 were terminated immediately post procedure and will be referred to as non-recovery animals

Group 2 were terminated at 2 days.

Group 3 were terminated at 2 weeks.

Group 4 were terminated at 4 weeks.

Group 5 were terminated at 8 weeks.

Blood Analysis.

An important aspect of the *in vivo* porcine studies is the animals' reaction to the insult of BETA. A biochemical profile examining the liver and renal functions (Table 6.5 & 6.6) and a series of inflammatory markers specific to the porcine species (Table 6.1-6.4) (Alava et al, 1997, Eckersall et al, 1999a, Hiss et al, 2003, Grau-Roma et al, 2009, Pineiro et al, 2009) were tested. The Group 1 animals were not acclimatised for 2 weeks prior to ablation procedures, as were groups 2-5, however all blood samples were obtained according to the same protocol (-1 to -2 days pre ablation).

The following protocol was used for blood sample acquisition for the animal groups.

Pretreatment: Day -1 or -2	All animals
Immediately post-ablation	All animals
24 hours post-ablation	Animals in Groups 2, 3, 4 and 5
48 hours post-ablation	Animals in Groups 2, 3, 4 and 5
72 hours post-ablation	Animals in Groups 3, 4 and 5

The initial analysis of the inflammatory markers was obtained following ablation of animal 24. Consultation with the supervisors and Dr L Bence (ReactivLab) suggested additional samples

should be obtained for inflammatory marker analysis pretermination. The pre-termination bloods were extended to include biochemical markers to ensure the liver and renal functions had returned to normal.

The protocol for the additional blood samples were as follows:

Pretermination	Animals in Groups 3, 4 and 5.

C-Reactive Protein (CRP):

Background:

C-reactive protein (CRP) is a protein found in the blood, which rises in response to inflammation (an acute phase protein). It is synthesised in the liver in response to a rise in the plasma concentration of IL-6, which is produced predominantly by macrophages as well as adipocytes (Pepys and Hirschfield, 2003). CRP binds to phosphocholine expressed on the surface of dead or dying cells in order to activate the complement system, which in turn stimulates an inflammatory response. It is a member of the Pentraxin family of proteins but is not related to C-Peptide or Protein C. It is thought to assist in complement binding to foreign and damaged cells and enhances phagocytosis by macrophages (opsonin mediated phagocytosis), which express a receptor for CRP. CRP rises up to 50,000-fold in acute inflammation, such as infection. It rises above normal limits within 6 hours, and peaks at 48 hours. Its half-life is constant, and therefore its level is mainly determined by the rate of production (and hence the severity of the precipitating cause) (Pepys and Hirschfield, 2003).

Method:

The porcine CRP assay is performed using an enzyme linked immunosorbent assay (ELISA) developed and validated at Reactivlab.

Sample and Standards

Serum samples were obtained from the 10 domestic large white hybrid pigs. Each serum sample was labelled, detailing the animal, the unique identifier code and the nature of the sample for analysis. All samples were frozen and transported as a batch to the ReactivLab laboratory. On receipt, the frozen samples were stored in a -80^{o}C freezer for analysis.

All samples were diluted 1:10000 in assay buffer prior to use.

Standards were prepared to give a range from 70ug/ml.

Calculation of Results:

The assay was read using a Fluostar Optima platereader pre-programmed with the assay details so that standard curve and sample concentrations were calculated automatically applying the

dilution factor. CRP concentration in unknown samples was calculated by comparison with the standard curve. Results from the control samples were assessed and confirmed to be within an acceptable range. All samples were analysed twice.

Serum Amyloid A (SAA):

Background:

Serum amyloid A (SAA) proteins are a family of apolipiproteins associated with high-density lipoprotein (HDL) in plasma and are synthesised predominantly in the liver. Different isoforms of SAA are expressed at different levels or in response to inflammatory stimuli (acute phase SAAs). The conservation of these proteins throughout invertebrates and vertebrates suggests that SAAs play a highly essential role in all animals. Acute-phase serum amyloid A proteins (A-SAAs) are secreted during the acute phase of inflammation. These proteins have several roles: transport of cholesterol to the liver for secretion into the bile, recruitment of immune cells to inflammatory sites, and the induction of enzymes that degrade extracellular matrix. SAA genes are regulated in liver cells by the proinflammatory cytokines IL-1, IL-6, and TNF-α (Uhlar and Whitehead, 1999).

Method:

The SAA assay was performed using an enzyme linked immunosorbent assay (ELISA) provided by Tridelta (Dublin, Ireland), on a Triturus automatic ELISA processor (Grifols, UK). A qualified engineer services this machine annually. A record of annual service visits is kept for laboratory compliance purposes.

Samples and Standards:

Serum samples were obtained from the 10 domestic large white hybrid pigs. Each serum sample was labelled, detailing the animal, the unique identifier code and the nature of the sample for analysis. All samples were frozen and transported as a batch to the ReactivLab laboratory. On receipt, the frozen samples were stored in a -80^{o}C freezer for analysis.

All samples were initially diluted 1:500 in assay buffer prior to use then, if necessary depending on results, further diluted to 1:5000 or rediluted at 1:100. Standards were prepared to give a range from 2000ng/ml.

Calculation of Results:

The assay was read on the Triturus automatic ELISA processor pre-programmed with the assay details so that standard curve and sample concentrations were calculated automatically applying the dilution factor. pMAP concentrations in unknown samples was calculated by comparison with the standard curve. Results from the control samples were assessed and confirmed to be within an acceptable range. All samples were analysed twice.

Pig – Major Acute Phase Protein (Pig-MAP)

Background:

Pig-MAP is an acute phase protein, which is the pig counterpart of a recently cloned human serum protein denominated PK-120, which is a putative substrate for kallikrein (Gonzalez-Ramon et al, 1995). The protein exists in other mammalian species and it is also an acute phase protein, at least in the rat. Pig-MAP shows homology, as PK-120, with the heavy chain 2 (HC-2) of the inter-α-trypsin inhibitor superfamily but does not possess trypsin inhibitory activity (Alava et al, 1997). The protein rises following stimulation of the inflammatory cascade, reaching maximum concentration at 24-48 hours after the initial insult. Pig-MAP is induced in a variety of experimental models and under different physiological and pathological conditions, such as inflammation and small bowel surgery. Pig-MAP concentration exhibits the most obvious increase in pigs, which show more severe symptoms following inflammation and surgical trauma (Gonzalez-Ramon et al, 1995).

Method:

The pig MAP assay was performed using an enzyme linked immunosorbent assay (ELISA) provided by PigChamp (Spain), on a Triturus automatic ELISA processor (Grifols, UK). A qualified engineer services this machine annually. A record of annual service visits is kept for laboratory compliance purposes

Sample and Standards

Serum samples were obtained from the 10 domestic large white hybrid pigs. Each serum sample was labelled, detailing the animal, the unique identifier code and the nature of the sample for analysis.

All samples were frozen and transported as a batch to the ReactivLab laboratory. On receipt, the frozen samples were stored in a -80^{o}C freezer for analysis.

All samples were diluted 1:1000 in assay buffer prior to use. Standards were prepared to give a range from 3.5ug/ml.

Calculation of Results

The assay was read on the Triturus automatic ELISA processor pre-programmed with the assay details so that standard curve and sample concentrations were calculated automatically applying the dilution factor. pMAP concentrations in unknown samples was calculated by comparison with the standard curve. Results from the control samples were assessed and confirmed to be within an acceptable range. All samples were analysed twice.

Haptoglobin (Hp):

Background:

Haptoglobin (abbreviated as Hp) is a protein encoded by the HP gene in human subjects. In blood plasma, haptoglobin binds free hemoglobin (Hb) released from erythrocytes with high affinity and thereby inhibits its oxidative activity (Dobryszycka, 1997). The haptoglobin-haemoglobin complex is then removed by the retuculoendothelial system (mostly the spleen but also in the liver). In clinical setting, the haptoglobin assay is used to screen for and monitor intravascular hemolytic anaemia; the reticuloendothelial system removes the haptoglobin-haemoglobin complex from the body and thus haptoglobin levels are decreased in haemolytic anaemia. In the process of binding haemoglobin, haptoglobin sequesters the iron within haemoglobin, preventing iron-utilising bacteria from benefiting from haemolysis. It is theorised that, because of this, haptoglobin has evolved into an acute phase protein. Eckersall et al (Eckersall et al, 1996) investigated the most appropriate proteins as markers of inflammation. The study demonstrated C-reactive protein and haptoglobin likely to be the best markers for the identification of inflammatory lesions in pigs.

Method:

Haptoglobin (Hp) present in the samples provided for biochemical analysis combines with haemoglobin and at low pH preserves the peroxidase activity of the bound haemoglobin. Preservation of the peroxidase activity of haemoglobin is directly proportional to the amount of haptoglobin present in the sample. This method is described and validated by Eckersall et al (Eckersall et al, 1996).

The haptoglobin assay is performed on an automated biochemical analyser – the Pentra 400. This machine was calibrated before use and is serviced bi-annually by a qualified engineer. ReactivLab keeps a record of service visits for Laboratory compliance purposes.

Standards and Samples

Serum samples were obtained from the 10 domestic large white hybrid pigs. Each serum sample was labelled, detailing the animal, the unique identifier code and the nature of the sample for analysis. All samples were frozen and transported as a batch to the ReactivLab laboratory. On receipt, the frozen samples were stored in a -80^{o}C freezer for analysis.

All samples were analysed in the same laboratory by ReactivLab. A stock pool of serum with a haptoglobin concentration of 1.48g/L was aliquoted and stored at -20^{o}C. This material was thawed and diluted in 2% Bovine serum albumin (BSA), to give standards at haptoglobin concentrations of 1.48, 0.73 and 0.38g/L. A zero standard (2% BSA) was also included.

Pools of serum with known Hp concentration were kept aliquoted at -20^{o}C.

Serum samples were applied to the assay neat and if necessary analysis was repeated with samples diluted to 1:5 in saline.

Calculation of Results

The increase in absorbance at 600nm over the 50s after substrate addition was used to calculate the standard curve by the Pentra 400 computer program. Haptoglobin concentration in unknown samples was calculated by comparison with the standard curve. Results from the control samples were assessed and confirmed to be within an acceptable range. All samples were analysed twice.

Biochemical Profile:

Liver Functions:

Alkaline Phosphatase (ALP)

Alkaline Phosphatase (ALP) is an enzyme in the cells lining the biliary ducts of the liver. ALP levels in plasma increase with large bile duct obstruction, intrahepatic cholestasis or infiltrative diseases of the liver. ALP originates in bones and is therefore increased in growing animals.

Alanine Transaminase (ALT)

Alanine Transaminase (ALT), also called Serum Glutamic Pyruvate Transaminase (SGPT) or Alanine aminotransferase (ALAT) is an enzyme present in functioning hepatocytes. When a hepatocyte is damaged, the enzyme is release into the extracellular space and is absorbed by the circulatory system, where it is measured. ALT rises dramatically in acute liver damage and a raised ALT is entirely consistent with surgery or thermal ablation of the liver. The degree of increase is dependant on the volume of hepatocytes damaged and is therefore in this context related to the amount of tissue ablated. The use of Propofol for total intravenous anaesthetic (TIVA) influences the liver functions, specifically ALT due to the breakdown of hepatocytes during metabolism of the anaesthetic agent (Chen et al, 2000).

Aspartate Transaminase (AST)

Aspartate Transaminase (AST) also called Serum Glutamic Oxaloacetic Transaminase (SGOT) or aspartate aminotransferase (ASAT) is similar to ALT in that it is another enzyme associated with liver parenchymal cells. It is raised in acute liver damage, but is also present in red blood cells, and cardiac and skeletal muscle and is therefore not specific to the liver. Elevated AST levels are not specific for liver damage, and AST has also been used as a cardiac marker. Given the non-specific nature of the enzyme, it is difficult to differentiate liver damage cause by thermal ablation, the effects of Propofol anaesthetic agent and the contribution of both red blood cells and skeletal muscles. All the animals underwent general anaesthesia and laparotomy – the results obtained during this study must be evaluated with caution, as the aetiology of the enzyme abnormality is multi-factorial.

Gamma Glutamyl Transpeptidase (γ-GT)

Gamma Glutamyl Transpeptidase is reasonably specific to the liver and is an indicator of cholestatic damage, more specific than ALP. It may be elevated with even minor, sub-clinical levels of liver dysfunction. An important function of γ-GT in the context of possible liver damage is that, when evaluated in conjunction with ALP, indicates specific liver damage.
The levels of γ-GT are often raised following propofol administration most commonly reaching their peak at 24 hours following surgery (Ture et al, 2009).

Lactate Dehydrogenase (LDH).

LDH is an enzyme found in many tissues in animals including the liver. LDH is commonly elevated following haemolysis and is also elevated following liver damage. It is not specific and is probably related to haemolysis in this context rather than liver damage.

Bilirubin.

Bilirubin is a breakdown product of haemolysis and is metabolized by the liver to remove it from circulating blood. An increased bilirubin is an indicator of liver failure; this may be due to excessive bilirubin production (pre-hepatic), liver damage (hepatic) or due to obstruction of the liver (post-hepatic). In this context, the presence of raised bilirubin indicates liver failure, which may be due to direct effects of thermal ablation, or be related to the surgery itself or the anaesthetic.

Renal Function.

Sodium.

Sodium is an essential serum electrolyte, responsible for nerve conduction and active transport in cell membranes. It is filtered by the renal glomerulus and reabsorbed in the proximal convoluted tubule, the descending Loop of Henle and in the distal convoluted tubule. Renal failure causes a decrease in the reabsorbtion of sodium resulting in hyponatremia. Although serum sodium levels are not a diagnostic marker of renal failure, the importance of sodium on cell function makes it an important electrolyte for postoperative evaluation of renal function, rather than renal function specifically.

Potassium.

Potassium is an electrolyte essential to the active transport system in the cell membrane and cell function. It is reabsorbed from the proximal convoluted tubule and descending Loop of Henle. Acute renal failure results in a raised potassium (hyperkalemia), which may result in cardiac rhythm disturbances. It is for this reason that potassium is closely monitored in renal failure and must be treated if levels rise significantly.

Urea.

Urea is a waste product of protein metabolism. It is produced in the liver and excreted by the kidney. The levels of serum urea are a direct indicator of acute renal failure.
Elevated urea levels may cause a coagulopathy or a pericardial effusion.

Creatinine.

Creatinine is the most commonly quoted marker of renal function as it is both filtered and secreted by the kidney for excretion. It is a breakdown product of creatine found in muscles. Creatinine is produced at a fairly constant rate in the body depending on muscle mass. For this reason is an extremely sensitive marker for renal failure.
Creatinine should be interpreted in relation to the urea concentration in blood with regards to determining a possible cause. An elevated urea out of proportion to the creatinine level indicated a pre-renal cause of failure, such as dehydration or fluid depletion.

Standards and Samples for Biochemical Markers

Serum samples were obtained from the 10 domestic large white hybrid pigs. Each serum sample was labelled, detailing the animal, the unique identifier code and the nature of the sample for analysis. All samples were collected in a standard Serum Separator Tube (SST) containing clot activator and a gel for separation of the serum and blood cells.
All samples were analysed in the same laboratory by Huntingdon Life Sciences.

Calculation of Results

The blood analysis was performed with reference to normal serum levels in pigs. Each sample was analysed twice to ensure accurate analysis. The samples were tested using proprietary chemical pathology equipment at Huntingdon Life Sciences. All machines are regularly calibrated and serviced according to the minimum recommendations set out by the manufacturer.

Regulatory compliance

The assays were not conducted in accordance with the OECD Principles of GLP, however the work was performed generally following the principles of GLP.

Results:

The results are expressed as means ± standard deviation (SD) for normally distributed variables or the median and the interquartile range for non-normal variables (Appendix 5). Differences in both APP and biochemical values in each animal at each specified time point were tested with paired student's t-test. A *P* value <0.05 was considered statistically significant. SPSS 17 was used for all statistical data analysis. The values of each APP and biochemical marker are quoted according to the standard international unit for each specific marker unless specified.

Haptoglobin (Hp) Results

In pigs, an Hp concentration of 1.0g/L and above is considered to be biologically relevant. The results show that in animal numbers 15, 16 and 20 there was an elevated Hp level at pretreatment. This could be attributed to an underlying subclinical infection or to stress. Animals 15 and 16 were not acclimatised prior to surgery and the elevated Hp levels may be attributed to transport. This was also reflected in a high CRP concentration in these animals at pretreatment. In the remaining animals, there was an overall trend for the Hp to increase up 2-4x from 24 hours to 72 hours (maximum Hp 2.16g/L with animal 22 at 72 hours) then decreased to below reference level by termination. The increase in Hp post treatment was statistically significant at 48 hrs (p=0.034). The immediate post procedure value, 24 hrs and 72 hrs were not significant (p=0.168, p=0.205, p=0.115)

No animal showed any signs of a systemic inflammatory response (SIRS) post surgery.

Table 6.1 tabulates the results for the mean Haptoglobin levels at each time point, including the standard deviation (SD), standard error of the mean (SEM), 95% confidence interval (CI) and range.
Table 6.2 tabulates the individual Haptoglobin levels for each animal at each time point.
Graph 6.1 demonstrates the Haptoglobin levels for each animal with error bars at each time point.

Haptoglobin (g/L)								
					95% CI for Mean			
	N	Mean	SD	SEM	Lower Bound	Upper Bound	Min	Max
Pre (PT)	10	0.521	0.44079	0.13939	0.2057	0.836	0	1.48
0hrs post (IAD)	10	0.385	0.27265	0.08622	0.19	0.58	0.13	1
24hrs post	8	0.8312	0.27663	0.09781	0.6	1.063	0.46	1.27
48hrs post	8	1.105	0.37306	0.1319	0.7931	1.417	0.59	1.78
72hrs post	6	1.1983	0.38928	0.15892	0.7898	1.607	0.83	1.85
Termination	4	0.3275	0.0943	0.04715	0.1775	0.478	0.26	0.46
Total	46	0.7185	0.45956	0.06776	0.582	0.855	0	1.85

Table 6.1 The results for the mean Haptoglobin levels at each time point, including the standard deviation (SD), standard error of the mean (SEM), 95% confidence interval (CI) and range.

C-Reactive Protein (CRP) Results

In pigs, a CRP concentration of <100mg/L is considered to be biologically relevant. As stated above the results show that in animal numbers 15, 16 and 20 there was an elevated CRP (and Hp) level at pretreatment which could be attributed to an underlying subclinical infection or to stress. Animals 15 and 16 were not acclimatised prior to surgery and the elevated Hp levels may be attributed to transport. The overall trend in the remaining animals showed CRP to increase from 24 hours up to 72 hours (p=0.018, p=0.015 and p=0.01; Tables 6.23-6.25) exception was animal 23 (56d termination); the CRP peaked at 24 hours post surgery and then decreased at 48 and 72 hours. The immediate post procedure CRP was not elevated significantly (p=0.952; Table 6.22). Several of the animals showed a >10x increase in CRP levels from pre-treatment (PT) to 72 hours, with a maximum CRP concentration of 387mg/L with animal 24 at 72 hours. By termination date CRP levels had reduced to slightly above reference level. No animal showed any signs of a systemic inflammatory response (SIRS) post surgery.

Table 6.3 tabulates the results for the mean CRP levels at each time point, including the standard deviation (SD), standard error of the mean (SEM), 95% confidence interval (CI) and range.
Table 6.4 tabulates the results for the CRP levels at each time point for each animal.
Graph 6.2 demonstrates the CRP levels for each animal with error bars at each time point.

CRP (mmol/L)								
					95% CI for Mean			
	N	Mean	SD	SEM	Lower Bound	Upper Bound	Min	Max
Pre (PT)	10	338.31	323.41692	102.27341	106.9515	569.6685	67	936.3
0hrs post (IAD)	10	343.82	318.27273	100.64667	116.1414	571.4986	56	1103.1
24hrs post	8	1471.125	742.72746	262.59381	850.1893	2092.0607	544.5	2806.6
48hrs post	8	1613.6125	868.51224	307.06545	887.5181	2339.7069	591	3192.4
72hrs post	6	2051.1333	1114.8761	455.14626	881.1426	3221.124	734.5	3877.3
Termination	4	126.6	31.58681	15.79341	76.3383	176.8617	95.4	169.1
Total	46	963.313	946.37414	139.53525	682.2746	1244.3515	56	3877.3

Table 6.3 The Mean CRP levels at each time point are tabulated, including the standard deviation (SD), standard error of the (SEM), 95% confidence interval (CI) and range.

Serum Amyloid A (SAA) Results

In pigs, an SAA concentration of >50mg/L is considered to be biologically relevant. In animals 17-26 (2d-56d terminations) the SAA level peaked at 24 hours, decreased by 72 hours and returned to below reference level by termination. Most of the animals showed a >200 times increase in SAA levels from PT to 24 hours with a maximum SAA response of 776.5mg/L seen with animal 17 (14d termination) at 24 hours. The elevated SAA level was not statistically significant immediately post surgery (p=0.471), but was statistically significant at 24, 48 and 72 hrs post surgery (p=0.001, p=0.001, p=0.01) and were normal at termination.
No animal showed any signs of a systemic inflammatory response (SIRS) post surgery.

Table 6.5 tabulates the results for the mean SAA levels at each time point, including the standard deviation (SD), standard error of the mean (SEM), 95% confidence interval (CI) and range.
Table 6.6 tabulates the results for the SAA levels at each time point for each animal.
Graph 6.3 demonstrates the SAA levels for each animal with error bars at each time point.

SAA (mg/L)								
					95% CI for Mean			
	N	Mean	SD	SEM	Lower Bound	Upper Bound	Min	Max
Pre	10	9.133	9.14827	2.89294	2.5887	15.677	0.23	29.73
0hrs post	10	14.975	24.51846	7.75342	-2.5644	32.514	2.02	82.25
24hrs post	8	536	252.07262	89.12113	325.262	746.74	67.75	776.5
48hrs post	8	402.8438	207.33569	73.30424	229.507	576.18	69.75	652.5
72hrs post	6	144.5417	76.50285	31.23216	64.2569	224.83	55	284.25
Termination	4	5.735	5.88263	2.94132	-3.6256	15.096	0.23	13.68
Total	46	187.87	253.10736	37.31864	112.706	263.03	0.23	776.5

Table 6.5 The mean SAA levels at each time point, including the standard deviation (SD), standard error of the mean (SEM), 95% confidence interval (CI) and range.

Pig – Major Acute Phase (pMAP) Results

In pigs a pMAP concentration of >0.6g/L is considered to be biologically relevant.
In animals 17-26 (2d-56d terminations) the overall trend showed pMAP to increase from 24 hours up to 48-72 hours. Most of the animals showed a >5-20 times increase in pMAP levels from PT to 72 hours, with a maximum pMAP concentration of 2.45g/L with animal 25 (2d termination) at 48 hours. The elevated pMAP was statistically significant at each time point post surgery ($p=0.003$, $p<0.0001$, $p<0.0001$, $p=0.1$). By termination date pMAP levels had reduced to below reference level. No animal showed any signs of a systemic inflammatory response (SIRS) post surgery.

Table 6.7 tabulates the results for the mean pMAP levels at each time point, including the standard deviation (SD), standard error of the mean (SEM), 95% confidence interval (CI) and range.
Table 6.8 tabulates the results for the pMAP levels at each time point for each animal.
Graph 6.4 demonstrates the pMAP levels at each time point for each animal with error bars.

pMAP (g/L)								
					95% CI for Mean			
	N	Mean	SD	SEM	Lower Bound	Upper Bound	Min	Max
Pre	**10**	**0.304**	**0.14385**	**0.04549**	**0.2011**	**0.4069**	**0.13**	**0.61**
0hrs post	**10**	**0.167**	**0.12239**	**0.0387**	**0.0794**	**0.2546**	**0.02**	**0.37**
24hrs post	**8**	**1.39**	**0.46081**	**0.16292**	**1.0048**	**1.7752**	**0.46**	**1.91**
48hrs post	**8**	**1.7438**	**0.61558**	**0.21764**	**1.2291**	**2.2584**	**0.85**	**2.45**
72hrs post	**6**	**1.5233**	**0.43385**	**0.17712**	**1.068**	**1.9786**	**0.99**	**2.03**
Termination	**4**	**0.1675**	**0.14683**	**0.07341**	**-0.0661**	**0.4011**	**0.03**	**0.36**
Total	**46**	**0.8607**	**0.76613**	**0.11296**	**0.6331**	**1.0882**	**0.02**	**2.45**

Table 6.7 The mean pMAP levels at each time point, including the standard deviation (SD), standard error of the mean (SEM), 95% confidence interval (CI) and range

Biochemical Results

Liver Function.

Table 6.9 summarises the mean values for each liver function, LDH, Albumin and Bilirubin at each specified time point tested, with the corresponding 95% confidence interval (Radostits et al, 2005).

Alkaline Phosphatase (ALP)

In pigs the normal reference range for ALP is 120-400 U/L.

The ALP increased above the pre treatment PT range in animal 25 (2d termination) and 26 (28d termination), peaking at 48hrs but overall there was no significant increase in the levels of ALP at 24hrs, 48hrs or 72hrs (p=0.829, p=0.06, p=0.089). The ALP showed a significant increase immediately post surgery (p=0.016), however this enzyme is affected by anaesthetic agents and therefore the transient significant increase is probably due to a combination of the surgery and anaesthetic, given the values of ALP at 24, 48 and 72 hrs post surgery.

All levels of ALP returned to the pre-treatment levels at termination.

Table 6.10 tabulates the results for the mean ALP levels at each time point, including the standard deviation (SD), standard error of the mean (SEM), 95% confidence interval (CI) and range.

Table 6.11 tabulates the results for the ALP levels at each time point for each animal.

tabulates the results for the ALP levels at each time point.

Graph 6.5 demonstrates the ALP levels at each time point for each animal with error bars.

ALP (U/L)								
					95% CI for Mean			
	N	Mean (U/L)	SD	SEM	Lower Bound	Upper Bound	Min	Max
Pre	10	148.6	40	12.66	119.96	177.24	96	211
0hrs post	10	124.5	27.8	8.79	104.61	144.39	76	180
24hrs post	8	143.88	31	10.98	117.92	169.83	99	189
48hrs post	8	112.25	19.1	6.747	96.3	128.2	84	139
72hrs post	6	97.5	14	5.731	82.77	112.23	77	119
Termination	4	118.5	20.2	10.12	86.29	150.71	100	147
Total	46	126.93	32.4	4.772	117.32	136.55	76	211

Table 6.10 The mean pMAP levels at each time point, including the standard deviation (SD), standard error of the mean (SEM), 95% confidence interval (CI) and range.

Alanine Transaminase (ALT) Results

In pigs the normal reference range for ALT is 31-58 U/L.

The ALT demonstrated significant increases above the pre-treatment level at 24, 48 and 72hrs (P=0.001, p=0.001, p=0.001), peaking at 24-48hrs. No significant difference was noted at 0hrs (p=1.00).

All the enzyme levels returned to normal at termination.

Table 6.12 tabulates the results for the mean ALT levels at each time point, including the standard deviation (SD), standard error of the mean (SEM), 95% confidence interval (CI) and range.

Table 6.13 tabulates the results for the ALT levels at each time point for each animal.

Graph 6.6 demonstrates the ALT levels at each time point for each animal with error bars.

ALT U/L								
					95% Confidence Interval for Mean			
	N	Mean	SD	SEM	Lower Bound	Upper Bound	Min	Max
Pre	10	44.4	7.71	2.437	38.89	49.91	35	61
0hrs post	10	44.4	9.4	2.971	37.68	51.12	33	62
24hrs post	8	104.5	32	11.33	77.71	131.29	55	150
48hrs post	8	109.3	34.4	12.15	80.51	137.99	59	157
72hrs post	6	95.83	18.7	7.635	76.21	115.46	70	116
Termination	6	58.83	8.91	3.637	49.48	68.18	48	70
Total	48	73.46	35.1	5.073	63.25	83.66	33	157

Table 6.12 The mean ALT levels at each time point, including the standard deviation (SD), standard error of the mean (SEM), 95% confidence interval (CI) and range.

Aspartate Transaminase (AST) Results

In pigs the normal reference range for AST is 32-84 U/L.

The AST demonstrated significant increases at 0hrs, 24hrs, 48hrs and 72hrs ($p<0.0001$, $p=0.001$, $p=0.024$, $p=0.006$), peaking at 24 hours post treatment. The initial rise and peak 24 hrs may in part be due to the combination of general anaesthetic, surgery and ablations, however it is not possible to quantify this and it is beyond the scope of this research.

The enzymes returned to normal pre-treatment levels at termination.

Table 6.14 tabulates the results for the mean AST levels at each time point, including the standard deviation (SD), standard error of the mean (SEM), 95% confidence interval (CI) and range.

Table 6.15 tabulates the results for the AST levels at each time point for each animal.

Graph 6.7 demonstrates the AST levels at each time point for each animal with error bars.

AST (U/L)								
					95% CI for Mean			
	N	Mean	SD	SEM	Lower Bound	Upper Bound	Min	Max
Pre	10	41.9	15.989	5.056	30.46	53.34	22	67
0hrs post	10	246.8	76.947	24.333	191.76	301.84	116	379
24hrs post	8	625.88	275.29	97.33	395.73	856.02	211	1130
48hrs post	8	370.38	320.48	113.31	102.44	638.31	97	889
72hrs post	6	160.33	57.158	23.335	100.35	220.32	101	243
Termination	6	54	16.358	6.678	36.83	71.17	29	70
Total	48	252.98	264.19	38.132	176.27	329.69	22	1130

Table 6.14 The results for the mean AST levels at each time point, including the standard deviation (SD), standard error of the mean (SEM), 95% confidence interval (CI) and range.

Gamma Glutamyl Transpeptidase (γ-GT) Results

In pigs the normal reference range for γ-GT is 10-60 U/L.

The γ-GT demonstrated an increase in animal 16 (0d termination) at 0hrs post surgery, but this was the only observed significant increase in any animal and may be spurious. There was no significant increase in the γ-GT level at 0hrs, 24hrs, 48hrs or 72hrs (p=0.894, p=0.920, p=0.889, p=0.613).

The levels overall remained within the normal reference range.

Table 6.16 tabulates the results for the mean γ-GT levels at each time point, including the standard deviation (SD), standard error of the mean (SEM), 95% confidence interval (CI) and range.

Table 6.17 tabulates the results for the γ-GT levels at each time point for each animal.

Graph 6.8 demonstrates the γ-GT levels at each time point for each animal with error bars.

γ - GT (U/L)								
					95% CI for Mean			
		Mean	SD	SEM	Lower Bound	Upper Bound	Min	Max
Pre	10	45.7	16.59	5.247	33.83	57.57	18	73
0hrs post	10	45	23.32	7.374	28.32	61.68	23	103
24hrs post	8	44.62	13.74	4.858	33.14	56.11	21	61
48hrs post	8	44.38	15.1	5.338	31.75	57	21	70
72hrs post	6	41.33	7.005	2.86	33.98	48.68	31	50
Termination	6	40.17	7.468	3.049	32.33	48	28	49
Total	48	43.92	15.29	2.207	39.48	48.36	18	103

Table 6.16 The results for the mean γ-GT levels at each time point, including the standard deviation (SD), standard error of the mean (SEM), 95% confidence interval (CI) and range.

Lactate Dehydrogenase (LDH) Results

In pigs the normal reference range for LDH is 380-630 U/L.

The LDH demonstrated a significant increase at 0hrs, 24hrs, 48 hrs and 72hrs ($p<0.010$, $p<0.003$, $p<0.024$, $p<0.014$), peaking at 24 hours. The causes of an elevated LDH are numerous and the likely reason for the observed rise is a combination of general anaesthetic, surgery, thermal ablation and haemolysis associated with the surgery.

Table 6.18 tabulates the results for the mean LDH levels at each time point, including the standard deviation (SD), standard error of the mean (SEM), 95% confidence interval (CI) and range.

Table 6.19 tabulates the results for the LDH levels at each time point for each animal.

Graph 6.9 demonstrates the LDH levels at each time point for each animal with error bars.

LDH (U/L)								
					95% CI for Mean			
	N	Mean	SD	SEM	Lower Bound	Upper Bound	Min	Max
Pre	10	1313.3	417.074	131.89	1014.94	1611.66	957	2239
0hrs post	10	1785.8	310.427	98.165	1563.73	2007.87	1354	2271
24hrs post	8	5338.6	2601.87	919.9	3163.41	7513.84	2728	9903
48hrs post	8	3497	2278.42	805.54	1592.2	5401.8	2153	8606
72hrs post	6	2243.7	469.495	191.67	1750.96	2736.37	1846	2965
Termination	6	1157.7	219.036	89.421	927.8	1387.53	949	1566
Total	48	2543.4	2011.74	290.37	1959.27	3127.57	949	9903

Table 6.18 The results for the mean LDH levels at each time point, including the standard deviation (SD), standard error of the mean (SEM), 95% confidence interval (CI) and range.

Bilirubin Results

In pigs the normal reference range for Bilirubin is 0-17.1 μmol/L.

The bilirubin demonstrated a significant increase at 0hrs ($p<0.004$; Table 6.62), however returned to normal levels by 24 hours (Tables 6.63-6.65).

Table 6.20 tabulates the results for the mean Bilirubin levels at each time point, including the standard deviation (SD), standard error of the mean (SEM), 95% confidence interval (CI) and range.

Table 6.21 tabulates the results for the Bilirubin levels at each time point for each animal.

Graph 6.10 demonstrates the Bilirubin levels at each time point for each animal with error bars.

Bilirubin (U/L)								
					95% CI for Mean			
	N	Mean	SD	SEM	Lower Bound	Upper Bound	Min	Max
Pre	10	1.5	1.269	0.401	0.59	2.41	1	5
0hrs post	10	3.9	2.132	0.674	2.38	5.42	1	8
24hrs post	8	1.38	0.518	0.183	0.94	1.81	1	2
48hrs post	8	1	0.535	0.189	0.55	1.45	0	2
72hrs post	6	0.5	0.548	0.224	-0.07	1.07	0	1
Termination	6	1	0	0	1	1	1	1
Total	48	1.71	1.637	0.236	1.23	2.18	0	8

Table 6.20 The results for the mean Bilirubin levels at each time point, including the standard deviation (SD), standard error of the mean (SEM), 95% confidence interval (CI) and range.

Renal Function.

Table 6.22 summarises the mean values for each marker tested (Sodium (Na), Potassium (K), Urea and Creatinine) at each specified time point tested, with the corresponding 95% confidence interval (Radostits et al, 2005).

Serum Sodium Results

In pigs the normal reference range for serum Sodium is 140-150 mmol/L.

The serum sodium concentration levels remained stable throughout in all animals apart from animal 25 (2d) and 26 (28d) where a single elevated sodium level was observed.

No statistically significant elevations were seen at 24, 48 or 72 hrs post procedure (p=0.542, p=0.747, p=0.292). The levels immediately post procedure were significantly elevated (p=0.041), however this may be in part due to the intravenous administration of 0.9% Saline during the procedure for maintenance. In part, the mildly elevated levels observed in some animals (Animals 25 and 26) may be due to the accepted laboratory reference error of 10%. In the clinical context, these isolated results would not be regarded as a true value and would in all likelihood be repeated.

All results were normal at termination.

Table 6.23 tabulates the results for the mean Na levels at each time point, including the standard deviation (SD), standard error of the mean (SEM), 95% confidence interval (CI) and range.

Table 6.24 tabulates the results for the Na levels at each time point for each animal.

Graph 6.11 demonstrates the Na levels at each time point for each animal with error bars.

Na (mmol/L)								
					95% CI for Mean			
	N	Mean	SD	SEM	Lower Bound	Upper Bound	Min	Max
Pre (PT)	10	145.5	3.342	1.057	143.11	147.89	142	153
0hrs post (IAD)	10	142.3	1.418	0.448	141.29	143.31	140	145
24hrs post	8	145	2.507	0.886	142.9	147.1	142	149
48hrs post	8	146.5	3.817	1.35	143.31	149.69	143	153
72hrs post	6	145	2.757	1.125	142.11	147.89	142	149
Termination	6	144.7	3.983	1.626	140.49	148.85	141	152
Total	48	144.8	3.172	0.458	143.83	145.67	140	153

Table 6.23 tabulates the results for the mean Na levels at each time point, including the standard deviation (SD), standard error of the mean (SEM), 95% confidence interval (CI) and range.

Serum Potassium Results

In pigs the normal reference range for serum Potassium is 4.7-7.1 mmol/L.

The serum potassium concentration levels remain stable throughout in all animals apart from animal 26 (28d) where elevated serum potassium levels were measured at 24 and 48 hrs post treatment. The levels were not associated with any clinical symptoms and the levels may be due to trauma associated with the phlebotomy procedure. The potassium levels at 24, 48 and 72hrs were not significantly elevated (p=0.285, p=0.284, p=0.717).

The serum potassium (K) was seen to decrease significantly immediately post procedure (p=0.038), however this is still within normal limits for potassium and again may reflect intravenous administration of potassium poor crystalloid solution as maintenance fluids.

This phenomenon is seen commonly in the clinical context and unless the decrease in potassium is significant (below 3mmol/L), this biochemical abnormality is not corrected with medication, rather by reabsorbtion of potassium in the kidney.

All serum potassium levels were normal at termination.

Table 6.25 tabulates the results for the mean K levels at each time point, including the standard deviation (SD), standard error of the mean (SEM), 95% confidence interval (CI) and range.

Table 6.26 tabulates the results for the K levels at each time point for each animal.

Graph 6.12 demonstrates the K levels at each time point for each animal with error bars.

K (mmol/L)								
					95% CI for Mean			
	N	Mean	SD	SEM	Lower Bound	Upper Bound	Min	Max
Pre (PT)	10	5.15	0.409	0.129	4.86	5.44	4	6
0hrs post (IAD)	10	4.8	0.245	0.077	4.62	4.98	4	5
24hrs post	8	5.8	1.376	0.487	4.65	6.95	4	9
48hrs post	8	5.8	1.429	0.505	4.61	6.99	4	9
72hrs post	6	5.35	1.084	0.443	4.21	6.49	4	7
Termination	6	4.68	0.488	0.199	4.17	5.19	4	6
Total	48	5.26	0.985	0.142	4.97	5.55	4	9

Table 6.25 The results for the mean K levels at each time point, including the standard deviation (SD), standard error of the mean (SEM), 95% confidence interval (CI) and range.

Urea Results

In pigs the normal reference range for urea is 3-8.5 mmol/L.

The serum urea levels remained stable throughout, peaking at 24hrs post surgery, however this was not significant (p=0.079) and all urea measurements remained within the normal reference range at 0, 24, 48, 72 hrs post procedure and at termination.

Table 6.27 tabulates the results for the mean Urea levels at each time point, including the standard deviation (SD), standard error of the mean (SEM), 95% confidence interval (CI) and range.

Table 6.28 tabulates the results for the Urea levels at each time point for each animal.

Graph 6.13 demonstrates the Urea levels at each time point for each animal with error bars.

Urea (mmol/L)								
					95% CI for Mean			
	N	Mean	SD	SEM	Lower Bound	Upper Bound	Min	Max
Pre (PT)	10	4.3	0.539	0.171	3.91	4.68	4	5
0hrs post (IAD)	10	4.28	0.874	0.276	3.65	4.9	3	5
24hrs post	8	5.28	1.381	0.488	4.13	6.44	4	8
48hrs post	8	3.67	0.961	0.34	2.87	4.47	2	5
72hrs post	6	4.1	0.917	0.374	3.14	5.07	3	6
Termination	6	4.67	1.317	0.538	3.29	6.05	3	7
Total	48	4.37	1.071	0.155	4.06	4.69	2	8

Table 6.27 The results for the mean Urea levels at each time point, including the standard deviation (SD), standard error of the mean (SEM), 95% confidence interval (CI) and range.

Creatinine Results

In pigs the normal reference range for creatinine is 90-240 μmol/L.

The serum Creatinine levels remained within normal limits throughout the study, with all the serum creatinine levels improving from the pre-treatment levels apart from animal 26 (28d termination). The improved levels of Creatinine may be due to the controlled living conditions of the animals throughout the study and the careful dietary requirements set out by the study protocol.

The statistically significant observation at 0 hrs and 72 hrs was an improvement in Creatinine levels (p=0.006, p=0.034).

Table 6.29 tabulates the results for the mean Creatinine levels at each time point, including the standard deviation (SD), standard error of the mean (SEM), 95% confidence interval (CI) and range.

Table 6.30 tabulates the results for the Creatinine levels at each time point for each animal.

Graph 6.14 demonstrates the Creatinine levels at each time point for each animal with error bars.

Creatinine (mmol/L)								
					95% CI for Mean			
	N	Mean	SD	SEM	Lower Bound	Upper Bound	Min	Max
Pre	10	141.2	18.546	5.865	127.93	154.47	102	163
0hrs post	10	125.2	11.593	3.666	116.91	133.49	104	142
24hrs post	8	121	19.603	6.931	104.61	137.39	87	141
48hrs post	8	121.5	13.213	4.671	110.45	132.55	97	135
72hrs post	6	106.17	31.429	12.831	73.18	139.15	61	136
Termination	6	125.67	13.292	5.426	111.72	139.62	109	146
Total	48	124.9	20.117	2.904	119.05	130.74	61	163

Table 6.29 tabulates the results for the mean Creatinine levels at each time point, including the standard deviation (SD), standard error of the mean (SEM), 95% confidence interval (CI) and range.

Haptoglobin g/L						
Sample	PT	IAD	24 Hrs	48 Hrs	72 Hrs	Termination
	Mean	Mean	Mean	Mean	Mean	Mean
15-0d	0.52	0.25	NS	NS	NS	NS
16-0d	1.48	0.22	NS	NS	NS	NS
18-2d	0.58	0.48	0.79	1.20	NS	NS
25-2d	0.16	0.13	0.59	0.76	NS	NS
20-14d	0.94	1.00	1.27	1.78	1.85	0.54
17-14d	0.11	0.19	0.62	0.91	0.98	0.43
21-28d	0.34	0.35	1.00	1.31	1.27	0.33
26-28d	0.56	0.31	0.46	0.59	0.83	0.26
23-56d	0.37	0.22	0.82	1.00	0.87	0.46
24-56d	0.67	0.70	1.10	1.29	1.39	0.26

Table 6.2 tabulates the individual Haptoglobin levels for each animal at each time point for each animal.

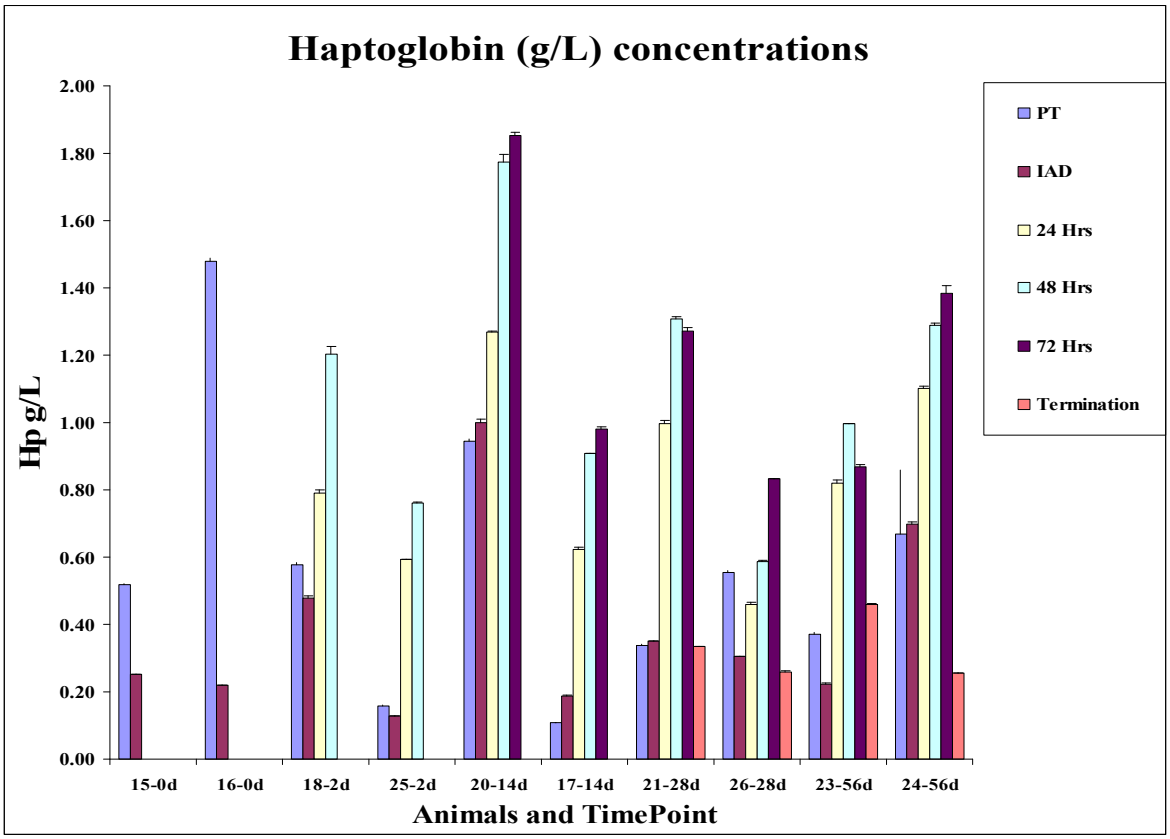

Graph 6.1 Haptoglobin levels for each animal with error bars at each time point.

CRP mg/L						
Sample	PT	IAD	24 Hrs	48 Hrs	72 Hrs	Termination
	Mean	Mean	Mean	Mean	Mean	Mean
15-0d	540.7	570.7	NS	NS	NS	NS
16-0d	936.3	223.7	NS	NS	NS	NS
18-2d	96.9	190.1	1183.7	1318.7	NS	NS
25-2d	67.0	213.3	568.4	1032.1	1032.5	NS
17-14d	101.4	207.4	1453.8	1847.6	1879.6	69.5
20-14d	705.7	1103.1	1996.3	2555.9	2570.2	88.3
21-28d	206.2	179.1	1543.2	1247.7	2112.6	129.6
26-28d	67.2	56.0	544.5	591.0	734.5	95.4
23-56d	77.1	123.8	1672.5	1123.5	1132.6	112.3
24-56d	584.6	571.0	2806.6	3192.4	3877.3	169.1

Table 6.4 tabulates the individual CRP levels for each animal at each time point for each animal.

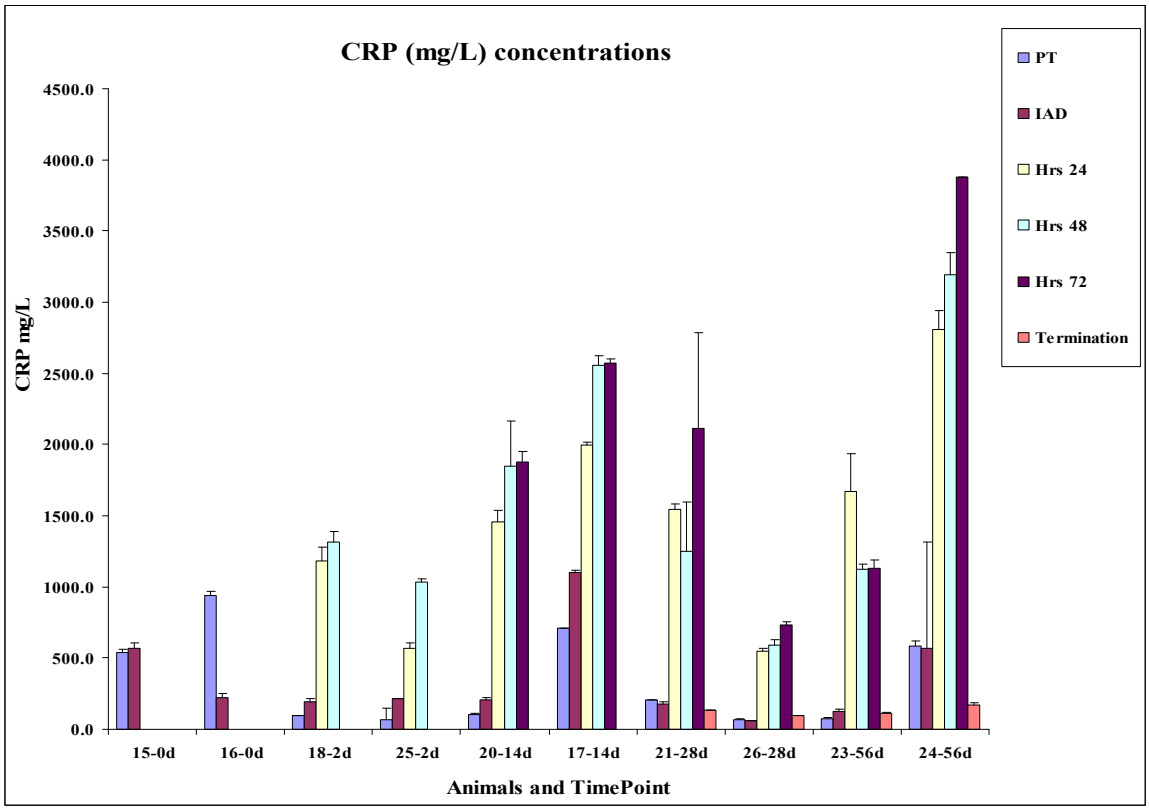

Graph 6.2 CRP levels for each animal with error bars at each time point.

SAA mg/L						
Sample	PT	IAD	24 Hrs	48 Hrs	72 Hrs	Termination
	Mean	Mean	Mean	Mean	Mean	Mean
15-0d	9.28	82.25	NS	NS	NS	NS
16-0d	18.98	3.26	NS	NS	NS	NS
18-2d	2.34	2.66	744.25	508.50	NS	NS
25-2d	3.54	12.53	476.50	506.25	NS	NS
20-14d	29.73	23.50	665.75	290.25	128.50	NS
17-14d	1.57	8.55	776.50	611.00	110.25	NS
21-28d	0.23	7.23	684.50	652.50	284.25	13.68
26-28d	4.73	4.71	67.75	69.75	55.00	6.44
23-56d	2.75	13.67	612.50	404.75	132.50	0.23
24-56d	4.54	2.02	260.25	179.75	156.75	2.59

Table 6.6 tabulates the individual SAA levels for each animal at each time point for each animal.

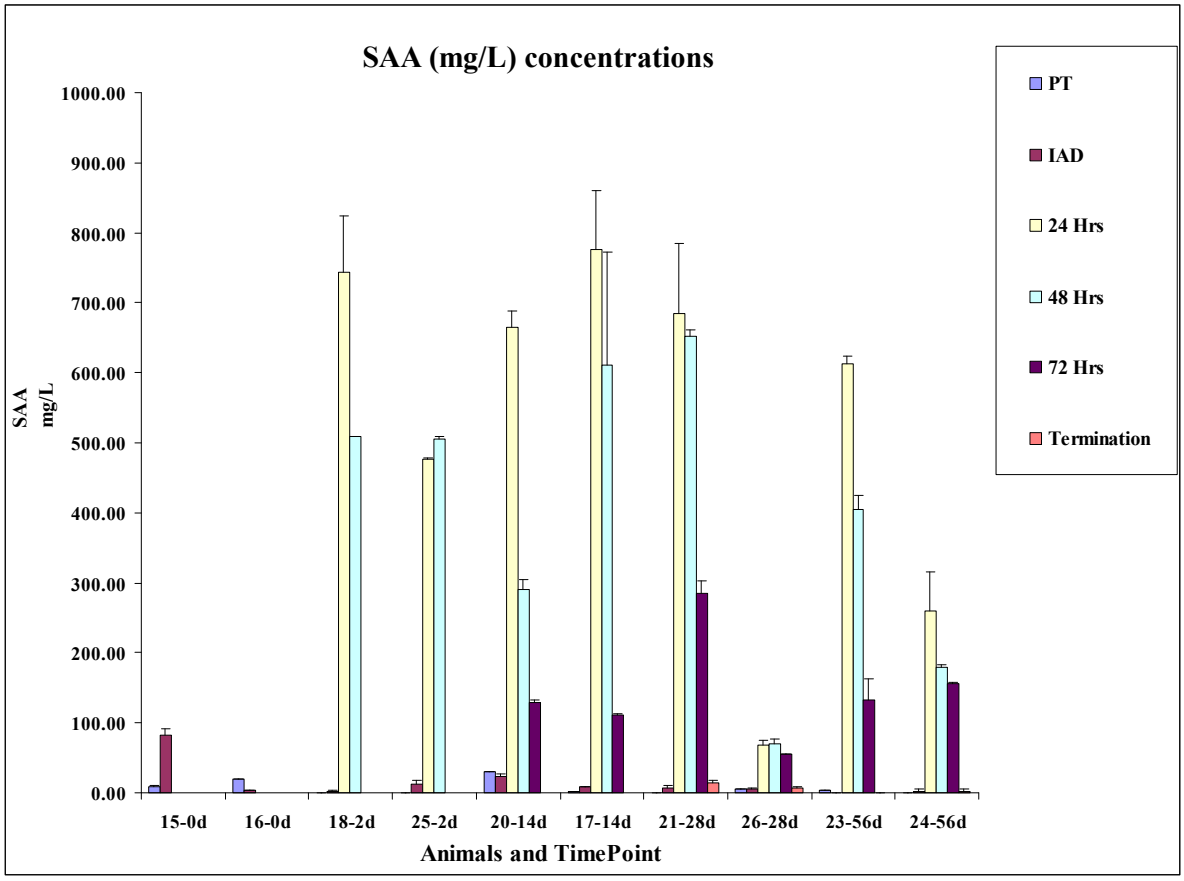

Graph 6.3 SAA levels for each animal with error bars at each time point.

pMAP g/L						
Sample	PT	IAD	24 Hrs	48 Hrs	72 Hrs	Termination
	Mean	Mean	Mean	Mean	Mean	Mean
15-0d	0.34	0.36	NS	NS	NS	NS
16-0d	0.61	0.37	NS	NS	NS	NS
25-2d	0.23	0.09	1.60	2.45	NS	NS
18-2d	0.34	0.19	1.91	2.16	NS	NS
20-14d	0.25	0.04	1.80	2.08	1.56	NS
17-14d	0.18	0.02	0.46	1.02	1.20	NS
21-28d	0.13	0.09	1.61	2.13	2.03	0.03
26-28d	0.22	0.16	1.13	0.85	0.99	0.36
23-56d	0.18	0.12	1.24	1.20	1.33	0.20
24-56d	0.36	0.23	1.37	2.06	2.03	0.08

Table 6.8 The mean pMAP levels at each time point, including the standard deviation (SD), standard error of the mean (SEM), 95% confidence interval (CI) and range.

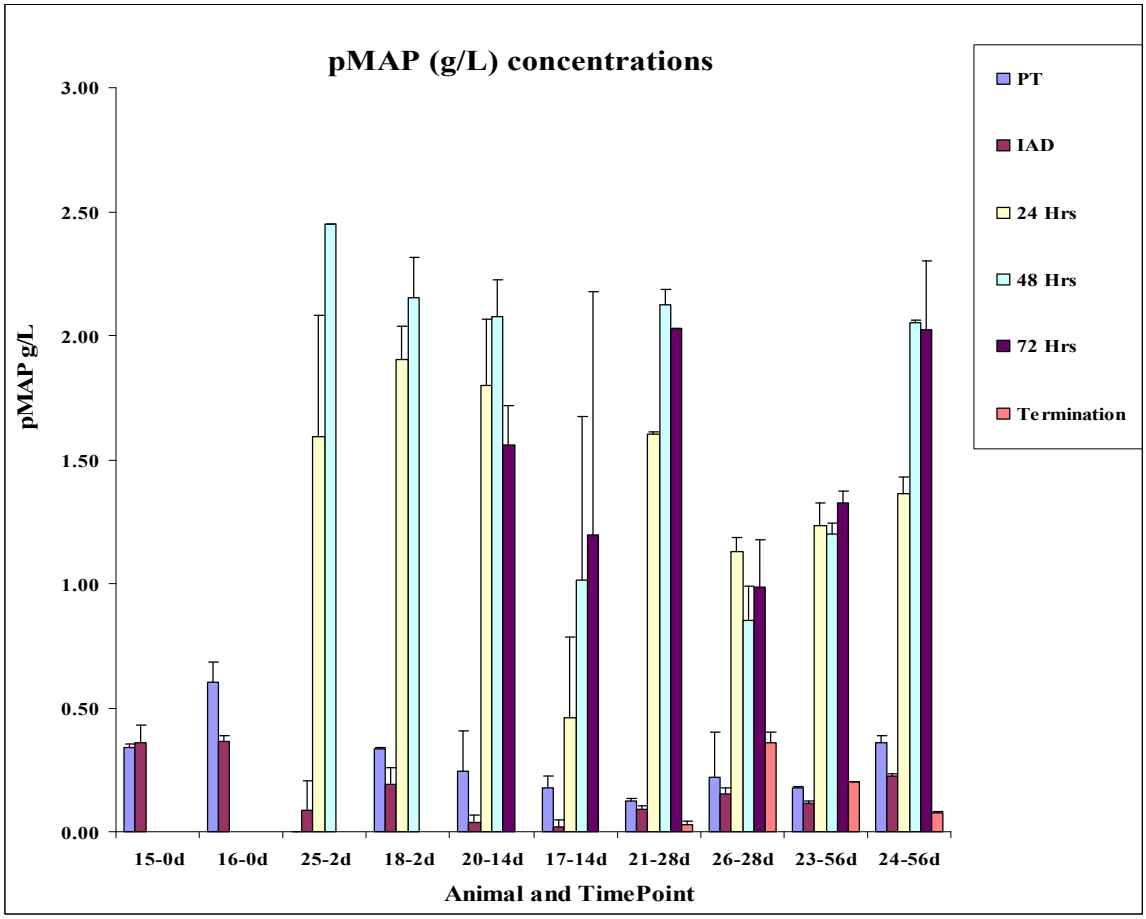

Graph 6.4 SAA levels for each animal with error bars at each time point.

Liver Function Summary												
Marker	**PT**		**IAD**		**24 Hrs**		**48 Hrs**		**72 Hrs**		**Termination**	
	Mean	**95% CI**	**Mean**	**95% CI**	**Mean**	**95% CI**	**Mean**	**95% CI**	**Mean**	**95% CI**	**Mean**	**95% CI**
ALP (U/L)	**148.6**	**23.54**	**124.5**	**16.34**	**143.88**	**20.12**	**112.25**	**12.37**	**97.5**	**10.25**	**117.17**	**11.83**
ALT (U/L)	**44.4**	**4.53**	**44.4**	**5.52**	**104.50**	**22.20**	**109.25**	**23.82**	**95.83**	**14.96**	**58.83**	**7.12**
AST (U/L)	**41.9**	**9.91**	**246.8**	**47.7**	**625.88**	**190.76**	**370.375**	**222.08**	**160.33**	**45.73**	**54**	**13.08**
GGT (U/L)	**45.7**	**10.28**	**45**	**14.45**	**44.63**	**9.52**	**44.38**	**10.47**	**41.3**	**5.6**	**40.17**	**5.98**
LDH (U/L)	**1313.3**	**258.5**	**1785.8**	**192.4**	**5338.63**	**1802.97**	**3497**	**1578.83**	**2243.67**	**375.67**	**1224.75**	**193.13**
Bilirubin (U/L)	**1.5**	**0.79**	**3.9**	**1.27**	**1.375**	**0.36**	**1**	**0.37**	**0.5**	**0.44**	**1**	**0**
Albumin (g/L)	**39**	**2.02**	**31.3**	**1.7**	**37.5**	**3.5**	**37.5**	**2.85**	**37.5**	**2.76**	**40.5**	**2.13**

Table 6.9 Summarises the mean values for each liver function, LDH, Albumin and Bilirubin at each specified time point tested, with the corresponding 95% confidence interval (Radostits et al, 2005).

Renal Function Summary												
Marker	**PT**		**IAD**		**24 Hrs**		**48 Hrs**		**72 Hrs**		**Termination**	
	Mean	**95% CI**	**Mean**	**95% CI**	**Mean**	**95% CI**	**Mean**	**95% CI**	**Mean**	**95% CI**	**Mean**	**95% CI**
Na mmol/L	**145.5**	**1.96**	**142.3**	**0.833**	**145**	**1.62**	**146.5**	**2.47**	**145**	**2.01**	**144.67**	**2.91**
K mmol/L	**5.15**	**0.24**	**4.8**	**0.15**	**5.8**	**0.95**	**5.8**	**0.92**	**5.35**	**0.86**	**4.68**	**0.39**
Urea mmol/L	**4.3**	**0.33**	**4.28**	**0.54**	**5.28**	**0.96**	**3.67**	**0.62**	**4.11**	**0.67**	**4.67**	**1.05**
Creat mmol/L	**141.2**	**11.5**	**125.2**	**7.18**	**121**	**13.58**	**121.5**	**9.15**	**106.17**	**25.14**	**125.67**	**10.63**

Table 6.22 Summarises the mean values for each marker tested (Sodium (Na), Potassium (K), Urea and Creatinine) at each specified time point tested, with the corresponding 95% confidence interval (Radostits et al, 2005).

ALP U/L						
Sample	PT	IAD	24 Hrs	48 Hrs	72 Hrs	Termination
	Mean	Mean	Mean	Mean	Mean	Mean
15-0d	211	180	NS	NS	NS	NS
16-0d	109	105	NS	NS	NS	NS
18-2d	205	141	189	139	NS	NS
25-2d	114	127	146	122	NS	NS
20-14d	96	76	99	84	77	120
17-14d	165	117	135	102	90	109
21-28d	157	116	138	100	96	147
26-28d	124	139	167	110	104	110
23-56d	173	138	170	137	119	117
24-56d	132	106	107	104	99	100

Table 6.11 tabulates the results for the ALP levels at each time point for each animal.

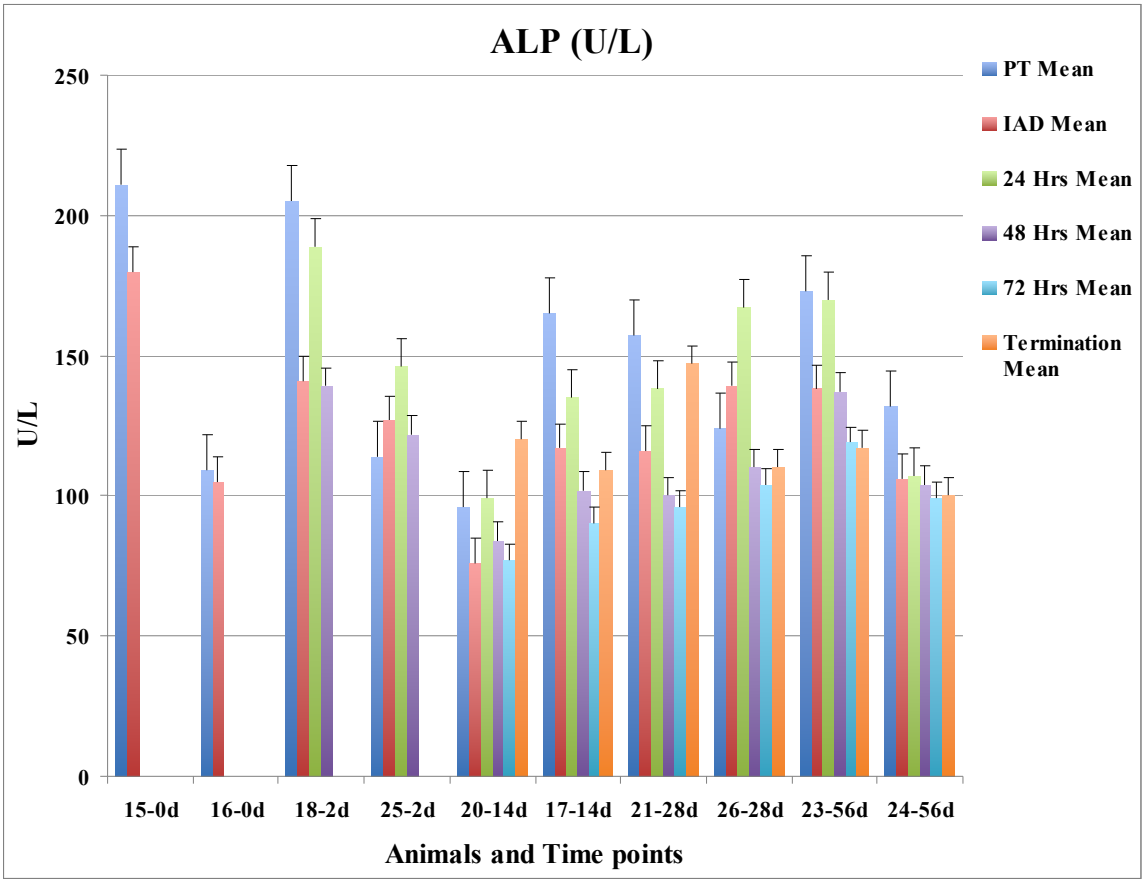

Graph 6.5 demonstrates the ALP levels at each time point for each animal with error bars.

ALT U/L						
Sample	PT	IAD	24 Hrs	48 Hrs	72 Hrs	Termination
	Mean	Mean	Mean	Mean	Mean	Mean
15-0d	50	46	NS	NS	NS	NS
16-0d	46	48	NS	NS	NS	NS
18-2d	38	41	67	59	NS	NS
25-2d	44	42	150	129	NS	NS
20-14d	41	37	100	149	110	48
17-14d	36	36	95	82	78	56
21-28d	61	58	119	106	108	70
26-28d	48	62	118	82	70	68
23-56d	35	33	132	157	116	60
24-56d	45	41	55	110	93	51

Table 6.13 The results for the ALT levels at each time point for each animal.

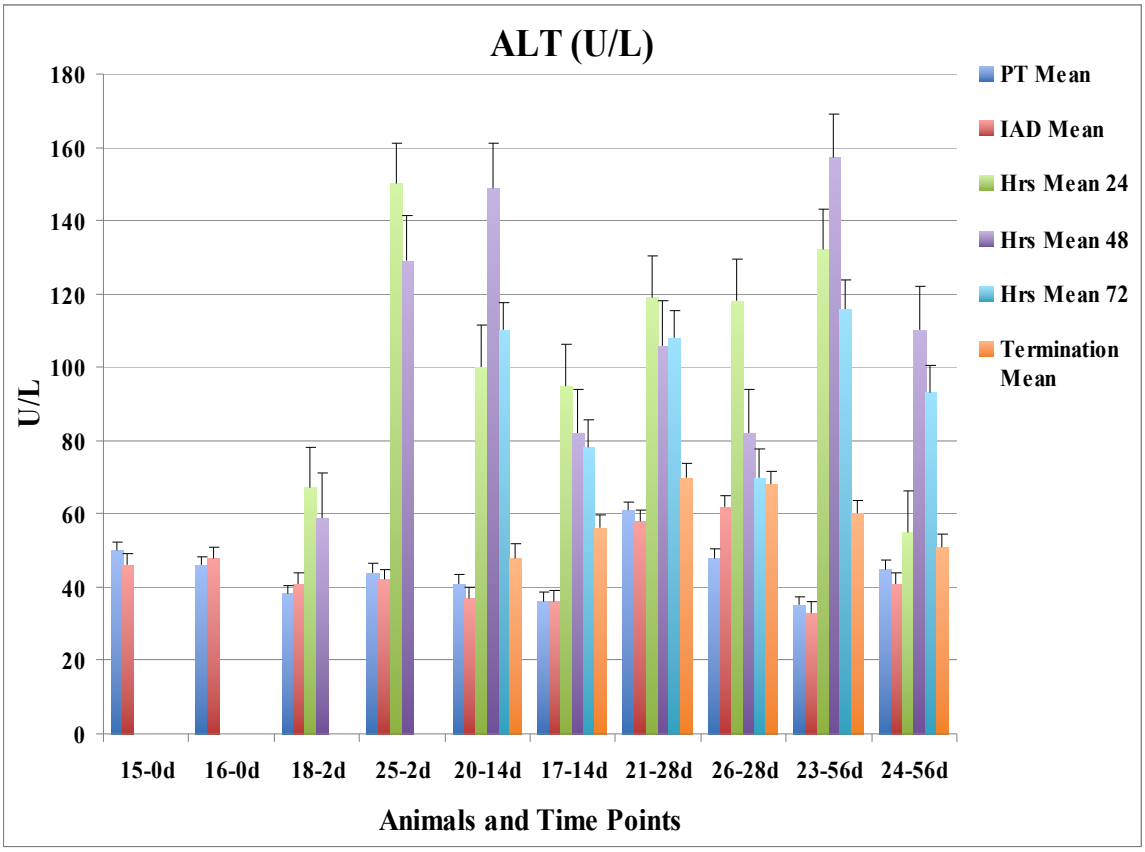

Graph 6.6 The ALT levels at each time point for each animal with error bars

AST U/L						
Sample	PT	IAD	24 Hrs	48 Hrs	72 Hrs	Termination
	Mean	Mean	Mean	Mean	Mean	Mean
15-0d	67	303	NS	NS	NS	NS
16-0d	50	249	NS	NS	NS	NS
18-2d	27	185	211	97	NS	NS
25-2d	26	176	826	212	NS	NS
20-14d	48	271	506	183	116	55
17-14d	37	222	658	862	101	68
21-28d	39	321	662	221	178	70
26-28d	22	379	605	145	119	29
23-56d	36	116	1130	889	205	62
24-56d	67	246	409	354	243	40

Table 6.15 tabulates the results for the AST levels at each time point for each animal.

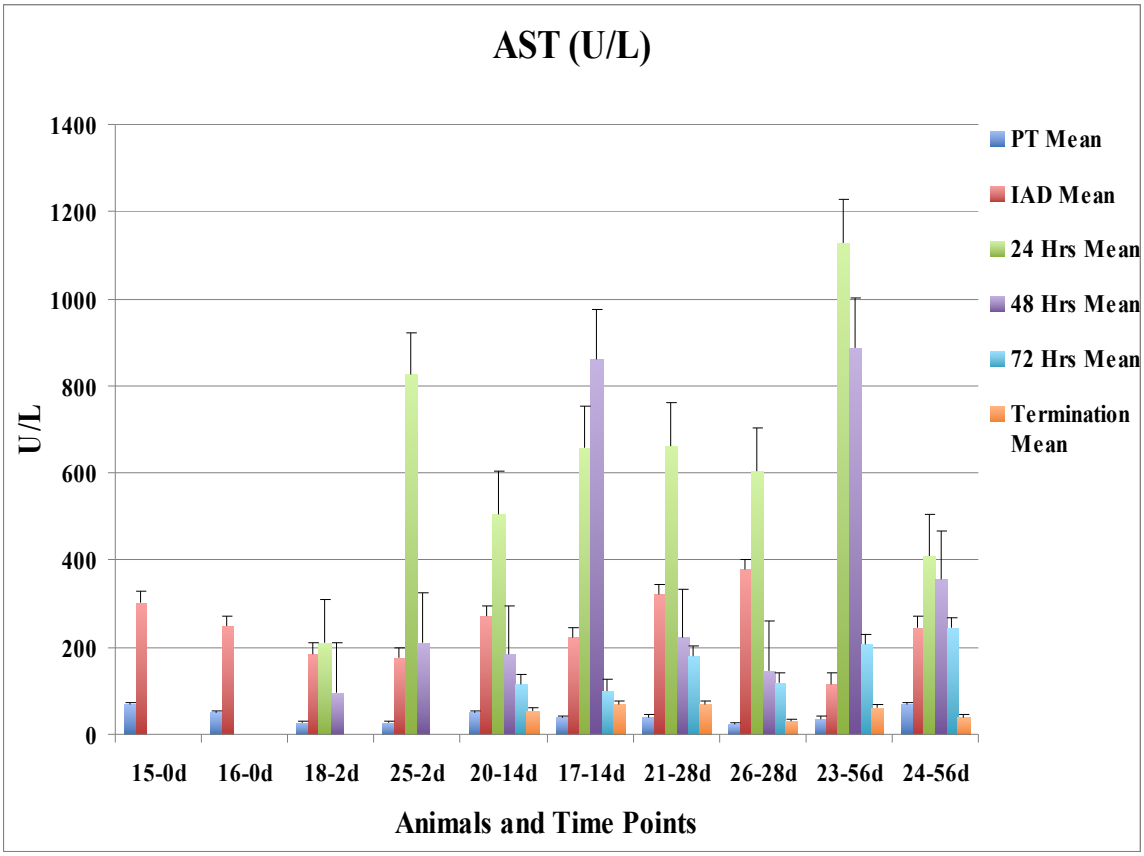

Graph 6.7 demonstrates the AST levels at each time point for each animal with error bars.

GGT U/L						
Sample	PT	IAD	24 Hrs	48 Hrs	72 Hrs	Termination
	Mean	Mean	Mean	Mean	Mean	Mean
15-0d	49	34	NS	NS	NS	NS
16-0d	61	103	NS	NS	NS	NS
18-2d	73	59	59	70	NS	NS
25-2d	18	23	21	21	NS	NS
20-14d	33	32	40	47	43	38
17-14d	43	40	47	41	44	40
21-28d	38	34	36	34	35	39
26-28d	49	47	56	51	45	49
23-56d	31	26	37	35	31	28
24-56d	62	52	61	56	50	47

Table 6.17 tabulates the results for the γ-GT levels at each time point for each animal.

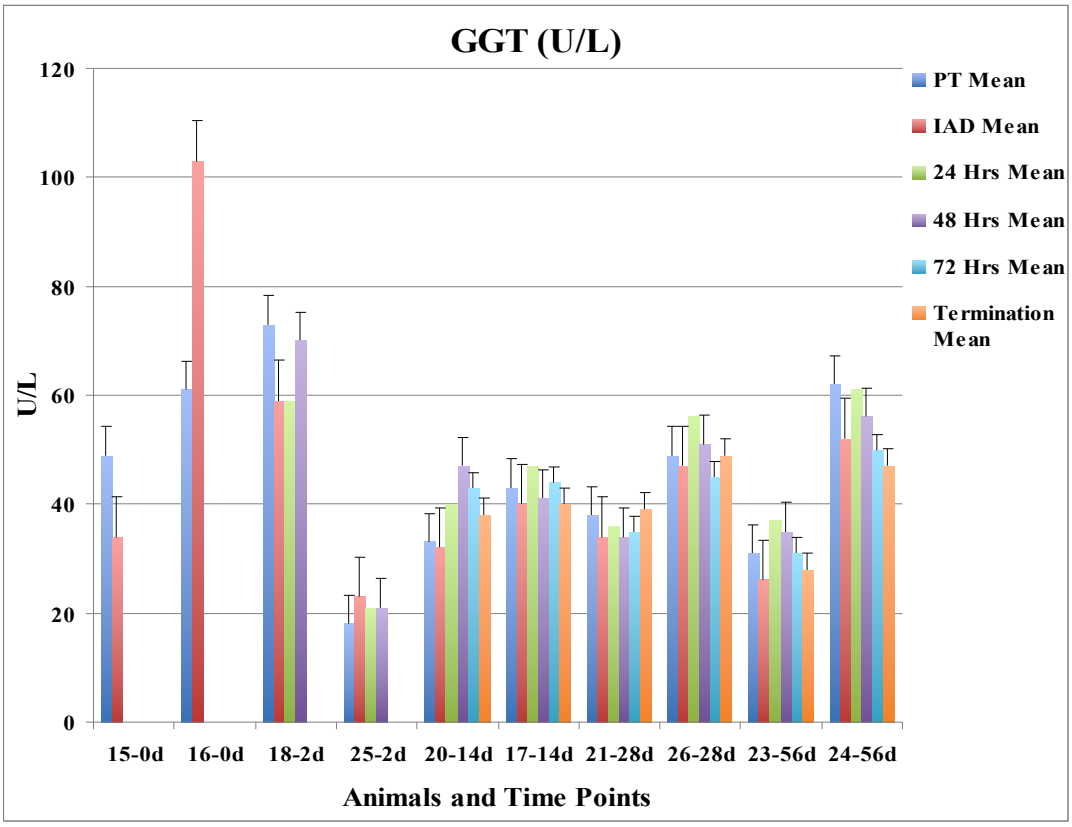

Graph 6.8 demonstrates the γ-GT levels at each time point for each animal with error bars.

LDH U/L						
Sample	PT	IAD	24 Hrs	48 Hrs	72 Hrs	Termination
	Mean	Mean	Mean	Mean	Mean	Mean
15-0d	1735	1734	NS	NS	NS	NS
16-0d	1504	2035	NS	NS	NS	NS
18-2d	1423	1377	3136	2475	NS	NS
25-2d	979	1756	7600	2153	NS	NS
20-14d	957	1541	3325	8606	1876	986
17-14d	1095	2271	4177	2217	1846	1102
21-28d	1161	1687	4561	2340	2965	1566
26-28d	1000	2081	9903	2515	2239	1165
23-56d	1040	1354	7279	5103	2647	997
24-56d	2239	2022	2728	2567	1889	1171

Table 6.19 tabulates the results for the LDH levels at each time point for each animal.

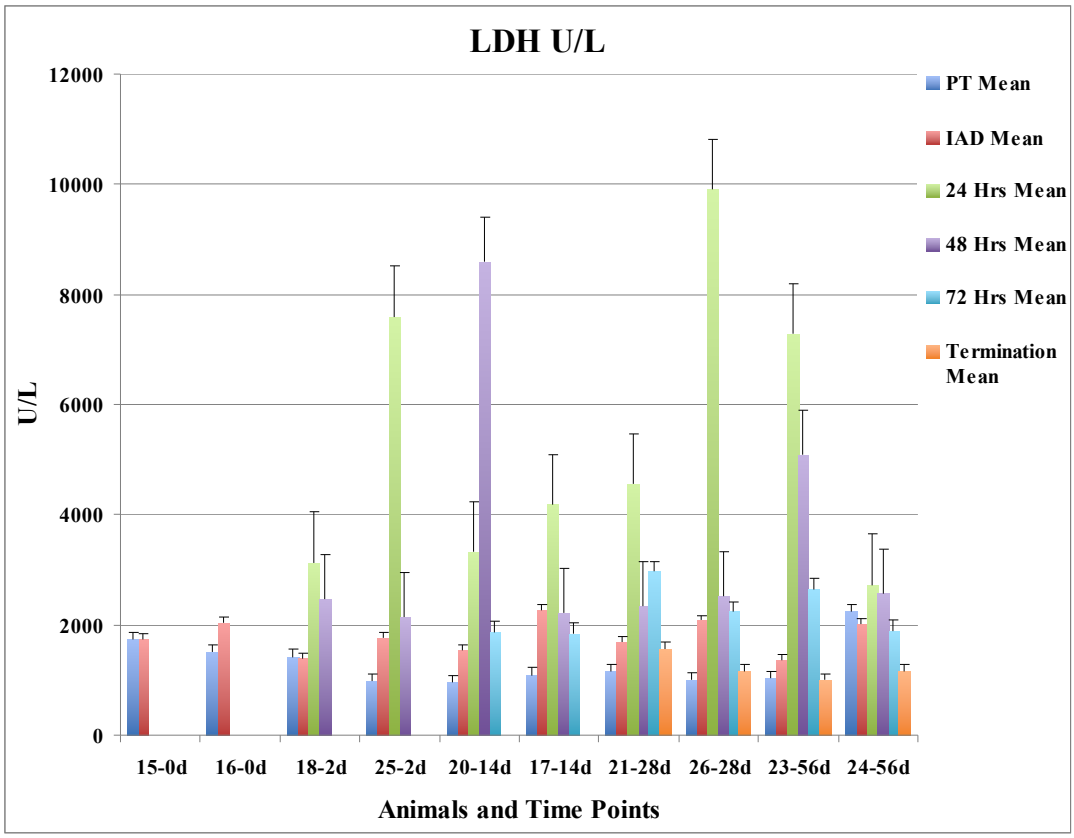

Graph 6.9 demonstrates the LDH levels at each time point for each animal with error bars.

Bilirubin µmol/L						
Sample	PT	IAD	24 Hrs	48 Hrs	72 Hrs	Termination
	Mean	Mean	Mean	Mean	Mean	Mean
15-0d	5	7	NS	NS	NS	NS
16-0d	1	4	NS	NS	NS	NS
18-2d	1	4	1	1	NS	NS
25-2d	1	3	1	1	NS	NS
20-14d	1	4	2	1	1	1
17-14d	2	2	1	2	1	1
21-28d	1	1	1	1	1	1
26-28d	1	8	1	1	1	1
23-56d	1	3	2	1	1	1
24-56d	1	3	2	1	1	1

Table 6.19 tabulates the results for the Bilirubin levels at each time point for each animal.

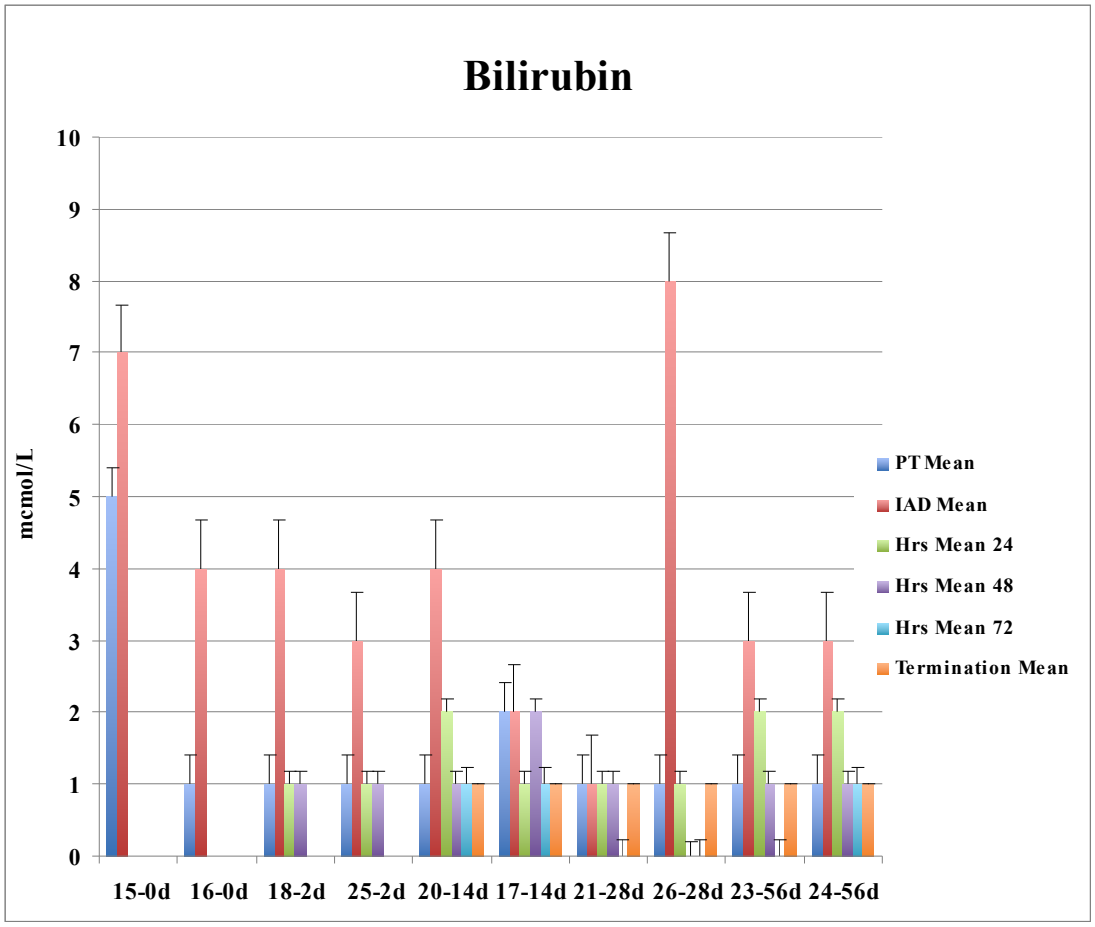

Graph 6.10 demonstrates the Bilirubin levels at each time point for each animal with error bars.

Na mmol/L						
Sample	PT	IAD	24 Hrs	48 Hrs	72 Hrs	Termination
	Mean	Mean	Mean	Mean	Mean	Mean
15-0d	149	140	NS	NS	NS	NS
16-0d	145	142	NS	NS	NS	NS
18-2d	153	141	146	153	NS	NS
25-2d	146	143	148	152	NS	NS
20-14d	145	143	144	146	143	144
17-14d	143	143	142	145	143	143
21-28d	142	142	149	144	147	142
26-28d	145	145	143	143	146	152
23-56d	145	141	145	145	149	141
24-56d	142	143	143	144	142	146

Table 6.24 tabulates the results for the Na levels at each time point for each animal.

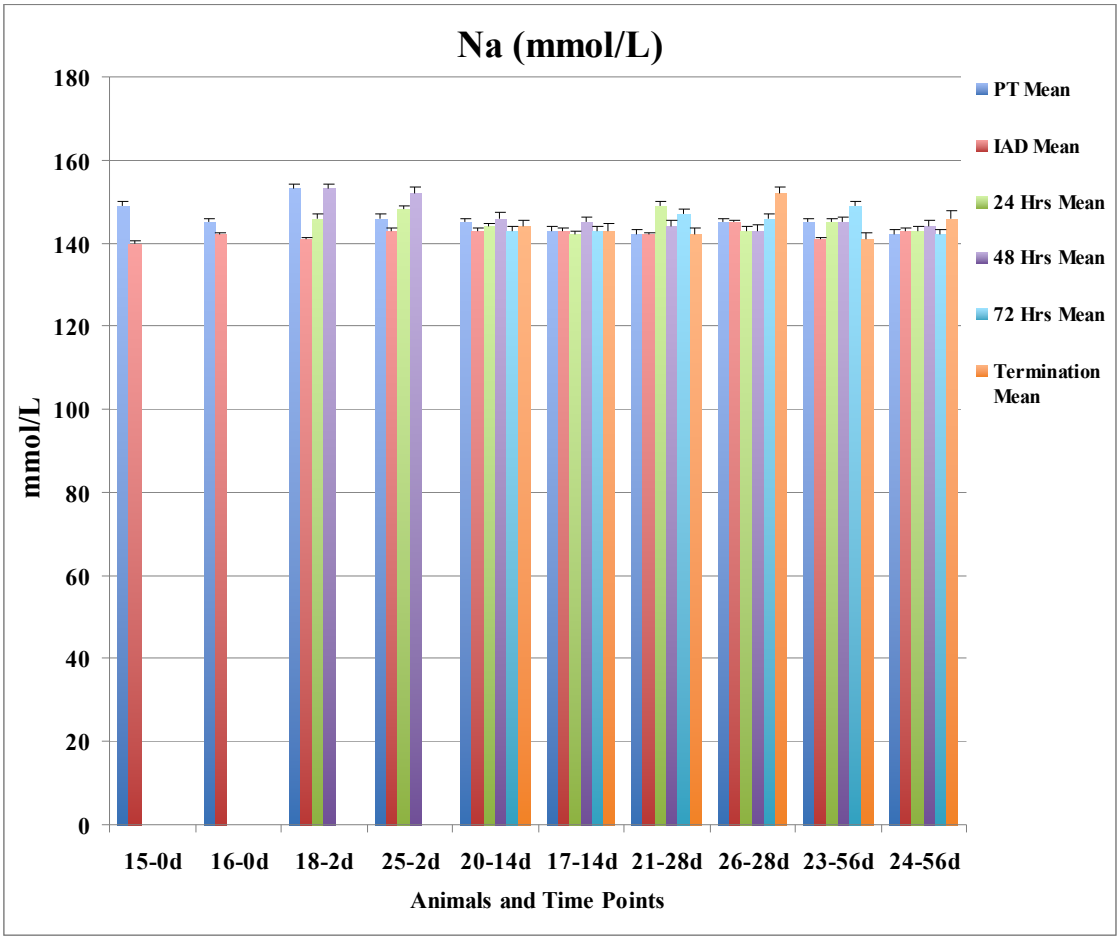

Graph 6.11 demonstrates the Na levels at each time point for each animal with error bars.

K mmol/L						
Sample	PT	IAD	24 Hrs	48 Hrs	72 Hrs	Termination
	Mean	Mean	Mean	Mean	Mean	Mean
15-0d	6	5.2	NS	NS	NS	NS
16-0d	4.9	4.9	NS	NS	NS	NS
18-2d	4.5	4.9	4.3	4.9	NS	NS
25-2d	5.1	4.9	5.5	6.3	NS	NS
20-14d	5.2	4.6	5.4	5	4.2	4.1
17-14d	5	5.1	5	6.1	4.9	4.3
21-28d	5.5	4.4	6.3	4.5	7.3	4.6
26-28d	5	4.7	8.9	9	5.3	5.5
23-56d	5.4	4.7	5.3	5.5	5.7	4.8
24-56d	4.9	4.6	5.7	5.1	4.7	4.8

Table 6.26 tabulates the results for the K levels at each time point for each animal.

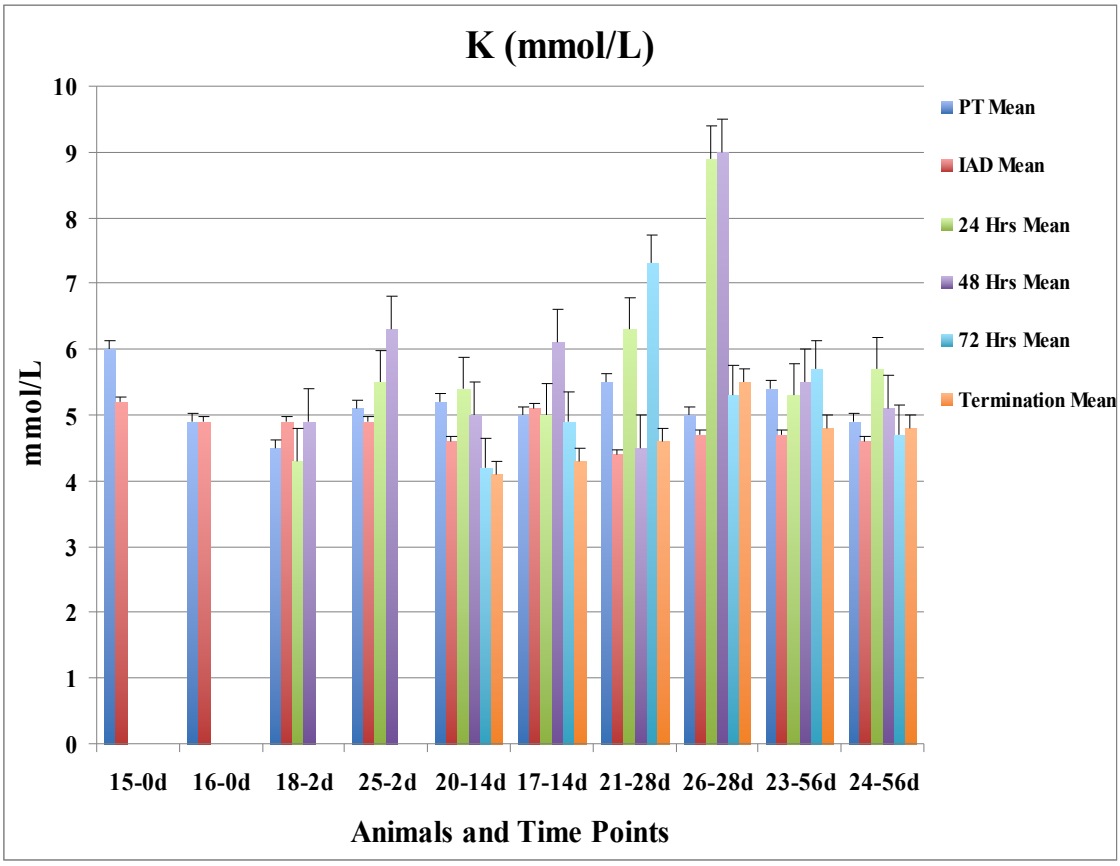

Graph 6.12 demonstrates the K levels at each time point for each animal with error bars.

Urea mmol/L						
Sample	PT	IAD	24 Hrs	48 Hrs	72 Hrs	Termination
	Mean	Mean	Mean	Mean	Mean	Mean
15-0d	4.88	3.79	NS	NS	NS	NS
16-0d	4.05	2.81	NS	NS	NS	NS
18-2d	4.31	3.57	4.01	2.21	NS	NS
25-2d	3.51	3.7	4.6	4.48	NS	NS
20-14d	4.81	5.46	6.05	2.94	3.01	3.43
17-14d	5.17	5.14	4.76	3.01	4.73	3.65
21-28d	4.13	3.85	7.51	5.08	5.5	4.24
26-28d	3.58	5.03	4.91	3.51	4.3	4.73
23-56d	4.14	5.15	6.83	4.5	3.53	7.09
24-56d	4.38	4.25	3.58	3.62	3.56	4.89

Table 6.28 tabulates the results for the Urea levels at each time point for each animal.

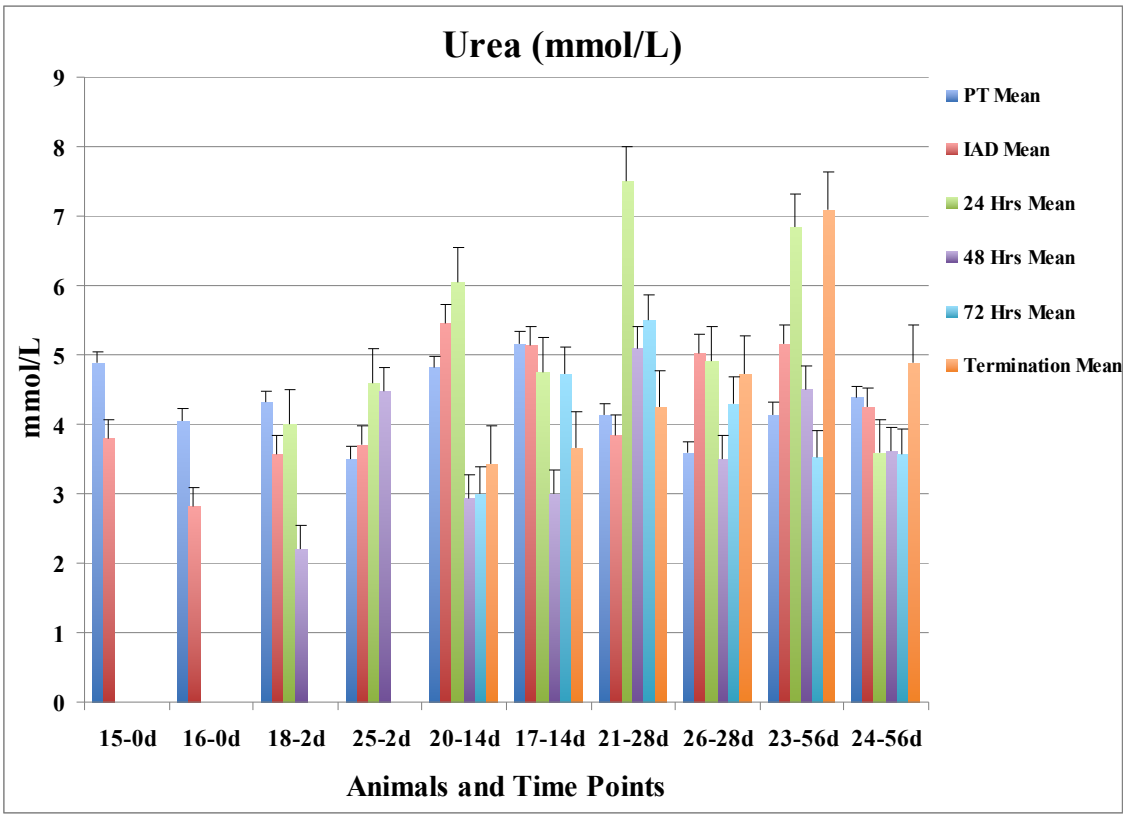

Graph 6.13 demonstrates the Urea levels at each time point for each animal with error bars.

Creatinine mmol/L						
Sample	PT	IAD	24 Hrs	48 Hrs	72 Hrs	Termination
	Mean	Mean	Mean	Mean	Mean	Mean
15-0d	146	119	NS	NS	NS	NS
16-0d	130	111	NS	NS	NS	NS
18-2d	162	125	102	135	NS	NS
25-2d	123	134	87	123	NS	NS
20-14d	149	122	134	97	112	109
17-14d	163	142	132	132	121	115
21-28d	151	135	141	120	61	122
26-28d	102	104	110	107	74	129
23-56d	145	132	140	130	133	146
24-56d	141	128	122	128	136	133

Table 6.30 tabulates the results for the Creatinine levels at each time point for each animal.

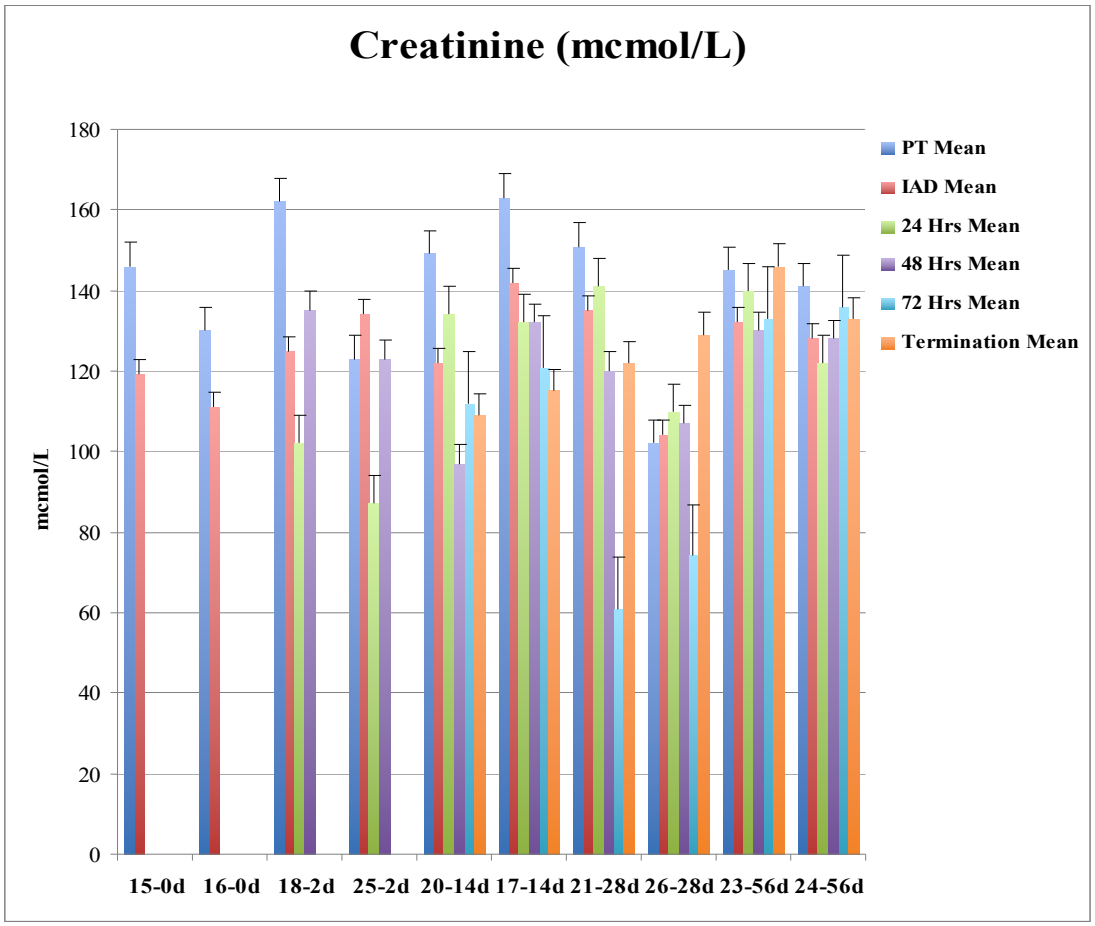

Graph 6.14 demonstrates the Creatinine levels at each time point for each animal with error bars.

Discussion:

General.

RFA has a low complication rate (Rhim et al, 2003, Tateishi et al, 2005) when compared to cryoablation (Seifert and Morris, 1999, Seifert et al, 1999) and similar complication rates when compared to ethanol ablation (Di Stasi et al, 1997, Livraghi et al, 1998) despite the recent complication reported using ethanol ablation (Chiu et al, 2009).

Establishing the safety profile of BETA is essential before embarking on clinical trials. The clinical response of the animal models together with the biochemical and Acute Phase Protein (APP) analysis provides important information regarding the response to BETA. The results however must be viewed with the knowledge that the insult to the animals was not just BETA; the animals were subjected to surgical laparotomy and 8 ablation cycles, including a general anaesthetic which was over 6 hours duration in one animal (Animal 15). The length of general anaesthetic itself stimulates the inflammatory cascade, the animal's respiratory system is compromised in the supine position, the abdominal contents splint the diaphragm, often causing lower lobe consolidation. This can in turn lead to infection or lobar collapse, which can often manifest as non specific respiratory symptoms, which may not be clinically significant, but may cause an elevated acute phase response, becoming apparent with raised inflammatory markers. The volume of tissue ablated during these studies in each animal is significantly very much larger than would be ablated in a clinical situation. This volume of necrotic tissue therefore initiates a greater inflammatory response in the tissue, with release of inflammatory cytokines. The results therefore represent the combination of these procedures and must be evaluated accordingly.

The inflammatory response to ablation is well documented in the literature in both clinical (Ng et al, 2004, Jansen et al, 2008) and research contexts (Teague et al, 2002, Teague et al, 2004a, Teague et al, 2004b).

Systemic Inflammatory Response:

Cryoablation has a well-documented complication profile, the most serious complication being the "cryoshock phenomenon" (Seifert and Morris, 1999). This significant, but relatively rare complication consists of thrombocytopenia, disseminated intravascular coagulation (DIC), renal failure and adult respiratory distress syndrome. The cryoshock phenomenon was observed in 21 of 2173 patients following cryotherapy. Of these 21 patients, 6 patients died during the

postoperative period (Seifert and Morris, 1999). The incomplete syndrome however, is observed more frequently and consists of one or more of the complications described. The safety profile of RFA and electrolysis is considerably more favourable than cryotherapy, however RFA is associated with an inflammatory response, similar to surgical resection; this is only observed on a biochemical level, the clinical manifestations are considerably less (Jansen et al, 2008). Jansen et al compared the inflammatory response in 39 patients undergoing RFA, major resection (MR) or minor hepatic resection (mR). RFA induced an elevation of CRP higher than MR and mR (77 mg/L vs 50 mg/L and 59 mg/L). IL-6 levels were elevated earlier in the RFA group compared to the mR group (96 pg/ml vs 4 pg/ml). A further protein; serum Plasma Secretory Phospholipase A2 (sPLA2) was measured in addition in order to determine an overall inflammatory response. This inflammatory protein however appears unreliable when comparing the inflammatory response (sPLA2) using different treatments (Jansen et al, 2008). These results highlight the inflammatory response of RFA being similar to surgical resection, despite it being a minimally invasive procedure. However Jansen's patients underwent open RFA performed at open surgery. The results therefore are a combination of the response to surgical laparotomy and RFA, rather than response to percutaneous RFA.

Ng et al (Ng et al, 2004) evaluated the inflammatory response following RFA, cryoablation and surgical resection in porcine models. Peak tumor necrosis factor - α (TNF-α) and interleukin-1β (IL-1β) in the RFA group were significantly lower than in the cryotherapy group (96.4pg/mL vs >225pg/mL for TNF-α and ≤90pg/mL vs ≥180pg/mL for IL-1β).

The safety of electrolysis is well described in the literature (Wemyss-Holden et al, 2000, Teague et al, 2004a, Teague et al, 2004b). Teague et al (Teague et al, 2004a) performed electrolytic liver ablation in 16 pigs. Platelet count and serum levels of urea, creatinine, liver enzymes, C-reactive protein (CRP), TNF-α and IL-1β were measured before treatment and for 72 h post procedure. There were significant dose-related increases in CRP levels with liver electrolysis, however this was not seen in the serum TNF-α and IL-1β levels. The rise in CRP levels appeared to plateau at 72 hours and there was no documented clinical abnormalities detected, despite the elevated CRP levels.

The inflammatory response of BETA has not previously been evaluated to date and the acute phase marker proteins were discussed with HLS. The measurement of acute phase proteins is not a routine procedure, as it requires ELISA and expert analysis. HLS did not provide this service and thus a laboratory had to be found which would be able to analyse the blood samples and return reliable results.

Professor D. Eckersall of the University of Glasgow has a special interest in inflammatory proteins and his expertise was sought in order to determine which proteins would be most appropriate for inflammatory marker analysis in porcine models. Following discussions with Prof D Eckersall, it was agreed to measure CRP (C Reactive Protein), Serum Amyloid A

(SAA), Pig MAP and serum Haptoglobin. Studies by Eckersall et al (Eckersall et al, 1996, Eckersall et al, 1999a, Eckersall et al, 1999b, Eckersall, 2000, Bence et al, 2004, Eckersall, 2004) have shown these to be more reliable than TNF-α and IL-1β. These inflammatory markers have not been described in the medical literature as markers for the inflammatory response in animals, but are well described in the veterinary literature as reliable markers for the inflammatory response measurement (Alava et al, 1997, Horadagoda et al, 1999, Hiss et al, 2003, Ceron et al, 2005, Jonasson et al, 2006, Gutierrez et al, 2008, Grau-Roma et al, 2009, Gutierrez et al, 2009b). CRP, however is the most commonly quoted marker of inflammation in both medical and veterinary literature (Gutierrez et al, 2008, Gutierrez et al, 2009b).

The results of the CRP analysis demonstrated a marked rise in the CRP at 24 hours, peaking at 48 hours, with a small rise at 72 hours post ablation, however the pattern demonstrated a plateau appearance at 72 hours rather than a sustained rise in the CRP levels. The results of the CRP analysis are comparable with the literature (Teague et al, 2004a) with the levels returning to normal pre-termination.

An interesting observation was the pre ablation CRP levels noted in a number of animals. A normal CRP value is less than 100mg/L, however animals 15, 16, 20 and 24 had abnormal CRP levels pre ablation. Animals 15 and 16 were not acclimatised for 2 weeks prior to treatment and the stress of transportation from the commercial pig farm in Shropshire may be a contributing factor in the abnormal results. Animals 20 and 24 were acclimatised for 2 weeks prior to the procedure and were deemed clinically suitable for general anaesthetic prior to the procedure. None of the animals demonstrated clinical signs of infection and were examined by the treating veterinary surgeon on the day of the procedure and deemed well. The reason for the abnormal CRP is unknown, however an important observation is the normal Haptoglobin levels in all the animals prior to the procedure, apart from animal 16, however again this abnormal marker may well be due to the stress following transportation.

The encouraging plateau of the CRP and Haptoglobin levels at 72 hours demonstrates an inflammatory response, which appears to settle biochemically at 72 hours and by 1 month, has completely resolved and returned to normal levels. It is not possible to compare BETA to standard RFA with regards to the inflammatory response as there were no control animals in this study, however the response to BETA appears to similar to the response to electrolysis (Teague et al, 2004a, Teague et al, 2004b) and RFA (Ng et al, 2004, Jansen et al, 2008). None of the animals developed a systemic inflammatory response to BETA and the inflammatory response observed clinically and biochemically in Animal 22 must be directly attributed to the morbidity and mortality resulting from the perforated gastric ulcer. Alava et al (Alava et al, 1997) described a 5-7 times increase in the concentration of CRP following trauma and a 10-30 times increase in Haptoglobin. Both of these markers peaked at 48 hours, similar results to those obtained during this research. If each of the CRP and Haptoglobin values are analysed using this

trend of 5-7 times for CRP and 10-30 times for Haptoglobin, the results of the APP analysis following BETA demonstrates a CRP elevation of over 100 times the normal, however the corresponding Haptoglobin results reached a peak of 1.78g/L at 72 hours which corresponds to a rise of less than 2 times the normal value (<1g/L). Haptoglobin is the most studied APP in pigs (Pineiro et al, 2007). A mean value of 1.24g/L in animals 18-24 weeks of life was reported by Pineiro et al (Pineiro et al, 2009) and therefore the laboratory value of less than 1g/L are not species-specific levels. Pineiro et al however concluded that levels above 1g/L could be found in commercially available farm animals, without evidence of clinical disease.
The levels of CRP in this research study were extremely variable without any animal displaying signs of clinical disease. The CRP levels in both the non-recovery animals were 540mg/L and 1213mg/L respectively, however these animals were not acclimatised for 2 weeks prior to the procedure and the abnormal CRP may well be due to stress of the road transport (Pineiro et al, 2007). The abnormal CRP levels observed in animals 20 and 24 however cannot be attributed to the stress of road transport as groups 2-5 were all acclimatised for 2 weeks prior to ablation. None of the pigs displayed clinical signs of infection or inflammation and both had normal Haptoglobin levels pre treatment. Given the normal serum values of HP, SAA and pig-MAP, the abnormal levels of the CRP may indicate this to be a poor marker of specific inflammation, or CRP may well have a poor correlation with clinical signs, however this a hypothesis of observed results and the sample size is too small to make any significant observations.
Serum Amyloid-A (SAA) is considered to be a clinically relevant acute phase protein in pigs (Jacobson et al, 2004, Jonasson et al, 2006). A biochemical response of SAA is most commonly observed during the first 3 days following an insult (Heegaard et al, 2000, Jacobson et al, 2004, Jonasson et al, 2006) and is rarely seen in chronic inflammation (Horadagoda et al, 1999), making it another favourable APP in evaluating an acute phase response. In pigs, an SAA concentration of <50mg/L is considered to be biologically relevant. In animals 17-26 (2d-56d terminations) the SAA level peaked at 24 hours, decreased by 72 hours and returned to below reference level by termination. This is entirely consistent with the published literature (Jacobson et al, 2004, Jonasson et al, 2006). Most of the animals showed a >200 times increase in SAA levels from PT (pre-test) to 24 hours with a maximum SAA response of 776.5mg/L seen with animal 17 (14d termination) at 24 hours. Although this rise in the baseline SAA levels is significant, no animal showed any signs of a systemic inflammatory response (SIRS) post surgery.

The porcine Major Acute Phase Protein (pMAP) has been identified and shown to be the most sensitive protein to use as a marker of inflammation in this species (Alava et al, 1997, Eckersall et al, 1999a). Both pMAP and haptoglobin have been shown to be valid markers of disease in animals (Pineiro et al, 2009) and display similar kinetics of induction following inflammation or

bacterial infection (Grau-Roma et al, 2009, Pineiro et al, 2009). Both the proteins are classified as intermediate fast and protracted responders.
In pigs, a pMAP concentration of <0.6g/L is considered to be biologically relevant.
In animals 17-26 (2d-56d terminations) the overall trend showed pMAP to increase from 24 hours up to 48-72 hours. Most of the animals showed a >5-20 times increase in pMAP levels from PT to 72 hours, with a maximum pMAP concentration of 2.45g/L with animal 25 (2d termination) at 48 hours. By termination date pMAP levels had reduced to below reference level. No animal showed any signs of a systemic inflammatory response (SIRS) post surgery. The trend of pMAP both pre and post surgery demonstrated a favourable profile, similar to that observed with Hp. The levels of Hp may rise over 10 times in different acute-phase models, with a 10 fold rise noted in animals injected with turpentine, surgical trauma or acute bacterial and viral infection (Eckersall et al, 1996, Eckersall et al, 1999b, Horadagoda et al, 1999, Grau-Roma et al, 2009, Gutierrez et al, 2009a, Pineiro et al, 2009, Skovgaard et al, 2009).

The body's response to trauma however is both a clinical and subclinical one. Often, the subclinical response to trauma is a precursor to the observed clinical manifestations. The clinical and gross pathological abnormalities, although few were discussed in the previous chapter. The purpose of the staggered termination profiles of the *in vivo* studies was to observe ay immediate, intermediate or delayed response to the insult of BETA. This was evaluated in 3 ways; the clinical state of the animals throughout the post operative course, the biochemical state, observed with both APPs and the liver and renal function of the pigs. Finally the postmortem findings confirmed these clinical and biochemical observations.
All the animals in the study recovered well from the surgery apart from the anaesthetic-associated death and the animal, which developed peritonitis secondary to a perforated gastric ulcer. Both of these deaths can not reasonably be ascribed to BETA as discussed earlier. All the animals gained weight throughout the postoperative period and no observed complications were noted at post mortem. The favourable biochemical profile of the animals demonstrates BETA to have a similar profile to conventional RFA and electrolysis (Teague et al, 2004a, Teague et al, 2004b).

In a clinical setting, the Haptoglobin (Hp) assay is used to screen for and monitor intravascular hemolytic anaemia; the reticuloendothelial system removes the haptoglobin-haemoglobin complex from the body and thus haptoglobin levels are decreased in haemolytic anaemia. This process has lead to a theory of Haptoglobin being associated with the inflammatory response and therefore a sensitive APP. Eckersall et al (Eckersall et al, 1996) investigated the most appropriate proteins as markers of inflammation. The study demonstrated C-reactive protein and haptoglobin likely to be the best markers for the identification of inflammatory lesions in pigs.

In pigs, an Hp concentration of 1.0g/L is considered to be biologically relevant. The results of this study show that in animal numbers 15, 16 and 20 (0d, 0d and 2 week terminations respectively) the Hp level was raised at pretreatment. This could be attributed to an underlying subclinical infection or to stress. Animals 15 and 16 were not acclimatised prior to surgery and the elevated Hp levels may be attributed to transport. This was also reflected in a high CRP concentration in these animals at pretreatment. The elevated Hp level in animal 20 cannot be attributed to transport as all the animals apart from the 0d terminations were acclimatised for 14 days prior to treatment. This single result is probably spurious, given the normal Hp levels in all the remaining animals pre-treatment. In all animals apart from animals 15, 16 and 20, there was an overall trend for the Hp to increase 2-4 times from 24 hours to 72 hours (maximum Hp 2.16g/L with animal 22 at 72 hours) then decrease to below reference level by termination. No animal showed any signs of a systemic inflammatory response (SIRS) post surgery.

Biochemical Markers.

Both liver function and renal function biochemical markers demonstrated some evaluation during this study, however not all markers were elevated.

The liver functions included hepatic enzymes (ALT, AST, ALP, GGT), bilirubin, albumin and LDH. The LDH is the least reliable of all the hepatic markers evaluated, as it is influenced by a large number of factors, including surgery, the ablation cycles, the anaesthetic agents and haemolysis.

The liver enzymes provide a representative analysis of hepatic function before and after the ablations. The ALT and AST showed significant increases up to 72 hours post ablation, which is expected following 8 ablation cycles, importantly the ALP and GGT, which are markers of biliary obstruction did not increase significantly following the ablations. The Bilirubin decreased significantly at 24 hours post ablation, but returned to normal at 48 hours. This observation is probably related to the volume of hepatocytes affected by the ablations, however the rapid recovery demonstrates this to be a transient abnormality.

The LDH levels increased significantly following ablation but returned to normal at termination. This data must be viewed in the context of a surgical laparotomy and when viewed together with the other liver enzymes, does not demonstrate a significantly abnormal trend.

Bilirubin demonstrated a significant increase immediately post procedure (Table 6.61), however this was the single significant observation and given the time frame following the procedure, the Bilirubin levels were influenced by not only the ablations, but by the anaesthetic agent administration. Propofol, the anaesthetic drug used for intravenous anaesthesia during this study is rapidly metabolised by the liver and excreted by the kidney. This, in part may have influenced the immediate post procedural Bilirubin level. The reassuring decrease and normal values observed at 24, 48, 72 hrs post procedure and at termination reinforce this hypothesis.

The biochemical markers for renal function used in this study (Na, K, Urea and Creatinine) did not demonstrate any significant increase following the procedure. In contrast, the Creatinine levels improved following the procedure. However this is probably due to the strict dietary control and the constant supply of fresh drinking water for all the animals during the study (Chapter 5).

The trends in liver function observed during this study are similar to observations made by Teague et al following RFA in porcine subjects (Teague et al, 2004).
Although used in combination in all animals, the lack of any significant adverse incidents regarding the liver function during the study demonstrate BETA to have similar effects on the liver as RFA. The transient rises in liver enzymes post procedure occur following and insult to the liver, BETA does not appear to increase this any more than other thermal ablation techniques.

The stable renal function following the procedures is similar to the published literature for RFA and BETA appears to have similar effects *in vivo* as RFA.
The addition of DC does not cause a significant biochemical abnormality.
Elcetrolysis has been proven to be a safe modality, as has RFA. The combination of these two ablation techniques does not have a detrimental synergistic effect.
The lack of any clinical observation of SIRS during the study compliments is in accordance with the biochemical and inflammatory marker results.

Limitation of this Research:

I accept there are a number of limitations with this research.

1. All the animals underwent general anaesthetic, laparotomy, 4 BETA cycles and 4 conventional RFA cycles. The inflammatory markers measured in this research therefore reflect a multitude of clinical insults to each animal and therefore not just the insult of BETA.

   Due to the study design, it would not have been possible to assess the animals' response to BETA alone. The use of a 'sham' animal in order to create a control for the ablations, where an animal would undergo general anaesthetic and laparotomy only, in order to compare the inflammatory response to those animals exposed to BETA and control RFA was discussed prior to the research study. Due to financial constraints, this was not deemed feasible. The aim of this study was to determine the significance of the inflammatory response as a trend rather than an absolute value. The inflammatory response to ablation is well documented in the literature in both clinical (Ng et al, 2004, Jansen et al, 2008) and research contexts (Teague et al, 2002, Teague et al, 2004a, Teague et al, 2004b). The use of a 'sham' animal would have provided greater information regarding the contribution of ablation to the inflammatory response in this study; the general anaesthetic and the laparotomy alone cause a significant inflammatory response and I accept the values for each inflammatory marker measured cannot assess each aspect of the intervention, it does provide essential information regarding a sustained inflammatory response or the lack thereof. The information obtained and analysed during this research demonstrates BETA to have greater effects on the inflammatory response that conventional RFA, given the similar trends obtained in this study to the literature (Teague et al, 2002, Teague et al, 2004a, Teague et al, 2004b). A sustained inflammatory response may well have required deeper analysis into the individual contribution of BETA, however the results obtained were in keeping with the findings of Teague et al.
2. The results of the biochemical marker analysis, as with the inflammatory markers were influenced by the general anaesthetic, laparotomy and the ablation cycles. The ALT and AST were the only liver enzymes, which demonstrated a significant rise post treatment, however these had returned to normal by termination. The ALP and γ-GT levels increased, but this was not significant.
3. The renal function analysis remained normal throughout despite the surgery and ablation cycles and in some cases improved, almost certainly due to the controlled diet and water supply.

> As with the hepatic biochemical analysis, the renal biochemical analysis suffered the same limitations, but again, the lack of a significant abnormality was reassuring.

The lack of a ‘sham’ animal for this study does raise questions regarding the validity of the study, however the use of ‘sham’ animals is not well described in the literature & with ‘sham’ animals, the experimental animals would have received the same protocol (4 control and 4 BETA cycles). This still would have left the question of the individual contributions of conventional RFA and BETA to the inflammatory and biochemical response. The only way to have answered this question would have been to have 3 groups of animals; 1 group undergoing RFA, one control RFA and a third ‘sham’ group, this model, I think would have been rejected by the ethical committee given the lack of data to support the use of ‘sham’ animals for this study design.

If the inflammatory marker and biochemical analysis had revealed a significant abnormality, which translated into clinical signs, leading to animal death, the study would have been stopped immediately had the post mortem results attributed the death to BETA. This did not occur and the animals all recovered well, apart from the two unrelated deaths.

Conclusions:

1. Significant elevations in Acute Phase Protein (APP) levels are observed at 24 and 48 hours post procedure.

2. The elevated APPs are not associated with a clinical Systemic Inflammatory Response (SIR).

3. All inflammatory markers return to normal levels by the time of termination.

4. The liver transaminase enzymes demonstrated a significant increase post procedure, peaking at 24-48 hours post procedure, but returned to normal levels by the time of termination. No biochemical sign of biliary obstruction was observed.

5. The renal function did not demonstrate any significant transient or permanent renal impairment. In contrast, an improvement in certain biochemical markers was observed during the study.

6. BETA does not appear to cause a significant, sustained impairment in liver function.

7. The transient impairment in liver function peaks at 24-48 hrs post procedure and is not associated with any clinical signs.

Chapter 7:

Conclusions and Future Work

Chapter 1

Radiofrequency Ablation and Competing Therapies

Conclusions.

Chapter 1 discussed ablation therapies and their development for use in the treatment of HCC and colorectal metastases to the liver. The development of ablation therapies has progressed rapidly and tumours previously deemed untreatable are now suitable for percutaneous, laparoscopic or occasionally open ablation therapies.

The varieties of ablation therapies and their impact on treatment have been discussed in detail. Each of the ablation therapies available has been researched with a single aim – increasing the size of the ablation zone. The size of the ablation zone has a direct influence on the rate of recurrence of treated tumours (Glaiberman et al, 2005). Increasing the size of the ablation zone allows a margin of normal tissue to be ablated adjacent to the tumour (Liu et al, 2010c) thus decreasing the risk of recurrence. However, recent literature describes differing "safe" margins of ablation of HCC and colorectal metastases (Liu et al, 2010c). Each ablation technique discussed in Chapter 1 has been modified or manipulated in order to increase the size of the ablation zone. Some of the techniques described in Chapter 1 have proved successful, specifically:

(1) Electrode design; Expandable electrodes by LeVeen (LeVeen, 1997, Rossi et al, 1998) and the internally cooled electrode, the Cool-Tip Needle (Covidien plc, Dublin, Irl) has become commonplace in current practice.

(2) Adjuvant chemotherapy in the form of direct injection or TACE (Ahmed and Goldberg, 2004, Goldberg et al 2004, Goldberg et al, 2002) which shows promising results in both animal tumour models and in small clinical cohorts of patients.

Very little research has been conducted on the RF generator compared to the published literature on needle modification techniques. Work has been conducted on the use of pulsed RFA (Goldberg et al, 1999, Goldberg and Gazelle, 2001) and the use of multi-polar RFA combining the switching generator technique (Weisbrod et al, 2007, Brace et al, 2009). However, these techniques require multiple needles and thus an increase in the morbidity risk. BETA is the first technique, which modifies the RF generator in order to achieve larger ablation zones (Cockburn et al, 2007). The combination of DC and AC influences the bio-heat equation discussed in Chapter 1, allowing longer times for ablation and subsequently larger ablation zones.

The competing therapies discussed in Chapter 1 include thermal ablation (MW ablation and laser ablation), cryoablation and chemical ablation (Acetic Acid, Ethanol and Chemotherapy). RFA has been shown to be a superior method of ablation compared to all of these competing therapies specifically:

(1) Ethanol ablation has been discussed in detail in Chapter 1 regarding its complication profile and effectiveness. Until 2005 this technique was probably the most widely used treatment for inoperable HCC (Dodd et al, 2000, Barnett and Curley, 2002). A number of RCTs have shown RFA to be superior to ethanol ablation for the treatment of hepatic tumours (Marlow et al, 2006), this may be due to the relatively poor efficacy of ethanol ablation for metastatic tumours and the relative increase in the incidence of hepatic metastatic disease this decade (Cancer Research UK, 2009).

Ethanol ablation carries a similar complication profile (Livraghi et al, 1998) but a higher re-intervention rate when compared to RFA (Livraghi et al, 1999, Dodd et al, 2000), however its use an as adjunct to RFA has been evaluated (Goldberg et al, 2000) in the laboratory setting with promising results.

(2) Microwave ablation was discussed in detail in Chapter 1, including risks associated with treatment and developing techniques. RFA has been shown to have a superior efficacy profile to MW ablation following results of randomised control trials (RCTs)(Marlow et al, 2006). A debate continues as to the ideal microwave frequency required in order to generate the largest ablation zones (Sun et al, 2009), which, together with the size of the antenna and the heating generated in the antenna cord have left MW ablation with a number of unanswered questions. MW ablation has been shown to be free of effects caused by “heat-sink” discussed in Chapter 1 (Wright et al, 2005), which may prove beneficial.

(3) Laser Ablation has shown promising results for the treatment of hepatic tumours (Vogl et al, 2008), however there is little data comparing laser ablation to RFA (Marlow et al, 2006).

(4) The lack of RCT data comparing RFA to cryoablation does not detract from published data comparing these techniques in non-randomised patients, however some of the data series are small (Marlow et al, 2006). Cryoablation however has demonstrated a favourable safety profile in treating smaller tumours such as renal cell carcinoma (RCC) (Dominguez-Escrig et al, 2008). The long-term outcome of treating patients with small renal tumours has yet to be evaluated and the natural history of these tumours is not yet completely understood (Dominguez-Escrig et al, 2008). The reported data for cryoablation is relatively small compared to RFA for the treatment of renal tumours, however cryoablation is increasing for the treatment of RCC (Brown, 2005) in a select group of patients.

Published data historically has favoured surgical resection superior to RFA (Abdalla et al, 2004, Stang et al, 2009); this is accepted as the treatment of choice for colorectal liver metastases and HCC- making the primary role for ablation limited to those patients who are unfit for curative surgery (Kudo, 2010, Liu et al, 2010a).

Recently, however RFA has shown similar mortality outcomes to surgical resection for small (<3cm) hepatocellular tumours (Huang et al, 2010, Hung et al, 2010) and colorectal liver metastases (CRLM) (Otto et al, 2010). Favourable outcomes following RFA for multiple colorectal liver metastases (≤ 3.5cm) have been shown with a 5-year survival of 33%.

Future Work.

Resection.

The lack of quality randomised control trials comparing RFA to resection and to competing therapies indicates a necessity for large multi-centre trials comparing these techniques. The historical published data however does demonstrate resection to be superior to RFA (Abdalla et al, 2004, Marlow et al, 2006, Stang et al, 2009) and this is accepted as the treatment of choice for colorectal liver metastases and HCC.

Recently, retrospective studies have shown comparable 5-year survival in patients following resection of RFA for HCCs less than 3cm (Huang et al, 2010). Huang et al demonstrated similar survivals at 5 years in patients with tumours less than 3cm, however for tumours >3 ≤5cm, surgical resection remained the treatment of choice. Recent meta-analyses (Liu et al, 2010a, Liu et al, 2010b, Zhou et al, 2010) have confirmed this, however have made note of the higher recurrence rate following RFA. Importantly, RFA carries significantly lower peri-procedural morbidity compared to surgical resection. Zhou et al highlighted the lack of good evidence in the literature to date, comparing RFA and surgical resection. Hung et al (Hung et al, 2010) showed comparable survival in patients with tumours ≤ 5cm, however a higher recurrence rate following RFA. Peng et al (Peng et al, 2010) demonstrated favourable outcomes in patients with HCCs ≤5cm treated with RFA as first line treatment. The literature demonstrates a lack of well-constructed randomised control trials, assessing these treatments in potentially curable patients.

Microwave Ablation.

The size of the antenna currently marketed for percutaneous use may be too large for use in the lung, due to the increased risk of pneumothorax (Simon et al, 2005), a further limitation is the lack of *in vivo* data comparing ablative techniques in the lung (Dupuy, 2009). Randomised control trials comparing RFA and MW ablation are needed in order to evaluate the use of MW ablation for hepatic tumours (Carrafiello et al, 2008).

Recent pre-clinical experiments have demonstrated MWA to have promising potential for thermal treatment of tumours (Yu et al, 2010), however to date there are no clinical studies supporting this.

Cryoablation.

Further research into the benefit of treating small renal tumour is needed in order to determine the risk-benefit profile of this treatment. The complication profile of cryoablation appears to preclude it from treating large hepatic tumours, however. Recent literature suggests (Brown, 2005) that it is of benefit in the kidney. An RCT comparing cryoablation to RFA in renal tumours would provide important data. The risks associated with cryotherapy, including cryoshock, however limit the clinical application of this modality (Jansen et al, 2010, Sandomirsky et al, 2010).

Adjuvant Chemotherapy.

The benefits of adjuvant chemotherapy are well described in laboratory animals, but less so in a clinical context. The favourable data from animal studies suggest this combination therapy to be of benefit in patients with HCC (Ahmed et al, 2003). Newer therapies using a heat sensitive polymer (Celsion Corporation, 2010) show great promise, and Phase III trials are currently underway evaluating this new product.

Chapter 2

Ex vivo studies for optimisation of ablation parameters.

Conclusions.

Chapter 2 describes the *ex vivo* studies carried out in order to determine the parameters, which would produce the largest ablation zone. Previous work conducted into BETA utilised (Cockburn et al, 2007, Dobbins et al, 2008, Dobbins et al, 2008a, Dobbins et al, 2008b) a commercially available RFA generator and a DC transformer to perform the ablations. A Mark II machine specifically designed for this research was manufactured with no impedance feedback algorithm. An ablation matrix was designed (Appendix 1) and ablations performed at a variety of RF and DC settings (n=6) initially.

Following the results an RF setting of 600mA using 9V of DC were used to determine the combination which would produce the largest ablation zone without prolonging the time of ablation significantly. The results demonstrated this parameter to produce the largest ablation zone. Initially it was thought that pretreatment with DC alone prior to a DC and RF combination would produce larger ablation zones (Cockburn et al, 2007). The research described in this thesis did not reproduce the results by Cockburn et al, as it did not demonstrate a statistical difference between the ablation zones obtained with BETA and no pre-treatment compared to BETA with 300 and 600 seconds of pre-RF DC.

Future Work.

The time taken to produce BETA lesions is longer than for standard RFA, however this may be in part due to the larger ablation zones. Time for ablation remains a factor for radiologists when deciding on an ablation technique (Malczyk and Sutherland, 2009). However this does not translate into a change of practice given the faster ablation times achieved with MW ablation (Simon et al, 2005). The effect of electroosmosis may allow for smaller ablation zones of a given size to be achieved in a shorter time frame when compared to standard RFA. This possibility fell beyond the scope of this thesis but future studies may show a significant improvement in ablation times using BETA for smaller tumours.

Chapter 3

Hydration Studies.

Conclusions.

Chapter 3 describes the results of hydration studies comparing BETA zones to standard RFA zones. Electroosmosis, described in 1809 by Reuss (Reuss, 1809) and detailed in laboratory experiments by Nordenstrom (Nordenstrom, 1983) is the theoretical basis for the results achieved with BETA (Chapter 2). The net movement of water from the anode to the cathode increases the hydration in the liver, thus allowing for longer ablation times by decreasing the charring of tissue at the needle. The hydration experiments conducted provide proof of electroosmosis during BETA with statistically significant differences in the hydration of liver following ablation using BETA and standard RFA, specifically:

(1) The degree of hydration increases as the duration of the direct current application increases when compared to the control radiofrequency ablation hydration percentage.

(2) There is no significant difference in the degree of hydration in liver treated with simultaneous DC and RFA, 300 seconds of pre DC or 600 seconds of pre DC.

(3) The increase in hydration due to electroosmosis decreases the charring of tissue at the cathode and hence adherence of tissue to the electrode, with resultant larger ablation zones.

Future Work.

A principal aim of this research was to examine the theory of electroosmosis induced by BETA, causing a larger ablation zone by increasing the degree of hydration at the needle tip, minimising the negative effects of desiccation on ablation zone size. The process of electroosmosis is described in detail by Nordenstrom (Nordenstrom, 1983) through a series of experiments whereby four types of electroosmosis were described. The hydration changes occurring with BETA are due to type II electroosmosis. This increased hydration in the tissue allows the RF energy to be distributed for longer in the tissue, by decreasing the degree of charring at the needle tip. This allows for increased ablation zones without changing the needle design or RF parameters. The experiments conducted described in this thesis have shown a significant difference in tissue hydration post ablation as described in chapter 3. While this does not determine cause and effect, it allows a reasonable conclusion to be made: the anti-desiccating effect of direct current is associated with larger ablation zones caused by RF ablation.

Planned future work is based on a phenomenon associated with improved hydration at the needle tip – namely less tissue adherence associated with a ‘slippier’ needle. This will be examined *ex vivo* initially. The clinical importance of this finding lies in the potential to reduce the ‘seeding’ of live tumour cells along the needle track, using BETA.

Chapter 4

Temperature Distribution Studies.

Conclusions.

Chapter 4 describes the results of temperature analysis at fixed distances from the electrode (5, 10, 15 and 20mm). The results of the analysis are described and demonstrated. The results described in Chapter 4 compare favourably with the literature. The effects of temperature on cellular function during RFA are well described in the literature (Goldberg et al, 1996a, Goldberg et al, 1996b, Goldberg et al, 2000, Dupuy and Goldberg, 2001, Nahum Goldberg and Dupuy, 2001, Mertyna et al, 2008). The effects of BETA on tissue temperature are described in Chapter 4, specifically:

(1) BETA reaches cytocidal temperatures in ablated tissue faster than control RFA. 4-6 minutes has been quoted as the minimum time needed at this temperature to induce cell death (Goldberg et al, 1996a, Goldberg et al, 1996b, Goldberg et al, 2000), however temperatures at the margin of the ablation zone remain above the minimum temperature required for necrosis for longer than standard RFA.

(2) The mean temperatures at 5mm, 10mm, 15mm and 20mm are significantly higher following BETA compared to standard RFA.

(3) Tissue remains above cyitocidal temperatures up to 20mm from the active electrode for longer than standard RFA due to the longer time needed to produce a BETA lesion. This larger cytocidal zone may prove beneficial for thermosensitive chemotherapeutic agents (Celsion Corporation, 2010), increasing the area of necrosis beyond the ablation zone. The cells exposed to hyperthermic temperatures may be sensitised to adjuvant chemotherapeutic agents, which in turn decrease blood supply to the affected liver (Padhani, 2009).

(4) BETA produces a similar mean end-temperature profile to multipolar (Lee et al, 2006) and bipolar techniques (Lee et al, 2004a), but with decreased potential morbidity given the single electrode needed. The higher temperatures obtained with BETA may be due to the longer ablation times and the favourable heat distribution through the tissue due to decreased charring of tissue adjacent to the electrode.

Future Work.

The results of this research provide important data regarding temperature distribution in the tissue during BETA. Thermosensitive adjuvant chemotherapeutic agents show promise in increasing the ablation zone following thermal therapy (Celsion Corporation, 2010).

The temperature distribution of BETA shows favourable results, with potential cytocidal effects at 2cm from a single electrode.

Further work has been conducted into adjuvant therapies to complement RFA, namely radiation therapy (Horkan et al, 2005). The study evaluated external-beam radiotherapy and RFA with promising results, however significant advances have been made in the filed of radio-embolisation (Lewandowski et al, 2007, Bilbao et al, 2010) using Yttrium-90 microspheres. The results of external beam radiotherapy by Horkan et al (Horkan et al, 2005) were promising, however RFA with adjunct targeted endovascular radiation treatment remains an exciting prospect. There have been no papers in the literature to date describing this technique, however the results of hyperthermia in tissue using BETA may prove to be a catalyst in the development of Yttrium-90 embolisation and RFA as a treatment for inoperable HCC or a bridging procedure to transplant.

The treatment of HCC or colorectal liver metastases by percutaneous methods relies on imaging following the ablation in order to determine the likelihood of recurrence, depending on the zone of ablation. It is often difficult to be sure of the exact dimensions of the ablation zone post ablation as the enhancement of the tumour changes due to the application of heat to the tissue. Follow-up is characteristically performed from 1 month onwards depending on the operator preference (Liu et al, 2010b). The use of temperature monitoring during RFA may provide the operator with information on temperature distribution during the treatment, allowing changes to be made to electrode position (Chung et al, 1999, Keserci et al, 2006, Vigen et al, 2006). This real-time feedback may allow for more accurate localisation of the ablation zone (Breen et al, 2004) thus allowing for change in position of the electrode during open MRI ablation procedures (Steiner et al, 1997, Steiner et al, 1998). Vigen et al (Vigen et al, 2006) demonstrated successful *in vivo* temperature monitoring during RF ablation. The temperature maps generated were consistent with the dimensions of the RF ablation probe however some asymmetry occurred, which was likely due to ventilation. The research however demonstrated the feasibility of temperature monitoring during RFA. Terraz et al (Terraz et al, 2009) described the use of temperature monitoring in 16 malignant nodules in the liver, with results comparable to Vigen et al (Vigen et al, 2006). The use of MRI temperature monitoring requires further investigation in order to determine the potential clinical benefits.

Phase III trials into the efficacy of a thermally controlled release of Doxorubicin (Celsion Corporation, 2010) are being conducted at present. The favourable temperature distribution profile of BETA as demonstrated in Chapter 4 suggests BETA to have a wider thermal distribution in tissue compared to RFA alone. This may benefit a thermally controlled Doxorubicin based release platform, the ‘red zone’ of ablation, where cells are exposed to hyperthermic temperatures, but not sufficient temperatures to induce cell necrosis will then be exposed to an endovascular dose of chemotherapy, thus increasing the ablation zone.

Work into this hypothesis is required, in order to determine the extent of necrosis, which could potentially be created using a combination of BETA and Thermodox (Celsion Corporation,

2010). The potential of cell necrosis, using the temperature data obtained in chapter 4, would be significantly larger than using BETA alone. The temperature at 2cm from the electrode was in excess of 55 °C, which would equate to a greater than 4cm ablation diameter.
This however is a hypothesis and the effects would need to be correlated with both macroscopic and microscopic pathological findings.

Chapter 5 and 6

In Vivo Porcine studies

Conclusions.

Chapter 5 describes the results of *in vivo* comparison of BETA and conventional RFA.

In this study 10 White Hybrid pigs were used in order to evaluate the ablation created by BETA compared to conventional RFA.

For this study, each animal was treated with four conventional RFA cycles and four BETA cycles during a laparotomy conducted under general anaesthesia.

The immediate and intermediate term effects were evaluated, with interval termination at terminal anaesthesia, 2 days, 2 weeks, 1 month and 2 months post procedure.

Each of the termination intervals were used to evaluate the size of the BETA zone compared to the conventional RFA zones and to evaluate the effect of BETA on the tissue response at both gross pathological level and histological level.

The results obtained compare favourably with the results from earlier BETA studies (Cockburn et al, 2007, Dobbins et al, 2008, Dobbins et al, 2008a, Dobbins et al, 2008b) and with the published literature comparing the *ex vivo* and *in vivo* results (Cha et al, 2009).

The results by Cha et al demonstrated a 34% reduction in the size of the ablation zone in *in vivo* tissue compared to *ex vivo* tissue. These results demonstrate a 12% reduction in the maximum mean ablation zone size in *in vivo* liver compared to *ex vivo* liver. The reasons for the size reduction are in part due to the heat sink effect in liver and the use of a 2mm diameter needle in *in vivo* testing compared to a 2.5mm needle in *ex vivo* testing (Patterson et al, 1998, Goldberg et al, 1995).

The lengths of the BETA treatments were longer than the conventional RFA treatments (Chapter 2), which can be explained by the production of a larger ablation zone, however this contradicts the findings of Patterson et al (Patterson et al, 1998). However this research demonstrates a relationship between lesion diameter and ablation zone size. This is beyond the scope of the research, but the lack of an impedance feedback algorithm may in part explain the reason for this finding.

The intermediate term morbidity data (14, 28 and 56 days) did not reveal an abnormal inflammatory response, with comparable macroscopic and microscopic findings when comparing BETA to conventional RFA.

The results of the *in vivo* study are similar to those described by Dobbins et al (Dobbins et al, 2008a), the macroscopic appearance of the ablation zones at each time point decreased. However, there remained a significant difference in size in each treatment group when comparing BETA and conventional RFA.

The Acute Phase Proteins and biochemical profiles demonstrate similar trends to the published literature. Teague et al (Teague et al, 2004) reported significantly elevated CRP levels post procedure, peaking at 24 hours and remaining raised at 72 hours, the TNF- α levels showed a similar trend.

The use of porcine specific APPs for this study, together with the CRP has not been described in the medical literature, but extensively in the veterinary literature (Alava et al, 1997, Eckersall et al, 1999, Eckersall, 2000, Pepys and Hirschfield, 2003, Eckersall, 2004, Pineiro et al, 2009).

SAA peaked at 24 hours, p-MAP at 48 hours and CRP at 72 hours, Haptoglobin peaked at 48-72 hours, however all returned to normal levels at termination.

The biochemical markers for liver function remained stable apart from the transaminase enzymes, which were significantly elevated post procedure, peaking at 24-48 hours, but returning to normal at termination. Similar observations were described by Wemyss-Holden et al (Wemyss-Holden et al, 2000), where transaminase increased post treatment, but the bilirubin and γ-GT did not. The theory for this is due to the volume of tissue ablated, in combination with the effects of the anaesthetic agents administered for the procedure (Chen et al, 2000, Ture et al, 2009).

The renal function remained stable throughout the study, with no adverse biochemical events, similar to the safety profile described by Kinn et al (Kinn et al, 1991).

Future Work:

1) The promising results obtained from the *in vivo* study demonstrate BETA to be a safe and predictable ablation technique, with similar biochemical and clinical effects to conventional RFA and electrolysis.

In man studies need to be conducted in order to replicate the data obtained from the animal data. The animal and *ex vivo* data however do have a limitation in that only healthy tissue was ablated. BETA has not been tested in tumour tissue (Cockburn et al, 2007, Dobbins et al, 2008, Dobbins et al, 2008a, Dobbins et al, 2008b).

In order for BETA to progress, however, its efficacy must be tested in human subjects and in tumour tissue. For research to continue to this stage, a mark III machine must be designed, which meets with industry standard for human use. A safety circuit must be incorporated into the machine, to prevent voltage or current surges being transmitted to the patient and the limitations described in chapter 5 must be addressed.

The initial impedance encountered in liver on commencement of an ablation cycle must be compensated for in order to decrease the risk of early roll-off of the ablation cycle.

Research and Ethics approval for the first-in-man BETA study will be sought in order to determine the efficacy of BETA in liver tumours.
The research will be conducted at the Norfolk and Norwich University Hospital under the direction of Mr SA Wemyss-Holden and Dr. JF Cockburn. Patients will, after informed consent be treated with BETA prior to completion of a hemi-hepatectomy for a curable liver tumour. BETA will not be administered as a definitive treatment, but rather as an adjunct for research purposes prior to resection, however the ablation will take place at the time of the resection as an open procedure. The purpose of this study will be to determine the efficacy of BETA in tumour tissue and to determine the effects of BETA at a microscopic level. Acute phase reactants will be measured and the overall safety and outcome will be monitored.

2) The effects of BETA and adjunctive therapies has promising potential, given the temperature distribution profile of BETA in tissue (chapter 4).
New technologies such as temperature-controlled doxorubicin chemotherapeutic endovascular agents (Celsion Corporation, 2010) have the potential to significantly increase the ablation zone of BETA with the higher tissue temperature distribution of BETA compared to conventional RFA.

3) BETA has been shown to produce significantly larger ablation zones than conventional RFA using a smaller gauge needle (unpublished data), which may have a place in lung ablation (Lee et al, 2004). The smaller gauge needle may decrease the potential for complications such as pneumothorax and pulmonary haemorrhage compared to the 14G needle used currently. BETA has never been tested in pulmonary tissue where the effects of electroosmosis are unknown. The potential, however for BETA to produce an ablation zone similar in diameter to conventional RFA with a 14G needle is encouraging, given that that BETA produces comparable ablation zone diameters using a 19G needle (unpublished data).

This however is theoretical and requires both *ex vivo* and *in vivo* studies in order to determine the efficacy of BETA in pulmonary tissue.

BETA produces larger ablation zones than conventional RFA, with a similar systemic response encountered in porcine subjects, to the published literature for both RFA and electrolysis.
It has the potential to significantly impact on the current management of liver tumours and may, in certain instances provide a curative option in cases where conventional RFA or any ablation technique was limited by the size of the tumour.
It is for this reason that in-man studies are essential for this technology to progress.

ABBREVIATIONS:

AC	Alternating Current
ALP	Alkaline Phosphatase
ALT	Alanine Transaminase
APP	Acute Phase Proteins
AST	Aspartartate Transaminase
CI	Confidence Interval
CRP	C Reactive Protein
CT	Computer Tomography
BETA	Bimodal Electric Tissue Ablation
CLRM	Colorectal metastases
DC	Direct Current
ESWL	Extra Corporeal Shockwave Lithotripsy
GGT	Gamma Glutamyl Transpeptidase
HCC	Hepatocellular Carcinoma
HIFU	High-Intensity Focused Ultrasound
HLS	Huntingdon Life Sciences
Hp	Haptoglobin
IL	Interleukin
INR	International Normalised Ratio
IRE	Irreversible Electroporation
IVC	Inferior Vena Cava
K	Potassium

LITT	Laser Interstitial Thermotherapy
mH	milliHenry (unit of inductance)
MRI	Magnetic Resonance Imaging
ms	milliseconds
MWA	Microwave Ablation
Na	Sodium
pMAP	pig-Major Acute Phase Protein
PT	pre treatment
PV	Portal vein
RF	Radiofrequency
RFA	Radiofrequency Ablation
SAA	Serum Amyloid A
SD	Standard Deviation
SEM	Standard Error of the Mean
TAE	Transarterial Embolisation
TACE	Transarterial Chemoembolisation
TIVA	Total Intravenous Anaesthetic
TNF-α	Tumour Necrosis Factor-alpha
TUNEL	Terminal deoxynucleotidyl transferase (TdT)-mediated dUTP Nick End-Labeling
US	Ultrasound

RF (mA)	min (cm)	p25 (cm)	p50 (cm)	p75 (cm)	max (cm)	mean (cm)	SD
500	**1.1**	**1.5**	**1.5**	**1.7**	**1.8**	**1.55**	**0.17**
600	**1.2**	**1.4**	**1.5**	**1.5**	**1.6**	**1.45**	**0.09**
650	**1.3**	**1.3**	**1.4**	**1.5**	**1.6**	**1.43**	**0.12**
750	**0.8**	**1.2**	**1.2**	**1.3**	**1.4**	**1.14**	**0.19**
1000	**0.9**	**1**	**1**	**1.1**	**1.2**	**1.05**	**0.07**

Table 2.1 control sample size calculations together with the minimum, maximum and means for each radiofrequency energy value measured. The interquartile ranges and standard deviations are also shown.

RF (mA)	min (cm)	p25 (cm)	p50 (cm)	p75 (cm)	max (cm)	mean (cm)	SD
500	**1.2**	**2.25**	**2.4**	**2.6**	**3.5**	**2.38**	**0.33**
600	**2.1**	**2.3**	**2.4**	**2.7**	**2.9**	**2.48**	**0.22**
650	**2.2**	**2.3**	**2.4**	**2.6**	**3.3**	**2.43**	**0.23**
750	**1.1**	**1.8**	**2**	**2.2**	**2.5**	**1.96**	**0.32**
1000	**1**	**1.3**	**1.4**	**1.8**	**2.1**	**1.5**	**0.32**

Table 2.2 experimental sample size calculations together with the minimum, maximum and means for each radiofrequency energy value measured. The interquartile ranges and standard deviations are also shown.

DC-Pre (s)	DC (V)	RF (mA)	Size (cm)	Run-off (s)	Mean (cm)	SD	95% CI
0	0	400	1.2	688	1.2	0.07	0.01
0	0	400	1.3	785			
0	0	400	1.2	584			
0	0	400	1.2	687			
0	0	400	1.1	689			
0	0	450	1.2	587	1.24	0.0554	0.05
0	0	450	1.2	667			
0	0	450	1.3	654			
0	0	450	1.2	701			
0	0	450	1.3	599			
0	0	500	1.5	639	1.57	0.166	0.07
0	0	500	1.7	547			
0	0	500	1.6	609			
0	0	500	1.5	499			
0	0	500	1.7	565			
0	0	500	1.1	392			
0	0	500	1.7	696			
0	0	500	1.5	501			
0	0	500	1.7	579			
0	0	500	1.5	503			
0	0	500	1.4	460			
0	0	500	1.5	489			
0	0	500	1.4	467			
0	0	500	1.7	540			
0	0	500	1.8	602			
0	0	500	1.5	676			
0	0	500	1.5	600			
0	0	500	1.8	807			
0	0	500	1.6	758			
0	0	500	1.7	776			

Table 2.3 Matrix of tested parameters.

DC-Pre (s)	DC (V)	RF (mA)	Size (cm)	Run-off (s)	Mean (cm)	SD	95% CI
0	0	600	1.6	635			
0	0	600	1.5	361			
0	0	600	1.4	328			
0	0	600	1.5	419			
0	0	600	1.2	276			
0	0	600	1.4	349			
0	0	600	1.5	401			
0	0	600	1.4	359			
0	0	600	1.5	388			
0	0	600	1.4	374			
0	0	600	1.5	482			
0	0	600	1.5	425			
0	0	600	1.4	202			
0	0	600	1.4	282			
0	0	600	1.6	511			
0	0	600	1.5	328			
0	0	600	1.4	263			
0	0	600	1.4	281			
0	0	600	1.6	518			
0	0	600	1.5	468	1.58	0.1662	0.04
0	0	600	1.5	435			
0	0	600	1.4	301			
0	0	600	1.5	446			
0	0	600	1.5	389			
0	0	600	1.8	401			
0	0	600	1.7	581			
0	0	600	1.6	550			
0	0	600	1.6	559			
0	0	600	1.8	651			
0	0	600	1.7	601			
0	0	600	1.7	476			
0	0	600	1.8	359			
0	0	600	1.7	337			
0	0	600	1.7	377			
0	0	600	1.6	366			
0	0	600	1.6	301			
0	0	600	1.4	278			
0	0	600	1.6	244			
0	0	600	1.6	458			

Table 2.3 Matrix of tested parameters

DC-Pre (s)	DC (V)	RF (mA)	Size (cm)	Run-off (s)	Mean (cm)	SD	95% CI
0	0	600	1.5	247	1.58	0.1662	0.04
0	0	600	1.5	457			
0	0	600	1.7	508			
0	0	600	1.8	554			
0	0	600	1.8	486			
0	0	600	1.6	231			
0	0	600	1.9	480			
0	0	600	1.4	262			
0	0	600	2	485			
0	0	600	1.8	387			
0	0	600	1.7	326			
0	0	600	1.5	307			
0	0	600	1.8	391			
0	0	600	1.5	327			
0	0	600	1.7	337			
0	0	600	1.5	257			
0	0	600	1.8	458			
0	0	600	1.6	318			
0	0	600	1.5	435			
0	0	600	1.6	355			
0	0	600	1.4	312			
0	0	600	2.1	718			
0	0	600	1.9	465			
0	0	600	2	527			
0	0	600	1.4	321			
0	0	600	1.6	397			
0	0	600	1.6	463			
0	0	600	1.6	479			
0	0	600	1.8	863			
0	0	600	1.7	688			
0	0	600	1.9	896			
0	0	600	1.6	627			
0	0	600	1.5	593			
0	0	600	1.6	807			
0	0	600	1.4	541			
0	0	600	1.4	502			
0	0	600	1.5	654			
0	0	600	1.5	528			
0	0	600	1.6	508			
0	0	600	1.6	446			

Table 2.3 Matrix of tested parameters

DC-Pre (s)	DC (V)	RF (mA)	Size (cm)	Run-off (s)	Mean (cm)	SD	95% CI
0	0	600	1.5	518	1.58	0.662	0.04
0	0	600	1.5	400			
0	0	600	1.5	398			
0	0	600	1.4	362			
0	0	600	1.5	533			
0	0	600	1.5	403			

DC-Pre (s)	DC (V)	RF (mA)	Size (cm)	Run-off (s)	Mean (cm)	SD	95% CI
0	0	650	1.5	286	1.41	0.115	0.05
0	0	650	1.6	321			
0	0	650	1.5	311			
0	0	650	1.4	239			
0	0	650	1.3	231			
0	0	650	1.6	320			
0	0	650	1.5	266			
0	0	650	1.4	238			
0	0	650	1.4	248			
0	0	650	1.3	245			
0	0	650	1.3	287			
0	0	650	1.4	300			
0	0	650	1.6	321			
0	0	650	1.3	297			
0	0	650	1.3	300			
0	0	650	1.5	473			
0	0	650	1.3	376			
0	0	650	1.3	381			

Table 2.3 Matrix of tested parameters

DC-Pre (s)	DC (V)	RF (mA)	Size (cm)	Run-off (s)	Mean (cm)	SD	95% CI
0	0	750	1.1	131			
0	0	750	0.9	101			
0	0	750	0.9	117			
0	0	750	1	113			
0	0	750	0.8	101			
0	0	750	0.9	98			
0	0	750	1.3	134			
0	0	750	1.3	126			
0	0	750	1.4	237	1.16	0.1998	0.09
0	0	750	1.2	104			
0	0	750	1.3	98			
0	0	750	1.2	94			
0	0	750	1.2	96			
0	0	750	1.3	167			
0	0	750	1.2	110			
0	0	750	1.3	206			
0	0	750	1.5	215			

DC-Pre (s)	DC (V)	RF (mA)	Size (cm)	Run-off (s)	Mean (cm)	SD	95% CI
0	0	1000	1.1	85			
0	0	1000	1	101			
0	0	1000	0.9	78			
0	0	1000	1.1	106			
0	0	1000	1.2	112			
0	0	1000	1	88			
0	0	1000	1	78			
0	0	1000	1.1	97			
0	0	1000	1	88	1.05	0.073	0.04
0	0	1000	1.1	91			
0	0	1000	1	78			
0	0	1000	1.1	56			
0	0	1000	1	47			
0	0	1000	1.1	123			
0	0	1000	1	56			
0	0	1000	1.1	101			

Table 2.3 Matrix of tested parameters

DC-Pre (s)	DC (V)	RF (mA)	Size (cm)	Run-off (s)	Mean (cm)	SD	95% CI
0	3	500	1.4	535	1.333	0.121	0.1
0	3	500	1.5	529			
0	3	500	1.4	619			
0	3	500	1.2	343			
0	3	500	1.2	368			
0	3	500	1.3	401			
0	3	750	1.3	98	1.2	0.075	0.06
0	3	750	1.2	88			
0	3	750	1.2	75			
0	3	750	1.1	78			
0	3	750	1.2	80			
0	3	750	1.1	75			
0	3	1000	1	56	1.025	0.052	0.04
0	3	1000	1	45			
0	3	1000	1.1	78			
0	3	1000	1	65			
0	3	1000	1	69			
0	3	1000	1.1	71			
0	9	500	2.6	1458	2.69	0.262	0.13
0	9	500	2.6	2000			
0	9	500	2.7	2192			
0	9	500	2.6	2093			
0	9	500	2.6	1509			
0	9	500	2.7	2193			
0	9	500	2.6	1239			
0	9	500	2.6	1588			
0	9	500	2.7	1889			
0	9	500	2.5	1567			
0	9	500	2.6	2001			
0	9	500	2.6	2049			
0	9	500	2.7	1249			
0	9	500	3.6	2915			
0	9	500	2.5	1201			

Table 2.3 Matrix of tested parameters

DC-Pre (s)	DC (V)	RF (mA)	Size (cm)	Run-off (s)	Mean (cm)	SD	95% CI
0	**9**	**550**	**3.3**	**1087**	**2.65**	**0.264**	**0.15**
0	**9**	**550**	**2.7**	**806**			
0	**9**	**550**	**2.8**	**897**			
0	**9**	**550**	**2.4**	**527**			
0	**9**	**550**	**2.5**	**675**			
0	**9**	**550**	**2.9**	**829**			
0	**9**	**550**	**2.5**	**629**			
0	**9**	**550**	**2.3**	**599**			
0	**9**	**550**	**2.7**	**883**			
0	**9**	**550**	**2.5**	**818**			
0	**9**	**550**	**2.6**	**845**			
0	**9**	**550**	**2.7**	**890**			

Table 2.3 Matrix of tested parameters

DC-Pre (s)	DC (V)	RF (mA)	Size (cm)	Run-off (s)	Mean (cm)	SD	95% CI
0	9	600	3	1179	2.83	0.4212	0.09
0	9	600	2.5	989			
0	9	600	2	537			
0	9	600	2	469			
0	9	600	2	383			
0	9	600	2	297			
0	9	600	2.5	459			
0	9	600	2.3	651			
0	9	600	2.8	891			
0	9	600	3	1020			
0	9	600	2.5	758			
0	9	600	2.9	951			
0	9	600	2.5	778			
0	9	600	2.5	925			
0	9	600	2	582			
0	9	600	2.5	777			
0	9	600	2.5	758			
0	9	600	2.7	1097			
0	9	600	2.6	836			
0	9	600	2.6	803			
0	9	600	2.7	823			
0	9	600	2.8	895			
0	9	600	2.6	617			
0	9	600	2.9	569			
0	9	600	3	668			
0	9	600	3	826			
0	9	600	3	759			
0	9	600	2.9	671			
0	9	600	3	872			
0	9	600	2.4	535			
0	9	600	2.7	589			
0	9	600	2.5	611			
0	9	600	3	1079			
0	9	600	2.5	586			
0	9	600	2.8	972			
0	9	600	2.7	860			
0	9	600	3.4	1128			
0	9	600	3	1544			
0	9	600	3	879			
0	9	600	2.7	585			

Table 2.3 Matrix of tested parameters

DC-Pre (s)	DC (V)	RF (mA)	Size (cm)	Run-off (s)	Mean (cm)	SD	95% CI
0	9	600	3.3	1772			
0	9	600	3.6	1936			
0	9	600	3	678			
0	9	600	2.9	955			
0	9	600	2.8	781			
0	9	600	2.5	488			
0	9	600	3	797			
0	9	600	2.8	796			
0	9	600	2.5	664			
0	9	600	3.6	2261			
0	9	600	2.7	693			
0	9	600	2.7	750			
0	9	600	2.4	601			
0	9	600	3.6	3007			
0	9	600	2.6	616			
0	9	600	4.4	2812			
0	9	600	2.8	781			
0	9	600	3.3	962			
0	9	600	3.1	988			
0	9	600	2.7	715			
0	9	600	2.8	788			
0	9	600	3.4	797	2.83	0.4212	0.09
0	9	600	3.1	802			
0	9	600	2.5	589			
0	9	600	3.2	708			
0	9	600	2.6	589			
0	9	600	3	970			
0	9	600	2.9	992			
0	9	600	2.6	772			
0	9	600	3.5	1518			
0	9	600	3.1	977			
0	9	600	2.9	797			
0	9	600	3.6	1011			
0	9	600	3.3	1101			
0	9	600	3.5	1106			
0	9	600	2.8	761			
0	9	600	3.6	1096			
0	9	600	2.6	752			
0	9	600	2.6	4.7			
0	9	600	2.8	893			
0	9	600	3	917			
0	9	600	2.9	892			

Table 2.3 Matrix of tested parameters

DC-Pre (s)	DC (V)	RF (mA)	Size (cm)	Run-off (s)	Mean (cm)	SD	95% CI
0	9	750	1.8	364			
0	9	750	2.2	369			
0	9	750	2	358			
0	9	750	2	371			
0	9	750	1.8	350			
0	9	750	1.8	370			
0	9	750	3	426	2.26	0.46	0.25
0	9	750	2.2	398			
0	9	750	3	431			
0	9	750	2.1	261			
0	9	750	3	425			
0	9	750	2.5	514			
0	9	750	2.5	543			
0	9	1000	1	132			
0	9	1000	1	109			
0	9	1000	1.3	110	1.13	0.121	0.1
0	9	1000	1.2	98			
0	9	1000	1.2	105			
0	9	1000	1.1	99			
0	18	500	2.5	1352			
0	18	500	2.6	1188			
0	18	500	2.4	1005	2.37	0.186	0.15
0	18	500	2.4	875			
0	18	500	2.1	565			
0	18	500	2.2	368			
0	18	750	2.2	197			
0	18	750	2.3	201			
0	18	750	2.2	176	2.15	0.122	0.1
0	18	750	2	184			
0	18	750	2.2	200			
0	18	750	2	193			
0	18	1000	1.2	50			
0	18	1000	1	47			
0	18	1000	1	57	1.07	0.082	0.07
0	18	1000	1.1	77			
0	18	1000	1	60			
0	18	1000	1.1	88			

Table 2.3 Matrix of tested parameters

DC-Pre (s)	DC (V)	RF (mA)	Size (cm)	Run-off (s)	Mean (cm)	SD	95% CI
0	36	500	2	729	2.08	0.075	0.06
0	36	500	2	735			
0	36	500	2.1	439			
0	36	500	2.2	754			
0	36	500	2.1	457			
0	36	500	2.1	512			
0	36	750	2	180	1.9	0.098	0.08
0	36	750	2	169			
0	36	750	1.8	149			
0	36	750	1.8	175			
0	36	750	1.9	145			
0	36	750	1.8	167			
0	36	1000	1.4	105	1.5	0.098	0.8
0	36	1000	1.6	128			
0	36	1000	1.6	132			
0	36	1000	1.4	109			
0	36	1000	1.5	128			
0	36	1000	1.4	115			
300	3	500	2.6	1544	2.5	0.179	0.14
300	3	500	2.2	2343			
300	3	500	2.6	2500			
300	3	500	2.7	2375			
300	3	500	2.4	2301			
300	3	500	2.5	2332			
300	3	750	1.8	138	1.9	0.133	0.11
300	3	750	2	550			
300	3	750	2	546			
300	3	750	1.7	581			
300	3	750	1.8	286			
300	3	750	2	505			
300	3	1000	1.4	95	1.27	0.082	0.7
300	3	1000	1.2	135			
300	3	1000	1.2	89			
300	3	1000	1.3	90			
300	3	1000	1.2	138			
300	3	1000	1.3	140			

Table 2.3 Matrix of tested parameters

DC-Pre (s)	DC (V)	RF (mA)	Size (cm)	Run-off (s)	Mean (cm)	SD	95% CI
300	**9**	**500**	**2.1**	**535**			
300	**9**	**500**	**1.8**	**568**			
300	**9**	**500**	**2.5**	**1022**			
300	**9**	**500**	**1.9**	**544**			
300	**9**	**500**	**2.4**	**1101**			
300	**9**	**500**	**2.1**	**698**			
300	**9**	**500**	**2.3**	**874**			
300	**9**	**500**	**2.6**	**1321**	**2.32**	**0.268**	**0.14**
300	**9**	**500**	**2.3**	**1109**			
300	**9**	**500**	**2.4**	**1087**			
300	**9**	**500**	**2.1**	**889**			
300	**9**	**500**	**2.6**	**1219**			
300	**9**	**500**	**2.7**	**1512**			
300	**9**	**500**	**2.5**	**1206**			
300	**9**	**500**	**2.5**	**1363**			

Table 2.3 Matrix of tested parameters

DC-Pre (s)	DC (V)	RF (mA)	Size (cm)	Run-off (s)	Mean (cm)	SD	95% CI
300	9	600	2.5	768			
300	9	600	2.1	432			
300	9	600	2.4	724			
300	9	600	2.3	585			
300	9	600	2.4	756			
300	9	600	2.9	907			
300	9	600	2.5	871			
300	9	600	2.9	871			
300	9	600	2.2	608			
300	9	600	2.5	726			
300	9	600	2.5	789			
300	9	600	2.7	889			
300	9	600	2.7	876			
300	9	600	2.6	803			
300	9	600	2.7	875			
300	9	600	2.5	593	2.55	0.269	0.09
300	9	600	2.2	451			
300	9	600	3	651			
300	9	600	2.5	529			
300	9	600	2.3	617			
300	9	600	2.6	689			
300	9	600	2.6	694			
300	9	600	2.5	546			
300	9	600	2.5	600			
300	9	600	2.7	675			
300	9	600	3	998			
300	9	600	3.3	790			
300	9	600	2.5	662			
300	9	600	2.9	570			
300	9	600	2.8	801			
300	9	600	2.9	820			

Table 2.3 Matrix of tested parameters

DC-Pre (s)	DC (V)	RF (mA)	Size (cm)	Run-off (s)	Mean (cm)	SD	95% CI
300	9	750	1.6	98	1.96	0.353	0.2
300	9	750	1.7	117			
300	9	750	1.8	121			
300	9	750	2.1	132			
300	9	750	1.8	88			
300	9	750	1.7	112			
300	9	750	1.8	128			
300	9	750	1.6	121			
300	9	750	1.9	149			
300	9	750	2.5	471			
300	9	750	2.5	482			
300	9	750	2.5	608			
300	9	1000	1.6	223	1.67	0.076	0.06
300	9	1000	1.8	50			
300	9	1000	1.6	140			
300	9	1000	1.7	156			
300	9	1000	1.6	137			
300	9	1000	1.7	159			
300	9	1000	1.7	161			
300	18	500	2.5	789	2.3	0.103	0.08
300	18	500	2.4	701			
300	18	500	2.3	698			
300	18	500	2.3	676			
300	18	500	2.2	640			
300	18	500	2.3	680			
300	18	750	1.4	98	1.35	0.105	0.08
300	18	750	1.5	136			
300	18	750	1.3	129			
300	18	750	1.2	143			
300	18	750	1.3	138			
300	18	750	1.4	128			
300	18	1000	1.2	88	1.27	0.05	0.04
300	18	1000	1.3	76			
300	18	1000	1.3	64			
300	18	1000	1.3	98			
300	18	1000	1.2	77			
300	18	1000	1.3	89			

Table 2.3 Matrix of tested parameters

DC-Pre (s)	DC (V)	RF (mA)	Size (cm)	Run-off (s)	Mean (cm)	SD	95% CI
300	36	500	2	696	2.25	0.164	0.13
300	36	500	2.3	783			
300	36	500	2.2	598			
300	36	500	2.5	697			
300	36	500	2.2	609			
300	36	500	2.3	703			
300	36	750	2.1	276	1.75	0.25	0.2
300	36	750	1.7	301			
300	36	750	1.4	289			
300	36	750	1.8	268			
300	36	750	1.6	265			
300	36	750	1.5	226			
300	36	1000	1.5	143	1.3	0.133	0.2
300	36	1000	1.3	187			
300	36	1000	1.3	157			
300	36	1000	1.1	196			
300	36	1000	1.2	201			
300	36	1000	1.3	189			
600	3	500	2.4	1348	2.55	0.235	0.19
600	3	500	3	2012			
600	3	500	2.4	2077			
600	3	500	2.6	1876			
600	3	500	2.4	1321			
600	3	500	2.5	1804			
600	3	750	1.8	200	1.75	0.055	0.04
600	3	750	1.8	188			
600	3	750	1.7	150			
600	3	750	1.7	165			
600	3	750	1.8	191			
600	3	750	1.7	162			
600	3	1000	1	50	1.05	0.055	0.04
600	3	1000	1.1	58			
600	3	1000	1	54			
600	3	1000	1.1	61			
600	3	1000	1	63			
600	3	1000	1.1	70			

Table 2.3 Matrix of tested parameters

DC-Pre (s)	DC (V)	RF (mA)	Size (cm)	Run-off (s)	Mean (cm)	SD	95% CI
600	**9**	**500**	**2.4**	**700**			
600	**9**	**500**	**2.7**	**1090**			
600	**9**	**500**	**2.5**	**1056**			
600	**9**	**500**	**2.5**	**1093**			
600	**9**	**500**	**2.7**	**1211**			
600	**9**	**500**	**3.1**	**1398**			
600	**9**	**500**	**3.5**	**2409**			
600	**9**	**500**	**2.4**	**970**	**2.75**	**0.302**	**0.15**
600	**9**	**500**	**3.1**	**1812**			
600	**9**	**500**	**2.7**	**1987**			
600	**9**	**500**	**2.7**	**1954**			
600	**9**	**500**	**2.8**	**1652**			
600	**9**	**500**	**2.5**	**1016**			
600	**9**	**500**	**2.9**	**2012**			
600	**9**	**500**	**2.7**	**1987**			

Table 2.3 Matrix of tested parameters

DC-Pre (s)	DC (V)	RF (mA)	Size (cm)	Run-off (s)	Mean (cm)	SD	95% CI
600	9	600	2.8	789			
600	9	600	2.4	594			
600	9	600	2.5	511			
600	9	600	2.9	788			
600	9	600	2.7	589			
600	9	600	2.7	781			
600	9	600	2.6	657			
600	9	600	2.7	826			
600	9	600	2.7	611			
600	9	600	2.8	665			
600	9	600	2.7	534			
600	9	600	2.7	667			
600	9	600	2.8	689			
600	9	600	2.7	711			
600	9	600	2.8	694			
600	9	600	2.6	939	2.73	0.157	0.06
600	9	600	2.7	559			
600	9	600	2.7	800			
600	9	600	2.5	540			
600	9	600	3	611			
600	9	600	3	1036			
600	9	600	2.6	764			
600	9	600	3	703			
600	9	600	3	927			
600	9	600	2.7	673			
600	9	600	2.7	617			
600	9	600	2.7	623			
600	9	600	2.8	654			
600	9	600	3	698			
600	9	600	2.9	701			

Table 2.3 Matrix of tested parameters

DC-Pre (s)	DC (V)	RF (mA)	Size (cm)	Run-off (s)	Mean (cm)	SD	95% CI
600	9	650	3.3	505	2.57	0.247	0.12
600	9	650	2.2	467			
600	9	650	2.4	589			
600	9	650	2.7	489			
600	9	650	2.4	646			
600	9	650	2.4	397			
600	9	650	2.7	490			
600	9	650	2.6	472			
600	9	650	2.8	501			
600	9	650	2.4	399			
600	9	650	2.6	418			
600	9	650	2.6	437			
600	9	650	2.5	502			
600	9	650	2.4	401			
600	9	650	2.6	456			
600	9	650	2.5	666			
600	9	750	2	200	2.1	0.183	0.15
600	9	750	1.9	189			
600	9	750	2.4	207			
600	9	750	2	196			
600	9	750	2.2	201			
600	9	750	2.2	200			
600	9	1000	1.8	62	1.5	0.197	0.16
600	9	1000	1.3	44			
600	9	1000	1.3	48			
600	9	1000	1.5	59			
600	9	1000	1.3	52			
600	9	1000	1.4	60			
600	18	500	2.5	1098	2.4	0.19	0.12
600	18	500	2.4	554			
600	18	500	2.4	576			
600	18	500	2.3	497			
600	18	500	2.5	548			
600	18	500	2.4	835			
600	18	500	2.2	516			
600	18	500	2.5	1019			
600	18	500	2.7	838			
600	18	500	2	536			

Table 2.3 Matrix of tested parameters

DC-Pre (s)	DC (V)	RF (mA)	Size (cm)	Run-off (s)	Mean (cm)	SD	95% CI
600	18	600	2.2	425	2.33	0.107	0.05
600	18	600	2.4	515			
600	18	600	2.2	489			
600	18	600	2.3	478			
600	18	600	2.2	489			
600	18	600	2.4	519			
600	18	600	2.5	554			
600	18	600	2.2	407			
600	18	600	2.5	583			
600	18	600	2.2	401			
600	18	600	2.3	438			
600	18	600	2.3	459			
600	18	600	2.4	501			
600	18	600	2.3	427			
600	18	600	2.3	532			
600	18	600	2.3	401			
600	18	600	2.5	901			
600	18	600	2.4	528			
600	18	650	2.2	387	2.3	0.08	0.04
600	18	650	2.4	378			
600	18	650	2.2	275			
600	18	650	2.3	362			
600	18	650	2.4	493			
600	18	650	2.2	289			
600	18	650	2.3	371			
600	18	650	2.4	367			
600	18	650	2.3	563			
600	18	650	2.2	354			
600	18	650	2.3	389			
600	18	650	2.3	328			
600	18	650	2.4	601			
600	18	650	2.3	538			
600	18	650	2.2	512			
600	18	750	2.4	227	2.275	0.122	0.1
600	18	750	2.4	110			
600	18	750	2.2	161			
600	18	750	2.1	198			
600	18	750	2.2	221			
600	18	750	2.2	219			

Table 2.3 Matrix of tested parameters

DC-Pre (s)	DC (V)	RF (mA)	Size (cm)	Run-off (s)	Mean (cm)	SD	95% CI
600	18	1000	1.5	98	1.35	0.105	0.08
600	18	1000	1.2	86			
600	18	1000	1.3	101			
600	18	1000	1.4	88			
600	18	1000	1.3	89			
600	18	1000	1.4	93			
600	36	500	2.4	954	2.36	0.05	0.04
600	36	500	2.3	525			
600	36	500	2.4	798			
600	36	500	2.3	898			
600	36	500	2.4	967			
600	36	500	2.4	994			
600	36	750	2	308	2.1	0.109	0.09
600	36	750	2.2	276			
600	36	750	2	367			
600	36	750	2.2	267			
600	36	750	2.2	301			
600	36	1000	1.7	185	1.55	0.187	0.15
600	36	1000	1.3	121			
600	36	1000	1.4	115			
600	36	1000	1.8	187			
600	36	1000	1.6	137			
600	36	1000	1.5	123			
900	3	500	2.4	1010	2.375	0.098	0.08
900	3	500	2.3	988			
900	3	500	2.5	1210			
900	3	500	2.3	1023			
900	3	500	2.3	1029			
900	3	500	2.5	1226			
900	3	750	1.9	344	2.025	0.126	0.1
900	3	750	2.1	566			
900	3	750	2.2	500			
900	3	750	1.9	387			
900	3	750	2	499			
900	3	750	1.9	476			

Table 2.3 Matrix of tested parameters

DC-Pre (s)	DC (V)	RF (mA)	Size (cm)	Run-off (s)	Mean (cm)	SD	95% CI
900	3	1000	1.4	88	1.325	0.018	0.01
900	3	1000	1.2	108			
900	3	1000	1.4	118			
900	3	1000	1.3	97			
900	3	1000	1.4	126			
900	3	1000	1.3	99			
900	9	500	2.1	1350	2.45	0.204	0.16
900	9	500	2.5	1109			
900	9	500	2.7	1345			
900	9	500	2.5	1258			
900	9	500	2.6	1301			
900	9	500	2.5	1278			
900	9	750	2.2	501	2.2	0.147	0.12
900	9	750	2	368			
900	9	750	2.3	398			
900	9	750	2.3	458			
900	9	750	2	401			
900	9	750	2.3	539			
				)			
900	9	1000	1.4	260	1.65	0.213	0.17
900	9	1000	2	251			
900	9	1000	1.7	219			
900	9	1000	1.5	247			
900	9	1000	1.5	259			
900	9	1000	1.6	276			
900	18	500	2.4	1174	2.45	0.147	0.12
900	18	500	2.4	1169			
900	18	500	2.3	1181			
900	18	500	2.7	1261			
900	18	500	2.3	1193			
900	18	500	2.4	1221			
900	18	750	2.4	401	2.275	0.103	0.08
900	18	750	2.3	376			
900	18	750	2.1	298			
900	18	750	2.3	456			
900	18	750	2.2	301			
900	18	750	2.3	436			

Table 2.3 Matrix of tested parameters

DC-Pre (s)	DC (V)	RF (mA)	Size (cm)	Run-off (s)	Mean (cm)	SD	95% CI
900	18	1000	1.9	187	1.95	0.05	0.4
900	18	1000	2	173			
900	18	1000	2	166			
900	18	1000	1.9	165			
900	18	1000	2	171			
900	18	1000	1.9	156			
900	36	500	2.4	606	2.275	0.117	0.09
900	36	500	2.4	616			
900	36	500	2.1	587			
900	36	500	2.2	678			
900	36	500	2.3	626			
900	36	500	2.3	619			
900	36	750	2	486	2.175	0.103	0.08
900	36	750	2.3	356			
900	36	750	2.2	198			
900	36	750	2.2	397			
900	36	750	2.2	201			
900	36	750	2.1	188			
900	36	1000	2	400	1.875	0.018	0.01
900	36	1000	1.8	340			
900	36	1000	1.8	298			
900	36	1000	1.9	308			
900	36	1000	1.8	287			
900	36	1000	1.9	301			
1800	3	500	2.3	889	2.275	0.015	0.01
1800	3	500	2.3	978			
1800	3	500	2.2	859			
1800	3	500	2.3	937			
1800	3	500	2.2	847			
1800	3	500	2.3	926			
1800	3	750	2.1	243	2.2	0.075	0.06
1800	3	750	2.2	189			
1800	3	750	2.3	201			
1800	3	750	2.2	223			
1800	3	750	2.3	199			
1800	3	750	2.2	181			

Table 2.3 Matrix of tested parameters

DC-Pre (s)	DC (V)	RF (mA)	Size (cm)	Run-off (s)	Mean (cm)	SD	95% CI
1800	3	1000	1.9	136	1.9	0.075	0.06
1800	3	1000	2	101			
1800	3	1000	1.9	127			
1800	3	1000	1.8	176			
1800	3	1000	1.8	171			
1800	3	1000	1.9	191			
1800	9	500	2.7	1210	2.575	0.103	0.08
1800	9	500	2.4	1361			
1800	9	500	2.6	1288			
1800	9	500	2.6	1274			
1800	9	500	2.5	1288			
1800	9	500	2.6	1301			
1800	9	750	2.5	657	2.43	0.075	0.06
1800	9	750	2.5	588			
1800	9	750	2.4	598			
1800	9	750	2.3	607			
1800	9	750	2.4	601			
1800	9	750	2.4	623			
1800	9	1000	2	188	2.025	0.04	0.03
1800	9	1000	2	229			
1800	9	1000	2	246			
1800	9	1000	2.1	215			
1800	9	1000	2	230			
1800	9	1000	2	238			
1800	18	500	2.3	1354	2.425	0.08	0.06
1800	18	500	2.5	1544			
1800	18	500	2.4	1267			
1800	18	500	2.5	1301			
1800	18	500	2.4	1276			
1800	18	500	2.5	1301			

Table 2.3 Matrix of tested parameters

DC-Pre (s)	DC (V)	RF (mA)	Size (cm)	Run-off (s)	Mean (cm)	SD	95% CI
1800	18	750	2.1	327	1.975	0.103	0.08
1800	18	750	2	527			
1800	18	750	1.8	516			
1800	18	750	2	489			
1800	18	750	1.9	501			
1800	18	750	2	523			
1800	18	1000	1.8	92	1.75	0.104	0.08
1800	18	1000	1.7	100			
1800	18	1000	1.6	89			
1800	18	1000	1.9	109			
1800	18	1000	1.7	101			
1800	18	1000	1.8	110			
1800	36	500	N/A				
1800	36	500	N/A				
1800	36	500	N/A				
1800	36	750	N/A				
1800	36	750	N/A				
1800	36	750	N/A				
1800	36	1000	N/A				
1800	36	1000	N/A				
1800	36	1000	N/A				

Table 2.3 Matrix of tested parameters

No.	Parameter	% D	% R	g	% M	Mean %
1	600mA Control RFA	51.228	63.32	0.421	48.772	46.904
2		55.22	66.07	0.72	44.783	
3		57.62	73.53	0.606	42.384	
4		56.19	55.77	0.656	43.813	
5		54.964	12.2047	0.4885	43.035	
6		53.9748	92.8881	0.601	46.0252	
7		52.2587	95.0888	0.6414	47.7413	
8		51.9834	92.3692	0.3748	48.0166	
9		55.8459	69.9352	0.5405	44.1541	
10		50.5886	73.6456	0.3138	49.4114	
11		53.0274	70.2947	0.5587	46.9726	
12		51.1212	95.6136	0.2371	48.8788	
13		46.6941	11.4159	0.7267	53.3059	
14		52.7188	25.9826	0.6534	47.2812	
15		51.0018	18.2391	0.9182	48.9982	

Table 3.2

No.	Parameter	% D	% R	g	% M	Mean %
1	600mA - 9v - No pre RF DC	50.368	12.04	0.467	50.362	51.67
2		45.534	18.217	0.5042	54.646	
3		59.5647	67.8847	0.2846	40.435	
4		50.1186	99.5268	0.6974	49.8814	
5		48.9551	11.7751	0.7816	51.0449	
6		45.9263	11.774	0.8461	54.0737	
7		53.2803	87.6867	0.3748	48.0166	
8		49.6634	14.3519	0.4575	50.366	
9		49.0024	20.0028	0.9176	50.9976	
10		44.2094	14.2663	0.4566	55.7906	
11		42.2524	14.3519	0.4142	57.7476	
12		44.3421	12.0545	0.385	52.6579	
13		43.4278	15.3628	0.565	56.5722	
14		48.1139	22.1181	0.6862	51.8861	
15		49.4739	22.1816	0.9684	50.5261	

Table 3.3

No.	Parameter	% D	% R	g	% M	Mean %
1	300.0.9 - 600mA	50.067	99.73	0.4505	49.932	51.631
2		49.11	20.71	0.7913	50.892	
3		45.82	26.71	0.7112	54.183	
4		43.646	15.8759	1.0897	56.354	
5		48.335	11.1878	0.6143	51.665	
6		51.6145	76.6332	1.3669	48.3855	
7		53.3903	80.5368	0.5215	46.6097	
8		53.4745	87.0049	0.5833	46.5255	
9		45.0124	79.8998	0.8976	54.9876	
10		42.9902	75.2912	0.7936	57.0098	
11		47.9631	18.9843	0.8326	52.0369	
12		49.0072	16.7172	0.6917	50.9928	
13		47.9521	77.8987	0.4332	52.453	
14		52.8745	12.6765	0.5992	44.3434	
15		50.4543	81.9982	0.5412	51.3216	

Table 3.4

No.	Parameter	% D	% R	g	% M	Mean %
1	600.0.9 - 600mA	50.78	11.839	0.5084	50.214	52.34
2		51.8066	93.025	0.1993	48.193	
3		45.605	14.035	0.3767	54.394	
4		43.61	18.232	0.4584	56.39	
5		52.2767	91.287	0.7761	47.723	
6		48.0062	14.3865	0.4855	51.993	
7		44.4107	14.1483	0.9411	55.589	
8		47.0493	14.9692	0.6989	52.9507	
9		46.2716	13.6565	0.6301	53.7284	
10		47.6223	12.0984	0.7577	52.3777	
11		48.3326	12.0164	0.7827	51.6674	
12		47.1388	18.0936	0.9921	52.8612	
13		48.8675	14.912	0.4098	55.9876	
14		52.5434	13.2123	0.5567	47.5645	
15		47.9843	14.8978	0.6098	52.3387	

Table 3.5

No.	Parameter	% D	% R	g	% M	Mean %
1	Normal Liver	22.0079	13.805	0.8042	77.9921	72.193
2		27.292	26.6407	1.1467	72.708	
3		30.8018	20.4861	1.2013	69.1982	
4		24.4311	23.5672	0.9876	75.5689	
5		31.9834	17.1415	0.5559	68.1561	
6		27.5846	26.252	2.1113	72.4154	
7		28.9025	15.3874	1.0192	71.0975	
8		26.0124	20.1098	0.9987	73.9876	
9		30.5773	21.6683	0.7804	69.4227	
10		30.7806	17.948	0.4508	69.2194	
11		29.1395	22.135	0.9103	70.8605	
12		27.2645	26.6777	0.72	72.7355	
13		27.6608	26.1522	0.8566	72.3392	
14		25.8103	28.7442	1.169	74.1897	
15		26.9977	25.9976	0.7993	73.0023	

Table 3.6

% M percentage weight loss
displays change of mass registered during drying process in percents

% D part of dry mass received in drying process in percents.
part of sample which remained on the pan after humid evaporation is the result

% R humid / dry mass ratio received in drying process in percents
part of sample which vaporized during drying process is the result,

g mass change
mass of change registered during drying process is the result.

Table 3.7

Temperature Base Data Experiments 1 & 2 (˚c)																	
	Control				BETA					Control				BETA			
	1				1					2				2			
Time (sec)	5	10	15	20	5	10	15	20		5	10	15	20	5	10	15	20
0	23.2	15.7	23.2	16.9	17.8	26.5	18.7	21.8		18.6	20.8	14.4	20.5	20.0	27.7	19.4	23.6
30	24.6	15.8	24.3	16.9	17.9	49.9	18.8	22.8		27.8	21.4	15.1	20.7	28.2	34.8	22.9	25.9
60	24.3	15.9	24.6	17.0	28.8	55.6	20.3	23.1		35.4	26.0	16.0	21.4	38.7	37.6	27.6	27.5
90	14.1	16.1	16.3	17.0	53.1	60.2	25.7	23.6		41.5	31.0	17.0	22.1	48.3	42.1	32.5	29.3
120	13.8	16.5	14.5	17.2	63.3	64.7	32.3	24.0		46.0	36.3	18.2	22.9	55.5	47.4	36.7	32.9
150	13.9	19.4	14.6	18.1	68.1	68.3	38.3	24.6		50.0	42.4	19.4	23.8	61.1	51.2	40.7	36.0
180	16.3	22.9	15.6	19.0	72.0	71.0	43.5	25.4		53.9	46.9	20.7	24.7	65.2	53.9	44.4	38.1
210	19.8	26.1	16.8	19.9	76.1	73.5	48.0	25.4		57.8	50.9	22.0	25.7	68.3	54.7	47.5	39.2
240	23.6	28.9	18.0	20.9	77.4	75.4	51.5	27.0		62.1	55.8	23.3	26.7	70.7	55.3	50.2	39.7
270	27.0	31.3	19.4	21.9	77.7	78.1	54.1	29.0		65.8	60.5	24.6	27.8	72.8	56.0	52.7	40.6
300	38.2	33.5	25.4	23.0	77.9	79.9	56.4	30.9		69.8	61.6	25.9	28.9	74.5	58.5	54.9	42.9
330	40.7	35.6	27.0	24.1	78.8	81.2	58.4	41.4		73.3	63.3	27.1	30.0	76.3	61.0	56.9	43.4
360	45.1	37.6	28.6	25.1	76.6	81.6	60.0	45.0		76.4	65.3	28.4	31.1	78.0	63.7	58.8	44.5
390	50.6	39.5	30.2	26.2	75.6	82.5	61.3	47.1		78.7	66.9	29.6	32.3	79.6	64.9	60.6	45.0
420	55.2	41.3	31.9	27.3	75.6	83.3	62.5	48.8		80.9	68.6	30.7	33.4	81.0	66.7	62.2	46.7
450	59.5	43.0	33.3	28.4	75.9	84.3	63.6	50.2		83.5	70.4	31.7	34.5	82.3	68.7	63.7	47.3
480	65.4	44.6	36.8	29.5	76.5	85.2	64.7	51.5		84.6	72.4	33.9	35.5	83.5	69.8	65.1	48.4
510	68.0	46.3	38.5	30.6	77.0	85.7	65.7	52.7		85.7	74.6	35.8	36.4	84.6	72.9	66.4	49.6
540	72.5	47.9	40.4	31.6	77.4	85.9	66.7	53.8		86.4	76.8	41.7	37.7	85.7	74.7	67.6	50.0
570	77.9	49.6	42.6	32.9	77.9	86.8	67.7	54.7		87.6	78.3	42.5	39.4	86.9	75.8	68.8	51.5
600	81.9	51.7	44.7	35.3	78.1	87.0	68.6	55.7						87.8	76.8	69.9	52.7
630	83.7	52.2	44.9	36.6	78.5	86.7	69.4	56.6						88.6	78.6	71.0	53.5
660	85.8	53.6	45.4	36.9	78.9	87.5	70.1	57.4						89.3	80.2	71.9	54.7
690	88.4	58.5	45.9	37.5	81.4	87.4	71.2	58.3						89.8	82.9	72.8	55.9
720	90.3	60.3	46.1	38.6	83.5	87.4	72.5	59.1						90.3	83.6	73.7	56.7
750	92.7	62.4	46.5	40.0	85.1	87.8	73.7	59.9						90.9	84.7	74.5	58.1
780					86.0	88.3	74.8	60.6						91.4	85.6	75.5	59.7
810					86.7	88.8	75.8	61.2						92.1	87.8	76.5	60.4
840					87.4	89.3	76.8	61.8						92.9	88.3	77.1	61.3
870					88.1	89.7	77.8	62.3						92.7	88.9	78.0	62.5
900					89.0	90.0	78.7	62.9						93.4	90.2	81.2	63.0
930					89.8	90.1	79.6	62.9						94.5	90.3	82.3	63.1
960					90.3	87.6	80.0	59.7						95.1	87.0	82.9	59.9
990					91.2	89.5	80.6	60.4						96.4	87.8	83.7	55.3
1020					91.4	86.3	81.2	56.8						97.8	88.5	84.6	56.3
1050					91.8	86.7	81.8	57.5						98.6	89.2	85.7	57.2
1080					92.0	91.1	82.5	58.8						99.7	90.1	85.9	58.2
1110					92.2	91.5	83.0	59.2						101.0	90.9	86.1	58.5
1140					92.3	91.9	83.5	59.7						102.6	91.7	86.4	59.1

Table 4.1 Temperatures at each distance from the electrode at each 30 second time interval for the control (600mA RF) and the BETA (9V DC and 600mA) experiments at 5, 10, 15 and 20mm from the electrode.

Temperature Base Data Experiments 3 & 4 (˚c)																	
No.	**Control**				**BETA**					**Control**				**BETA**			
Time (sec)	**3**				**3**					**4**				**4**			
0	**5**	**10**	**15**	**20**	**5**	**10**	**15**	**20**		**5**	**10**	**15**	**20**	**5**	**10**	**15**	**20**
30	**24.0**	**22.3**	**17.6**	**22.5**	**21.7**	**25.9**	**21.7**	**25.9**		**18.7**	**27.8**	**17.5**	**23.1**	**21.6**	**34.4**	**21.4**	**26.9**
60	**32.7**	**22.4**	**19.3**	**22.5**	**28.6**	**25.7**	**23.1**	**25.5**		**24.1**	**32.5**	**18.7**	**23.5**	**28.9**	**48.9**	**22.2**	**33.3**
90	**39.1**	**24.5**	**21.1**	**23.0**	**45.1**	**22.6**	**28.3**	**22.8**		**28.9**	**34.8**	**20.1**	**23.5**	**48.4**	**59.1**	**26.1**	**35.6**
120	**44.5**	**34.6**	**23.0**	**24.1**	**55.0**	**23.8**	**34.3**	**22.9**		**32.7**	**37.9**	**21.8**	**23.8**	**60.8**	**66.0**	**31.5**	**36.4**
150	**49.2**	**42.9**	**25.1**	**25.1**	**60.3**	**29.5**	**39.0**	**24.0**		**35.9**	**40.7**	**23.7**	**24.0**	**67.5**	**71.1**	**36.8**	**37.6**
180	**53.0**	**49.3**	**27.1**	**26.0**	**63.5**	**35.0**	**42.5**	**25.2**		**38.8**	**43.6**	**25.8**	**24.2**	**71.3**	**74.4**	**41.5**	**39.9**
210	**56.3**	**54.5**	**29.1**	**27.0**	**66.0**	**39.5**	**45.2**	**26.8**		**41.4**	**46.5**	**27.9**	**24.7**	**73.4**	**76.8**	**45.3**	**40.7**
240	**59.2**	**56.5**	**31.1**	**27.3**	**68.2**	**43.8**	**47.4**	**28.9**		**43.7**	**48.3**	**30.0**	**24.8**	**75.0**	**78.0**	**48.5**	**42.0**
270	**61.9**	**57.6**	**32.9**	**27.9**	**69.7**	**47.1**	**49.4**	**31.0**		**45.8**	**50.3**	**31.9**	**24.9**	**76.5**	**78.0**	**51.2**	**43.6**
300	**64.5**	**58.7**	**34.8**	**28.2**	**71.0**	**50.1**	**51.1**	**33.1**		**47.8**	**52.6**	**33.7**	**25.2**	**78.3**	**78.4**	**53.6**	**44.7**
330	**67.1**	**62.5**	**36.6**	**29.4**	**72.1**	**52.7**	**52.6**	**35.0**		**50.0**	**55.5**	**35.5**	**25.7**	**79.6**	**79.0**	**55.9**	**45.1**
360	**69.6**	**64.6**	**38.3**	**30.2**	**73.2**	**55.0**	**53.9**	**36.7**		**52.2**	**57.5**	**37.2**	**26.0**	**81.1**	**80.2**	**58.0**	**46.7**
390	**72.7**	**66.3**	**40.1**	**30.8**	**74.0**	**56.9**	**55.1**	**38.3**		**54.4**	**59.9**	**38.7**	**26.6**	**82.3**	**81.2**	**59.8**	**47.6**
420	**74.9**	**68.9**	**41.6**	**31.4**	**74.9**	**58.5**	**56.2**	**39.7**		**56.1**	**63.9**	**40.0**	**27.5**	**83.9**	**82.1**	**61.6**	**48.1**
450	**75.5**	**70.3**	**42.0**	**32.3**	**75.6**	**60.0**	**57.2**	**41.1**		**59.1**	**65.8**	**41.4**	**28.0**	**84.3**	**82.7**	**63.5**	**49.0**
480	**77.8**	**72.4**	**42.6**	**33.1**	**76.2**	**61.3**	**58.1**	**42.2**		**64.9**	**67.3**	**41.7**	**28.5**	**85.3**	**82.7**	**65.7**	**50.7**
510	**79.8**	**73.5**	**42.9**	**33.8**	**76.8**	**62.5**	**58.9**	**43.5**		**73.3**	**70.0**	**42.6**	**29.5**	**85.9**	**83.3**	**67.8**	**51.6**
540	**81.7**	**76.6**	**43.2**	**35.4**	**77.5**	**63.7**	**59.7**	**44.8**		**75.7**	**73.1**	**43.1**	**30.6**	**86.6**	**84.0**	**70.0**	**51.9**
570	**83.6**	**79.7**	**43.5**	**36.9**	**78.2**	**65.0**	**60.3**	**45.8**		**77.9**	**75.2**	**43.7**	**31.6**	**87.0**	**84.4**	**71.2**	**52.3**
600	**85.9**	**81.9**	**43.8**	**38.4**	**79.1**	**66.5**	**61.0**	**47.0**		**80.1**	**77.0**	**43.9**	**32.6**	**87.9**	**84.7**	**72.1**	**53.3**
630	**88.4**	**82.4**	**43.9**	**38.7**	**79.9**	**68.2**	**61.6**	**48.3**		**81.7**	**80.9**	**44.1**	**35.4**	**89.3**	**86.2**	**73.2**	**54.5**
660					**80.9**	**69.8**	**62.2**	**49.5**		**83.6**	**81.5**	**44.5**	**36.3**	**91.9**	**87.5**	**74.0**	**55.1**
690					**82.0**	**71.1**	**62.9**	**50.6**		**88.6**	**82.1**	**44.7**	**37.9**	**94.2**	**88.2**	**74.6**	**56.6**
720					**83.1**	**72.3**	**63.8**	**51.6**		**90.4**	**82.6**	**45.1**	**38.6**	**95.1**	**88.9**	**75.8**	**57.8**
750					**84.5**	**73.8**	**64.8**	**52.6**		**91.9**	**83.7**	**45.5**	**39.6**	**96.4**	**90.1**	**76.2**	**58.6**
780					**85.6**	**75.3**	**65.7**	**53.8**		**93.9**	**85.5**	**45.9**	**40.6**	**98.0**	**90.5**	**76.8**	**59.6**
810					**86.9**	**77.8**	**66.5**	**54.7**						**99.3**	**90.7**	**78.0**	**60.4**
840					**87.9**	**79.1**	**67.3**	**55.7**						**101.0**	**91.3**	**79.2**	**61.2**
870					**88.4**	**81.3**	**68.1**	**56.2**						**103.2**	**92.7**	**80.6**	**61.9**
900					**89.0**	**82.5**	**69.1**	**56.9**						**103.8**	**92.8**	**82.1**	**52.6**
930					**87.9**	**83.9**	**69.5**	**57.4**						**103.6**	**93.2**	**84.3**	**57.5**
960					**88.3**	**85.7**	**71.5**	**58.3**						**103.7**	**93.9**	**85.1**	**58.8**
990					**90.1**	**85.9**	**73.2**	**54.9**						**103.7**	**94.6**	**85.6**	**55.2**
1020					**91.5**	**80.6**	**74.3**	**55.8**						**103.7**	**95.7**	**85.7**	**60.0**
1050					**92.5**	**82.9**	**75.1**	**60.8**						**103.9**	**96.9**	**86.1**	**52.6**
1080					**94.6**	**83.7**	**76.3**	**61.2**						**104.2**	**97.5**	**86.2**	**53.8**
1110					**96.8**	**83.2**	**77.9**	**61.4**						**104.6**	**97.9**	**96.8**	**55.7**
1140					**97.9**	**86.9**	**79.4**	**58.4**						**105.8**	**98.3**	**86.9**	**57.2**
1170					**99.6**	**87.0**	**79.7**	**58.7**						**106.3**	**98.6**	**86.9**	**57.3**

Table 4.1 Temperatures at each distance from the electrode at each 30 second time interval for the control (600mA RF) and the BETA (9V DC and 600mA) experiments at 5, 10, 15 and 20mm from the electrode.

Temperature Base Data Experiments 5 & 6 (˚c)

No.	Control				BETA					Control				BETA			
Time (sec)	5				5					6				6			
0	5	10	15	20	5	10	15	20		5	10	15	20	5	10	15	20
30	19.3	20.4	20.0	18.6	21.7	18.3	21.7	16.4		19.7	21.6	22.3	19.4	24.9	22.3	22.1	20.6
60	22.5	22.8	22.3	18.6	28.6	23.7	23.1	17.7		25.8	25.4	23.5	19.8	39.8	31.2	27.2	22.0
90	28.6	23.0	22.7	19.7	45.1	29.7	28.3	19.0		30.1	31.7	24.7	20.0	49.8	42.0	36.4	23.6
120	33.4	24.5	23.1	29.9	55.0	35.6	34.3	20.5		35.4	37.4	25.6	20.4	53.6	48.9	42.1	24.7
150	38.7	31.2	24.0	20.0	60.3	40.5	39.0	22.1		47.6	42.5	26.6	21.3	55.9	53.3	45.5	25.1
180	40.3	37.9	24.9	20.1	63.5	44.2	42.5	23.7		54.9	46.8	27.6	22.3	57.2	56.2	52.1	25.6
210	45.8	43.2	25.9	21.3	66.0	47.2	45.2	25.4		60.0	50.3	28.7	23.3	50.3	58.7	52.8	26.8
240	50.9	48.0	26.9	22.2	68.2	49.9	47.4	27.1		64.0	53.1	29.8	24.3	63.2	60.2	53.5	27.8
270	54.1	52.3	28.0	23.6	69.7	52.3	49.4	28.8		67.4	55.9	31.0	25.3	65.9	61.5	54.2	28.0
300	57.8	56.4	29.3	24.4	71.0	54.3	51.1	30.4		70.4	58.7	32.2	26.4	67.5	62.5	54.8	30.5
330	63.0	59.3	30.6	26.7	72.1	56.4	52.6	31.9		73.2	61.3	33.4	27.5	70.5	63.3	55.3	32.8
360	67.3	61.8	31.9	29.0	73.2	58.3	53.9	33.4		75.7	63.5	34.6	28.5	73.9	64.3	55.8	35.1
390	71.0	64.4	33.4	31.1	74.0	60.1	55.1	34.7		78.0	65.8	35.8	29.6	75.6	65.3	56.3	36.8
420	74.2	66.0	34.4	33.1	74.9	61.7	56.2	35.9		80.2	67.5	36.3	30.6	77.6	65.9	57.9	37.4
450	77.0	68.9	35.6	35.1	75.6	63.0	57.2	37.1		82.1	69.4	36.9	31.6	78.8	66.6	58.5	38.6
480	79.6	71.3	35.9	37.0	76.2	64.4	58.1	38.2		83.7	71.3	37.4	32.6	79.6	67.3	58.9	39.8
510	82.2	73.6	38.6	38.9	76.8	65.6	58.9	39.2		85.3	72.6	38.2	33.5	80.6	68.0	59.2	41.4
540	84.9	76.8	41.3	39.2	77.5	66.7	59.7	40.1		86.6	75.9	38.7	34.5	81.5	68.6	59.6	42.2
570	87.8	79.2	41.5	39.6	78.2	67.7	60.3	41.1		88.0	78.3	39.1	35.5	82.4	69.2	59.9	43.6
600	88.6	80.2	41.6	39.9	79.1	68.9	61.0	42.0		89.5	79.7	39.6	36.4	83.5	69.8	60.3	44.9
630	89.7	81.7	42.1	40.1	79.9	70.1	61.6	43.0		91.0	80.1	40.0	37.4	84.7	70.2	61.1	46.0
660	90.8	82.6	42.5	40.3	80.9	70.8	62.2	43.9						85.3	70.7	61.9	47.3
690	91.6	82.8	42.8	40.4	82.0	71.9	62.9	44.7						86.3	71.2	62.6	49.6
720	92.4	84.9	43.2	40.7	83.1	72.8	63.8	45.3						87.3	71.5	63.2	52.3
750	93.6	85.9	43.9	40.9	84.5	74.0	64.8	46.0						87.6	71.0	63.7	55.3
780	94.8	86.8	44.3	41.0	85.6	75.1	65.7	46.6						89.9	71.2	64.1	59.9
810					86.9	78.3	66.5	47.6						89.5	71.4	64.5	64.1
840					87.9	81.4	67.3	48.9						89.9	71.6	64.8	66.4
870					88.4	82.7	68.1	51.4						84.7	71.8	65.3	55.3
900					89.0	85.1	69.1	56.8						89.9	71.8	65.7	55.4
930					87.9	86.7	69.5	56.3						90.9	72.3	66.1	53.7
960					88.4	87.9	70.8	56.6						91.6	74.3	66.7	54.0
990					90.1	81.1	71.9	59.3						85.3	75.4	67.7	58.6
1020					91.6	86.5	72.7	55.9						82.7	76.2	69.0	51.7
1050					93.5	84.6	72.5	57.1						92.0	76.8	70.1	56.1
1080					95.8	85.4	73.8	57.6						92.8	76.9	71.4	56.7
1110					97.9	86.7	74.9	56.9						93.7	77.0	73.9	56.9
1140					98.6	87.1	75.4	57.2						94.8	77.0	76.3	57.3
1170					99.4	87.2	76.0	57.5						96.8	77.4	77.3	57.9

Table 4.1 Temperatures at each distance from the electrode at each 30 second time interval for the control (600mA RF) and the BETA (9V DC and 600mA) experiments at 5, 10, 15 and 20mm from the electrode.

Temperature Base Data Experiments 7 & 8 (˚c)																	
No.	**Control**				**BETA**					**Control**				**BETA**			
Time (sec)	**7**				**7**					**8**				**8**			
0	**5**	**10**	**15**	**20**	**5**	**10**	**15**	**20**		**5**	**10**	**15**	**20**	**5**	**10**	**15**	**20**
30	**23.9**	**24.7**	**24.0**	**23.9**	**22.0**	**22.0**	**24.1**	**22.0**		**24.1**	**24.7**	**24.1**	**24.0**	**25.0**	**25.0**	**22.5**	**21.7**
60	**31.5**	**27.8**	**24.3**	**24.1**	**32.0**	**28.0**	**27.8**	**23.6**		**31.4**	**27.8**	**24.3**	**24.3**	**28.5**	**26.3**	**29.3**	**22.5**
90	**35.3**	**33.5**	**24.7**	**24.5**	**37.5**	**34.0**	**31.9**	**25.6**		**35.6**	**33.5**	**25.2**	**24.7**	**33.4**	**30.2**	**36.7**	**23.3**
120	**40.1**	**38.7**	**25.1**	**24.7**	**44.7**	**41.7**	**35.8**	**28.0**		**40.2**	**38.7**	**26.2**	**25.1**	**37.2**	**35.7**	**38.6**	**24.3**
150	**46.0**	**43.5**	**25.6**	**25.6**	**58.5**	**51.3**	**39.2**	**30.5**		**45.7**	**43.5**	**27.1**	**25.6**	**41.6**	**40.7**	**40.9**	**25.6**
180	**50.6**	**47.4**	**26.1**	**25.9**	**67.4**	**58.5**	**42.1**	**31.7**		**51.2**	**47.4**	**28.0**	**26.1**	**52.1**	**50.2**	**42.7**	**27.0**
210	**54.0**	**50.6**	**26.7**	**26.4**	**72.1**	**62.4**	**44.6**	**32.8**		**57.8**	**50.6**	**28.6**	**26.7**	**60.9**	**57.7**	**47.5**	**28.6**
240	**57.2**	**53.3**	**27.4**	**27.4**	**75.5**	**65.7**	**46.9**	**33.6**		**62.9**	**53.3**	**29.5**	**27.4**	**66.6**	**63.4**	**51.8**	**30.1**
270	**60.0**	**56.5**	**28.1**	**28.5**	**77.9**	**68.3**	**48.9**	**34.6**		**67.0**	**56.5**	**30.8**	**28.1**	**70.2**	**67.4**	**55.4**	**31.7**
300	**62.4**	**61.1**	**28.8**	**29.1**	**80.0**	**70.3**	**50.7**	**35.1**		**70.4**	**61.1**	**31.4**	**28.8**	**73.2**	**71.8**	**58.6**	**33.2**
330	**64.6**	**64.1**	**29.6**	**30.7**	**81.8**	**72.2**	**52.4**	**35.9**		**73.4**	**64.1**	**32.1**	**29.6**	**75.1**	**74.8**	**61.7**	**34.6**
360	**66.5**	**65.4**	**30.3**	**31.2**	**83.3**	**73.9**	**53.9**	**36.6**		**75.8**	**65.4**	**33.4**	**30.3**	**76.3**	**76.7**	**64.6**	**36.0**
390	**68.5**	**66.8**	**31.1**	**32.0**	**84.6**	**75.3**	**55.3**	**37.4**		**78.0**	**66.8**	**34.7**	**31.1**	**77.4**	**78.1**	**67.0**	**37.2**
420	**70.2**	**68.2**	**31.9**	**33.1**	**86.9**	**77.1**	**56.7**	**38.6**		**79.7**	**68.2**	**35.9**	**31.9**	**78.5**	**80.1**	**69.5**	**38.5**
450	**71.9**	**70.6**	**32.6**	**34.2**	**89.4**	**79.0**	**58.0**	**39.8**		**81.4**	**69.7**	**36.1**	**33.6**	**79.8**	**81.8**	**72.0**	**39.7**
480	**73.5**	**72.5**	**33.9**	**35.4**	**92.0**	**80.9**	**59.3**	**40.7**		**82.9**	**72.5**	**37.1**	**33.9**	**81.3**	**83.3**	**73.5**	**40.9**
510	**75.0**	**75.7**	**35.1**	**36.5**	**94.1**	**82.6**	**60.6**	**41.5**		**84.2**	**74.1**	**38.2**	**34.8**	**82.8**	**83.4**	**74.4**	**41.8**
540	**78.2**	**77.1**	**36.8**	**37.5**	**95.1**	**82.7**	**61.7**	**42.2**		**85.3**	**74.6**	**39.3**	**36.8**	**84.2**	**83.6**	**75.8**	**42.6**
570	**80.6**	**78.6**	**38.0**	**38.6**	**95.9**	**83.0**	**62.8**	**43.6**		**86.3**	**75.0**	**40.4**	**38.7**	**85.2**	**83.9**	**76.7**	**43.9**
600	**82.4**	**81.7**	**39.7**	**39.5**	**95.5**	**83.4**	**63.8**	**44.9**		**87.2**	**75.3**	**41.4**	**39.3**	**86.3**	**84.2**	**76.9**	**44.5**
630	**84.9**	**82.3**	**41.0**	**40.5**	**96.1**	**83.6**	**65.1**	**45.8**		**88.1**	**75.9**	**42.4**	**40.2**	**89.4**	**84.5**	**77.8**	**45.6**
660					**96.6**	**83.9**	**68.7**	**47.3**		**89.4**	**76.1**	**43.4**	**40.5**	**92.0**	**85.5**	**78.3**	**46.8**
690					**96.8**	**84.2**	**71.4**	**49.6**		**89.6**	**76.5**	**44.1**	**40.2**	**94.1**	**86.8**	**78.9**	**47.9**
720					**96.9**	**84.5**	**73.6**	**50.4**		**91.0**	**76.9**	**45.2**	**41.3**	**95.1**	**86.9**	**79.1**	**48.8**
750					**97.0**	**85.5**	**75.9**	**51.7**		**92.3**	**77.1**	**46.5**	**42.7**	**96.3**	**87.3**	**79.4**	**49.5**
780					**98.1**	**86.8**	**78.0**	**52.7**		**92.5**	**77.2**	**47**	**43.6**	**97.1**	**87.6**	**79.8**	**51.3**
810					**99.2**	**86.9**	**80.2**	**53.8**						**98.2**	**88.1**	**80.0**	**52.7**
840					**100.2**	**87.3**	**83.5**	**54.9**						**98.5**	**88.3**	**80.3**	**53.8**
870					**98.3**	**87.6**	**89.7**	**54.9**						**98.8**	**89.1**	**81.2**	**55.5**
900					**99.8**	**88.1**	**85.2**	**55.9**						**99.1**	**90.2**	**81.4**	**53.3**
930					**100.3**	**88.3**	**85.1**	**53.8**						**99.7**	**91.0**	**81.6**	**54.2**
960					**100.6**	**88.9**	**86.0**	**54.3**						**100.1**	**91.4**	**81.8**	**54.8**
990					**100.8**	**89.1**	**85.3**	**54.7**						**100.3**	**91.5**	**81.9**	**51.2**
1020					**100.8**	**89.3**	**84.0**	**56.7**						**100.4**	**91.8**	**82.0**	**55.0**
1050					**101.5**	**90.6**	**87.3**	**57.4**						**101.5**	**92.8**	**82.1**	**55.7**

Table 4.1 Temperatures at each distance from the electrode at each 30 second time interval for the control (600mA RF) and the BETA (9V DC and 600mA) experiments at 5, 10, 15 and 20mm from the electrode.

Temperature Base Data Experiments 9 & 10 (˚c)																	
No.	**Control**				**BETA**					**Control**				**BETA**			
Time (sec)	**9**				**9**					**10**				**10**			
0	**5**	**10**	**15**	**20**	**5**	**10**	**15**	**9.2**		**5**	**10**	**15**	**20**	**5**	**10**	**15**	**20**
30	**25.8**	**20.5**	**17.2**	**23.9**	**25.1**	**26.2**	**25.1**	**22.6**		**14.8**	**23.1**	**11.0**	**18.8**	**19.2**	**14.5**	**22.4**	**21.7**
60	**30.3**	**24.9**	**25.0**	**24.1**	**28.3**	**34.0**	**27.5**	**24.7**		**26.2**	**24.3**	**11.3**	**24.5**	**38.3**	**23.2**	**33.2**	**22.5**
90	**35.8**	**26.4**	**25.8**	**24.4**	**29.4**	**39.8**	**28.3**	**27.0**		**35.7**	**29.3**	**13.2**	**25.4**	**51.7**	**36.2**	**44.4**	**23.6**
120	**40.1**	**32.6**	**26.9**	**24.9**	**33.4**	**44.0**	**31.2**	**29.3**		**42.4**	**34.4**	**15.4**	**26.3**	**59.9**	**47.3**	**47.6**	**24.8**
150	**43.8**	**38.9**	**27.7**	**25.3**	**35.2**	**47.3**	**33.1**	**31.4**		**47.3**	**38.5**	**17.7**	**27.5**	**63.1**	**55.4**	**49.3**	**26.2**
180	**48.5**	**44.2**	**28.5**	**25.8**	**35.2**	**50.0**	**33.7**	**33.4**		**51.2**	**41.8**	**19.9**	**28.8**	**66.2**	**61.6**	**51.7**	**27.6**
210	**55.3**	**48.4**	**29.3**	**26.3**	**37.0**	**52.0**	**35.6**	**35.1**		**54.7**	**44.4**	**22.1**	**30.1**	**68.9**	**65.8**	**53.5**	**29.1**
240	**62.6**	**52.1**	**30.1**	**26.8**	**37.6**	**53.8**	**36.1**	**36.7**		**57.9**	**46.8**	**24.5**	**31.4**	**71.6**	**68.9**	**55.7**	**30.7**
270	**67.2**	**55.3**	**31.0**	**27.4**	**41.6**	**55.3**	**40.2**	**38.1**		**60.8**	**48.9**	**27.1**	**32.6**	**73.6**	**71.4**	**57.8**	**32.2**
300	**70.8**	**58.2**	**31.9**	**28.0**	**47.8**	**56.7**	**44.3**	**39.4**		**63.3**	**50.8**	**29.6**	**33.9**	**75.3**	**73.4**	**59.1**	**33.9**
330	**73.1**	**60.6**	**32.9**	**28.6**	**53.4**	**58.1**	**48.8**	**40.5**		**65.4**	**52.6**	**32.1**	**35.1**	**76.5**	**74.8**	**61.8**	**35.2**
360	**75.7**	**62.7**	**34.0**	**29.2**	**57.9**	**59.5**	**52.5**	**41.6**		**67.4**	**54.4**	**34.3**	**36.2**	**77.4**	**75.7**	**63.7**	**36.5**
390	**78.2**	**64.8**	**35.1**	**29.8**	**61.5**	**61.1**	**55.8**	**42.7**		**69.3**	**56.4**	**36.4**	**37.3**	**78.2**	**76.7**	**64.3**	**37.7**
420	**80.7**	**65.2**	**36.1**	**30.4**	**64.4**	**62.8**	**58.8**	**43.6**		**71.8**	**58.6**	**38.5**	**38.4**	**79.1**	**77.6**	**66.1**	**38.9**
450	**83.0**	**67.8**	**37.9**	**31.6**	**66.9**	**64.2**	**61.4**	**44.6**		**74.7**	**61.5**	**40.3**	**39.5**	**80.1**	**78.4**	**67.7**	**40.1**
480	**84.7**	**70.2**	**38.6**	**32.2**	**69.1**	**65.6**	**63.6**	**45.5**		**77.5**	**65.5**	**42.2**	**40.4**	**81.2**	**79.4**	**70.6**	**41.2**
510	**86.3**	**73.1**	**39.2**	**33.4**	**70.9**	**67.1**	**65.5**	**46.3**		**80.3**	**68.3**	**43.3**	**41.2**	**82.4**	**80.3**	**73.0**	**42.3**
540	**87.7**	**75.2**	**39.7**	**34.0**	**72.4**	**68.8**	**67.0**	**47.1**		**82.6**	**70.1**	**44.1**	**41.9**	**84.9**	**80.5**	**76.8**	**43.4**
570	**89.0**	**76.7**	**40.1**	**34.6**	**73.8**	**70.3**	**68.3**	**48.0**		**84.4**	**72.4**	**45.1**	**42.4**	**88.5**	**80.8**	**77.6**	**44.5**
600	**90.1**	**79.1**	**40.7**	**35.1**	**75.1**	**71.6**	**69.5**	**48.8**		**86.3**	**74.8**	**45.5**	**42.8**	**91.0**	**81.8**	**78.9**	**45.6**
630					**76.3**	**72.8**	**70.4**	**49.6**		**88.2**	**75.6**	**45.9**	**43.0**	**92.5**	**83.1**	**79.5**	**46.7**
660					**77.5**	**73.7**	**71.1**	**50.5**		**89.1**	**76.8**	**46.0**	**43.2**	**93.5**	**83.8**	**80.3**	**47.8**
690					**78.6**	**74.6**	**71.8**	**51.5**		**90.1**	**77.0**	**46.2**	**43.3**	**94.4**	**84.6**	**81.7**	**48.2**
720					**79.7**	**75.8**	**72.6**	**52.6**		**90.9**	**77.2**	**46.5**	**43.5**	**95.2**	**85.3**	**82.7**	**48.9**
750					**80.7**	**77.3**	**73.3**	**53.9**		**91.6**	**77.4**	**46.8**	**43.6**	**95.9**	**85.7**	**82.9**	**49.3**
780					**81.8**	**78.5**	**74.1**	**54.1**		**93**	**77.5**	**47**	**43.6**	**96.7**	**85.9**	**83.0**	**50.2**
810					**82.8**	**79.6**	**74.8**	**54.5**						**97.0**	**86.0**	**83.1**	**51.5**
840					**83.7**	**80.2**	**75.4**	**55.1**						**97.6**	**86.3**	**83.4**	**52.1**
870					**84.3**	**81.2**	**76.0**	**55.9**						**98.0**	**86.9**	**83.7**	**51.7**
900					**84.9**	**82.6**	**76.6**	**56.0**						**98.4**	**87.1**	**83.9**	**53.9**
930					**85.2**	**83.5**	**77.0**	**56.7**						**99.2**	**87.5**	**84.0**	**55.8**
960					**88.9**	**83.9**	**77.3**	**56.9**						**100.4**	**88.1**	**84.2**	**57.1**
990					**90.1**	**83.3**	**77.6**	**57.1**						**101.0**	**88.3**	**84.3**	**53.9**
1020					**91.7**	**84.1**	**77.9**	**57.8**						**101.6**	**88.6**	**84.7**	**57.1**
1050					**92.6**	**84.3**	**78.3**	**58.2**									
1080					**93.9**	**84.8**	**78.7**	**58.4**									
1110					**94.9**	**85.1**	**79.1**	**58.6**									
1140					**96.2**	**85.6**	**79.6**	**58.8**									
1170					**98.2**	**86.8**	**80.0**	**59.0**									

Table 4.1 Temperatures at each distance from the electrode at each 30 second time interval for the control (600mA RF) and the BETA (9V DC and 600mA) experiments at 5, 10, 15 and 20mm from the electrode.

Temperature Base Data Experiments 11 & 12 (˚c)																	
No.	**Control**				**BETA**					**Control**				**BETA**			
Time (sec)	**11**				**11**					**12**				**12**			
0	**5**	**10**	**15**	**20**	**5**	**10**	**15**	**20**		**5**	**10**	**15**	**20**	**5**	**15**	**10**	**20**
30	**12.7**	**20.1**	**18.7**	**12.7**	**18.8**	**23.6**	**18.8**	**23.4**		**15.5**	**21.4**	**19.0**	**15.3**	**14.0**	**13.5**	**28.6**	**25.1**
60	**33.8**	**28.4**	**20.1**	**15.0**	**26.9**	**24.7**	**21.9**	**23.6**		**29.2**	**27.2**	**20.9**	**16.3**	**19.4**	**18.3**	**32.2**	**26.7**
90	**47.5**	**35.7**	**21.6**	**17.0**	**37.2**	**27.0**	**26.2**	**25.6**		**36.7**	**32.4**	**22.9**	**16.9**	**27.5**	**26.4**	**35.5**	**28.4**
120	**54.9**	**41.3**	**23.2**	**18.4**	**42.8**	**29.3**	**30.2**	**28.0**		**40.2**	**36.6**	**25.1**	**17.3**	**39.7**	**43.5**	**38.3**	**30.2**
150	**61.0**	**45.6**	**25.0**	**19.6**	**47.3**	**36.7**	**32.3**	**30.5**		**47.8**	**40.0**	**27.3**	**18.3**	**47.8**	**54.3**	**40.8**	**32.0**
180	**65.9**	**49.5**	**26.7**	**20.7**	**49.2**	**38.1**	**38.1**	**31.7**		**53.6**	**43.0**	**29.5**	**19.3**	**54.4**	**60.1**	**43.1**	**33.7**
210	**69.8**	**53.2**	**28.5**	**21.8**	**51.2**	**39.4**	**40.2**	**32.8**		**58.0**	**45.6**	**31.7**	**20.5**	**59.0**	**64.5**	**45.0**	**34.5**
240	**73.2**	**56.6**	**30.3**	**22.9**	**53.7**	**40.5**	**42.1**	**33.6**		**61.4**	**47.9**	**33.8**	**21.7**	**62.3**	**68.0**	**46.9**	**35.1**
270	**75.8**	**57.8**	**31.5**	**23.9**	**54.8**	**51.7**	**43.5**	**34.6**		**64.5**	**50.0**	**35.9**	**22.9**	**65.1**	**70.9**	**48.6**	**35.7**
300	**77.9**	**59.6**	**31.8**	**24.8**	**55.8**	**53.5**	**50.3**	**35.1**		**67.1**	**51.9**	**37.8**	**24.1**	**67.0**	**73.5**	**50.4**	**36.8**
330	**79.6**	**61.6**	**32.0**	**25.8**	**61.4**	**55.7**	**55.6**	**35.9**		**69.6**	**53.7**	**39.8**	**25.4**	**68.4**	**75.7**	**52.2**	**37.2**
360	**81.1**	**64.7**	**32.6**	**26.7**	**62.7**	**57.8**	**56.7**	**36.6**		**72.0**	**55.4**	**41.6**	**26.6**	**70.2**	**77.9**	**53.9**	**37.9**
390	**82.6**	**68.8**	**32.9**	**27.6**	**64.3**	**59.1**	**57.1**	**37.4**		**74.4**	**57.0**	**41.9**	**27.8**	**72.0**	**80.6**	**55.5**	**38.3**
420	**84.0**	**69.4**	**33.5**	**28.4**	**65.8**	**61.8**	**57.8**	**38.6**		**76.8**	**58.6**	**42.2**	**28.9**	**73.6**	**82.9**	**57.1**	**39.7**
450	**85.1**	**70.4**	**34.7**	**29.3**	**66.9**	**63.7**	**58.4**	**39.8**		**78.8**	**60.3**	**42.4**	**30.0**	**75.6**	**85.2**	**58.7**	**40.2**
480	**86.1**	**71.6**	**35.8**	**30.1**	**67.8**	**64.3**	**59.8**	**40.7**		**80.6**	**62.6**	**42.6**	**31.0**	**77.6**	**86.8**	**60.1**	**40.8**
510	**87.0**	**72.7**	**36.8**	**30.9**	**68.9**	**66.1**	**61.4**	**41.2**		**82.3**	**64.7**	**42.9**	**32.0**	**80.1**	**88.3**	**61.4**	**41.1**
540	**87.8**	**73.4**	**37.4**	**31.7**	**70.1**	**69.3**	**63.6**	**41.5**		**83.8**	**65.6**	**43.7**	**32.9**	**83.1**	**88.6**	**62.7**	**42.5**
570	**88.6**	**75.6**	**38.9**	**32.5**	**71.6**	**71.4**	**66.1**	**42.2**		**85.3**	**66.8**	**44.8**	**33.9**	**85.7**	**89.5**	**63.8**	**43.9**
600					**72.8**	**73.1**	**68.4**	**43.6**		**86.8**	**67.8**	**44.9**	**34.7**	**86.9**	**86.3**	**65.0**	**44.3**
630					**73.7**	**74.8**	**69.6**	**44.1**		**88.2**	**68.9**	**45.0**	**35.6**	**88.5**	**84.7**	**66.0**	**45.2**
660					**76.3**	**76.4**	**72.4**	**44.9**		**90.1**	**70.5**	**45.1**	**36.4**	**89.1**	**85.3**	**66.7**	**45.4**
690					**79.9**	**78.2**	**73.3**	**45.8**		**90.6**	**72.6**	**45.6**	**37.1**	**90.2**	**85.9**	**67.5**	**46.6**
720					**83.1**	**79.5**	**73.9**	**46.3**		**91.2**	**74.8**	**45.7**	**38.2**	**92.4**	**86.0**	**69.9**	**47.7**
750					**86.4**	**82.5**	**74.0**	**47.3**		**91.8**	**76.3**	**45.8**	**39.6**	**93.6**	**87.4**	**71.6**	**48.6**
780					**88.8**	**83.6**	**74.2**	**48.4**		**92.7**	**77.9**	**46**	**41.1**	**94.1**	**88.5**	**73.0**	**49.9**
810					**90.7**	**84.3**	**74.6**	**49.6**						**95.2**	**88.9**	**74.1**	**51.2**
840					**90.2**	**84.3**	**74.8**	**50.4**						**96.7**	**89.4**	**75.1**	**52.6**
870					**91.3**	**85.7**	**75.0**	**53.2**						**97.8**	**89.9**	**77.4**	**56.9**
900					**91.8**	**86.2**	**75.6**	**57.3**						**98.3**	**90.4**	**77.6**	**53.6**
930					**93.0**	**86.9**	**75.7**	**53.4**						**99.4**	**90.3**	**77.5**	**50.0**
960					**94.2**	**87.0**	**76.0**	**53.9**						**99.8**	**90.5**	**78.1**	**50.6**
990					**96.3**	**87.3**	**76.5**	**54.9**						**100.2**	**90.5**	**78.2**	**56.9**
1020					**97.4**	**87.5**	**76.8**	**55.2**						**101.3**	**90.6**	**78.6**	**57.0**
1050					**98.4**	**87.9**	**77.0**	**56.0**									

Table 4.1 Temperatures at each distance from the electrode at each 30 second time interval for the control (600mA RF) and the BETA (9V DC and 600mA) experiments at 5, 10, 15 and 20mm from the electrode.

Temperature Base Data Experiments 13 & 14 (˚c)																	
No.	**Control**				**BETA**					**Control**				**BETA**			
Time (sec)	**13**				**13**					**14**				**14**			
0	**5**	**10**	**15**	**20**	**5**	**10**	**15**	**20**		**5**	**10**	**15**	**20**	**5**	**15**	**10**	**20**
30	**19.5**	**19.7**	**19.7**	**18.7**	**17.8**	**23.8**	**18.3**	**24.0**		**22.4**	**21.3**	**23.4**	**20.9**	**20.8**	**20.8**	**21.8**	**18.3**
60	**30.2**	**23.6**	**20.9**	**19.9**	**19.0**	**16.5**	**19.3**	**20.2**		**24.3**	**25.3**	**22.1**	**22.1**	**24.6**	**20.5**	**25.9**	**19.2**
90	**40.4**	**28.5**	**21.9**	**20.8**	**26.1**	**16.2**	**23.8**	**16.5**		**34.2**	**30.8**	**23.6**	**23.1**	**27.9**	**27.9**	**30.0**	**20.3**
120	**46.9**	**33.2**	**23.0**	**21.6**	**35.4**	**16.1**	**28.4**	**16.4**		**42.1**	**35.6**	**24.7**	**23.9**	**27.9**	**28.0**	**33.9**	**21.5**
150	**52.2**	**37.5**	**24.1**	**22.2**	**42.7**	**17.8**	**32.3**	**17.0**		**47.5**	**39.6**	**25.9**	**24.7**	**27.9**	**27.9**	**37.4**	**22.8**
180	**56.6**	**41.2**	**25.3**	**22.8**	**48.2**	**23.7**	**35.8**	**18.7**		**51.6**	**42.8**	**27.1**	**25.6**	**38.5**	**39.7**	**40.4**	**25.5**
210	**60.0**	**44.4**	**26.7**	**23.5**	**53.1**	**31.9**	**39.1**	**20.7**		**55.0**	**45.7**	**28.3**	**26.6**	**54.5**	**53.5**	**43.1**	**26.8**
240	**65.4**	**47.5**	**28.1**	**24.7**	**57.9**	**39.5**	**42.0**	**23.1**		**57.8**	**48.2**	**29.6**	**27.6**	**63.2**	**59.6**	**45.5**	**28.0**
270	**67.5**	**50.7**	**29.5**	**25.4**	**60.7**	**44.9**	**44.6**	**25.7**		**60.3**	**50.5**	**30.8**	**28.6**	**68.8**	**63.7**	**47.5**	**29.2**
300	**69.3**	**56.9**	**30.9**	**26.0**	**62.8**	**48.9**	**46.9**	**28.4**		**62.4**	**52.7**	**32.0**	**29.7**	**74.7**	**67.8**	**49.3**	**30.4**
330	**72.2**	**62.0**	**32.3**	**27.3**	**64.5**	**52.1**	**49.2**	**31.3**		**64.3**	**54.9**	**33.2**	**30.7**	**79.7**	**71.8**	**50.9**	**31.5**
360	**74.6**	**63.2**	**32.5**	**28.6**	**66.1**	**54.7**	**51.2**	**33.9**		**66.0**	**57.1**	**34.3**	**31.8**	**81.3**	**73.4**	**52.4**	**32.5**
390	**76.8**	**65.2**	**33.0**	**29.8**	**67.6**	**56.9**	**53.1**	**36.2**		**67.5**	**59.3**	**35.4**	**32.9**	**81.4**	**73.8**	**53.7**	**33.5**
420	**78.7**	**66.9**	**33.3**	**31.0**	**69.0**	**58.7**	**55.0**	**38.3**		**74.8**	**61.8**	**36.4**	**33.9**	**82.6**	**75.1**	**55.0**	**34.5**
450	**79.5**	**68.4**	**33.4**	**31.6**	**70.2**	**60.1**	**56.8**	**40.1**		**78.9**	**64.9**	**37.4**	**35.0**	**83.4**	**76.2**	**56.3**	**35.4**
480	**80.4**	**70.1**	**33.8**	**32.1**	**71.2**	**61.4**	**58.7**	**41.7**		**80.6**	**67.0**	**38.4**	**35.3**	**84.6**	**77.7**	**57.7**	**36.3**
510	**83.2**	**71.6**	**34.0**	**33.3**	**72.2**	**62.5**	**60.6**	**43.4**		**84.9**	**68.9**	**39.3**	**35.8**	**85.2**	**78.9**	**58.9**	**37.2**
540	**84.7**	**72.6**	**34.4**	**33.8**	**73.2**	**63.5**	**62.3**	**45.0**		**87.8**	**70.3**	**40.1**	**36.0**	**86.0**	**80.6**	**60.1**	**38.8**
570	**86.9**	**73.5**	**36.4**	**34.4**	**74.2**	**64.6**	**64.0**	**46.6**		**88.4**	**72.8**	**41.0**	**36.6**	**86.6**	**82.4**	**61.3**	**40.5**
600	**88.1**	**74.6**	**38.5**	**35.4**	**75.1**	**65.8**	**65.6**	**47.8**		**89.6**	**73.1**	**42.6**	**36.9**	**87.3**	**83.8**	**64.6**	**42.0**
630	**89.3**	**75.7**	**40.1**	**37.8**	**75.8**	**67.5**	**67.0**	**49.1**		**90.1**	**73.9**	**43.1**	**37.2**	**88.3**	**83.6**	**67.9**	**42.7**
660	**90.4**	**79.8**	**40.6**	**38.3**	**76.4**	**69.1**	**68.2**	**50.4**		**90.5**	**74.2**	**44.7**	**37.9**	**88.9**	**84.1**	**69.0**	**43.4**
690	**91.4**	**80.2**	**41.4**	**39.1**	**76.7**	**70.5**	**69.3**	**51.6**		**91.0**	**75.0**	**45.3**	**38.4**	**89.3**	**85.1**	**70.7**	**44.2**
720	**91.6**	**81.3**	**42.6**	**39.3**	**77.2**	**72.0**	**70.4**	**52.4**		**91.4**	**75.8**	**46.1**	**39.0**	**90.5**	**85.8**	**72.9**	**45.0**
750	**92.0**	**82.6**	**43.4**	**39.6**	**77.5**	**73.2**	**71.6**	**53.7**		**92.0**	**76.5**	**46.5**	**40.4**	**91.4**	**87.0**	**73.9**	**46.5**
780	**92.5**	**78.8**	**45.3**	**41.1**	**75.8**	**74.4**	**70.7**	**55.1**		**92.7**	**77.5**	**47**	**41.6**	**92.6**	**87.5**	**75.8**	**47.8**
810					**77.9**	**75.4**	**72.3**	**55.7**						**93.7**	**87.9**	**76.8**	**48.2**
840					**79.0**	**76.4**	**73.8**	**56.8**						**94.8**	**88.4**	**77.9**	**50.3**
870					**82.5**	**80.6**	**75.1**	**51.9**						**95.4**	**88.8**	**81.6**	**51.4**
900					**84.6**	**82.6**	**76.0**	**52.9**						**97.0**	**89.7**	**79.4**	**52.6**
930					**86.3**	**82.0**	**77.4**	**55.0**						**98.3**	**90.1**	**84.7**	**54.8**
960					**88.0**	**82.7**	**78.3**	**55.6**						**99.1**	**90.4**	**85.2**	**56.9**
990					**89.3**	**84.3**	**78.9**	**56.1**						**100.5**	**90.8**	**85.6**	**58.4**
1020					**90.4**	**86.0**	**79.4**	**56.5**						**101.2**	**91.0**	**85.8**	**60.0**

Table 4.1 Temperatures at each distance from the electrode at each 30 second time interval for the control (600mA RF) and the BETA (9V DC and 600mA) experiments at 5, 10, 15 and 20mm from the electrode.

Temperature Base Data Experiments 15 & 16 (˚c)																	
No.	**Control**				**BETA**					**Control**				**BETA**			
Time (sec)	**15**				**15**					**16**				**16**			
0	**5**	**10**	**15**	**20**	**5**	**10**	**15**	**20**		**5**	**10**	**15**	**20**	**5**	**10**	**15**	**20**
30	**24.0**	**21.8**	**21.0**	**21.6**	**23.3**	**24.6**	**23.0**	**22.4**		**20.9**	**21.7**	**20.7**	**21.8**	**24.8**	**26.3**	**23.7**	**20.9**
60	**32.4**	**25.8**	**21.8**	**22.5**	**27.8**	**26.4**	**27.4**	**23.2**		**27.7**	**23.3**	**21.0**	**22.9**	**26.7**	**26.6**	**26.9**	**21.2**
90	**39.3**	**31.3**	**22.9**	**23.5**	**28.3**	**28.1**	**28.5**	**24.1**		**34.7**	**31.4**	**21.8**	**24.9**	**35.3**	**32.8**	**30.3**	**21.5**
120	**44.8**	**36.0**	**24.1**	**24.6**	**33.3**	**29.6**	**29.1**	**25.1**		**40.5**	**38.9**	**22.9**	**26.1**	**44.6**	**39.8**	**33.6**	**22.0**
150	**49.0**	**40.1**	**25.5**	**25.7**	**45.1**	**31.1**	**30.5**	**26.2**		**45.6**	**44.9**	**24.1**	**27.0**	**51.3**	**45.7**	**37.1**	**22.7**
180	**52.2**	**43.7**	**27.0**	**26.9**	**53.3**	**32.5**	**32.3**	**27.4**		**49.6**	**49.6**	**25.5**	**28.0**	**56.3**	**51.0**	**40.7**	**23.5**
210	**57.2**	**47.0**	**29.8**	**28.1**	**58.2**	**33.8**	**34.1**	**28.5**		**52.7**	**53.4**	**27.0**	**29.0**	**60.3**	**55.4**	**43.9**	**24.4**
240	**59.5**	**49.9**	**31.1**	**29.3**	**61.4**	**37.2**	**35.5**	**29.7**		**55.6**	**56.7**	**28.4**	**30.0**	**63.2**	**58.7**	**47.0**	**25.5**
270	**61.5**	**52.6**	**32.4**	**30.5**	**63.3**	**38.3**	**36.7**	**30.9**		**58.2**	**59.6**	**29.8**	**31.2**	**65.3**	**60.7**	**50.1**	**26.7**
300	**63.4**	**55.3**	**33.6**	**31.7**	**64.6**	**39.3**	**37.9**	**32.0**		**60.7**	**62.5**	**31.1**	**32.3**	**67.1**	**63.7**	**52.8**	**28.0**
330	**68.5**	**58.0**	**36.8**	**32.9**	**66.0**	**42.6**	**38.9**	**33.1**		**63.1**	**65.9**	**32.4**	**33.4**	**69.5**	**65.1**	**55.0**	**29.2**
360	**70.0**	**60.4**	**37.7**	**34.0**	**67.5**	**43.3**	**39.7**	**34.1**		**67.2**	**69.8**	**33.6**	**33.9**	**70.4**	**66.1**	**57.4**	**30.6**
390	**71.3**	**61.7**	**38.6**	**34.5**	**68.8**	**44.9**	**40.4**	**35.2**		**70.9**	**71.3**	**34.7**	**34.2**	**71.1**	**66.7**	**59.8**	**32.0**
420	**73.4**	**62.6**	**40.2**	**34.7**	**70.2**	**49.2**	**41.1**	**36.1**		**72.8**	**72.6**	**35.8**	**34.7**	**73.4**	**68.8**	**62.0**	**33.4**
450	**77.4**	**64.8**	**41.0**	**34.9**	**71.7**	**50.8**	**43.7**	**37.0**		**76.5**	**73.8**	**36.8**	**35.0**	**74.7**	**70.2**	**63.8**	**34.8**
480	**81.3**	**68.4**	**42.4**	**35.2**	**73.6**	**52.1**	**44.5**	**37.9**		**80.3**	**74.7**	**37.7**	**35.7**	**76.3**	**72.0**	**65.5**	**36.1**
510	**83.2**	**69.7**	**43.0**	**35.8**	**75.8**	**53.4**	**45.3**	**38.7**		**82.0**	**76.8**	**38.6**	**36.0**	**78.8**	**74.0**	**66.9**	**37.3**
540	**87.0**	**71.3**	**44.9**	**36.0**	**78.3**	**56.2**	**46.2**	**39.6**		**85.0**	**78.0**	**39.4**	**36.2**	**79.4**	**74.5**	**68.3**	**38.6**
570	**89.7**	**73.1**	**45.5**	**36.2**	**81.6**	**57.8**	**47.1**	**40.5**		**86.3**	**81.3**	**40.2**	**36.4**	**81.1**	**75.8**	**69.6**	**39.7**
600	**91.5**	**75.6**	**46.2**	**36.8**	**84.1**	**59.5**	**48.0**	**41.9**		**88.9**	**82.0**	**41.0**	**37.0**	**82.6**	**77.1**	**70.7**	**40.8**
630	**92.9**	**77.9**	**47.4**	**37.0**	**86.1**	**62.8**	**51.4**	**42.9**		**92.0**	**82.9**	**41.7**	**37.8**	**83.3**	**77.6**	**71.7**	**41.8**
660					**87.8**	**64.1**	**53.0**	**43.8**						**83.7**	**77.8**	**72.8**	**42.8**
690					**89.8**	**67.3**	**58.2**	**44.7**						**84.5**	**78.4**	**73.9**	**43.8**
720					**90.2**	**70.2**	**61.4**	**45.7**						**85.6**	**79.4**	**74.6**	**44.7**
750					**92.9**	**72.6**	**63.3**	**46.7**						**86.1**	**81.3**	**75.1**	**45.6**
780					**94.4**	**74.1**	**64.6**	**47.8**						**87.8**	**81.4**	**75.8**	**46.4**
810					**97.9**	**76.8**	**66.0**	**49.0**						**89.8**	**82.6**	**76.2**	**47.2**
840					**98.5**	**78.2**	**68.8**	**50.2**						**90.2**	**83.4**	**76.7**	**47.9**
870					**99.2**	**78.9**	**70.9**	**48.6**						**92.9**	**84.6**	**76.9**	**53.8**
900					**100.4**	**81.1**	**73.6**	**54.4**						**94.4**	**85.2**	**77.0**	**52.3**
930					**101.2**	**88.1**	**75.9**	**55.6**						**97.9**	**86.0**	**77.2**	**56.5**
960					**102.0**	**89.5**	**77.5**	**58.9**						**98.5**	**87.3**	**77.9**	**56.9**
990					**103.5**	**90.2**	**78.3**	**60.2**						**99.2**	**88.3**	**78.0**	**57.2**
1020					**105.7**	**90.6**	**79.0**	**60.5**						**100.4**	**88.9**	**78.1**	**57.4**

Table 4.1 Temperatures at each distance from the electrode at each 30 second time interval for the control (600mA RF) and the BETA (9V DC and 600mA) experiments at 5, 10, 15 and 20mm from the electrode.

Temperature Base Data Experiments 17 & 18 (˚c)																	
No.	**Control**				**BETA**					**Control**				**BETA**			
Time (sec)	**17**				**17**					**18**				**18**			
0	**5**	**10**	**15**	**20**	**5**	**10**	**15**	**20**		**5**	**10**	**15**	**20**	**5**	**15**	**10**	**20**
30	**21.2**	**22.4**	**21.8**	**22.2**	**24.3**	**21.8**	**22.3**	**21.3**		**23.0**	**22.0**	**23.0**	**21.9**	**24.7**	**23.9**	**23.0**	**23.3**
60	**27.2**	**24.1**	**23.3**	**22.6**	**29.6**	**28.6**	**25.8**	**22.6**		**29.6**	**24.5**	**23.0**	**22.3**	**28.7**	**25.6**	**23.3**	**23.6**
90	**35.0**	**29.1**	**25.5**	**23.4**	**48.0**	**35.6**	**29.5**	**24.3**		**34.8**	**29.9**	**23.5**	**23.1**	**40.7**	**29.3**	**23.6**	**23.7**
120	**41.5**	**34.2**	**28.0**	**24.2**	**59.9**	**38.4**	**34.0**	**26.1**		**42.2**	**35.0**	**23.8**	**23.9**	**51.0**	**34.0**	**24.1**	**23.9**
150	**46.7**	**38.5**	**30.7**	**25.2**	**66.7**	**41.1**	**38.3**	**27.8**		**46.9**	**39.6**	**24.0**	**24.7**	**56.7**	**38.3**	**30.0**	**24.8**
180	**51.1**	**42.1**	**31.5**	**26.3**	**70.8**	**45.5**	**41.6**	**29.6**		**50.6**	**43.2**	**24.6**	**25.6**	**60.0**	**41.7**	**37.3**	**25.9**
210	**54.8**	**45.1**	**31.2**	**27.5**	**74.1**	**49.4**	**44.2**	**31.4**		**57.0**	**46.2**	**25.3**	**26.5**	**62.8**	**40.5**	**43.4**	**27.1**
240	**57.9**	**47.7**	**32.0**	**28.7**	**76.1**	**52.6**	**46.4**	**33.2**		**62.5**	**49.0**	**26.2**	**27.6**	**65.5**	**57.9**	**48.0**	**28.5**
270	**60.6**	**50.0**	**32.8**	**30.0**	**77.2**	**55.4**	**48.3**	**35.1**		**67.1**	**51.8**	**27.0**	**28.7**	**68.2**	**55.1**	**51.5**	**30.0**
300	**62.9**	**52.1**	**33.5**	**31.1**	**78.9**	**57.7**	**50.3**	**36.9**		**71.3**	**54.5**	**27.9**	**30.0**	**71.6**	**57.1**	**54.1**	**31.6**
330	**65.2**	**54.0**	**34.2**	**32.2**	**79.3**	**59.6**	**52.1**	**38.5**		**75.1**	**57.0**	**28.9**	**31.6**	**75.3**	**59.2**	**56.3**	**33.1**
360	**67.5**	**55.8**	**34.9**	**33.2**	**79.5**	**61.4**	**53.9**	**40.0**		**78.6**	**59.1**	**29.9**	**33.5**	**79.0**	**61.4**	**57.9**	**34.6**
390	**71.0**	**57.7**	**35.5**	**34.2**	**82.1**	**62.9**	**55.4**	**41.4**		**82.4**	**61.5**	**30.9**	**35.2**	**83.0**	**63.8**	**59.4**	**36.0**
420	**74.3**	**59.4**	**36.2**	**35.1**	**82.7**	**64.3**	**56.8**	**42.6**		**84.4**	**63.6**	**31.9**	**36.9**	**87.0**	**65.8**	**60.6**	**37.3**
450	**77.5**	**61.2**	**36.8**	**36.1**	**83.6**	**65.8**	**58.2**	**43.8**		**85.9**	**65.2**	**33.0**	**38.6**	**87.2**	**71.0**	**61.7**	**38.5**
480	**80.2**	**63.0**	**37.5**	**37.0**	**84.5**	**67.1**	**59.5**	**44.8**		**86.9**	**66.4**	**33.6**	**40.8**	**87.6**	**71.0**	**62.8**	**39.6**
510	**83.0**	**64.9**	**38.1**	**37.9**	**84.9**	**68.4**	**61.0**	**45.7**		**88.0**	**67.3**	**34.0**	**41.3**	**89.4**	**72.0**	**64.1**	**40.7**
540	**85.4**	**66.8**	**38.4**	**38.7**	**85.1**	**69.6**	**62.7**	**46.6**		**90.2**	**69.4**	**35.1**	**41.7**	**91.7**	**73.0**	**65.2**	**41.7**
570	**86.7**	**68.7**	**39.1**	**39.7**	**85.4**	**70.8**	**64.4**	**47.4**		**91.5**	**70.6**	**35.7**	**41.9**	**92.1**	**73.1**	**66.3**	**42.7**
600	**86.4**	**70.5**	**40.0**	**40.5**	**85.1**	**71.9**	**66.5**	**48.2**		**92.2**	**72.4**	**36.2**	**42.6**	**92.1**	**73.2**	**67.4**	**43.6**
630	**86.8**	**72.1**	**41.8**	**41.3**	**84.9**	**72.9**	**68.5**	**48.9**		**94.1**	**75.8**	**37.4**	**43.4**	**92.6**	**73.3**	**68.5**	**44.4**
660	**86.6**	**73.7**	**43.5**	**42.1**	**86.8**	**73.8**	**69.6**	**49.6**		**95.7**	**79.0**	**38.9**	**45.0**	**93.5**	**75.0**	**69.8**	**45.3**
690	**86.1**	**75.2**	**45.1**	**43.0**	**88.6**	**74.7**	**70.1**	**50.2**						**94.4**	**77.1**	**71.5**	**46.1**
720	**87.0**	**76.6**	**46.6**	**43.9**	**90.2**	**75.7**	**71.4**	**50.8**						**94.5**	**78.4**	**71.4**	**47.0**
750	**89.3**	**79.1**	**46.9**	**44.9**	**91.8**	**76.6**	**72.6**	**51.4**						**95.7**	**79.2**	**71.9**	**47.9**
780	**93.1**	**80.4**	**47.0**	**45.0**	**93.0**	**77.5**	**73.2**	**52.0**						**96.9**	**80.6**	**72.6**	**48.8**
810					**94.6**	**78.4**	**74.3**	**52.6**						**98.1**	**81.7**	**73.1**	**49.7**
840					**95.3**	**79.3**	**74.8**	**53.2**						**98.8**	**82.4**	**73.0**	**50.6**
870					**97.9**	**80.1**	**75.3**	**51.2**						**99.5**	**83.2**	**73.6**	**52.5**
900					**99.3**	**82.4**	**75.8**	**53.2**						**100.1**	**83.7**	**74.0**	**53.5**
930														**100.6**	**84.1**	**74.7**	**54.6**
960														**101.5**	**84.9**	**75.0**	**55.2**
990														**102.9**	**85.3**	**75.2**	**55.5**
1020														**104.7**	**85.8**	**75.5**	**55.7**
1050														**112.6**	**86.1**	**75.9**	**55.9**

Table 4.1 Temperatures at each distance from the electrode at each 30 second time interval for the control (600mA RF) and the BETA (9V DC and 600mA) experiments at 5, 10, 15 and 20mm from the electrode.

Temperature Base Data Experiments 19 & 20 (˚c)																	
No.	**Control**				**BETA**					**Control**				**BETA**			
Time (sec)	**19**				**19**					**20**				**20**			
0	**5**	**10**	**15**	**20**	**5**	**10**	**15**	**20**		**5**	**10**	**15**	**20**	**5**	**10**	**15**	**20**
30	**22.9**	**24.2**	**24.3**	**22.3**	**25.8**	**23.0**	**25.4**	**22.5**		**17.6**	**22.4**	**22.4**	**16.0**	**26.0**	**25.3**	**24.0**	**24.3**
60	**29.4**	**27.0**	**24.8**	**23.5**	**42.4**	**31.5**	**28.3**	**23.4**		**25.9**	**23.3**	**22.7**	**17.0**	**26.9**	**26.3**	**26.6**	**25.0**
90	**36.2**	**30.6**	**25.3**	**25.0**	**52.1**	**35.7**	**32.7**	**24.4**		**33.2**	**27.0**	**24.3**	**18.2**	**36.0**	**33.3**	**29.7**	**25.6**
120	**41.4**	**34.1**	**25.9**	**26.5**	**57.5**	**39.9**	**37.0**	**25.6**		**38.5**	**30.6**	**26.1**	**19.5**	**46.2**	**41.2**	**32.8**	**26.0**
150	**45.6**	**37.3**	**26.5**	**28.2**	**61.6**	**43.8**	**40.6**	**26.8**		**42.9**	**33.7**	**28.1**	**20.9**	**51.8**	**45.2**	**37.8**	**26.9**
180	**49.1**	**40.2**	**27.2**	**29.9**	**64.6**	**48.9**	**43.4**	**28.3**		**46.8**	**36.5**	**30.2**	**22.5**	**56.6**	**48.2**	**40.0**	**27.4**
210	**54.4**	**42.8**	**27.9**	**32.9**	**67.2**	**51.2**	**46.2**	**29.8**		**50.0**	**38.9**	**32.1**	**24.2**	**60.2**	**50.8**	**43.7**	**28.4**
240	**56.5**	**45.1**	**28.7**	**34.2**	**70.2**	**53.7**	**48.6**	**31.3**		**52.8**	**40.9**	**33.9**	**25.8**	**63.3**	**52.9**	**45.3**	**29.0**
270	**60.0**	**47.2**	**29.5**	**36.6**	**72.9**	**55.6**	**51.2**	**32.7**		**55.3**	**42.7**	**35.5**	**27.5**	**66.2**	**55.4**	**48.0**	**30.1**
300	**61.4**	**49.3**	**30.3**	**37.7**	**75.4**	**57.8**	**53.5**	**34.1**		**57.5**	**44.4**	**37.1**	**29.0**	**68.7**	**57.5**	**49.3**	**30.7**
330	**64.0**	**51.4**	**31.2**	**39.7**	**77.6**	**60.3**	**55.8**	**35.4**		**59.6**	**45.9**	**38.5**	**30.6**	**71.0**	**59.5**	**52.6**	**32.6**
360	**65.2**	**53.5**	**32.1**	**40.7**	**79.8**	**62.8**	**58.4**	**36.7**		**62.0**	**47.1**	**39.8**	**32.1**	**73.2**	**61.3**	**53.5**	**33.3**
390	**67.8**	**55.5**	**33.0**	**42.4**	**81.6**	**64.2**	**60.0**	**37.9**		**74.0**	**48.3**	**36.7**	**33.5**	**75.1**	**63.1**	**54.5**	**34.1**
420	**69.5**	**57.6**	**33.9**	**43.2**	**83.3**	**67.2**	**61.2**	**39.0**		**77.1**	**49.2**	**34.5**	**35.0**	**76.7**	**64.7**	**57.0**	**36.9**
450	**71.4**	**59.8**	**34.9**	**44.1**	**84.5**	**69.8**	**62.7**	**40.2**		**78.7**	**50.6**	**36.0**	**36.4**	**78.3**	**66.2**	**60.8**	**38.4**
480	**73.6**	**62.1**	**36.1**	**45.0**	**85.9**	**70.9**	**64.0**	**41.2**		**82.8**	**52.1**	**37.3**	**37.9**	**79.9**	**67.6**	**61.9**	**39.8**
510	**76.6**	**64.7**	**37.2**	**45.9**	**87.3**	**72.2**	**65.2**	**42.2**		**86.5**	**53.6**	**38.4**	**39.3**	**81.4**	**69.0**	**62.3**	**41.1**
540	**81.1**	**68.0**	**38.4**	**43.3**	**88.5**	**74.6**	**66.3**	**43.2**		**88.5**	**55.3**	**39.6**	**39.9**	**83.1**	**70.3**	**64.2**	**42.4**
570	**83.0**	**68.2**	**39.0**	**43.4**	**89.7**	**75.9**	**67.4**	**44.1**		**89.9**	**57.2**	**40.7**	**40.4**	**85.0**	**71.5**	**66.1**	**43.7**
600	**85.7**	**70.2**	**39.3**	**43.6**	**90.6**	**76.5**	**68.5**	**44.9**		**91.0**	**60.7**	**41.9**	**40.9**	**86.8**	**72.4**	**67.7**	**44.9**
630	**88.9**	**73.2**	**39.4**	**43.9**	**91.5**	**77.9**	**69.8**	**45.7**		**91.7**	**65.7**	**43.0**	**41.3**	**88.3**	**73.6**	**69.2**	**46.1**
660	**90.2**	**76.8**	**40.1**	**44.1**	**92.1**	**78.2**	**71.3**	**46.3**		**92.1**	**68.6**	**44.1**	**41.8**	**89.4**	**74.6**	**70.6**	**47.3**
690					**93.1**	**79.7**	**72.5**	**46.9**		**92.5**	**71.7**	**45.3**	**42.6**	**91.3**	**75.7**	**72.4**	**48.7**
720					**94.1**	**81.0**	**73.7**	**47.5**		**93.7**	**74.6**	**46.4**	**42.8**	**92.4**	**77.4**	**73.1**	**50.2**
750					**94.9**	**82.6**	**74.9**	**48.0**		**94.8**	**77.9**	**46.8**	**43.0**	**94.5**	**78.8**	**73.9**	**51.5**
780					**95.7**	**83.8**	**75.7**	**49.0**		**95.9**	**80.2**	**47.0**	**43.2**	**95.8**	**79.9**	**74.3**	**52.5**
810					**97.1**	**84.9**	**77.1**	**50.2**						**96.2**	**80.2**	**74.8**	**53.7**
840					**98.2**	**85.6**	**78.2**	**51.4**						**97.4**	**80.9**	**75.6**	**54.9**
870					**98.9**	**86.8**	**78.5**	**55.8**						**98.7**	**81.3**	**75.8**	**55.6**
900					**99.7**	**87.0**	**78.7**	**56.6**						**98.9**	**81.9**	**76.2**	**56.1**
930														**99.5**	**82.4**	**76.4**	**56.2**
960														**100.1**	**82.9**	**76.7**	**56.7**

Table 4.1 Temperatures at each distance from the electrode at each 30 second time interval for the control (600mA RF) and the BETA (9V DC and 600mA) experiments at 5, 10, 15 and 20mm from the electrode.

	BETA MEAN				Control Mean			
Time (sec)	5-BETA	10-BETA	15-BETA	20-BETA	5-Control	10-Control	15-Control	20-Control
0	22	24.5	21.6	22.4	20.6	21.9	26.6	21.1
30	28.2	30.5	24.5	23.5	28.3	24.9	28	22.5
60	37.8	35	30.5	24.3	35.4	29.3	29.1	23.3
90	46.4	38.2	36.4	25.4	40	34.1	31	24.3
120	52	42	41.1	27	45	38.6	32	25.2
150	57.3	45.4	46	28.3	49	42.6	33.3	26.3
180	61.4	48.1	49.5	30	53.2	46.3	34.5	27.4
210	64.4	51.4	53	31	57	48.9	35.6	28.4
240	66.8	54.2	55.2	32.3	60	51.5	36.6	29.5
270	69	56	57.7	33.7	62.7	54.4	37.7	30.5
300	71	58.4	60	35.1	66	57	38.5	31.6
330	72.2	60.3	61.7	37	68.3	59	39.4	32.6
360	74.1	62	63.1	38.2	71.3	61	40.2	33.3
390	75.6	64	64.7	39.5	74	62.4	41.1	34
420	76.7	65.4	66.3	41	76	64.1	41.8	34
450	77.7	67	68	42	78	65.7	42.6	35.8
480	79.2	68	68.9	43	80.5	67.7	43.2	36.6
510	80.4	70	70	44	82.4	69.4	44.2	37.4
540	81.6	71	71	45	84	71.6	45	38.3
570	82.5	72.2	71.7	46	85.6	73.8	44.4	39
600	83.5	74	72.6	47	87.2	75	44.5	39.7
630	84.5	75	75	48	88.4	76.8	44.4	39.7
660	85.9	76.2	76	49	89	77.2	44.6	40.8
690	86.9	78	77.1	50	90	78.1	44.8	41.1
720	88	79.1	77.8	51	91.3	78.6	45	40.9
750	88.9	80.4	78.6	52.2	92.5	79.1	45.3	41.1
780	90	82	79.4	53.3				
810	90.8	83	80.2	54.4				
840	91.7	83.7	81.1	54.6				
870	92.5	84.1	82	55.1				
900	93.4	84.7	82.5	55.9				
930	94.2	85.7	82.5	56.5				
960	94.4	85	83.3	56.3				
990	94.7	85.7	83.6	56.3				
1020	95.1	85.4	83.8	56.7				
1050	95.2	85.8	83.9	57.3				
1080	95.4	87.6	84.1	58.7				
1110	95.6	89.3	84.2	58.3				
1140	95.8	90	84.4	59.4				

Table 4.2 The mean temperatures at each distance from the electrode at each 30 second time interval for the control (600mA RF) and the BETA (9V simultaneous DC and 600mA RF) experiments at 5, 10, 15 and 20mm from the electrode.

Animal	Control (mm)	Control (mm)	Mean (mm)	SD	95% CI	BETA (mm)	BETA (mm)	Mean (mm)	SD	95% CI
Terminal Anaesthesia (0D)	10 x 8	10	11.25	1.28	0.89	21 x 18	24	20.9	3.91	2.71
	10 x 8	10				23 x 19	23			
	11 x 9	11				24 x 21	24			
	11 x 10	11				24 x 23	24			
	11 x 8	11				22 x 21	22			
	11 x 9	11				21 x 19	21			
	12 x 10	12				11 x 7	11			
	14 x 12	14				23 x 18	23			
						20 x 18	20			
						20 x 15	20			

Animal	Control (mm)	Control (mm)	Mean (mm)	SD	95% CI	BETA (mm)	BETA (mm)	Mean (mm)	SD	95% CI
2 day Termination (2D)	15 x 13	15	15.13	1.21	0.84	18 x 16	18	25	3.96	2.75
	13 x 10	13				28 x 26	28			
	11 x 10	11				22 x 18	22			
	16 x 14	16				22 x 20	22			
	18 x 15	18				25 x 22	25			
	16 x 13	16				28 x 28	28			
	16 x 15	16				29 x 27	29			
	16 x 15	16				28 x 26	28			

Animal	Control (mm)	Control (mm)	Mean (mm)	SD	95% CI	BETA (mm)	BETA (mm)	Mean (mm)	SD	95% CI
1 week Termination (14D)	11 x 9	11	11.38	1.19	0.82	15 x 13	15	14.88	1.8	1.25
	10 x 8	10				17 x 16	17			
	11 x 9	11				13 x 11	13			
	13 x 8	13				17 x 15	17			
	10 x 9	10				16 x 14	16			
	13 x 11	13				14 x 12	14			
	11 x 9	11				15 x 13	15			
	12 x 9	12				12 x 10	12			

Animal	Control (mm)	Control (mm)	Mean (mm)	SD	95% CI	BETA (mm)	BETA (mm)	Mean (mm)	SD	95% CI
4 week termination (28D)	5 x 5	5	7.75	2.05	1.42	12 x 9	12	11.5	1.69	1.17
	4 x 3	4				9 x 9	9			
	9 x 6	9				12 x 11	12			
	9 x 9	9				14 x 12	14			
	9 x 7	9				13 x 11	13			
	8 x 8	8				10 x 7	10			
	9 x 7	9				10 x 7	10			
	9 x 8	9				12 x 9	12			

Animal	Control (mm)	Control (mm)	Mean (mm)	SD	95% CI	BETA (mm)	BETA (mm)	Mean (mm)	SD	95% CI
8 week termination (56D)	6 x 4	6	5.13	2.03	1.41	12 x 11	12	10.38	1.6	1.11
	6 x 5	6				10 x 9	10			
	8 x 4	8				10 x 9	10			
	3 x 3	3				7 x 6	7			
	5 x 5	5				10 x 10	10			
	7 x 6	7				11 x 10	11			
	2 x 1	2				12 x 11	12			
	4 x 4	4				11 x 9	11			

Table 5.1 demonstrates the largest short axis diameter ablation zone for each control (600mA RF only) and corresponding BETA experiment (600mA, 9V DC) at post mortem examination. The mean, standard deviation (SD) and 95% confidence intervals (95% CI) are tabulated.

BIBLIOGRAPHY.

A

Abdalla EK, Hicks ME & Vauthey JN (2001). Portal vein embolization: rationale, technique and future prospects. *Br J Surg* 88, 165-175.

Abdalla EK, Vauthey JN, Ellis LM, Ellis V, Pollock R, Broglio KR, Hess K & Curley SA (2004). Recurrence and outcomes following hepatic resection, radiofrequency ablation, and combined resection/ablation for colorectal liver metastases.
Ann Surg 239, 818-25; discussion 825-7.

Abitabile P & Maurer CA (2010). Radiofrequency ablation of liver tumors: a novel needle perfusion technique enhances efficiency. *J Surg Res* 159, 532-537.

Adam R, Akpinar E, Johann M, Kunstlinger F, Majno P & Bismuth H (1997). Place of cryosurgery in the treatment of malignant liver tumors. *Ann Surg* 225, 39-8; discussion 48-50.

Adam R, Laurent A, Azoulay D, Castaing D & Bismuth H (2000). Two-stage hepatectomy: A planned strategy to treat irresectable liver tumors. *Ann Surg* 232, 777-785.

Adam R, Avisar E, Ariche A, Giachetti S, Azoulay D, Castaing D, Kunstlinger F, Levi F & Bismuth F (2001). Five-year survival following hepatic resection after neoadjuvant therapy for nonresectable colorectal [Liver] Metastases. *Ann Surg Oncol* 8, 347-353.

Ahmad F, Gravante G, Bhardwaj N, Strickland A, Basit R, West K, Sorge R, Dennison AR & Lloyd DM (2010). Large volume hepatic microwave ablation elicits fewer pulmonary changes than radiofrequency or cryotherapy. *J Gastrointest Surg* 14, 1963-1968.

Ahmad F, Gravante G, Bhardwaj N, Strickland A, Basit R, West K, Sorge R, Dennison AR & Lloyd DM (2010). Changes in interleukin-1beta and 6 after hepatic microwave tissue ablation compared with radiofrequency, cryotherapy and surgical resections. *Am J Surg* 200, 500-506.

Ahmad SA (2004). Limitations of radiofrequency ablation in treating liver metastases: a lesson in geometry. *Ann Surg Oncol* 11, 358-359.

Ahmed M, Lobo SM, Weinstein J, Kruskal JB, Gazelle GS, Halpern EF, Afzal SK, Lenkinski RE & Goldberg SN (2002). Improved coagulation with saline solution pretreatment during radiofrequency tumor ablation in a canine model. *J Vasc Interv Radiol* 13, 717-724.

Ahmed M, Weinstein J, Liu Z, Afzal KS, Horkan C, Kruskal JB & Goldberg SN (2003). Image-guided percutaneous chemical and radiofrequency tumor ablation in an animal model. *J Vasc Interv Radiol* 14, 1045-1052.

Ahmed M, Monsky WE, Girnun G, Lukyanov A, D'Ippolito G, Kruskal JB, Stuart KE, Torchilin VP & Goldberg SN (2003). Radiofrequency thermal ablation sharply increases intratumoral liposomal doxorubicin accumulation and tumor coagulation. *Cancer Res* 63, 6327-6333.

Ahmed M, Liu Z, Afzal KS, Weeks D, Lobo SM, Kruskal JB, Lenkinski RE & Goldberg SN (2004). Radiofrequency ablation: effect of surrounding tissue composition on coagulation necrosis in a canine tumor model. *Radiology* 230, 761-767.

Ahmed M & Goldberg SN (2004). Combination radiofrequency thermal ablation and adjuvant IV liposomal doxorubicin increases tissue coagulation and intratumoural drug accumulation. *Int J Hyperthermia* 20, 781-802.

Ahmed M, Liu Z, Lukyanov AN, Signoretti S, Horkan C, Monsky WL, Torchilin VP & Goldberg SN (2005). Combination radiofrequency ablation with intratumoral liposomal doxorubicin: effect on drug accumulation and coagulation in multiple tissues and tumor types in animals. *Radiology* 235, 469-477.

Ahmed M, Lukyanov AN, Torchilin V, Tournier H, Schneider AN & Goldberg SN (2005). Combined radiofrequency ablation and adjuvant liposomal chemotherapy: effect of chemotherapeutic agent, nanoparticle size, and circulation time. *J Vasc Interv Radiol* 16, 1365-1371.

Akahane M, Koga H, Kato N, Yamada H, Uozumi K, Tateishi R, Teratani T, Shiina S & Ohtomo K (2005). Complications of percutaneous radiofrequency ablation for hepato-cellular carcinoma: imaging spectrum and management. *Radiographics* 25 Suppl 1, S57-68.

Al-Sakere B, Andre F, Bernat C, Connault E, Opolon P, Davalos RV, Rubinsky B & Mir LM (2007). Tumor ablation with irreversible electroporation. *PLoS One* 2, e1135.

Alava MA, Gonzalez-Ramon N, Heegaard P, Guzylack S, Toussaint MJM, Lipperheide C, Madec F, Gruys E, Eckersall PD, Lampreave F & Pineiro A (1997). Pig-MAP, Porcine Acute Phase Proteins and Standardisation of Assays in Europe. *Comparative Haematology International* 7, 208-213.

Amin Z, Harries SA, Lees WR & Bown SG (1993). Interstitial tumour photocoagulation. *Endosc Surg Allied Technol* 1, 224-229.

Amin Z, Donald JJ, Masters A, Kant R, Steger AC, Bown SG & Lees WR (1993). Hepatic metastases: interstitial laser photocoagulation with real-time US monitoring and dynamic CT evaluation of treatment. *Radiology* 187, 339-347.

Amin Z, Bown SG & Lees WR (1993). Local treatment of colorectal liver metastases: a comparison of interstitial laser photocoagulation (ILP) and percutaneous alcohol injection (PAI). *Clin Radiol* 48, 166-171.

Anderson EM, Lees WR & Gillams AR (2009). Early indicators of treatment success after percutaneous radiofrequency of pulmonary tumors. *Cardiovasc Intervent Radiol* 32, 478-483.

Arellano RS, Flanders VL, Lee SI, Mueller PR & Gervais DA (2010). Imaging-guided percutaneous radiofrequency ablation of retroperitoneal metastatic disease in patients with gynecologic malignancies: clinical experience with eight patients.
AJR Am J Roentgenol 194, 1635-1638.

Arienti V & Pretolani S (2006). Complication rates of ablation therapies for hepatocellular carcinoma: a difficult comparison with an easy solution. *Gut* 55, 1211-1212.

Arienti V, Pretolani S, Goldberg SN, Silverman SG, Gervais DA, Lencioni R, Sacks D & Dupuy D (2006). How to report and compare complications of image-guided ablation therapies: comments on seeding and the use of a sole common denominator for liver tumors.
Radiology 241, 625-6; author reply 626-7.

Arienti V, Pretolani S, Pacella CM, Magnolfi F, Caspani B, Francica G, Megna AS, Regine R, Sponza M, Antico E & Di Lascio FM (2008). Complications of laser ablation for hepatocellular carcinoma: a multicenter study. *Radiology* 246, 947-955.

Aube C, Schmidt D, Brieger J, Schenk M, Kroeber S, Vielle B, Claussen CD, Goldberg SN & Pereira PL (2007). Influence of NaCl concentrations on coagulation, temperature, and electrical conductivity using a perfusion radiofrequency ablation system: an ex vivo experimental study. *Cardiovasc Intervent Radiol* 30, 92-97.

Azavedo E, Svane G & Nordenstrom B (1991). Radiological evidence of response to electrochemical treatment of breast cancer. *Clin Radiol* 43, 84-87.

B

Barnett CC & Curley SA (2002). Ablation Techniques: Ethanol Injection, Cryoablation and Radiofrequency Ablation. *Operative Techniques in General Surgery* 4, 65-75.

Baxter PS, Wemyss-Holden SA, Dennison AR & Maddern GJ (1998). Electrochemically induced hepatic necrosis: the next step forward in patients with unresectable liver tumours? *Aust N Z J Surg* 68, 637-640.

Bence LM, Eckersall PD, Vahe V, Gardner JP & O'Brien P (2004). Development of an Enzyme Linked Immunosorbent Assay (ELISA) for measurment of rat alpha-2-macroglobulin. *Veterinary Clinical Pathology* 33, 265.

Berendson J & Simonsson D (1994). Electrochemical aspects of treatment of tissue with direct current. *Eur J Surg Suppl* 111-115.

Berendson J & Olsson JM (1998). Bioelectrochemical aspects of the treatment of tissue with direct current. *Electromagnetic Biology and Medicine* 17, 1-16.

Bhardwaj N, Strickland AD, Ahmad F, Atanesyan L, West K & Lloyd DM (2009). A comparative histological evaluation of the ablations produced by microwave, cryotherapy and radiofrequency in the liver. *Pathology* 41, 168-172.

Bhardwaj N, Gravante G, Strickland AD, Ahmad F, Dormer J, Dennison AR & Lloyd DM (2010). Cryotherapy of the liver: a histological review. *Cryobiology* 61, 1-9.

Bilbao JI, Garrastachu P, Herraiz MJ, Rodriguez M, Inarrairaegui M, Rodriguez J, Hernandez C, de la Cuesta AM, Arbizu J & Sangro B (2010). Safety and efficacy assessment of flow redistribution by occlusion of intrahepatic vessels prior to radioembolization in the treatment of liver tumors. *Cardiovasc Intervent Radiol* 33, 523-531.

Boaz TL, Lewin JS, Chung YC, Duerk JL, Clampitt ME & Haaga JR (1998). MR monitoring of MR-guided radiofrequency thermal ablation of normal liver in an animal model. *J Magn Reson Imaging* 8, 64-69.

Boehm T, Malich A, Goldberg SN, Hauff P, Reinhardt M, Reichenbach JR, Muller W, Fleck M, Seifert B & Kaiser WA (2002). Radio-frequency ablation of VX2 rabbit tumors: assessment of completeness of treatment by using contrast-enhanced harmonic power Doppler US. *Radiology* 225, 815-821.

Boehm T, Malich A, Goldberg SN, Reichenbach JR, Hilger I, Hauff P, Reinhardt M, Fleck M & Kaiser WA (2002). Radio-frequency tumor ablation: internally cooled electrode versus saline-enhanced technique in an aggressive rabbit tumor model. *Radiology* 222, 805-813.

Boss A, Clasen S, Kuczyk M, Anastasiadis A, Schmidt D, Graf H, Schick F, Claussen CD & Pereira PL (2005). Magnetic resonance-guided percutaneous radiofrequency ablation of renal cell carcinomas: a pilot clinical study. *Invest Radiol* 40, 583-590.

Boss A, Rempp H, Martirosian P, Clasen S, Schraml C, Stenzl A, Claussen CD, Schick F & Pereira PL (2008). Wide-bore 1.5 Tesla MR imagers for guidance and monitoring of radiofrequency ablation of renal cell carcinoma: initial experience on feasibility. *Eur Radiol* 18, 1449-1455.

Bouza C, Lopez-Cuadrado T, Alcazar R, Saz-Parkinson Z & Amate JM (2009). Meta-analysis of percutaneous radiofrequency ablation versus ethanol injection in hepatocellular carcinoma. *BMC Gastroenterol* 9, 31.

Brace CL, Laeseke PF, van der Weide DW & Lee FT (2005). Microwave Ablation With a Triaxial Antenna: Results in ex vivo Bovine Liver. *IEEE Trans Microw Theory Tech* 53, 215-220.

Brace CL, Laeseke PF, Sampson LA, Frey TM, van der Weide DW & Lee FTJ (2007). Microwave ablation with a single small-gauge triaxial antenna: in vivo porcine liver model. *Radiology* 242, 435-440.

Brace CL, Laeseke PF, Sampson LA, Frey TM, van der Weide DW & Lee FTJ (2007). Microwave ablation with multiple simultaneously powered small-gauge triaxial antennas: results from an in vivo swine liver model. *Radiology* 244, 151-156.

Brace CL, Sampson LA, Hinshaw JL, Sandhu N & Lee FTJ (2009). Radiofrequency ablation: simultaneous application of multiple electrodes via switching creates larger, more confluent ablations than sequential application in a large animal model. *J Vasc Interv Radiol* 20, 118-124.

Brace CL, Hinshaw JL, Laeseke PF, Sampson LA & Lee FTJ (2009). Pulmonary thermal ablation: comparison of radiofrequency and microwave devices by using gross pathologic and CT findings in a swine model. *Radiology* 251, 705-711.

Brace CL, Diaz TA, Hinshaw JL & Lee FTJ (2010). Tissue contraction caused by radiofrequency and microwave ablation: a laboratory study in liver and lung. *J Vasc Interv Radiol* 21, 1280-1286.

Breen MS, Lazebnik RS, Fitzmaurice M, Nour SG, Lewin JS & Wilson DL (2004). Radiofrequency thermal ablation: correlation of hyperacute MR lesion images with tissue response. *J Magn Reson Imaging* 20, 475-486.

Brennan DD, Appelbaum L, Raptopolous V, Kruskal JB & Goldberg SN (2006). CT artifact introduced by radiofrequency ablation. *AJR Am J Roentgenol* 186, S284-6.

Brennan DD, Ganguli S, Brecher CW & Goldberg SN (2008). Thinking outside the abdominal box: safe use of the epipericardial fat pad window for percutaneous radiofrequency ablation of hepatic dome tumors. *J Vasc Interv Radiol* 19, 133-136.

Brillet PY, Paradis V, Brancatelli G, Rangheard AS, Consigny Y, Plessier A, Durand F, Belghiti J, Sommacale D & Vilgrain V (2006). Percutaneous radiofrequency ablation for hepatocellular carcinoma before liver transplantation: a prospective study with histopathologic comparison. *AJR Am J Roentgenol* 186, S296-305.

Brown DB (2005). Concepts, considerations, and concerns on the cutting edge of radiofrequency ablation. *J Vasc Interv Radiol* 16, 597-613.

Bruix J, Sherman M, Llovet JM, Beaugrand M, Lencioni R, Burroughs AK, Christensen E, Pagliaro L, Colombo M & Rodes J (2001). Clinical management of hepatocellular carcinoma. Conclusions of the Barcelona-2000 EASL conference. European Association for the Study of the Liver. *J Hepatol* 35, 421-430.

Brunello F, Veltri A, Carucci P, Pagano E, Ciccone G, Moretto P, Sacchetto P, Gandini G & Rizzetto M (2008). Radiofrequency ablation versus ethanol injection for early hepatocellular carcinoma: A randomized controlled trial. *Scand J Gastroenterol* 43, 727-735.

Buijs M, Vossen JA, Frangakis C, Hong K, Georgiades CS, Chen Y, Liapi E & Geschwind JF (2008). Nonresectable hepatocellular carcinoma: long-term toxicity in patients treated with transarterial chemoembolization--single-center experience. *Radiology* 249, 346-354.

Burdio F, Guemes A, Burdio JM, Navarro A, Sousa R, Castiella T, Cruz I, Burzaco O, Guirao X & Lozano R (2003). Large hepatic ablation with bipolar saline-enhanced radiofrequency: an experimental study in in vivo porcine liver with a novel approach. *J Surg Res* 110, 193-201.

Burdio F, Guemes A, Burdio JM, Navarro A, Sousa R, Castiella T, Cruz I, Burzaco O & Lozano R (2003). Bipolar saline-enhanced electrode for radiofrequency ablation: results of experimental study of in vivo porcine liver. *Radiology* 229, 447-456.

Buy X, Basile A, Bierry G, Cupelli J & Gangi A (2006). Saline-infused bipolar radiofrequency ablation of high-risk spinal and paraspinal neoplasms. *AJR Am J Roentgenol* 186, S322-6.

C

Cabassa P, Donato F, Simeone F, Grazioli L & Romanini L (2006). Radiofrequency ablation of hepatocellular carcinoma: long-term experience with expandable needle electrodes. *AJR Am J Roentgenol* 186, S316-21.

Callstrom MR & Charboneau JW (2008). Technologies for ablation of hepatocellular carcinoma. *Gastroenterology* 134, 1831-1835.

Cancer Research UK (14 Aug 2009). UK Liver Cancer incidence Statistics, London UK, accessed 28 Oct 2009, http://www.cancerresearchuk.org

Carrafiello G, Lagana D, Mangini M, Fontana F, Dionigi G, Boni L, Rovera F, Cuffari S & Fugazzola C (2008). Microwave tumors ablation: principles, clinical applications and review of preliminary experiences. *Int J Surg* 6 Suppl 1, S65-9.

Celsion Corporation (10 Aug 2010). Phase III Study of ThermoDox With Radiofrequency Ablation (RFA) in Treatment of Hepatocellular Carcinoma (HCC), New York, USA, accessed 30 Oct 2010, http://www.clinicaltrials.gov

Ceron JJ, Eckersall PD & Martynez-Subiela S (2005). Acute phase proteins in dogs and cats: current knowledge and future perspectives. *Vet Clin Pathol* 34, 85-99.

Cha J, Choi D, Lee MW, Rhim H, Kim YS, Lim HK, Yoon JH & Park CK (2009). Radiofrequency ablation zones in ex vivo bovine and in vivo porcine livers: comparison of the use of internally cooled electrodes and internally cooled wet electrodes. *Cardiovasc Intervent Radiol* 32, 1235-1240.

Chang I, Mikityansky I, Wray-Cahen D, Pritchard WF, Karanian JW & Wood BJ (2004). Effects of perfusion on radiofrequency ablation in swine kidneys. *Radiology* 231, 500-505.

Chen MH, Yang W, Yan K, Zou MW, Solbiati L, Liu JB & Dai Y (2004). Large liver tumors: protocol for radiofrequency ablation and its clinical application in 110 patients--mathematic model, overlapping mode, and electrode placement process. *Radiology* 232, 260-271.

Chen TL, Wu CH, Chen TG, Tai YT, Chang HC & Lin CJ (2000). Effects of propofol on functional activities of hepatic and extrahepatic conjugation enzyme systems. *Br J Anaesth* 84, 771-776.

Cheng BQ, Jia CQ, Liu CT, Fan W, Wang QL, Zhang ZL & Yi CH (2008). Chemoembolization combined with radiofrequency ablation for patients with hepatocellular carcinoma larger than 3 cm: a randomized controlled trial. *JAMA* 299, 1669-1677.

Cheng Z, Xiao Q, Wang Y, Sun Y, Lu T & Liang P (2010). 915MHz microwave ablation with implanted internal cooled-shaft antenna: Initial experimental study in in vivo porcine livers. *Eur J Radiol* Jan 12, [Epub].

Cheung TT, Ng KK, Poon RT & Fan ST (2009). Tolerance of radiofrequency ablation by patients of hepatocellular carcinoma. *J Hepatobiliary Pancreat Surg* 16, 655-660.

Chiu YC, Chuang CH, Tsai HM & Chen CY (2009). Massive hepatic infarction after pure ethanol injection and radiofrequency ablation therapy for hepatocellular carcinoma: a case report. *Kaohsiung J Med Sci* 25, 156-159.

Cho YK, Rhim H, Ahn YS, Kim MY & Lim HK (2006). Percutaneous radiofrequency ablation therapy of hepatocellular carcinoma using multitined expandable electrodes: comparison of subcapsular and nonsubcapsular tumors. *AJR Am J Roentgenol* 186, S269-74.

Cho YK, Kim JK, Kim MY, Rhim H & Han JK (2009). Systematic review of randomized trials for hepatocellular carcinoma treated with percutaneous ablation therapies. *Hepatology* 49, 453-459.

Choi D, Lim HK, Kim SH, Lee WJ, Jang HJ, Lee JY, Paik SW, Koh KC & Lee JH (2000). Hepatocellular carcinoma treated with percutaneous radio-frequency ablation: usefulness of power Doppler US with a microbubble contrast agent in evaluating therapeutic response-preliminary results. *Radiology* 217, 558-563.

Choi D, Lim HK, Kim MJ, Lee SH, Kim SH, Lee WJ, Lim JH, Joh JW & Kim YI (2004). Recurrent hepatocellular carcinoma: percutaneous radiofrequency ablation after hepatectomy. *Radiology* 230, 135-141.

Chua TC, Sarkar A, Saxena A, Glenn D, Zhao J & Morris DL (2010). Long-term outcome of image-guided percutaneous radiofrequency ablation of lung metastases: an open-labeled prospective trial of 148 patients. *Ann Oncol* 21, 2017-2022.

Chung YC, Duerk JL, Shankaranarayanan A, Hampke M, Merkle EM & Lewin JS (1999). Temperature measurement using echo-shifted FLASH at low field for interventional MRI. *J Magn Reson Imaging* 9, 138-145.

Clasen S, Boss A, Schmidt D, Fritz J, Schraml C, Claussen CD & Pereira PL (2006). Magnetic resonance imaging for hepatic radiofrequency ablation. *Eur J Radiol* 59, 140-148.

Clasen S, Schmidt D, Boss A, Dietz K, Krober SM, Claussen CD & Pereira PL (2006). Multipolar radiofrequency ablation with internally cooled electrodes: experimental study in ex vivo bovine liver with mathematic modeling. *Radiology* 238, 881-890.

Clasen S, Schmidt D, Dietz K, Boss A, Krober SM, Schraml C, Fritz J, Claussen CD & Pereira PL (2007). Bipolar radiofrequency ablation using internally cooled electrodes in ex vivo bovine liver: prediction of coagulation volume from applied energy. *Invest Radiol* 42, 29-36.

Cockburn JF, Maddern GJ & Wemyss-Holden SA (2007). Bimodal electric tissue ablation (BETA) - in-vivo evaluation of the effect of applying direct current before and during radiofrequency ablation of porcine liver. *Clin Radiol* 62, 213-220.

Cosman ER, Nashold BS & Ovelman-Levitt J (1984). Theoretical aspects of radiofrequency lesions in the dorsal root entry zone. *Neurosurgery* 15, 945-950.

Court FG, Wemyss-Holden SA, Morrison CP, Teague BD, Laws PE, Kew J, Dennison AR & Maddern GJ (2003). Segmental nature of the porcine liver and its potential as a model for experimental partial hepatectomy. *Br J Surg* 90, 440-444.

Court FG, Laws PE, Morrison CP, Teague BD, Metcalfe MS, Wemyss-Holden SA, Dennison AR & Maddern GJ (2004). Subtotal hepatectomy: a porcine model for the study of liver regeneration. *J Surg Res* 116, 181-186.

Curley MG & Hamilton PS (1997). Creation of large thermal lesions in liver using saline-enhanced RFablation. *Engineering in Medicine and Biology Society. Proceedings of the 19th Annual International Conference of the IEEE* 6, 2516-2519.

D

D'Ippolito G & Goldberg SN (2002). Radiofrequency ablation of hepatic tumors. *Tech Vasc Interv Radiol* 5, 141-155.

D'Ippolito G, Ahmed M, Girnun GD, Stuart KE, Kruskal JB, Halpern EF & Goldberg SN (2003). Percutaneous tumor ablation: reduced tumor growth with combined radio-frequency ablation and liposomal doxorubicin in a rat breast tumor model. *Radiology* 228, 112-118.

Davalos RV, Rubinsky B & Mir LM (2003). Theoretical analysis of the thermal effects during in vivo tissue electroporation. *Bioelectrochemistry* 61, 99-107.

Davalos RV, Mir IL & Rubinsky B (2005). Tissue ablation with irreversible electroporation. *Ann Biomed Eng* 33, 223-231.

Davalos RV & Rubinsky B (2008) Temperature considerations during irreversible electroporation. *Int J Heat Mass Transfer* 51, 5617-5622.

David SL, Absolom DR, Smith CR, Gams J & Herbert MA (1985). Effect of low level direct current on in vivo tumor growth in hamsters. *Cancer Res* 45, 5625-5631.

de Baere T, Denys A, Wood BJ, Lassau N, Kardache M, Vilgrain V, Menu Y & Roche A (2001). Radiofrequency liver ablation: experimental comparative study of water-cooled versus expandable systems. *AJR Am J Roentgenol* 176, 187-192.

de Baere T, Deschamps F, Briggs P, Dromain C, Boige V, Hechelhammer L, Abdel-Rehim M, Auperin A, Goere D & Elias D (2008). Hepatic malignancies: percutaneous radiofrequency ablation during percutaneous portal or hepatic vein occlusion. *Radiology* 248, 1056-1066.

De Sanctis JT, Goldberg SN & Mueller PR (1998). Percutaneous treatment of hepatic neoplasms: A review of current techniques. *Cardiovasc Intervent Radiol* 21, 273-296.

Decadt B & Siriwardena AK (2004). Radiofrequency ablation of liver tumours: systematic review. *Lancet Oncol* 5, 550-560.

Delis S, Bramis I, Triantopoulou C, Madariaga J & Dervenis C (2006). The imprint of radiofrequency in the management of hepatocellular carcinoma. *HPB (Oxford)* 8, 255-263.

Dev SB & Hofmann GA (1994). Electrochemotherapy--a novel method of cancer treatment. *Cancer Treat Rev* 20, 105-115.

Di Stasi M, Buscarini L, Livraghi T, Giorgio A, Salmi A, De Sio I, Brunello F, Solmi L, Caturelli E, Magnolfi F, Caremani M & Filice C (1997). Percutaneous ethanol injection in the treatment of hepatocellular carcinoma. A multicenter survey of evaluation practices and complication rates. *Scand J Gastroenterol* 32, 1168-1173.

Dick EA, Joarder R, de Jode M, Taylor-Robinson SD, Thomas HC, Foster GR & Gedroyc WM (2003). MR-guided laser thermal ablation of primary and secondary liver tumours. *Clin Radiol* 58, 112-120.

Dobbins C, Brennan C, Wemyss-Holden S, Cockburn J & Maddern G (2008). Bimodal electric tissue ablation-long term studies of morbidity and pathological change. *J Surg Res* 148, 251-259.

Dobbins C, Wemyss-Holden SA, Cockburn J & Maddern GJ (2008). Bimodal electric tissue ablation-modified radiofrequency ablation with a le veen electrode in a pig model. *J Surg Res* 144, 111-116.

Dobbins C, Brennan C, Wemyss-Holden SA, Cockburn J & Maddern GJ (2008). Bimodal electric tissue ablation: positive electrode studies. *ANZ J Surg* 78, 568-572.

Dobryszycka W (1997). Biological functions of haptoglobin--new pieces to an old puzzle. *Eur J Clin Chem Clin Biochem* 35, 647-654.

Dodd GDr, Soulen MC, Kane RA, Livraghi T, Lees WR, Yamashita Y, Gillams AR, Karahan OI & Rhim H (2000). Minimally invasive treatment of malignant hepatic tumors: at the threshold of a major breakthrough. *Radiographics* 20, 9-27.

Dodd GDr, Napier D, Schoolfield JD & Hubbard L (2005). Percutaneous radiofrequency ablation of hepatic tumors: postablation syndrome. *AJR Am J Roentgenol* 185, 51-57.

Dominguez-Escrig JL, Sahadevan K & Johnson P (2008). Cryoablation for Small Renal Masses. Advances in Urology, vol. 2008, Article ID 479495, 10 pages, 2008. doi:10.1155/2008

Dubinsky TJ, Cuevas C, Dighe MK, Kolokythas O & Hwang JH (2008). High-intensity focused ultrasound: current potential and oncologic applications. *AJR Am J Roentgenol* 190, 191-199.

Dupuy DE & Goldberg SN (2001). Image-guided radiofrequency tumor ablation: challenges and opportunities--part II. *J Vasc Interv Radiol* 12, 1135-1148.

Dupuy DE (2009). Microwave ablation compared with radiofrequency ablation in lung tissue-is microwave not just for popcorn anymore? *Radiology* 251, 617-618.

E

Eckersall PD, Saini PK & McComb C (1996). The acute phase response of acid soluble glycoprotein, alpha(1)-acid glycoprotein, ceruloplasmin, haptoglobin and C-reactive protein, in the pig. *Vet Immunol Immunopathol* 51, 377-385.

Eckersall PD, Duthie S, Toussaint MJ, Gruys E, Heegaard P, Alava M, Lipperheide C & Madec F (1999). Standardization of diagnostic assays for animal acute phase proteins. *Adv Vet Med* 41, 643-655.

Eckersall PD, Rodgers J, Murray M & Kennedy PG (1999). Haptoglobin, the acute phase response and natural human immunity to trypanosomes. *Parasitol Today* 15(6), 251-252.

Eckersall PD (2000). Recent advances and future prospects for the use of acute phase proteins as markers of disease in animals. *Revue De Medicine Veterinaire* 151, 577-584.

Eckersall PD (2004). The time is right for acute phase protein assays. *Vet J* 168, 3-5.

Edd JF, Horowitz L, Davalos RV, Mir LM & Rubinsky B (2006). In vivo results of a new focal tissue ablation technique: irreversible electroporation. *IEEE Trans Biomed Eng* 53, 1409-1415.

El-Serag HB & Rudolph KL (2007). Hepatocellular carcinoma: epidemiology and molecular carcinogenesis. *Gastroenterology* 132, 2557-2576.

Erinjeri JP & Clark TW (2010). Cryoablation: mechanism of action and devices. *J Vasc Interv Radiol* 21, S187-91.

Esser AT, Smith KC, Gowrishankar TR & Weaver JC (2007). Towards solid tumor treatment by irreversible electroporation: intrinsic redistribution of fields and currents in tissue. *Technol Cancer Res Treat* 6, 261-274.

F

Finch JG, Fosh BG, Anthony AA, Texler M, Pearson S, Dennison AR & Maddern GJ (2004). The use of a "liquid" electrode in hepatic electrolysis. *J Surg Res* 120, 272-277.

Flanders VL & Gervais DA (2010). Ablation of liver metastases: current status. *J Vasc Interv Radiol* 21, S214-22.

Fosh BG, Finch JG, Lea M, Black C, Wong S, Wemyss-Holden S & Maddern GJ (2002). Use of electrolysis as an adjunct to liver resection. *Br J Surg* 89, 999-1002.

Frericks BB, Ritz JP, Roggan A, Wolf KJ & Albrecht T (2005). Multipolar radiofrequency ablation of hepatic tumors: initial experience. *Radiology* 237, 1056-1062.

Frieser M, Haensler J, Schaber S, Peters A, Mohelsky E, Bernatik T, Hahn EG & Strobel D (2004). Radiofrequency ablation of liver tumors: how to enlarge the necrotic zones? *Eur Surg Res* 36, 357-361.

Fuentes D, Cardan R, Stafford RJ, Yung J, Dodd GDr & Feng Y (2010). High-fidelity computer models for prospective treatment planning of radiofrequency ablation with in vitro experimental correlation. *J Vasc Interv Radiol* 21, 1725-1732.

G

Galandi D & Antes G (2004). Radiofrequency thermal ablation versus other interventions for hepatocellular carcinoma. *Cochrane Database Syst Rev* 4, CD003046.

Gao Y, Wang Y, Duan Y, Li C, Sun Y, Zhang D, Lu T & Liang P (2010). 915MHz microwave ablation with high output power in in vivo porcine spleens. *Eur J Radiol* **75**, 87-90.

Garrean S, Hering J, Saied A, Helton WS & Espat NJ (2008). Radiofrequency ablation of primary and metastatic liver tumors: a critical review of the literature. *Am J Surg* 195, 508-520.

Gazelle GS, Goldberg SN, Solbiati L & Livraghi T (2000). Tumor ablation with radio-frequency energy. *Radiology* 217, 633-646.

Gazelle GS, McMahon PM, Beinfeld MT, Halpern EF & Weinstein MC (2004). Metastatic colorectal carcinoma: cost-effectiveness of percutaneous radiofrequency ablation versus that of hepatic resection. *Radiology* 233, 729-739.

Gervais DA, McGovern FJ, Wood BJ, Goldberg SN, McDougal WS & Mueller PR (2000). Radio-frequency ablation of renal cell carcinoma: early clinical experience. *Radiology* 217, 665-672.

Gervais DA, Goldberg SN, Brown DB, Soulen MC, Millward SF & Rajan DK (2009). Society of interventional radiology position statement on percutaneous radiofrequency ablation for the treatment of liver tumors. *J Vasc Interv Radiol* 20, 3-8.

Gillams AR & Lees WR (2007). Analysis of the factors associated with radiofrequency ablation-induced pneumothorax. *Clin Radiol* 62, 639-644.

Gillams AR & Lees WR (2008). Five-year survival following radiofrequency ablation of small, solitary, hepatic colorectal metastases. *J Vasc Interv Radiol* 19, 712-717.

Gillams AR & Lees WR (2009). Five-year survival in 309 patients with colorectal liver metastases treated with radiofrequency ablation. *Eur Radiol* 19, 1206-1213.

Glaiberman CB, Pilgram TK & Brown DB (2005). Patient factors affecting thermal lesion size with an impedance-based radiofrequency ablation system. *J Vasc Interv Radiol* 16, 1341-1348.

Gleisner AL, Choti MA, Assumpcao L, Nathan H, Schulick RD & Pawlik TM (2008). Colorectal liver metastases: recurrence and survival following hepatic resection, radiofrequency ablation, and combined resection-radiofrequency ablation. *Arch Surg* 143, 1204-1212.

Golberg A & Rubinsky B (2010). A statistical model for multidimensional irreversible electroporation cell death in tissue. *Biomed Eng Online* 9, 13.

Goldberg SN, Gazelle GS, Dawson SL, Rittman WJ, Mueller PR & Rosenthal DI (1995). Tissue ablation with radiofrequency using multiprobe arrays. *Acad Radiol* 2, 670-674.

Goldberg SN, Gazelle GS, Dawson SL, Rittman WJ, Mueller PR & Rosenthal DI (1995). Tissue ablation with radiofrequency: effect of probe size, gauge, duration, and temperature on lesion volume. *Acad Radiol* 2, 399-404.

Goldberg SN, Gazelle GS, Solbiati L, Rittman WJ & Mueller PR (1996). Radiofrequency tissue ablation: increased lesion diameter with a perfusion electrode. *Acad Radiol* 3, 636-644.

Goldberg SN, Gazelle GS, Halpern EF, Rittman WJ, Mueller PR & Rosenthal DI (1996). Radiofrequency tissue ablation: importance of local temperature along the electrode tip exposure in determining lesion shape and size. *Acad Radiol* 3, 212-218.

Goldberg SN, Gazelle GS, Compton CC, Mueller PR & McLoud TC (1996). Radio-frequency tissue ablation of VX2 tumor nodules in the rabbit lung. *Acad Radiol* 3, 929-935.

Goldberg SN, Gazelle GS, Solbiati L, Livraghi T, Tanabe KK, Hahn PF & Mueller PR (1998). Ablation of liver tumors using percutaneous RF therapy. *AJR Am J Roentgenol* 170, 1023-1028.

Goldberg SN, Hahn PF, Halpern EF, Fogle RM & Gazelle GS (1998). Radio-frequency tissue ablation: effect of pharmacologic modulation of blood flow on coagulation diameter. *Radiology* 209, 761-767.

Goldberg SN, Hahn PF, Tanabe KK, Mueller PR, Schima W, Athanasoulis CA, Compton CC, Solbiati L & Gazelle GS (1998). Percutaneous radiofrequency tissue ablation: does perfusion-mediated tissue cooling limit coagulation necrosis? *J Vasc Interv Radiol* 9, 101-111.

Goldberg SN, Solbiati L, Hahn PF, Cosman E, Conrad JE, Fogle R & Gazelle GS (1998). Large-volume tissue ablation with radio frequency by using a clustered, internally cooled electrode technique: laboratory and clinical experience in liver metastases. *Radiology* 209, 371-379.

Goldberg SN, Stein MC, Gazelle GS, Sheiman RG, Kruskal JB & Clouse ME (1999). Percutaneous radiofrequency tissue ablation: optimization of pulsed-radiofrequency technique to increase coagulation necrosis. *J Vasc Interv Radiol* 10, 907-916.

Goldberg SN, Walovitch RC, Straub JA, Shore MT & Gazelle GS (1999). Radio-frequency-induced coagulation necrosis in rabbits: immediate detection at US with a synthetic microsphere contrast agent. *Radiology* 213, 438-444.

Goldberg SN, Kruskal JB, Oliver BS, Clouse ME & Gazelle GS (2000). Percutaneous tumor ablation: increased coagulation by combining radio-frequency ablation and ethanol instillation in a rat breast tumor model. *Radiology* 217, 827-831.

Goldberg SN, Gazelle GS & Mueller PR (2000). Thermal ablation therapy for focal malignancy: a unified approach to underlying principles, techniques, and diagnostic imaging guidance. *AJR Am J Roentgenol* 174, 323-331.

Goldberg SN, Solbiati L, Halpern EF & Gazelle GS (2000). Variables affecting proper system grounding for radiofrequency ablation in an animal model.*J Vasc Interv Radiol* 11, 1069-1075.

Goldberg SN, Ahmed M, Gazelle GS, Kruskal JB, Huertas JC, Halpern EF, Oliver BS & Lenkinski RE (2001). Radio-frequency thermal ablation with NaCl solution injection: effect of electrical conductivity on tissue heating and coagulation-phantom and porcine liver study. *Radiology* 219, 157-165.

Goldberg SN, Saldinger PF, Gazelle GS, Huertas JC, Stuart KE, Jacobs T & Kruskal JB (2001). Percutaneous tumor ablation: increased necrosis with combined radio-frequency ablation and intratumoral doxorubicin injection in a rat breast tumor model. *Radiology* 220, 420-427.

Goldberg SN (2001). Radiofrequency tumor ablation: principles and techniques. *Eur J Ultrasound* 13, 129-147.

Goldberg SN & Gazelle GS (2001). Radiofrequency tissue ablation: physical principles and techniques for increasing coagulation necrosis. *Hepatogastroenterology* 48, 359-367.

Goldberg SN & Solbiati L (2001). Tumor dissemination after radiofrequency ablation of hepatocellular carcinoma. *Hepatology* 34, 609; author reply 610-609; author reply 611.

Goldberg SN, Kamel IR, Kruskal JB, Reynolds K, Monsky WL, Stuart KE, Ahmed M & Raptopoulos V (2002). Radiofrequency ablation of hepatic tumors: increased tumor destruction with adjuvant liposomal doxorubicin therapy. *AJR Am J Roentgenol* 179, 93-101.

Goldberg SN & Ahmed M (2002). Minimally invasive image-guided therapies for hepatocellular carcinoma. *J Clin Gastroenterol* 35, S115-29.

Goldberg SN (2005). Science to practice: can we differentiate residual untreated tumor from tissue responses to heat following thermal tumor ablation? *Radiology* 234, 317-318.

Goldberg SN, Grassi CJ, Cardella JF, Charboneau JW, Dodd GDr, Dupuy DE, Gervais D, Gillams AR, Kane RA, Lee FTJ, Livraghi T, McGahan J, Phillips DA, Rhim H & Silverman SG (2005). Image-guided tumor ablation: standardization of terminology and reporting criteria. *Radiology* 235, 728-739.

Goldberg SN, Grassi CJ, Cardella JF, Charboneau JW, Dodd GDr, Dupuy DE, Gervais D, Gillams AR, Kane RA, Lee FTJ, Livraghi T, McGahan J, Phillips DA, Rhim H & Silverman SG (2005). Image-guided tumor ablation: standardization of terminology and reporting criteria. *J Vasc Interv Radiol* 16, 765-778.

Goldberg SN (2005). Is radiofrequency ablation effective in patients with early-stage hepatocellular carcinoma and cirrhosis? *Nat Clin Pract Oncol* 2, 438-439.

Gonzalez-Ramon N, Alava MA, Sarsa JA, Pineiro M, Escartin A, Garcia-Gil A, Lampreave F & Pineiro A (1995). The major acute phase serum protein in pigs is homologous to human plasma kallikrein sensitive PK-120. *FEBS Lett* 371, 227-230.

Grau-Roma L, Heegaard PM, Hjulsager CK, Sibila M, Kristensen CS, Allepuz A, Pineiro M, Larsen LE, Segales J & Fraile L (2009). Pig-major acute phase protein and haptoglobin serum concentrations correlate with PCV2 viremia and the clinical course of postweaning multisystemic wasting syndrome. *Vet Microbiol* 138, 53-61.

Gulesserian T, Mahnken AH, Schernthaner R, Memarsadeghi M, Weber M, Tacke A & Kettenbach J (2006). Comparison of expandable electrodes in percutaneous radiofrequency ablation of renal cell carcinoma. *Eur J Radiol* 59, 133-139.

Guo Y, Zhang Y, Nijm GM, Sahakian AV, Yang GY, Omary RA & Larson AC (2010). Irreversible Electroporation in the Liver: Contrast-enhanced Inversion-Recovery MR Imaging Approaches to Differentiate Reversibly Electroporated Penumbra from Irreversibly Electroporated Ablation Zones. *Radiology Dec* 3 [Epub]

Guo Y, Zhang Y, Klein R, Nijm GM, Sahakian AV, Omary RA, Yang GY & Larson AC (2010). Irreversible electroporation therapy in the liver: longitudinal efficacy studies in a rat model of hepatocellular carcinoma. *Cancer Res* 70, 1555-1563.

Gutierrez AM, Martinez-Subiela S, Montes A, Parra MD & Ceron JJ (2008). C-reactive protein measurements in meat juice of pigs. *Vet Immunol Immunopathol* 122, 250-255.

Gutierrez AM, Martinez-Subiela S & Ceron JJ (2009). Evaluation of an immunoassay for determination of haptoglobin concentration in various biological specimens from swine. *Am J Vet Res* 70, 691-696.

Gutierrez AM, Martinez-Subiela S, Eckersall PD & Ceron JJ (2009). C-reactive protein quantification in porcine saliva: a minimally invasive test for pig health monitoring. *Vet J* 181, 261-265.

H

Haar G & Coussios C (2007). High intensity focused ultrasound: past, present and future. *International Journal of Hyperthermia* 23, 85-87.

Haemmerich D, Lee FTJ, Schutt DJ, Sampson LA, Webster JG, Fine JP & Mahvi DM (2005). Large-volume radiofrequency ablation of ex vivo bovine liver with multiple cooled cluster electrodes. *Radiology* 234, 563-568.

Hakime A, Hines-Peralta A, Peddi H, Atkins MB, Sukhatme VP, Signoretti S, Regan M & Goldberg SN (2007). Combination of radiofrequency ablation with antiangiogenic therapy for tumor ablation efficacy: study in mice. *Radiology* 244, 464-470.

Hamazoe R, Hirooka Y, Ohtani S, Katoh T & Kaibara N (1995). Intraoperative microwave tissue coagulation as treatment for patients with nonresectable hepatocellular carcinoma. *Cancer* 75, 794-800.

Head HW, Dodd GDr, Dalrymple NC, Prasad SR, El-Merhi FM, Freckleton MW & Hubbard LG (2007). Percutaneous radiofrequency ablation of hepatic tumors against the diaphragm: frequency of diaphragmatic injury. *Radiology* 243, 877-884.

Heegaard PM, Godson DL, Toussaint MJ, Tjornehoj K, Larsen LE, Viuff B & Ronsholt L (2000). The acute phase response of haptoglobin and serum amyloid A (SAA) in cattle undergoing experimental infection with bovine respiratory syncytial virus. *Vet Immunol Immunopathol* 77, 151-159.

JM H (1993). sg:15 Sample size determination for means and proportions. *Stata Technical Bulletin* 11, 17-20.

Hines-Peralta A, Hollander CY, Solazzo S, Horkan C, Liu ZJ & Goldberg SN (2004). Hybrid radiofrequency and cryoablation device: preliminary results in an animal model. *J Vasc Interv Radiol* 15, 1111-1120.

Hines-Peralta A, Liu ZJ, Horkan C, Solazzo S & Goldberg SN (2006). Chemical tumor ablation with use of a novel multiple-tine infusion system in a canine sarcoma model. *J Vasc Interv Radiol* 17, 351-358.

Hines-Peralta A, Sukhatme V, Regan M, Signoretti S, Liu ZJ & Goldberg SN (2006). Improved tumor destruction with arsenic trioxide and radiofrequency ablation in three animal models. *Radiology* 240, 82-89.

Hines-Peralta AU, Pirani N, Clegg P, Cronin N, Ryan TP, Liu Z & Goldberg SN (2006). Microwave ablation: results with a 2.45-GHz applicator in ex vivo bovine and in vivo porcine liver. *Radiology* 239, 94-102.

Hinshaw JL, Laeseke PF, Winter TCr, Kliewer MA, Fine JP & Lee FTJ (2006). Radiofrequency ablation of peripheral liver tumors: intraperitoneal 5% dextrose in water decreases postprocedural pain. *AJR Am J Roentgenol* 186, S306-10.

Hinshaw JL, Lee FTJ, Laeseke PF, Sampson LA & Brace C (2010). Temperature isotherms during pulmonary cryoablation and their correlation with the zone of ablation. *J Vasc Interv Radiol* 21, 1424-1428.

Hiss S, Knura-Deszczka S, Regula G, Hennies M, Gymnich S, Petersen B & Sauerwein H (2003). Development of an enzyme immuno assay for the determination of porcine haptoglobin in various body fluids: testing the significance of meat juice measurements for quality monitoring programs. *Vet Immunol Immunopathol* 96, 73-82.

Hoffmann RT, Jakobs TF, Lubienski A, Schrader A, Trumm C, Reiser MF & Helmberger TK (2006). Percutaneous radiofrequency ablation of pulmonary tumors--is there a difference between treatment under general anaesthesia and under conscious sedation? *Eur J Radiol* 59, 168-174.

Hompes R, Fieuws S, Aerts R, Thijs M, Penninckx F & Topal B (2010). Results of single-probe microwave ablation of metastatic liver cancer. *Eur J Surg Oncol* 36, 725-730.

Hong K & Georgiades C (2010). Radiofrequency ablation: mechanism of action and devices. *J Vasc Interv Radiol* 21, S179-86.

Hope WW, Arru JM, McKee JQ, Vrochides D, Aswad B, Simon CJ, Dupuy DE & Iannitti DA (2007). Evaluation of mulitprobe radiofrequency technology in a porcine model. *HPB (Oxford)* 9, 363-367.

Hope WW, Schmelzer TM, Newcomb WL, Heath JJ, Lincourt AE, Norton HJ, Heniford BT & Iannitti DA (2009). Guidelines for power and time variables for microwave ablation in an in vivo porcine kidney. *J Surg Res* 153, 263-267.

Horadagoda NU, Knox KM, Gibbs HA, Reid SW, Horadagoda A, Edwards SE & Eckersall PD (1999). Acute phase proteins in cattle: discrimination between acute and chronic inflammation. *Vet Rec* 144, 437-441.

Horkan C, Ahmed M, Liu Z, Gazelle GS, Solazzo SA, Kruskal JB & Goldberg SN (2004). Radiofrequency ablation: Effect of pharmacologic modulation of hepatic and renal blood flow on coagulation diameter in a VX2 tumor model. *J Vasc Interv Radiol* 15, 269-274.

Horkan C, Dalal K, Coderre JA, Kiger JL, Dupuy DE, Signoretti S, Halpern EF & Goldberg SN (2005). Reduced tumor growth with combined radiofrequency ablation and radiation therapy in a rat breast tumor model. *Radiology* 235, 81-88.

Hsieh CB, Chang HM, Chen TW, Chen CJ, Chan DC, Yu JC, Liu YC, Chang TM & Shen KL (2004). Comparison of transcatheter arterial chemoembolization, laparoscopic radiofrequency ablation, and conservative treatment for decompensated cirrhotic patients with hepatocellular carcinoma. *World J Gastroenterol* 10, 505-508.

Huang J, Hernandez-Alejandro R, Croome KP, Yan L, Wu H, Chen Z, Prasoon P & Zeng Y (2010). Radiofrequency Ablation Versus Surgical Resection for Hepatocellular Carcinoma in Childs A Cirrhotics-a Retrospective Study of 1,061 Cases. *J Gastrointest Surg* Oct 30 [Epub]

Huang L, Han Y, Zhao J, Wang X, Cheng Q, Li X, Xu H & Gao K (2010). Is radiofrequency thermal ablation a safe and effective procedure in the treatment of pulmonary malignancies? *Eur J Cardiothorac Surg,* Jul 19 [Epub]

Hung BP (2009). Surgery or ablation for hepatocellular carcinoma. *Ann Surg* 249, 350.

Hung HH, Chiou YY, Hsia CY, Su CW, Chou YH, Chiang JH, Kao WY, Huo TI, Huang YH, Su YH, Lin HC, Lee SD & Wu JC (2010). Survival Rates Are Comparable After Radiofrequency Ablation or Surgery in Patients With Small Hepatocellular Carcinomas. *Clin Gastroenterol Hepatol,* Sep 8 [Epub]

Hur H, Ko YT, Min BS, Kim KS, Choi JS, Sohn SK, Cho CH, Ko HK, Lee JT & Kim NK (2009). Comparative study of resection and radiofrequency ablation in the treatment of solitary colorectal liver metastases. *Am J Surg* 197, 728-736.

Hynynen K & McDannold N (2004). MRI guided and monitored focused ultrasound thermal ablation methods: a review of progress. *Int J Hyperthermia* 20, 725-737.

I

Iannitti DA, Dupuy DE, Mayo-Smith WW & Murphy B (2002). Hepatic radiofrequency ablation. *Archives of Surgery* 137, 422-6; discussion 427.

Iannitti DA, Martin RC, Simon CJ, Hope WW, Newcomb WL, McMasters KM & Dupuy D (2007). Hepatic tumor ablation with clustered microwave antennae: the US Phase II Trial. *HPB (Oxford)* 9, 120-124.

Iwamoto T, Kawai N, Sato M, Tanihata H, Takasaka I, Minamiguchi H, Sahara S, Nakata K & Shirai S (2008). Effectiveness of hepatic arterial embolization on radiofrequency ablation volume in a swine model: relationship to portal venous flow and liver parenchymal pressure. *J Vasc Interv Radiol* 19, 1646-1651.

Izzo F (2003). Other thermal ablation techniques: microwave and interstitial laser ablation of liver tumors. *Ann Surg Oncol* 10, 491-497.

J

Jacobson M, Fellstrom C, Lindberg R, Wallgren P & Jensen-Waern M (2004). Experimental swine dysentery: comparison between infection models. *J Med Microbiol* 53, 273-280.

Jang HJ, Lee JY, Lee DH, Kim WH & Hwang JH (2010). Current and Future Clinical Applications of High-Intensity Focused Ultrasound (HIFU) for Pancreatic Cancer. *Gut Liver* 4, S57-S61.

Jansen MC, van Hillegersberg R, Chamuleau RA, van Delden OM, Gouma DJ & van Gulik TM (2005). Outcome of regional and local ablative therapies for hepatocellular carcinoma: a collective review. *Eur J Surg Oncol* 31, 331-347.

Jansen MC, van Wanrooy S, van Hillegersberg R, Rijken AM, van Coevorden F, Prevoo W & van Gulik TM (2008). Assessment of systemic inflammatory response (SIR) in patients undergoing radiofrequency ablation or partial liver resection for liver tumors. *Eur J Surg Oncol* 34, 662-667.

Jansen MC, van Hillegersberg R, Schoots IG, Levi M, Beek JF, Crezee H & van Gulik TM (2010). Cryoablation induces greater inflammatory and coagulative responses than radiofrequency ablation or laser induced thermotherapy in a rat liver model. *Surgery* 147, 686-695.

Jaskolka JD, Kachura JR, Hwang DM, Tsao MS, Waddell TK, Asch MR, Darling GE & Johnston MR (2010). Pathologic assessment of radiofrequency ablation of pulmonary metastases. *J Vasc Interv Radiol* 21, 1689-1696.

Jin C, Zhu H, Wang Z, Wu F, Chen W, Li K, Su H, Zhou K & Gong W (2010). High-intensity focused ultrasound combined with transarterial chemoembolization for unresectable hepatocellular carcinoma: Long-term follow-up and clinical analysis. *Eur J Radiol,* Sep 21 [Epub]

Jonasson R, Andersson M, Rasback T, Johannisson A & Jensen-Waern M (2006). Immunological alterations during the clinical and recovery phases of experimental swine dysentery. *J Med Microbiol* 55, 845-855.

Joosten J, Jager G, Oyen W, Wobbes T & Ruers T (2005). Cryosurgery and radiofrequency ablation for unresectable colorectal liver metastases. *Eur J Surg Oncol* 31, 1152-1159.

K

Kadivar F & Soulen MC (2010). Enhancing ablation: synergies with regional and systemic therapies. *J Vasc Interv Radiol* 21, S251-6.

Ke S, Ding XM, Kong J, Gao J, Wang SH, Cheng Y & Sun WB (2010). Low temperature of radiofrequency ablation at the target sites can facilitate rapid progression of residual hepatic VX2 carcinoma. *J Transl Med* 8, 73.

Kennedy A, Nag S, Salem R, Murthy R, McEwan AJ, Nutting C, Benson Ar, Espat J, Bilbao JI, Sharma RA, Thomas JP & Coldwell D (2007). Recommendations for radioembolization of hepatic malignancies using yttrium-90 microsphere brachytherapy: a consensus panel report from the radioembolization brachytherapy oncology consortium.
Int J Radiat Oncol Biol Phys 68, 13-23.

Kelekis AD, Thanos L, Mylona S, Ptohis N, Malagari K, Nikita A, Christodoulidou J & Kelekis N (2006). Percutaneous radiofrequency ablation of lung tumors with expandable needle electrodes: current status. *Eur Radiol* 16, 2471-2482.

Keserci BM, Kokuryo D, Suzuki K, Kumamoto E, Okada A, Khankan AA & Kuroda K (2006). Near-real-time feedback control system for liver thermal ablations based on self-referenced temperature imaging. *Eur J Radiol* 59, 175-182.

Kettenbach J, Kostler W, Rucklinger E, Gustorff B, Hupfl M, Wolf F, Peer K, Weigner M, Lammer J, Muller W & Goldberg SN (2003). Percutaneous saline-enhanced radiofrequency ablation of unresectable hepatic tumors: initial experience in 26 patients.
AJR Am J Roentgenol 180, 1537-1545.

Kettenbach J & Jolesz FA (2006). Editorial comment on percutaneous tumor ablation.
Eur J Radiol 59, 131-132.

Kim SH, Lim HK, Choi D, Lee WJ, Kim SH, Kim MJ, Kim CK, Jeon YH, Lee JM & Rhim H (2006). Percutaneous radiofrequency ablation of hepatocellular carcinoma: effect of histologic grade on therapeutic results. *AJR Am J Roentgenol* 186, S327-33.

Kim SK, Lim HK, Kim YH, Lee WJ, Lee SJ, Kim SH, Lim JH & Kim SA (2003). Hepatocellular carcinoma treated with radio-frequency ablation: spectrum of imaging findings. *Radiographics* 23, 107-121.

Kim SK, Lim HK, Ryu JA, Choi D, Lee WJ, Lee JY, Lee JH, Sung YM, Cho EY, Hong SM & Kim JS (2004). Radiofrequency ablation of rabbit liver in vivo: effect of the pringle maneuver on pathologic changes in liver surrounding the ablation zone. *Korean J Radiol* 5, 240-249.

Kim YK, Kim CS, Chung GH, Han YM, Lee SY, Jin GY & Lee JM (2006). Radiofrequency ablation of hepatocellular carcinoma in patients with decompensated cirrhosis: evaluation of therapeutic efficacy and safety. *AJR Am J Roentgenol* 186, S261-8.

Kinn AC, Nordenstrom BE, Elbarouni J & Nilsson I (1991). Effects of direct current on renal function. An experimental study in pigs. *Urol Res* 19, 397-400.

Kong WT, Zhang WW, Qiu YD, Zhou T, Qiu JL, Zhang W & Ding YT (2009). Major complications after radiofrequency ablation for liver tumors: analysis of 255 patients. *World J Gastroenterol* 15, 2651-2656.

Kopelman D, Inbar Y, Hanannel A, Freundlich D, Castel D, Perel A, Greenfeld A, Salamon T, Sareli M, Valeanu A & Papa M (2006). Magnetic resonance-guided focused ultrasound surgery (MRgFUS): ablation of liver tissue in a porcine model. *Eur J Radiol* 59, 157-162.

Kopelman D, Inbar Y, Hanannel A, Freundlich D, Vitek S, Schmidt R, Sokolov A, Hatoum OA & Rabinovici J (2006). Magnetic resonance-guided focused ultrasound surgery using an enhanced sonication technique in a pig muscle model. *Eur J Radiol* 59, 190-197.

Korpan NN (1997). Hepatic cryosurgery for liver metastases. Long-term follow-up. *Ann Surg* 225, 193-201.

Korpan NN (2008). Cryosurgery: Early Ultrastructural Changes in Liver Tissue In Vivo. *J Surg Res* 153, 54-65.

Kruse R, Essen-Gustavsson B, Fossum C & Jensen-Waern M (2008). Blood concentrations of the cytokines IL-1beta, IL-6, IL-10, TNF-alpha and IFN-gamma during experimentally induced swine dysentery. *Acta Vet Scand* 50, 32.

Kruskal JB, Oliver B, Huertas JC & Goldberg SN (2001). Dynamic intrahepatic flow and cellular alterations during radiofrequency ablation of liver tissue in mice. *J Vasc Interv Radiol* 12, 1193-1201.

Kuang M, Lu MD, Xie XY, Xu HX, Mo LQ, Liu GJ, Xu ZF, Zheng YL & Liang JY (2007). Liver cancer: increased microwave delivery to ablation zone with cooled-shaft antenna--experimental and clinical studies. *Radiology* 242, 914-924.

Kudo M (2010). Radiofrequency ablation for hepatocellular carcinoma: updated review in 2010. *Oncology* 78 Suppl 1, 113-124.

Kuehl H, Stattaus J, Hertel S, Hunold P, Kaiser G, Bockisch A & Forsting M (2008). Mid-term outcome of positron emission tomography/computed tomography-assisted radiofrequency ablation in primary and secondary liver tumours--a single-centre experience. *Clin Oncol (R Coll Radiol)* 20, 234-240.

Kuehl H, Antoch G, Stergar H, Veit-Haibach P, Rosenbaum-Krumme S, Vogt F, Frilling A, Barkhausen J & Bockisch A (2008). Comparison of FDG-PET, PET/CT and MRI for follow-up of colorectal liver metastases treated with radiofrequency ablation: initial results. *Eur J Radiol* 67, 362-371.

Kunkle DA & Uzzo RG (2008). Cryoablation or radiofrequency ablation of the small renal mass : a meta-analysis. *Cancer* 113, 2671-2680.

Kurup AN & Callstrom MR (2010). Ablation of skeletal metastases: current status. *J Vasc Interv Radiol* 21, S242-50.

Kuvshinoff BW & Ota DM (2002). Radiofrequency ablation of liver tumors: influence of technique and tumor size. *Surgery* 132, 605-11; discussion 611-2.

Kwon JH (2010). Is Percutaneous Ethanol Injection Therapy Still Effective for Hepatocellular Carcinoma in the Era of Radiofrequency Ablation? *Gut Liver* 4, S105-S112.

L

Laeseke PF, Sampson LA, Haemmerich D, Brace CL, Fine JP, Frey TM, Winter TCr & Lee FTJ (2005). Multiple-electrode radiofrequency ablation: simultaneous production of separate zones of coagulation in an in vivo porcine liver model. *J Vasc Interv Radiol* 16, 1727-1735.

Laeseke PF, Sampson LA, Brace CL, Winter TCr, Fine JP & Lee FTJ (2006). Unintended thermal injuries from radiofrequency ablation: protection with 5% dextrose in water. *AJR Am J Roentgenol* 186, S249-54.

Laeseke PF, Sampson LA, Haemmerich D, Brace CL, Fine JP, Frey TM, Winter TCr & Lee FTJ (2006). Multiple-electrode radiofrequency ablation creates confluent areas of necrosis: in vivo porcine liver results. *Radiology* 241, 116-124.

Laeseke PF, Sampson LA, Frey TM, Mukherjee R, Winter TCr, Lee FTJ & Brace CL (2007). Multiple-electrode radiofrequency ablation: comparison with a conventional cluster electrode in an in vivo porcine kidney model. *J Vasc Interv Radiol* 18, 1005-1010.

Lafon C, Melodelima D, Salomir R & Chapelon JY (2007). Interstitial devices for minimally invasive thermal ablation by high-intensity ultrasound. *Int J Hyperthermia* 23, 153-163.

Lau WY & Lai EC (2009). The current role of radiofrequency ablation in the management of hepatocellular carcinoma: a systematic review. *Ann Surg* 249, 20-25.

Laufer S, Ivorra A, Reuter VE, Rubinsky B & Solomon SB (2010). Electrical impedance characterization of normal and cancerous human hepatic tissue. *Physiol Meas* 31, 995-1009.

Lawes D, Chopada A, Gillams A, Lees W & Taylor I (2006). Radiofrequency ablation (RFA) as a cytoreductive strategy for hepatic metastasis from breast cancer.
Ann R Coll Surg Engl 88, 639-642.

Leblanc F, Fonck M, Brunet R, Becouarn Y, Mathoulin-Pelissier S & Evrard S (2008). Comparison of hepatic recurrences after resection or intraoperative radiofrequency ablation indicated by size and topographical characteristics of the metastases.
Eur J Surg Oncol 34, 185-190.

Lee EW, Loh CT & Kee ST (2007). Imaging guided percutaneous irreversible electroporation: ultrasound and immunohistological correlation. *Technol Cancer Res Treat* 6, 287-294.

Lee EW, Chen C, Prieto VE, Dry SM, Loh CT & Kee ST (2010). Advanced hepatic ablation technique for creating complete cell death: irreversible electroporation. *Radiology* 255, 426-433.

Lee EW, Thai S & Kee ST (2010). Irreversible Electroporation: A Novel Image-Guided Cancer Therapy. *Gut Liver* 4, S99-S104.

Lee JD, Lee JM, Kim SW, Kim CS & Mun WS (2001). MR imaging-histopathologic correlation of radiofrequency thermal ablation lesion in a rabbit liver model: observation during acute and chronic stages. *Korean J Radiol* 2, 151-158.

Lee JM, Han JK, Kim SH, Lee JY, Kim DJ, Lee MW, Cho GG, Han CJ & Choi BI (2004). Saline-enhanced hepatic radiofrequency ablation using a perfused-cooled electrode: comparison of dual probe bipolar mode with monopolar and single probe bipolar modes. *Korean J Radiol* 5, 121-127.

Lee JM, Jin GY, Goldberg SN, Lee YC, Chung GH, Han YM, Lee SY & Kim CS (2004). Percutaneous radiofrequency ablation for inoperable non-small cell lung cancer and metastases: preliminary report. *Radiology* 230, 125-134.

Lee JM, Kim YK, Kim SW, Han JK, Kim SH & Choi BI (2004). Combined radiofrequency ablation and acetic acid hypertonic saline solution instillation: an in vivo study of rabbit liver. *Korean J Radiol* 5, 31-38.

Lee JM, Lee YH, Kim YK, Kim SW, Kim SH, Han JK & Choi BI (2004). Combined treatment of radiofrequency ablation and acetic acid injection: an in vivo feasibility study in rabbit liver. *Eur Radiol* 14, 1303-1310.

Lee JM, Han JK, Kim SH, Lee JY, Choi SH & Choi BI (2004). Hepatic bipolar radiofrequency ablation using perfused-cooled electrodes: a comparative study in the ex vivo bovine liver. *Br J Radiol* 77, 944-949.

Lee JM, Han JK, Kim SH, Shin KS, Lee JY, Park HS, Hur H & Choi BI (2004). Comparison of wet radiofrequency ablation with dry radiofrequency ablation and radiofrequency ablation using hypertonic saline preinjection: ex vivo bovine liver. *Korean J Radiol* 5, 258-265.

Lee JM, Kim SH, Han JK, Sohn KL & Choi BI (2005). Ex vivo experiment of saline-enhanced hepatic bipolar radiofrequency ablation with a perfused needle electrode: comparison with conventional monopolar and simultaneous monopolar modes. *Cardiovasc Intervent Radiol* 28, 338-345.

Lee JM, Han JK, Eoh H, Kim SH, Lee JY, Lee MW & Choi BI (2006). Intraoperative radiofrequency ablation using a loop internally cooled-perfusion electrode: in vitro and in vivo experiments.
J Surg Res 131, 215-224.

Lee JM, Han JK, Lee JY, Kim SH, Choi JY, Lee MW, Choi SH, Eo H & Choi BI (2006). Hepatic radiofrequency ablation using multiple probes: ex vivo and in vivo comparative studies of monopolar versus multipolar modes. *Korean J Radiol* 7, 106-117.

Lee JM, Han JK, Chang JM, Chung SY, Kim SH, Lee JY, Lee MW & Choi BI (2006). Radiofrequency ablation of the porcine liver in vivo: increased coagulation with an internally cooled perfusion electrode. *Acad Radiol* 13, 343-352.

Lee JM, Han JK, Kim SH, Son KR, Kim HC, Kim SJ & Choi BI (2007). In vivo efficiency of multipolar radiofrequency ablation with two bipolar electrodes: a comparative experimental study in pig kidney. *J Vasc Interv Radiol* 18, 1553-1560.

Lee JM, Han JK, Kim HC, Choi YH, Kim SH, Choi JY & Choi BI (2007). Switching monopolar radiofrequency ablation technique using multiple, internally cooled electrodes and a multichannel generator: ex vivo and in vivo pilot study. *Invest Radiol* 42, 163-171.

Leen E & Horgan PG (2007). Radiofrequency ablation of colorectal liver metastases.
Surg Oncol 16, 47-51.

Leen E, Kumar S, Khan SA, Low G, Ong KO, Tait P & Averkiou M (2009). Contrast-enhanced 3D ultrasound in the radiofrequency ablation of liver tumors.
World J Gastroenterol 15, 289-299.

Lencioni R, Della Pina C & Bartolozzi C (2005). Percutaneous image-guided radiofrequency ablation in the therapeutic management of hepatocellular carcinoma.
Abdom Imaging 30, 401-408.

Lencioni R & Crocetti L (2007). Radiofrequency ablation of liver cancer.
Tech Vasc Interv Radiol 10, 38-46.

Lencioni R, Crocetti L, Cioni R, Suh R, Glenn D, Regge D, Helmberger T, Gillams AR, Frilling A, Ambrogi M, Bartolozzi C & Mussi A (2008). Response to radiofrequency ablation of pulmonary tumours: a prospective, intention-to-treat, multicentre clinical trial (the RAPTURE study). *Lancet Oncol* 9, 621-628.

Lencioni R, Crocetti L, Pina MC & Cioni D (2009). Percutaneous image-guided radiofrequency ablation of liver tumors. *Abdom Imaging* 34, 547-556.

Lencioni R, Crocetti L, Cioni D, Pina CD, Oliveri F, De Simone P, Brunetto M & Filipponi F (2010). Single-session percutaneous ethanol ablation of early-stage hepatocellular carcinoma with a multipronged injection needle: results of a pilot clinical study.
J Vasc Interv Radiol 21, 1533-1538.

Lepetit-Coiffe M, Laumonier H, Seror O, Quesson B, Sesay MB, Moonen CT, Grenier N & Trillaud H (2010). Real-time monitoring of radiofrequency ablation of liver tumors using thermal-dose calculation by MR temperature imaging: initial results in nine patients, including follow-up. *Eur Radiol* 20, 193-201.

Leslie TA & Kennedy JE (2007). High intensity focused ultrasound in the treatment of abdominal and gynaecological diseases. *Int J Hyperthermia* 23, 173-182.

LeVeen RF (1997). Laser hyperthermia and radiofrequency ablation of hepatic lesions. *Seminars in Interventional Radiology* 14, 313-324.

Lewandowski RJ, Wang D, Gehl J, Atassi B, Ryu RK, Sato K, Nemcek AAJ, Miller FH, Mulcahy MF, Kulik L, Larson AC, Salem R & Omary RA (2007). A comparison of chemoembolization endpoints using angiographic versus transcatheter intraarterial perfusion/MR imaging monitoring. *J Vasc Interv Radiol* 18, 1249-1257.

Lewin JS, Connell CF, Duerk JL, Chung YC, Clampitt ME, Spisak J, Gazelle GS & Haaga JR (1998). Interactive MRI-guided radiofrequency interstitial thermal ablation of abdominal tumors: clinical trial for evaluation of safety and feasibility. *J Magn Reson Imaging* 8, 40-47.

Li YY, Sha WH, Zhou YJ & Nie YQ (2007). Short and long term efficacy of high intensity focused ultrasound therapy for advanced hepatocellular carcinoma.
J Gastroenterol Hepatol 22, 2148-2154.

Liang HH, Chen MS, Peng ZW, Zhang YJ, Zhang YQ, Li JQ & Lau WY (2008). Percutaneous radiofrequency ablation versus repeat hepatectomy for recurrent hepatocellular carcinoma: a retrospective study. *Ann Surg Oncol* 15, 3484-3493.

Liang P, Wang Y, Yu X & Dong B (2009). Malignant liver tumors: treatment with percutaneous microwave ablation--complications among cohort of 1136 patients. *Radiology* 251, 933-940.

Liao WJ, Shi M, Chen JZ & Li AM (2010). Local recurrence of hepatocellular carcinoma after radiofrequency ablation. *World J Gastroenterol* 16, 5135-5138.

Lin SM, Lin CJ, Chung HJ, Hsu CW & Peng CY (2003). Power rolloff during interactive radiofrequency ablation can enhance necrosis when treating hepatocellular carcinoma. *AJR Am J Roentgenol* 180, 151-157.

Lin SM, Lin CJ, Lin CC, Hsu CW & Chen YC (2005). Randomised controlled trial comparing percutaneous radiofrequency thermal ablation, percutaneous ethanol injection, and percutaneous acetic acid injection to treat hepatocellular carcinoma of 3 cm or less. *Gut* 54, 1151-1156.

Liu CH, Arellano RS, Uppot RN, Samir AE, Gervais DA & Mueller PR (2010). Radiofrequency ablation of hepatic tumours: effect of post-ablation margin on local tumour progression. *Eur Radiol* 20, 877-885.

Liu JG, Wang YJ & Du Z (2010). Radiofrequency ablation in the treatment of small hepatocellular carcinoma: a meta analysis. *World J Gastroenterol* 16, 3450-3456.

Liu Z, Lobo SM, Humphries S, Horkan C, Solazzo SA, Hines-Peralta AU, Lenkinski RE & Goldberg SN (2005). Radiofrequency tumor ablation: insight into improved efficacy using computer modeling. *AJR Am J Roentgenol* 184, 1347-1352.

Liu Z, Ahmed M, Weinstein Y, Yi M, Mahajan RL & Goldberg SN (2006). Characterization of the RF ablation-induced 'oven effect': the importance of background tissue thermal conductivity on tissue heating. *Int J Hyperthermia* 22, 327-342.

Liu Z, Ahmed M, Sabir A, Humphries S & Goldberg SN (2007). Computer modeling of the effect of perfusion on heating patterns in radiofrequency tumor ablation. *Int J Hyperthermia* 23, 49-58.

Liu Z, Ahmed M, Gervais D, Humphries S & Goldberg SN (2008). Computer modeling of factors that affect the minimum safety distance required for radiofrequency ablation near adjacent nontarget structures. *J Vasc Interv Radiol* 19, 1079-1086.

Liu Z, Zhou Y, Zhang P & Qin H (2010). Meta-analysis of the therapeutic effect of hepatectomy versus radiofrequency ablation for the treatment of hepatocellular carcinoma. *Surg Laparosc Endosc Percutan Tech* 20, 130-140.

Liu ZY, Chang ZH, Lu ZM & Guo QY (2010). Early PET/CT after radiofrequency ablation in colorectal cancer liver metastases: is it useful? *Chin Med J (Engl)* 123, 1690-1694.

Livraghi T, Festi D, Monti F, Salmi A & Vettori C (1986). US-guided percutaneous alcohol injection of small hepatic and abdominal tumors. *Radiology* 161, 309-312.

Livraghi T & Vettori C (1990). Percutaneous ethanol injection therapy of hepatoma. *Cardiovasc Intervent Radiol* 13, 146-152.

Livraghi T, Vettori C & Lazzaroni S (1991). Liver metastases: results of percutaneous ethanol injection in 14 patients. *Radiology* 179, 709-712.

Livraghi T, Goldberg SN, Monti F, Bizzini A, Lazzaroni S, Meloni F, Pellicano S, Solbiati L & Gazelle GS (1997). Saline-enhanced radio-frequency tissue ablation in the treatment of liver metastases. *Radiology* 202, 205-210.

Livraghi T (1998). Percutaneous ethanol injection in hepatocellular carcinoma. *Digestion* 59 Suppl 2, 80-82.

Livraghi T, Benedini V, Lazzaroni S, Meloni F, Torzilli G & Vettori C (1998). Long term results of single session percutaneous ethanol injection in patients with large hepatocellular carcinoma. *Cancer* 83, 48-57.

Livraghi T, Goldberg SN, Lazzaroni S, Meloni F, Solbiati L & Gazelle GS (1999). Small hepatocellular carcinoma: treatment with radio-frequency ablation versus ethanol injection. *Radiology* 210, 655-661.

Livraghi T, Goldberg SN, Lazzaroni S, Meloni F, Ierace T, Solbiati L & Gazelle GS (2000). Hepatocellular carcinoma: radio-frequency ablation of medium and large lesions. *Radiology* 214, 761-768.

Livraghi T, Goldberg SN, Solbiati L, Meloni F, Ierace T & Gazelle GS (2001). Percutaneous radio-frequency ablation of liver metastases from breast cancer: initial experience in 24 patients. *Radiology* 220, 145-149.

Livraghi T, Solbiati L, Meloni MF, Gazelle GS, Halpern EF & Goldberg SN (2003). Treatment of focal liver tumors with percutaneous radio-frequency ablation: complications encountered in a multicenter study. *Radiology* 226, 441-451.

Livraghi T, Solbiati L, Meloni F, Ierace T, Goldberg SN & Gazelle GS (2003). Percutaneous radiofrequency ablation of liver metastases in potential candidates for resection: the "test-of-time approach". *Cancer* 97, 3027-3035.

Llovet JM, Vilana R, Bru C, Bianchi L, Salmeron JM, Boix L, Ganau S, Sala M, Pages M, Ayuso C, Sole M, Rodes J & Bruix J (2001). Increased risk of tumor seeding after percutaneous radiofrequency ablation for single hepatocellular carcinoma. *Hepatology* 33, 1124-1129.

Lobo SM, Afzal KS, Ahmed M, Kruskal JB, Lenkinski RE & Goldberg SN (2004). Radiofrequency ablation: modeling the enhanced temperature response to adjuvant NaCl pretreatment. *Radiology* 230, 175-182.

Lobo SM, Liu ZJ, Yu NC, Humphries S, Ahmed M, Cosman ER, Lenkinski RE, Goldberg W & Goldberg SN (2005). RF tumour ablation: computer simulation and mathematical modelling of the effects of electrical and thermal conductivity. *Int J Hyperthermia* 21, 199-213.

Lorentzen T (1996). A cooled needle electrode for radiofrequency tissue ablation: thermodynamic aspects of improved performance compared with conventional needle design. *Acad Radiol* 3, 556-563.

Lu DS, Yu NC, Raman SS, Limanond P, Lassman C, Murray K, Tong MJ, Amado RG & Busuttil RW (2005). Radiofrequency ablation of hepatocellular carcinoma: treatment success as defined by histologic examination of the explanted liver. *Radiology* 234, 954-960.

Lubner MG, Brace CL, Hinshaw JL & Lee FTJ (2010). Microwave tumor ablation: mechanism of action, clinical results, and devices. *J Vasc Interv Radiol* 21, S192-203.

Lucey BC (2006). Radiofrequency ablation: the future is now.
AJR Am J Roentgenol 186, S237-9.

Lui KW, Gervais DA, Arellano RA & Mueller PR (2003). Radiofrequency ablation of renal cell carcinoma. *Clin Radiol* 58, 905-913.

Luo W, Zhou X, Yu M, He G, Zheng X, Li Q, Liu Q, Z. (2009). Ablation of High-Intensity Focused Ultrasound Assisted with SonoVue on Rabbit VX2 Liver Tumors: Sequential findings with histopathology, immunohistochemistry and enzyme histochemistry.
Annals of surgical oncology 16, 2359-2368.

M

Maataoui A, Qian J, Mack MG, Khan MF, Oppermann E, Roozru M, Schmidt S, Bechstein WO & Vogl TJ (2005). Liver metastases in rats: chemoembolization combined with interstitial laser ablation for treatment. *Radiology* 237, 479-484.

Machi J, Oishi AJ, Sumida K, Sakamoto K, Furumoto NL, Oishi RH & Kylstra JW (2006). Long-term outcome of radiofrequency ablation for unresectable liver metastases from colorectal cancer: evaluation of prognostic factors and effectiveness in first- and second-line management. *Cancer J* 12, 318-326.

Malczyk R & Sutherland R (2009). BETA Market Research Report.

Maluccio MA, Covey AM, Schubert J, Brody LA, Sofocleous CT, Getrajdman GI, DeMatteo R & Brown KT (2006). Treatment of metastatic sarcoma to the liver with bland embolization. *Cancer* 107, 1617-1623.

Maor E, Ivorra A, Mitchell JJ & Rubinsky B (2010). Vascular smooth muscle cells ablation with endovascular nonthermal irreversible electroporation. *J Vasc Interv Radiol* 21, 1708-1715.

Marchal F, Elias D, Rauch P, Zarnegar R, Leroux A, Stines J, Verhaeghe JL, Guillemin F, Carteaux JP & Villemot JP (2006). Prevention of biliary lesions that may occur during radiofrequency ablation of the liver: study on the pig. *Ann Surg* 243, 82-88.

Marlow NE, Maddern GJ, Middleton PF, Tooher R & Babidge WJ (2006). Evaluating new surgical techniques in Australia: the Australian Safety and Efficacy Register of New Interventional Procedures-Surgical experience.
ASERNIP-S Report No. 56. Adelaide, South Australia: ASERNIP-S August 2006.

Martin RC (2006). Hepatic tumor ablation: cryo versus radiofrequency, which is better?
Am Surg 72, 391-392.

Martinez-Subiela S, Eckersall PD, Campbell FM, Parra MD, Fuentes P & Ceron JJ (2007). A time-resolved immunofluorometric assay for porcine C-reactive protein quantification in whole blood. *Luminescence* 22, 171-176.

Maruyama H, Yoshikawa M & Yokosuka O (2008). Current role of ultrasound for the management of hepatocellular carcinoma. *World J Gastroenterol* 14, 1710-1719.

Matsuda Y, Kawata S, Nagase T, Maeda Y, Yamasaki E, Kiso S, Ishiguro H & Matsuzawa Y (1994). Interleukin-6 in transcatheter arterial embolization for patients with hepatocellular carcinoma. Effects of serine protease inhibitor. *Cancer* 73, 53-57.

Matsumata T, Taketomi A, Kawahara N, Higashi H, Shirabe K & Takenaka K (1995). Morbidity and mortality after hepatic resection in the modern era.
Hepatogastroenterology 42, 456-460.

McGahan JP, Browning PD, Brock JM & Tesluk H (1990). Hepatic ablation using radiofrequency electrocautery. *Invest Radiol* 25, 267-270.

McGahan JP, Gu WZ, Brock JM, Tesluk H & Jones CD (1996). Hepatic ablation using bipolar radiofrequency electrocautery. *Acad Radiol* 3, 418-422.

McGahan JP, Loh S, Boschini FJ, Paoli EE, Brock JM, Monsky WL & Li CS (2010). Maximizing parameters for tissue ablation by using an internally cooled electrode.
Radiology 256, 397-405.

McWilliams JP, Yamamoto S, Raman SS, Loh CT, Lee EW, Liu DM & Kee ST (2010). Percutaneous ablation of hepatocellular carcinoma: current status. *J Vasc Interv Radiol* 21, S204-13.

Merkle EM, Boll DT, Boaz T, Duerk JL, Chung YC, Jacobs GH, Varnes ME & Lewin JS (1999). MRI-guided radiofrequency thermal ablation of implanted VX2 liver tumors in a rabbit model: demonstration of feasibility at 0.2 T. *Magn Reson Med* 42, 141-149.

Merkle EM, Haaga JR, Duerk JL, Jacobs GH, Brambs HJ & Lewin JS (1999). MR imaging-guided radio-frequency thermal ablation in the pancreas in a porcine model with a modified clinical C-arm system. *Radiology* 213, 461-467.

Merkle EM, Shonk JR, Duerk JL, Jacobs GH & Lewin JS (1999). MR-guided RF thermal ablation of the kidney in a porcine model. *AJR Am J Roentgenol* 173, 645-651.

Mertyna P, Hines-Peralta A, Liu ZJ, Halpern E, Goldberg W & Goldberg SN (2007). Radiofrequency ablation: variability in heat sensitivity in tumors and tissues. *J Vasc Interv Radiol* 18, 647-654.

Mertyna P, Dewhirst MW, Halpern E, Goldberg W & Goldberg SN (2008). Radiofrequency ablation: the effect of distance and baseline temperature on thermal dose required for coagulation. *Int J Hyperthermia* 24, 550-559.

Metcalfe MS, Mullin EJ, Texler M, Berry DP, Dennison AR & Maddern GJ (2007). The safety and efficacy of radiofrequency and electrolytic ablation created adjacent to large hepatic veins in a porcine model. *Eur J Surg Oncol* 33, 662-667.

Miao Y, Ni Y, Mulier S, Wang K, Hoey MF, Mulier P, Penninckx F, Yu J, De Scheerder I, Baert AL & Marchal G (1997). Ex vivo experiment on radiofrequency liver ablation with saline infusion through a screw-tip cannulated electrode. *J Surg Res* 71, 19-24.

Miller L, Leor J & Rubinsky B (2005). Cancer cells ablation with irreversible electroporation. *Technol Cancer Res Treat* 4, 699-705.

Miyamoto N, Tsuji K, Sakurai Y, Nishimori H, Kang JH, Mitsui S & Maguchi H (2004). Percutaneous radiofrequency ablation for unresectable large hepatic tumours during hepatic blood flow occlusion in four patients. *Clin Radiol* 59, 812-818.

Molinari M & Helton S (2009). Hepatic resection versus radiofrequency ablation for hepatocellular carcinoma in cirrhotic individuals not candidates for liver transplantation: A Markov model decision analysis. *Am J Surg* 198, 396-406.

Monsky WL, Kruskal JB, Lukyanov AN, Girnun GD, Ahmed M, Gazelle GS, Huertas JC, Stuart KE, Torchilin VP & Goldberg SN (2002). Radio-frequency ablation increases intratumoral liposomal doxorubicin accumulation in a rat breast tumor model. *Radiology* 224, 823-829.

Morimoto M, Numata K, Nozawa A, Kondo M, Nozaki A, Nakano M & Tanaka K (2010). Radiofrequency ablation of the liver: extended effect of transcatheter arterial embolization with iodized oil and gelatin sponge on histopathologic changes during follow-up in a pig model. *J Vasc Interv Radiol* 21, 1716-1724.

Morris DL, Ross WB, Iqbal J, McCall JL, King J, PR. (1996). Cryoablation of hepatic malignancy: an evaluation of tumour marker data and survival in 110 patients. *GI Cancer* 1, 247-251.

Mostafa EM, Ganguli S, Faintuch S, Mertyna P & Goldberg SN (2008). Optimal strategies for combining transcatheter arterial chemoembolization and radiofrequency ablation in rabbit VX2 hepatic tumors. *J Vasc Interv Radiol* 19, 1740-1748.

Moug SJ, Smith D, Leen E, Roxburgh C & Horgan PG (2010). Evidence for a synchronous operative approach in the treatment of colorectal cancer with hepatic metastases: a case matched study. *Eur J Surg Oncol* 36, 365-370.

Mulier S, Mulier P, Ni Y, Miao Y, Dupas B, Marchal G, De Wever I & Michel L (2002). Complications of radiofrequency coagulation of liver tumours. *Br J Surg* 89, 1206-1222.

Mulier S, Ni Y, Miao Y, Rosiere A, Khoury A, Marchal G & Michel L (2003). Size and geometry of hepatic radiofrequency lesions. *Eur J Surg Oncol* 29, 867-878.

Mulier S, Ni Y, Jamart J, Ruers T, Marchal G & Michel L (2005). Local recurrence after hepatic radiofrequency coagulation: multivariate meta-analysis and review of contributing factors. *Ann Surg* 242, 158-171.

Murakami R, Yoshimatsu S, Yamashita Y, Matsukawa T, Takahashi M & Sagara K (1995). Treatment of hepatocellular carcinoma: value of percutaneous microwave coagulation. *AJR Am J Roentgenol* 164, 1159-1164.

N

Nahum Goldberg S & Dupuy DE (2001). Image-guided radiofrequency tumor ablation: challenges and opportunities--part I. *J Vasc Interv Radiol* 12, 1021-1032.

Naugler WE & Sonnenberg A (2010). Survival and cost-effectiveness analysis of competing strategies in the management of small hepatocellular carcinoma. *Liver Transpl* 16, 1186-1194.

Ng KK, Lam CM, Poon RT, Shek TW, To JY, Wo YH, Ho DW & Fan ST (2004). Comparison of systemic responses of radiofrequency ablation, cryotherapy, and surgical resection in a porcine liver model. *Ann Surg Oncol* 11, 650-657.

Ni Y, Mulier S, Miao Y, Michel L & Marchal G (2005). A review of the general aspects of radiofrequency ablation. *Abdom Imaging* 30, 381-400.

Nikfarjam M & Christophi C (2003). Interstitial laser thermotherapy for liver tumours. *Br J Surg* 90, 1033-1047.

Nikfarjam M, Muralidharan V & Christophi C (2005). Mechanisms of focal heat destruction of liver tumors. *J Surg Res* 127, 208-223.

Nikfarjam M, Muralidharan V, Malcontenti-Wilson C, McLaren W & Christophi C (2006). Impact of blood flow occlusion on liver necrosis following thermal ablation. *ANZ J Surg* 76, 84-91.

Nikfarjam M, Shereef S, Kimchi ET, Gusani NJ, Jiang Y, Avella DM, Mahraj RP & Staveley-O'Carroll KF (2009). Survival outcomes of patients with colorectal liver metastases following hepatic resection or ablation in the era of effective chemotherapy. *Ann Surg Oncol* 16, 1860-1867.

Niu R, Yan TD, Zhu JC, Black D, Chu F & Morris DL (2007). Recurrence and survival outcomes after hepatic resection with or without cryotherapy for liver metastases from colorectal carcinoma. *Ann Surg Oncol* 14, 2078-2087.

Nordenstrom BE (1983) *Biologically Closed Electric Circuits: Clinical, Experimental and Theoretical Evidence for an Additional Circulatory System* (Nordic Medical Publications: Stockholm).

Nordenstrom BE (1985). Fleischner lecture. Biokinetic impacts on structure and imaging of the lung: the concept of biologically closed electric circuits. *AJR Am J Roentgenol* 145, 447-467.

Nordenstrom BE (1992). Impact of biologically closed electric circuits (BCEC) on structure and function. *Integr Physiol Behav Sci* 27, 285-303.

Nordenstrom BE (1994). Electrostatic field interference with cellular and tissue function, leading to dissolution of metastases that enhances the effect of chemotherapy. *Eur J Surg Suppl* 121-135.

Nordenstrom BE (1994). The paradigm of biologically closed electric circuits (BCEC) and the formation of an International Association (IABC) for BCEC systems. *Eur J Surg Suppl* 7-23.

Nordenstrom BE (1998) *Exploring BCEC-Systems (Biologically Closed Electric Systems)* (Nordic Medical Publications, Stockholm).

Nour SG, Lewin JS, Gutman M, Hillenbrand C, Wacker FK, Wong JW, Mitchell IC, Armstrong CB, Hashim MM, Duerk JL & Strauss M (2004). Percutaneous MR imaging-guided radiofrequency interstitial thermal ablation of tongue base in porcine models: implications for obstructive sleep apnea syndrome. *Radiology* 230, 359-368.

O

Oei T, vanSonnenberg E, Shankar S, Morrison PR, Tuncali K & Silverman SG (2005). Radiofrequency ablation of liver tumors: a new cause of benign portal venous gas. *Radiology* 237, 709-717.

Ohmoto K & Yamamoto S (2000). Percutaneous microwave coagulation therapy for superficial hepatocellular carcinoma on the liver surface. *Am J Gastroenterol* 95, 2401-2403.

Ohmoto K, Yoshioka N, Tomiyama Y, Shibata N, Kawase T, Yoshida K, Kuboki M & Yamamoto S (2006). Thermal ablation therapy for hepatocellular carcinoma: comparison between radiofrequency ablation and percutaneous microwave coagulation therapy. *Hepatogastroenterology* 53, 651-654.

Ohmoto K, Yoshioka N, Tomiyama Y, Shibata N, Kawase T, Yoshida K, Kuboki M & Yamamoto S (2009). Comparison of therapeutic effects between radiofrequency ablation and percutaneous microwave coagulation therapy for small hepatocellular carcinomas. *J Gastroenterol Hepatol* 24, 223-227.

Okuma T, Matsuoka T, Yamamoto A, Oyama Y, Hamamoto S, Toyoshima M, Nakamura K & Miki Y (2010). Determinants of local progression after computed tomography-guided percutaneous radiofrequency ablation for unresectable lung tumors: 9-year experience in a single institution. *Cardiovasc Intervent Radiol* 33, 787-793.

Onik G, Rubinsky B, Zemel R, Weaver L, Diamond D, Cobb C & Porterfield B (1991). Ultrasound-guided hepatic cryosurgery in the treatment of metastatic colon carcinoma. Preliminary results. *Cancer* 67, 901-907.

Onofrio BM (1975). Radiofrequency percutaneous Gasserian ganglion lesions. Results in 140 patients with trigeminal pain. *J Neurosurg* 42, 132-139.

Organ LW (1976). Electrophysiologic principles of radiofrequency lesion making. *Appl Neurophysiol* 39, 69-76.

Orlando A, Leandro G, Olivo M, Andriulli A & Cottone M (2009). Radiofrequency thermal ablation vs. percutaneous ethanol injection for small hepatocellular carcinoma in cirrhosis: meta-analysis of randomized controlled trials. *Am J Gastroenterol* 104, 514-524.

Otto G, Duber C, Hoppe-Lotichius M, Konig J, Heise M & Pitton MB (2010). Radiofrequency ablation as first-line treatment in patients with early colorectal liver metastases amenable to surgery. *Ann Surg* 251, 796-803.

P

Pacella CM, Stasi R, Bizzarri G, Pacella S, Graziano FM, Guglielmi R & Papini E (2008). Percutaneous laser ablation of unresectable primary and metastatic adrenocortical carcinoma. *Eur J Radiol* 66, 88-94.

Padhani A (2009). Unresectable hepatocellular carcinoma: serial early vascular and cellular changes after transarterial chemoembolization. *Radiology* 250, 324-326.

Park BK & Kim CK (2009). Complications of image-guided radiofrequency ablation of renal cell carcinoma: causes, imaging features and prevention methods. *Eur Radiol* 19, 2180-2190.

Park SY, Tak WY, Jeon SW, Cho CM, Kweon YO, Kim SK & Choi YH (2009). The efficacy of intraperitoneal saline infusion for percutaneous radiofrequency ablation for hepatocellular carcinoma. *Eur J Radiol* 74, 536-540.

Patterson EJ, Scudamore CH, Owen DA, Nagy AG & Buczkowski AK (1998). Radiofrequency ablation of porcine liver in vivo: effects of blood flow and treatment time on lesion size. *Ann Surg* 227, 559-565.

Pavy FW & Siau RL (1903). The influence of ablation of the liver on the sugar contents of the blood. *J Physiol* 29, 375-381.

Pech M, Janitzky A, Wendler JJ, Strang C, Blaschke S, Dudeck O, Ricke J & Liehr UB (2010). Irreversible Electroporation of Renal Cell Carcinoma: A First-in-Man Phase I Clinical Study. *Cardiovasc Intervent Radiol* Aug 15. [Epub]

Peng ZW, Zhang YJ, Chen MS, Lin XJ, Liang HH & Shi M (2010). Radiofrequency ablation as first-line treatment for small solitary hepatocellular carcinoma: long-term results. *Eur J Surg Oncol* 36, 1054-1060.

Peng ZW, Liang HH, Chen MS, Zhang YJ, Zhang YQ & Lau WY (2011). Conformal radiofrequency ablation of hepatocellular carcinoma with a multi-pin bipolar system. *J Surg Oncol* 103, 69-74.

Pennathur A, Abbas G, Qureshi I, Schuchert MJ, Wang Y, Gilbert S, Landreneau RJ & Luketich JD (2009). Radiofrequency ablation for the treatment of pulmonary metastases. *Ann Thorac Surg* 87, 1030-6; discussion 1036-9.

Pennathur A, Abbas G, Gooding WE, Schuchert MJ, Gilbert S, Christie NA, Landreneau RJ & Luketich JD (2009). Image-guided radiofrequency ablation of lung neoplasm in 100 consecutive patients by a thoracic surgical service. *Ann Thorac Surg* 88, 1601-6; discussion 1607-8.

Pennes HH (1998). Analysis of tissue and arterial blood temperatures in the resting human forearm. 1948. *J Appl Physiol* 85, 5-34.

Pepys MB & Hirschfield GM (2003). C-reactive protein: a critical update. *J Clin Invest* 111, 1805-1812.

Pereira PL, Trubenbach J, Schenk M, Subke J, Kroeber S, Schaefer I, Remy CT, Schmidt D, Brieger J & Claussen CD (2004). Radiofrequency ablation: in vivo comparison of four commercially available devices in pig livers. *Radiology* 232, 482-490.

Pereira PL (2007). Actual role of radiofrequency ablation of liver metastases. *Eur Radiol* 17, 2062-2070.

Permpongkosol S, Nicol TL, Link RE, Varkarakis I, Khurana H, Zhai QJ, Kavoussi LR & Solomon SB (2007). Differences in ablation size in porcine kidney, liver, and lung after cryoablation using the same ablation protocol. *AJR Am J Roentgenol* 188, 1028-1032.

Pfeifer U (1998). Pathology of hepatocellular carcinoma. *Digestion* 59 Suppl 2, 66-69.

Pineiro C, Pineiro M, Morales J, Andres M, Lorenzo E, Pozo MD, Alava MA & Lampreave F (2009). Pig-MAP and haptoglobin concentration reference values in swine from commercial farms. *Vet J* 179, 78-84.

Pineiro M, Pineiro C, Carpintero R, Morales J, Campbell FM, Eckersall PD, Toussaint MJ & Lampreave F (2007). Characterisation of the pig acute phase protein response to road transport. *Vet J* 173, 669-674.

Pompili M, Pacella CM, Francica G, Angelico M, Tisone G, Craboledda P, Nicolardi E, Rapaccini GL & Gasbarrini G (2010). Percutaneous laser ablation of hepatocellular carcinoma in patients with liver cirrhosis awaiting liver transplantation. *Eur J Radiol* 74, e6-e11.

Pringle JH (1908). V. Notes on the Arrest of Hepatic Hemorrhage Due to Trauma. *Ann Surg* 48, 541-549.

Probstein RF (1994) *Physicochemical hydrodynamics: an introduction* (John Wiley and Sons, New York).

Pua BB, Thornton RH & Solomon SB (2010). Ablation of pulmonary malignancy: current status. *J Vasc Interv Radiol* 21, S223-32.

Puls R, Langner S, Rosenberg C, Hegenscheid K, Kuehn JP, Noeckler K & Hosten N (2009). Laser ablation of liver metastases from colorectal cancer with MR thermometry: 5-year survival. *J Vasc Interv Radiol* 20, 225-234.

Pupulim LF, Hakime A, Barrau V, Abdel-Rehim M, Zappa M & Vilgrain V (2009). Fatty hepatocellular carcinoma: radiofrequency ablation--imaging findings. *Radiology* 250, 940-948.

R

Radostits OM, Gay CC, Blood DC & Hinchcliff KW (2005) *Veterinary medicine: a textbook of the diseases of cattle, sheep, pigs, goats and horses* (WB Saunders,

Rampone B, Schiavone B, Martino A, Viviano C & Confuorto G (2009). Current management strategy of hepatocellular carcinoma. *World J Gastroenterol* 15, 3210-3216.

Ravikumar TS, Kane R, Cady B, Jenkins RL, McDermott W, Onik G, Clouse M & Steele GJ (1987). Hepatic cryosurgery with intraoperative ultrasound monitoring for metastatic colon carcinoma. *Arch Surg* 122, 403-409.

Ravikumar TS, Kane R, Cady B, Jenkins R, Clouse M & Steele GJ (1991). A 5-year study of cryosurgery in the treatment of liver tumors. *Arch Surg* 126, 1520-3; discussion 1523-4.

Rempp H, Voigtlander M, Clasen S, Kempf S, Neugebauer A, Schraml C, Schmidt D, Claussen CD, Enderle MD, Goldberg SN & Pereira PL (2009). Increased ablation zones using a cryo-based internally cooled bipolar RF applicator in ex vivo bovine liver. *Invest Radiol* 44, 763-768.

Reuss FF (1809). *Memoires de la Societe Imperiale des Naturalists de Moscow* 2, 327-337.

Reuter NP, Woodall CE, Scoggins CR, McMasters KM & Martin RC (2009). Radiofrequency ablation vs. resection for hepatic colorectal metastasis: therapeutically equivalent? *J Gastrointest Surg* 13, 486-491.

Rhim H, Goldberg SN, Dodd GDr, Solbiati L, Lim HK, Tonolini M & Cho OK (2001). Essential techniques for successful radio-frequency thermal ablation of malignant hepatic tumors. *Radiographics* 21 Spec No, S17-35; discussion S36-9.

Rhim H, Yoon KH, Lee JM, Cho Y, Cho JS, Kim SH, Lee WJ, Lim HK, Nam GJ, Han SS, Kim YH, Park CM, Kim PN & Byun JY (2003). Major complications after radio-frequency thermal ablation of hepatic tumors: spectrum of imaging findings. *Radiographics* 23, 123-34; discussion 134-6.

Rhim H, Dodd GDr, Chintapalli KN, Wood BJ, Dupuy DE, Hvizda JL, Sewell PE & Goldberg SN (2004). Radiofrequency thermal ablation of abdominal tumors: lessons learned from complications. *Radiographics* 24, 41-52.

Rhim H (2004). Review of asian experience of thermal ablation techniques and clinical practice. *Int J Hyperthermia* 20, 699-712.

Rhim H & Lim HK (2010). Radiofrequency Ablation of Hepatocellular Carcinoma: Pros and Cons. *Gut Liver* 4, S113-S118.

Riaz A, Lewandowski RJ, Kulik L & Salem R (2009). Yttrium-90 radioembolization using TheraSphere in the management of primary and secondary liver tumors.
Q J Nucl Med Mol Imaging 53, 311-316.

Robertson GS, Wemyss-Holden SA, Dennison AR, Hall PM, Baxter P & Maddern GJ (1998). Experimental study of electrolysis-induced hepatic necrosis. *Br J Surg* 85, 1212-1216.

Rosenberg C, Puls R, Hegenscheid K, Kuehn J, Bollman T, Westerholt A, Weigel C & Hosten N (2009). Laser ablation of metastatic lesions of the lung: long-term outcome.
AJR Am J Roentgenol 192, 785-792.

Rosner B (2005) *Fundamentals of Biostatistics* 6th Ed (Duxbury Press, Pacific Grove, Calif).

Rossi S, Fornari F, Pathies C & Buscarini L (1990). Thermal lesions induced by 480 KHz localized current field in guinea pig and pig liver. *Tumori* 76, 54-57.

Rossi S, Di Stasi M, Buscarini E, Quaretti P, Garbagnati F, Squassante L, Paties CT, Silverman DE & Buscarini L (1996). Percutaneous RF interstitial thermal ablation in the treatment of hepatic cancer. *AJR Am J Roentgenol* 167, 759-768.

Rossi S, Buscarini E, Garbagnati F, Di Stasi M, Quaretti P, Rago M, Zangrandi A, Andreola S, Silverman D & Buscarini L (1998). Percutaneous treatment of small hepatic tumors by an expandable RF needle electrode. *AJR Am J Roentgenol* 170, 1015-1022.

Rubinsky B (2007). Irreversible electroporation in medicine.
Technol Cancer Res Treat 6, 255-260.

Rutherford EE, Cast JE & Breen DJ (2008). Immediate and long-term CT appearances following radiofrequency ablation of renal tumours. *Clin Radiol* 63, 220-230.

Ruutiainen AT, Soulen MC, Tuite CM, Clark TW, Mondschein JI, Stavropoulos SW & Trerotola SO (2007). Chemoembolization and bland embolization of neuroendocrine tumor metastases to the liver. *J Vasc Interv Radiol* 18, 847-855.

S

Sakr AA, Saleh AA, Moeaty AA & Moeaty AA (2005). The combined effect of radiofrequency and ethanol ablation in the management of large hepatocellular carcinoma. *Eur J Radiol* 54, 418-425.

Sakurai J, Hiraki T, Mimura H, Gobara H, Fujiwara H, Tajiri N, Sano Y & Kanazawa S (2010). Radiofrequency ablation of small lung metastases by a single application of a 2-cm expandable electrode: determination of favorable responders. *J Vasc Interv Radiol* 21, 231-236.

Salman HS, Cynamon J, Jagust M, Bakal C, Rozenblit A, Kaleya R, Negassa A & Wadler S (2002). Randomized phase II trial of embolization therapy versus chemoembolization therapy in previously treated patients with colorectal carcinoma metastatic to the liver. *Clin Colorectal Cancer* 2, 173-179.

Samuel M, Chow PK, Chan Shih-Yen E, Machin D & Soo KC (2009). Neoadjuvant and adjuvant therapy for surgical resection of hepatocellular carcinoma. *Cochrane Database Syst Rev* CD001199.

Samuelsson L & Jonsson L (1980). Electrolyte destruction of lung tissue. Electrochemical aspects. *Acta Radiol Diagn (Stockh)* 21, 711-714.

Samuelsson L (1981). Electrolysis and surgery in experimental tumours in the rat. *Acta Radiol Diagn (Stockh)* 22, 129-131.

Samuelsson L & Jonsson L (1981). Electrolytic destruction of tissue in the normal lung of the pig. *Acta Radiol Diagn (Stockh)* 22, 9-14.

Sandomirsky M, Crifasi JA, Long C & Mitchell EK (2010). Case Report of Fatal Complication in Prostatic Cryotherapy: First Reported Death Due to Argon Gas Emboli. *Am J Forensic Med Pathol* May 21. [Epub]

Santambrogio R, Bianchi P, Palmisano A, Donadon M, Moroni E & Montorsi M (2003). Radiofrequency of hepatocellular carcinoma in patients with liver cirrhosis: a critical appraisal of the laparoscopic approach. *J Exp Clin Cancer Res* 22, 251-255.

Santambrogio R, Podda M, Zuin M, Bertolini E, Bruno S, Cornalba GP, Costa M & Montorsi M (2003). Safety and efficacy of laparoscopic radiofrequency ablation of hepatocellular carcinoma in patients with liver cirrhosis. *Surg Endosc* 17, 1826-1832.

Sartori S, Tombesi P, Macario F, Nielsen I, Tassinari D, Catellani M & Abbasciano V (2008). Subcapsular liver tumors treated with percutaneous radiofrequency ablation: a prospective comparison with nonsubcapsular liver tumors for safety and effectiveness. *Radiology* 248, 670-679.

Schmit GD, Atwell TD, Callstrom MR, Kurup AN, Fleming CJ, Andrews JC & Charboneau JW (2010). Ice ball fractures during percutaneous renal cryoablation: risk factors and potential implications. *J Vasc Interv Radiol* 21, 1309-1312.

Schraml C, Graf H, Boss A, Clasen S, Leibfritz M, Pereira PL, Claussen CD & Schick F (2005). Interaction between grounding pads used for RF ablation therapy and magnetic resonance imaging. *MAGMA* 18, 309-315.

Schraml C, Aube C, Graf H, Boss A, Clasen S, Herberts T, Schmidt D, Schick F, Claussen CD & Pereira PL (2006). MR-guided radiofrequency ablation: do magnetic fields influence extent of coagulation in ex vivo bovine livers? *Radiology* 241, 746-752.

Seifert JK & Morris DL (1999). Repeat hepatic cryotherapy for recurrent metastases from colorectal cancer. *Surgery* 125, 233-235.

Seifert JK & Morris DL (1999). Indicators of recurrence following cryotherapy for hepatic metastases from colorectal cancer. *Br J Surg* 86, 234-240.

Seifert JK & Morris DL (1999). World survey on the complications of hepatic and prostate cryotherapy. *World J Surg* 23, 109-13; discussion 113-4.

Seifert JK, Stewart GJ, Hewitt PM, Bolton EJ, Junginger T & Morris DL (1999). Interleukin-6 and tumor necrosis factor-alpha levels following hepatic cryotherapy: association with volume and duration of freezing. *World J Surg* 23, 1019-1026.

Seifert JK, Achenbach T, Heintz A, Bottger TC & Junginger T (2000). Cryotherapy for liver metastases. *Int J Colorectal Dis* 15, 161-166.

Seki T, Wakabayashi M, Nakagawa T, Imamura M, Tamai T, Nishimura A, Yamashiki N, Okamura A & Inoue K (1998). Hepatic infarction following percutaneous ethanol injection therapy for hepatocellular carcinoma. *Eur J Gastroenterol Hepatol* 10, 915-918.

Seki T, Wakabayashi M, Nakagawa T, Imamura M, Tamai T, Nishimura A, Yamashiki N, Okamura A & Inoue K (1999). Percutaneous microwave coagulation therapy for patients with small hepatocellular carcinoma: comparison with percutaneous ethanol injection therapy. *Cancer* 85, 1694-1702.

Seki T, Wakabayashi M, Nakagawa T, Imamura M, Tamai T, Nishimura A, Yamashiki N & Inoue K (1999). Percutaneous microwave coagulation therapy for solitary metastatic liver tumors from colorectal cancer: a pilot clinical study. *Am J Gastroenterol* 94, 322-327.

Seror O, N'Kontchou G, Ibraheem M, Ajavon Y, Barrucand C, Ganne N, Coderc E, Trinchet JC, Beaugrand M & Sellier N (2008). Large (>or=5.0-cm) HCCs: multipolar RF ablation with three internally cooled bipolar electrodes--initial experience in 26 patients. *Radiology* 248, 288-296.

Shen P, Fleming S, Westcott C & Challa V (2003). Laparoscopic radiofrequency ablation of the liver in proximity to major vasculature: effect of the Pringle maneuver. *J Surg Oncol* 83, 36-41.

Shetty SK, Rosen MP, Raptopoulos V & Goldberg SN (2001). Cost-effectiveness of percutaneous radiofrequency ablation for malignant hepatic neoplasms. *J Vasc Interv Radiol* 12, 823-833.

Shibata T, Niinobu T, Ogata N & Takami M (2000). Microwave coagulation therapy for multiple hepatic metastases from colorectal carcinoma. *Cancer* 89, 276-284.

Shibata T, Iimuro Y, Yamamoto Y, Maetani Y, Ametani F, Itoh K & Konishi J (2002). Small hepatocellular carcinoma: comparison of radio-frequency ablation and percutaneous microwave coagulation therapy. *Radiology* 223, 331-337.

Shibata T, Shibata T, Maetani Y, Isoda H & Hiraoka M (2006). Radiofrequency ablation for small hepatocellular carcinoma: prospective comparison of internally cooled electrode and expandable electrode. *Radiology* 238, 346-353.

Shiina S (2009). Image-guided percutaneous ablation therapies for hepatocellular carcinoma. *J Gastroenterol* 44 Suppl 19, 122-131.

Shimada S, Hirota M, Beppu T, Matsuda T, Hayashi N, Tashima S, Takai E, Yamaguchi K, Inoue K & Ogawa M (1998). Complications and management of microwave coagulation therapy for primary and metastatic liver tumors. *Surg Today* 28, 1130-1137.

Shimozawa N & Hanazaki K (2004). Longterm prognosis after hepatic resection for small hepatocellular carcinoma. *J Am Coll Surg* 198, 356-365.

Shock SA, Meredith K, Warner TF, Sampson LA, Wright AS, Winter TCr, Mahvi DM, Fine JP & Lee FTJ (2004). Microwave ablation with loop antenna: in vivo porcine liver model. *Radiology* 231, 143-149.

Simon CJ, Dupuy DE & Mayo-Smith WW (2005). Microwave ablation: principles and applications. *Radiographics* 25 Suppl 1, S69-83.

Skinner MG, Iizuka MN, Kolios MC & Sherar MD (1998). A theoretical comparison of energy sources--microwave, ultrasound and laser--for interstitial thermal therapy. *Phys Med Biol* 43, 3535-3547.

Skovgaard K, Mortensen S, Boye M, Poulsen KT, Campbell FM, Eckersall PD & Heegaard PM (2009). Rapid and widely disseminated acute phase protein response after experimental bacterial infection of pigs. *Vet Res* 40, 23.

Smith S & Gillams A (2008). Imaging appearances following thermal ablation. *Clin Radiol* 63, 1-11.

Solazzo S, Mertyna P, Peddi H, Ahmed M, Horkan C & Goldberg SN (2008). RF ablation with adjuvant therapy: comparison of external beam radiation and liposomal doxorubicin on ablation efficacy in an animal tumor model. *Int J Hyperthermia* 24, 560-567.

Solazzo SA, Liu Z, Lobo SM, Ahmed M, Hines-Peralta AU, Lenkinski RE & Goldberg SN (2005). Radiofrequency ablation: importance of background tissue electrical conductivity--an agar phantom and computer modeling study. *Radiology* 236, 495-502.

Solazzo SA, Ahmed M, Liu Z, Hines-Peralta AU & Goldberg SN (2007). High-power generator for radiofrequency ablation: larger electrodes and pulsing algorithms in bovine ex vivo and porcine in vivo settings. *Radiology* 242, 743-750.

Solbiati L, Giangrande A, De Pra L, Bellotti E, Cantu P & Ravetto C (1985). Percutaneous ethanol injection of parathyroid tumors under US guidance: treatment for secondary hyperparathyroidism. *Radiology* 155, 607-610.

Solbiati L, Ierace T, Goldberg SN, Sironi S, Livraghi T, Fiocca R, Servadio G, Rizzatto G, Mueller PR, Del Maschio A & Gazelle GS (1997). Percutaneous US-guided radio-frequency tissue ablation of liver metastases: treatment and follow-up in 16 patients. *Radiology* 202, 195-203.

Solbiati L, Goldberg SN, Ierace T, Livraghi T, Meloni F, Dellanoce M, Sironi S & Gazelle GS (1997). Hepatic metastases: percutaneous radio-frequency ablation with cooled-tip electrodes. *Radiology* 205, 367-373.

Solbiati L, Goldberg SN, Ierace T, Dellanoce M, Livraghi T & Gazelle GS (1999). Radio-frequency ablation of hepatic metastases: postprocedural assessment with a US microbubble contrast agent--early experience. *Radiology* 211, 643-649.

Solbiati L, Livraghi T, Goldberg SN, Ierace T, Meloni F, Dellanoce M, Cova L, Halpern EF & Gazelle GS (2001). Percutaneous radio-frequency ablation of hepatic metastases from colorectal cancer: long-term results in 117 patients. *Radiology* 221, 159-166.

Spangenberg HC, Thimme R & Blum HE (2008). Evolving therapies in the treatment of hepatocellular carcinoma. *Biologics* 2, 453-462.

Stang A, Fischbach R, Teichmann W, Bokemeyer C & Braumann D (2009). A systematic review on the clinical benefit and role of radiofrequency ablation as treatment of colorectal liver metastases. *Eur J Cancer* 45, 1748-1756.

Stauffer PR & Goldberg SN (2004). Introduction: thermal ablation therapy. *Int J Hyperthermia* 20, 671-677.

Steiner P, Botnar R, Goldberg SN, Gazelle GS & Debatin JF (1997). Monitoring of radio frequency tissue ablation in an interventional magnetic resonance environment. Preliminary ex vivo and in vivo results. *Invest Radiol* 32, 671-678.

Steiner P, Botnar R, Dubno B, Zimmermann GG, Gazelle GS & Debatin JF (1998). Radio-frequency-induced thermoablation: monitoring with T1-weighted and proton-frequency-shift MR imaging in an interventional 0.5-T environment. *Radiology* 206, 803-810.

Stippel DL, Brochhagen HG, Arenja M, Hunkemoller J, Holscher AH & Beckurts KT (2004). Variability of size and shape of necrosis induced by radiofrequency ablation in human livers: a volumetric evaluation. *Ann Surg Oncol* 11, 420-425.

Stuart KE & ZK S (1 Jun 2010). Hepatic carcinoma, Primary. EMedicine, Harvard Medical School, Boston, MA. http:// http://emedicine.medscape.com/article/282814-overview

Sun Y, Wang Y, Ni X, Gao Y, Shao Q, Liu L & Liang P (2009). Comparison of ablation zone between 915- and 2,450-MHz cooled-shaft microwave antenna: results in in vivo porcine livers. *AJR Am J Roentgenol* 192, 511-514.

T

Taha JM, Tew JMJ & Buncher CR (1995). A prospective 15-year follow up of 154 consecutive patients with trigeminal neuralgia treated by percutaneous stereotactic radiofrequency thermal rhizotomy. *J Neurosurg* 83, 989-993.

Takaki H, Yamakado K, Nakatsuka A, Fuke H, Murata K, Shiraki K & Takeda K (2007). Radiofrequency ablation combined with chemoembolization for the treatment of hepatocellular carcinomas 5 cm or smaller: risk factors for local tumor progression.
J Vasc Interv Radiol 18, 856-861.

Tanabe KK, Curley SA, Dodd GD, Siperstein AE & Goldberg SN (2004). Radiofrequency ablation: the experts weigh in. *Cancer* 100, 641-650.

Tateishi R, Shiina S, Teratani T, Obi S, Sato S, Koike Y, Fujishima T, Yoshida H, Kawabe T & Omata M (2005). Percutaneous radiofrequency ablation for hepatocellular carcinoma. An analysis of 1000 cases. *Cancer* 103, 1201-1209.

Tateishi R, Shiina S, Ohki T, Sato T, Masuzaki R, Imamura J, Goto E, Goto T, Yoshida H, Obi S, Sato S, Kanai F, Yoshida H & Omata M (2009). Treatment strategy for hepatocellular carcinoma: expanding the indications for radiofrequency ablation. *J Gastroenterol* 44 Suppl 19, 142-146.

Tatli S, Acar M, Tuncali K, Morrison PR & Silverman S (2010). Percutaneous cryoablation techniques and clinical applications. *Diagn Interv Radiol* 16, 90-95.

Teague BD, Wemyss-Holden SA, Fosh BG, Dennison AR & Maddern GJ (2002). Electrolysis and other local ablative treatments for non-resectable colorectal liver metastases. *ANZ J Surg* 72, 137-141.

Teague BD, Court FG, Morrison CP, Kho M, Wemyss-Holden SA & Maddern GJ (2004). Electrolytic liver ablation is not associated with evidence of a systemic inflammatory response syndrome. *Br J Surg* 91, 178-183.

Teague BD, Morrison CP, Court FG, Nguyen T, Wemyss-Holden SA, Dennison AR & Maddern GJ (2004). The lack of a systemic inflammatory response syndrome supports the safety of pancreatic electrolysis: experimental studies. *J Surg Res* 116, 121-123.

Terraz S, Cernicanu A, Lepetit-Coiffe M, Viallon M, Salomir R, Mentha G & Becker CD (2010). Radiofrequency ablation of small liver malignancies under magnetic resonance guidance: progress in targeting and preliminary observations with temperature monitoring. *Eur Radiol* 20, 886-897.

Thanos L, Poulou LS, Mailli L, Pomoni M & Kelekis DA (2010). Image-guided radiofrequency ablation of a pancreatic tumor with a new triple spiral-shaped electrode. *Cardiovasc Intervent Radiol* 33, 215-218.

Thumar AB, Trabulsi EJ, Lallas CD & Brown DB (2010). Thermal ablation of renal cell carcinoma: triage, treatment, and follow-up. *J Vasc Interv Radiol* 21, S233-41.

Timmerman RD, Bizekis CS, Pass HI, Fong Y, Dupuy DE, Dawson LA & Lu D (2009). Local surgical, ablative, and radiation treatment of metastases. *CA Cancer J Clin* 59, 145-170.

Ture H, Mercan A, Koner O, Aykac B & Ture U (2009). The effects of propofol infusion on hepatic and pancreatic function and acid-base status in children undergoing craniotomy and receiving phenytoin. *Anesth Analg* 109, 366-371.

U

Uhlar CM & Whitehead AS (1999). Serum amyloid A, the major vertebrate acute-phase reactant. *Eur J Biochem* 265, 501-523.

Urata K, Uehara S, Hayashi H, Matsumata T, Takenaka K & Sugimachi K (1995). Radiofrequency hyperthermia for malignant liver tumors: the clinical results of seven patients. *Hepatogastroenterology* 42, 492-496.

V

van den Bosch MA, Josan S, Bouley DM, Chen J, Gill H, Rieke V, Butts-Pauly K & Daniel BL (2009). MR imaging-guided percutaneous cryoablation of the prostate in an animal model: in vivo imaging of cryoablation-induced tissue necrosis with immediate histopathologic correlation.
J Vasc Interv Radiol 20, 252-258.

van Hillegersberg R (1997). Fundamentals of laser surgery. *Eur J Surg* 163, 3-12.

Vigen KK, Jarrard J, Rieke V, Frisoli J, Daniel BL & Butts Pauly K (2006). In vivo porcine liver radiofrequency ablation with simultaneous MR temperature imaging.
J Magn Reson Imaging 23, 578-584.

Vogel TJ, Mack MG, Muller P, Straub R, Eichler K & Felix R (1998). Laser-induced and microwave thermotherapy of hepatocellular carcinoma. *Digestion* 59 Suppl 2, 86-88.

Vogl TJ, Muller PK, Hammerstingl R, Weinhold N, Mack MG, Philipp C, Deimling M, Beuthan J, Pegios W, Riess H & et a (1995). Malignant liver tumors treated with MR imaging-guided laser-induced thermotherapy: technique and prospective results. *Radiology* 196, 257-265.

Vogl TJ, Mack MG, Balzer JO, Engelmann K, Straub R, Eichler K, Woitaschek D & Zangos S (2003). Liver metastases: neoadjuvant downsizing with transarterial chemoembolization before laser-induced thermotherapy. *Radiology* 229, 457-464.

Vogl TJ, Straub R, Zangos S, Mack MG & Eichler K (2004). MR-guided laser-induced thermotherapy (LITT) of liver tumours: experimental and clinical data. *Int J Hyperthermia* 20, 713-724.

Vogl TJ, Naguib NN, Eichler K, Lehnert T, Ackermann H & Mack MG (2008). Volumetric evaluation of liver metastases after thermal ablation: long-term results following MR-guided laser-induced thermotherapy. *Radiology* 249, 865-871.

Vogl TJ, Gruber T, Balzer JO, Eichler K, Hammerstingl R & Zangos S (2009). Repeated transarterial chemoembolization in the treatment of liver metastases of colorectal cancer: prospective study. *Radiology* 250, 281-289.

W

Wang YH, Liu JF, Li F, Li A, Liu Q, Liu DB, Liu DG & Wang YJ (2009). Radiofrequency ablation combined with transarterial chemoembolization for unresectable primary liver cancer. *Chin Med J (Engl)* 122, 889-894.

Wah TM, Arellano RS, Gervais DA, Saltalamacchia CA, Martino J, Halpern EF, Maher M & Mueller PR (2005). Image-guided percutaneous radiofrequency ablation and incidence of post-radiofrequency ablation syndrome: prospective survey. *Radiology* 237, 1097-1102.

Weaver ML, Atkinson D & Zemel R (1995). Hepatic cryosurgery in treating colorectal metastases. *Cancer* 76, 210-214.

Weinberg BD, Krupka TM, Haaga JR & Exner AA (2008). Combination of sensitizing pretreatment and radiofrequency tumor ablation: evaluation in rat model. *Radiology* 246, 796-803.

Weisbrod AJ, Atwell TD, Callstrom MR, Farrell MA, Mandrekar JN & Charboneau JW (2007). Percutaneous radiofrequency ablation with a multiple-electrode switching-generator system. *J Vasc Interv Radiol* 18, 1528-1532.

Wemyss-Holden SA, Porter KJ, Baxter P, Rudkin GE & Maddern GJ (1999). The laryngeal mask airway in experimental pig anaesthesia. *Lab Anim* 33, 30-34.

Wemyss-Holden SA, Robertson GS, Hall PD, Dennison AR & Maddern GJ (2000). Electrolytic treatment of colorectal liver tumour deposits in a rat model: a technique with potential for patients with unresectable liver tumours. *Dig Dis* 18, 50-57.

Wemyss-Holden SA, de la MHP, Robertson GS, Dennison AR, Vanderzon PS & Maddern GJ (2000). The safety of electrolytically induced hepatic necrosis in a pig model. *Aust N Z J Surg* 70, 607-612.

Wemyss-Holden SA, Robertson GS, Dennison AR, Vanderzon PS, Hall PM & Maddern GJ (2000). A new treatment for unresectable liver tumours: long-term studies of electrolytic lesions in the pig liver. *Clin Sci (Lond)* 98, 561-567.

Wemyss-Holden SA, Robertson GS, Dennison AR, de la MHP, Fothergill JC, Jones B & Maddern GJ (2000). Electrochemical lesions in the rat liver support its potential for treatment of liver tumors. *J Surg Res* 93, 55-62.

Wemyss-Holden SA, Berry DP, Robertson GS, Dennison AR, De La MHP & Maddern GJ (2002). Electrolytic ablation as an adjunct to liver resection: Safety and efficacy in patients. *ANZ J Surg* 72, 589-593.

Wemyss-Holden SA, Dennison AR, Finch GJ, Hall Pd Pde L & Maddern GJ (2002). Electrolytic ablation as an adjunct to liver resection: experimental studies of predictability and safety. *Br J Surg* 89, 579-585.

Wemyss-Holden SA, Court FG, Morrison CP, Teague BD, Burrell A, Morales DR, Rodgers N, Anthony AA, Metcalfe MS, Dennison AR & Maddern GJ (2003). Palliation of pancreatic cancer using electrolytic ablation. *Surg Endosc* 17, 207-211.

Wemyss-Holden SA, Dennison AR, Berry DP & Maddern GJ (2004). Local ablation for unresectable liver tumors: is thermal best? *J Hepatobiliary Pancreat Surg* 11, 97-106.

Wong J, Lee KF, Lee PS, Ho SS, Yu SC, Ng WW, Cheung YS, Tsang YY, Ling E & Lai PB (2009). Radiofrequency ablation for 110 malignant liver tumours: preliminary results on percutaneous and surgical approaches. *Asian J Surg* 32, 13-20.

Wong SN, Santi GE, Nurjadin H, Aguilar R & Gosalvez-Pe S (2010). Temperature-dependent electrode repositioning for multiple overlapping radiofrequency ablation in ex vivo porcine livers. *J Vasc Interv Radiol* 21, 1733-1738.

Wright AS, Sampson LA, Warner TF, Mahvi DM & Lee FTJ (2005). Radiofrequency versus microwave ablation in a hepatic porcine model. *Radiology* 236, 132-139.

X

Xu HX, Xie XY, Lu MD, Chen JW, Yin XY, Xu ZF & Liu GJ (2004). Ultrasound-guided percutaneous thermal ablation of hepatocellular carcinoma using microwave and radiofrequency ablation. *Clin Radiol* 59, 53-61.

Y

Yamada R, Sato M, Kawabata M, Nakatsuka H, Nakamura K & Takashima S (1983). Hepatic artery embolization in 120 patients with unresectable hepatoma. *Radiology* 148, 397-401.

Yan K, Chen MH, Yang W, Wang YB, Gao W, Hao CY, Xing BC & Huang XF (2008). Radiofrequency ablation of hepatocellular carcinoma: long-term outcome and prognostic factors. *Eur J Radiol* 67, 336-347.

Yan TD, King J, Sjarif A, Glenn D, Steinke K & Morris DL (2006). Learning curve for percutaneous radiofrequency ablation of pulmonary metastases from colorectal carcinoma: a prospective study of 70 consecutive cases. *Ann Surg Oncol* 13, 1588-1595.

Yan TD, Nunn DR & Morris DL (2006). Recurrence after complete cryoablation of colorectal liver metastases: analysis of prognostic features. *Am Surg* 72, 382-390.

Yan TD, King J, Sjarif A, Glenn D, Steinke K & Morris DL (2006). Percutaneous radiofrequency ablation of pulmonary metastases from colorectal carcinoma: prognostic determinants for survival. *Ann Surg Oncol* 13, 1529-1537.

Yang W, Chen MH, Yin SS, Yan K, Gao W, Wang YB, Huo L, Zhang XP & Xing BC (2006). Radiofrequency ablation of recurrent hepatocellular carcinoma after hepatectomy: therapeutic efficacy on early- and late-phase recurrence. *AJR Am J Roentgenol* 186, S275-83.

Yin XY, Xie XY, Lu MD, Xu HX, Xu ZF, Kuang M, Liu GJ, Liang JY & Lau WY (2009). Percutaneous thermal ablation of medium and large hepatocellular carcinoma: long-term outcome and prognostic factors. *Cancer* 115, 1914-1923.

Yoshimatsu R, Yamagami T, Terayama K, Matsumoto T, Miura H & Nishimura T (2009). Delayed and recurrent pneumothorax after radiofrequency ablation of lung tumors. *Chest* 135, 1002-1009.

Yu J, Liang P, Yu X, Liu F, Chen L & Wang Y (2010). A comparison of microwave ablation and bipolar radiofrequency ablation both with an internally cooled probe: Results in ex vivo and in vivo porcine livers. *Eur J Radiol* Jan 2 [Epub].

Yu Z, Liu W, Fan L, Shao J, Huang Y & Si X (2009). The efficacy and safety of percutaneous microwave coagulation by a new microwave delivery system in large hepatocellular carcinomas: four case studies. *Int J Hyperthermia* 25, 392-398.

Z

Zagoria RJ, Chen MY, Shen P & Levine EA (2002). Complications from radiofrequency ablation of liver metastases. *Am Surg* 68, 204-209.

Zhang L, Zhu H, Jin C, Zhou K, Li K, Su H, Chen W, Bai J & Wang Z (2009). High-intensity focused ultrasound (HIFU): effective and safe therapy for hepatocellular carcinoma adjacent to major hepatic veins. *Eur Radiol* 19, 437-445.

Zhang Y, Guo Y, Ragin AB, Lewandowski RJ, Yang GY, Nijm GM, Sahakian AV, Omary RA & Larson AC (2010). MR imaging to assess immediate response to irreversible electroporation for targeted ablation of liver tissues: preclinical feasibility studies in a rodent model. *Radiology* 256, 424-432.

Zhou Y, Zhao Y, Li B, Xu D, Yin Z, Xie F & Yang J (2010). Meta-analysis of radiofrequency ablation versus hepatic resection for small hepatocellular carcinoma. *BMC Gastroenterol* 10, 78.

Zhu JC, Yan TD & Morris DL (2008). A systematic review of radiofrequency ablation for lung tumors. *Ann Surg Oncol* 15, 1765-1774.

Zhu JC, Yan TD, Glenn D & Morris DL (2009). Radiofrequency ablation of lung tumors: feasibility and safety. *Ann Thorac Surg* 87, 1023-1028.